Cyanide Responsive Lanthanide Complexes and Supramolecular Lanthanide Architectures

Xuejian Zhang

Somerville College
University of Oxford

A thesis submitted in partial fulfilment of the requirements

for the degree of *Doctor of Philosophy*

Trinity Term 2019

Table of Contents

Abstract v

Publications vi

1 Introduction 1

1.1 General Lanthanide Chemistry 1

1.2 Lanthanide Luminescence 2

1.3 Sensitised luminescence 3

1.4 Luminescence quenching 6

1.5 Lanthanides as luminescent probes 8

1.6 Paramagnetic properties 9

1.7 Isomers of lanthanide complexes 14

1.8 Lanthanide coordination chemistry 17

1.8.1 Macrocyclic effect 17

1.9 Stability 18

1.9.1 Thermodynamic Stability 19

1.9.2 Kinetically Stability 21

1.10 Responsive lanthanide complexes as Sensors 24

1.10.1 Design Principles 24

1.10.2 pH sensors 25

1.10.3 Anion sensors 26

1.10.4 Cation sensors 29

1.10.5 Ratiometric sensing 31

1.10.6 Cyanide sensing [64] 33

1.10.7 Cyanohydrin formation 34

1.11 Click reaction 35

1.12 Project aims 38

1.13 Reference 39
2 Study of 4'-substituted PhenacylDO3A complex as Cyanide Sensor 43
2.1 Introduction 43
2.2 Synthesis 46
2.3 NMR spectroscopy characterisation 47
2.4 Photophysical studies 49
2.5 Fluoride and Cyanide binding of tetra-amide terbium complex 56
2.5.1 Synthesis and characterisation 57
2.5.2 Fluoride binding studies 60
2.6 Cyanide binding studies 62
2.7 Conclusion 69
2.8 Reference 71
3 Heterobimetallic f-f' Arrays as Ratiometric Cyanide Sensors 71
3.1 Introduction 72
3.2 Alkyne appended DO3A lanthanide complexes 72
3.2.1 Introduction 72
3.2.2 Propargyl-appended DO3A 74
3.2.3 Crystal structure of propargylDO3 complex and computational studies 75
3.2.4 NMR spectroscopy characterisation 77
3.2.5 Photophysical Studies 79
3.3 Propargyl-DO3P complex 81
3.3.1 Synthesis 81
3.3.2 NMR characterisation 82
3.3.3 Photophysical Studies 85
3.4 EthynylbenzylDO3A 87
3.4.1 Synthesis 87
3.4.2 Photophysical Studies 89
3.5 Azidophenacyl DO3A lanthanide complexes 91
3.5.1 Introduction 91
3.5.2 Synthesis 92
3.5.3 NMR spectroscopy characterisation 95

3.5.4 Photophysical Studies 97
3.6 Preparation and study of Heterobimetallic arrays 102
3.6.1 Introduction 102
3.6.2 Synthesis 103
3.6.3 NMR 105
3.6.4 Photophysical Cyanide binding studies 110
3.7 Conclusion 121
3.8 Reference 122
4 Novel Rotaxane Ligands for Lanthanide Complexation 124
4.1 Introduction 124
4.2 Origin of the design and strategy of synthesis 128
4.3 Synthesis of the ligating rotaxane 130
4.4 Structure optimisation 133
4.5 Lanthanide Binding Studies 134
4.6 Association Constant Determination 141
4.7 Conclusions 144
4.8 Reference 146
5 Conclusion and Future Perspective 148
6 Experimental 150
6.1 General procedures 150
6.2 X-ray crystallography 152
6.3 Titration methodology 153
6.4 Dynafit 153
6.5 Synthesis 156
6.6 X-ray crystallographic data 197
6.7 Reference 199

Abstract

‘Cyanide responsive lanthanide complexes and supramolecular lanthanide architecture’

Xuejian Zhang, Somerville College**,** University of Oxford

DPhil. Thesis, Trinity Term 2019

This thesis describes the development of new lanthanide-based luminescent architectures with potential as chemosensors, exploring how the luminescence properties of lanthanide complexes can be altered as a consequence of changes in key analyte concentrations.

Chapter 1 provides some background to the field, relating the fundamental properties of lanthanide complexes to their interactions with their surroundings. It also outlines key objectives for sensing cyanide and fluoride in competitive media.

Chapter 2 describes the synthesis and properties of a series of lanthanide complexes which incorporate a phenacyl group attached to the well-known DO3A lanthanide binding domain. These complexes show a very limited response to fluoride ions as a consequence of their weak affinity for the charge-neutral lanthanide complex. By contrast, cyanide ions interact with the phenacyl carbonyl group, modulating emission from the lanthanide as a consequence of cyanohydrin formation.

These ideas are pursued further in chapter 3. In this chapter, a series of methods are used to explore whether selectivity can be enhanced by using bimetallic complexes. A variety of ligand structures were explored, but the best results were obtained using systems in which two lanthanide-containing complexes were linked together by click reactions. Of these, both the **TbEu** and **EuYb** complexes showed the ability to detect cyanide ratiometrically. The **EuYb** system is probably destined to remain a curiosity, owing to the weak (and hard to detect) emission from the ytterbium centre. However, the **TbEu** complex has significant potential - offering cyanide selectivity and two-colour emission.

Chapter 4 takes a different approach, describing the synthesis of a lanthanide binding rotaxane in which rotaxane formation generates a lanthanide binding site. Studies on this system reveal lanthanide binding in the assembled hosts, albeit with relatively low affinity for lanthanide ions.

Chapter 5 draws conclusions from the whole body of work and suggests some avenues that might be explored in future

Chapter 6 contains the experimental detail.

Publications

1. Routledge, J.D., Zhang, X., Connolly, M., Tropiano, M., Blackburn, O.A., Kenwright, A.M., Beer, P.D., Aldridge, S., Faulkner, S.: Lanthanide Complexes that Respond to Changes in Cyanide Concentration in Water. Angew. Chemie - Int. Ed. 56, 7783–7786 (2017). doi:10.1002/anie.201702296

Acknowledgements

First of all, I would like to thank my supervisor Stephen Faulkner for offering the great opportunity to be a member of his group and to his advice not regards chemistry but in every aspect of life. During the three years, he has been a fountain of constant help, joy and in particular knowledge. You helped me to become a person who can consider chemistry as a chemist and open the door to real scientific research. You are a great mentor.

I am grateful to all the staff at the Chemistry Research Laboratory for their help and expertise. Particularly, I would like to thank Dr Nick Rees for the help with the NMR facility. Thanks to Alan Kenwright for recording some nice spectra for my complexes and the useful suggestion about the tuning paramagnetic NMR. Thanks to Kristen for measuring the crystallographic data. Thanks to Xiaoxiong for the synthesis of the beautiful rotaxane used in this work and in general thanks to the Beer and Aldridge groups for the continuous help during my DPhil

I would like to give special thanks to Robert Edkins for teaching me everything in luminescence and the fundamental photophysics. You have been a great mentor and friend during my time in Oxford. Thanks to Laura and Louise for continuous help in the lab, in particular, Leila, you gave so much useful advice at the beginning of my first year and plenty of fun.

During my time in Oxford, I have met some great people and I must thank the past and present members of the Faulkner group. Thank you for the help, the chats and laughs made my time with tedious experiments so colourful.

Thanks to all my students for making me think as a teacher and giving me the chance to solidify my theoretical and practical knowledge.

Thanks to all the friends in Oxford, for not only the fun in drinking, social activities but also the help and advice you gave. In particular, I would like to thank Tang Yu for being there for me in my times of need and boredom as well as being a really good friend.

I would like to think my family for always being there for me, for the encouragement and endless love. Thanks to my dad for teaching me to be a real man, a responsible person, and the suggestions for me to go through hard times. Thanks to my mum for teaching me how to be a warm and kind person. Thanks to my family for giving me the opportunity for education and for always being proud of me. I wouldn't have got here without you.

Finally, thanks to Mengran, who has always been a source of happiness to make my writing time so enjoyable. With you, I have spent the best days of my life and thank you for your love and support.

Abbreviations

a.u.	arbitrary units
BeT	Back-energy transfer
Bn	benzyl
cbz	benzylchloroformate
CT	charge transfer
Cyclen	1,4,7,10-tetrazacyclododecane
d	days
d	doublet
DCM	dichloromethane
DMSO	dimethylsulfoxide
DO2A	1,4,7,10-Tetraazacyclododecane-1,7-diacetic acid
DO3A	1,4,7,10-Tetraazacyclododecane-1,4,7-triacetic acid
DOTA	1,4,7,10-Tetraazacyclododecane-1,4,7,10-tetraacetic acid
DTPA	diethylenetriaminepentaacetic acid
EDTA	ethylenediaminetetraacetic acid
EI	electron ionisation
ES	electrospray
ET	energy transfer
EtOAc	ethyl acetate
EtOH	ethanol
h	hours
HPLC	high performance liquid chromatography
HRMS	high resolution mass spectrometry

IC	internal conversion
ILCT	intra-ligand charge transfer
IR	infrared
ISC	inter-system crossing
LIS	lanthanide induced shift
LMCT	ligand to metal charge transfer
Ln	lanthanide
MALDI	matrix-assisted laser desorption ionisation
Me	methyl
MeCN	acetonitrile
MeOH	methanol
MLCT	metal to ligand charge transfer
MRI	magnetic resonance imaging
MWCO	molecular weight cut-off
NEt_3	triethylamine
NIR	near infrared
NMR	nuclear magnetic resonance
OTf	trifluoromethansulfonate (triflate)
PeT	photoelectron transfer
Ph	phenyl
RT	room temperature
S	singlet state
SAP	square anti-prism
T	triplet state

TETA	1,4,8,11-tetraazacyclotetradecane-1,4,8,11-tetraacetic acid
TFA	trifluoroacetic acid
THF	tetrahydrofuran
TLC	thin layer chromatography
TOF	time of flight
TSAP	twisted square anti-prism
UV	ultraviolet
UV-Vis	ultraviolet-visible

1 Introduction

This thesis explores the development of responsive lanthanide complexes that interact with their surroundings to report on the concentration of ionic analytes, and particularly of fluoride and cyanide ions. Achieving these goals requires an understanding of the chemistry and spectroscopy of the lanthanides themselves, but also effective methods for ligand synthesis if the complexes are to have practical merit. This introductory chapter outlines some of the key backgrounds to the field and explores the development of lanthanide complexes as probes of their surroundings.

1.1 General Lanthanide Chemistry

The trivalent lanthanide (Ln^{III}) ions are the most stable form throughout the lanthanide series and dominate lanthanide chemistry with the exception of a handful of cases where divalent or tetravalent anions can be formed as a consequence of unusually high 3rd ionisation energies or unusually low fourth ionisation energies.

Lanthanides have been extensively investigated for last decades due to their unique photo-physical properties, such as sharp emission, large pseudo-Stokes shift and long luminescent lifetime. Although 4f orbitals are the valence orbitals. the 4f orbitals are well shielded by the filled 5s and 5p orbitals, which are more spatially dispersed. Therefore, the bonding formation in lanthanide complexes is mainly dominated by the electrostatic interactions between the Lewis acidic lanthanide metal ion and ligand. The coordination number varies from 8 to 10 in aqueous solution. The coordination geometry is substantially governed by

the steric effects of the lanthanide ion, which has most common +3 oxidation state, making hard donors like N and O atoms more favourable to be bounded with hard lanthanide metal ions.

1.2 Lanthanide Luminescence

The versatile electronic configuration renders the emission profile of each lanthanide ion greatly different across the lanthanide series. As shown in Figure 1-1, most of the lanthanide ions (Ln^{III}) are luminescent and their characteristic emission spectrum can spread from the UV(Gd^{III}) to near-infrared (NIR) (Nd^{III}, Yb^{III}, Er^{III}), going through green (Tb^{III}), yellow (Dy^{III}) and red (Eu^{III}).

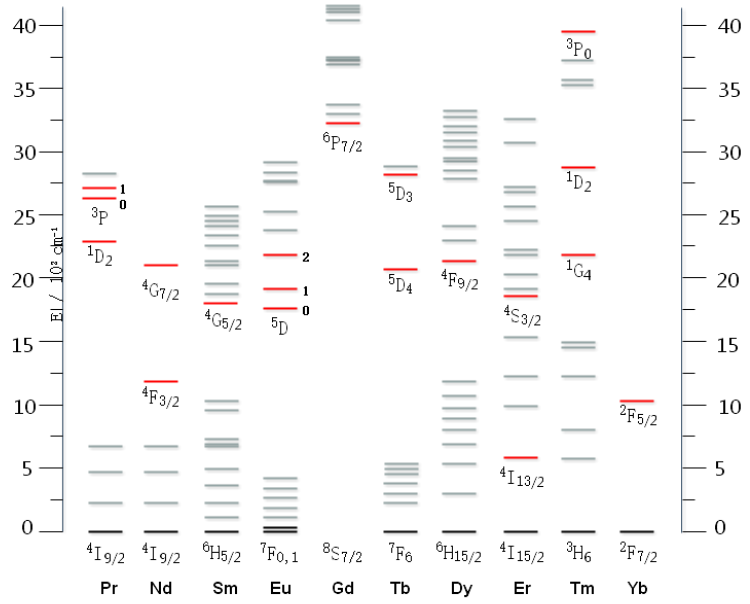


Figure 1-1. Partial energy diagram for Ln^{III} ions. The main excited states are marked in red, while the fundamental ground state is indicated in black.[1]

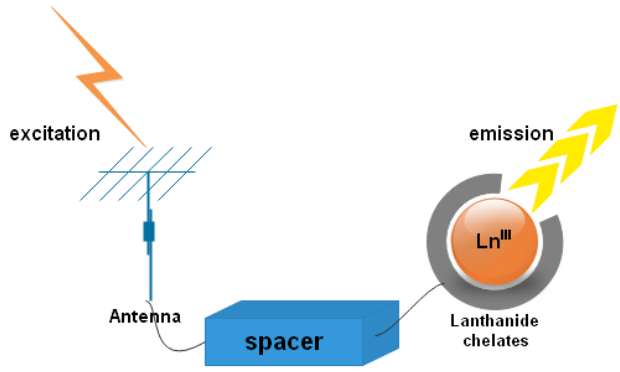
Lanthanide ions with partially filled 4f orbitals exhibit sharp line-like absorption and emission spectra as a consequence of the forbidden nature of f-f transitions, where the f-f transitions contain both electric dipole and magnetic dipole characters. Although magnetic dipole transitions are allowed, f-f transitions are significantly weak as a consequence of no changes in parity in transition, suggested by the Laporte rule (electric dipole selection rule). Nevertheless, the electric transitions are still the most significant in the spectrum since several mechanisms can be used to partially relax the selection rules (*e.g.*, vibronic coupling). Specifically, the vibronic coupling of excited states emerges due to the fact that the symmetry of metal ions is changed by molecular vibration, though the limited covalency of lanthanide compounds tends to mean that vibrations have low energy, resulting in very narrow transitions. More importantly, mixing of J-levels and mixing of wavefunctions becomes facile in non-centrosymmetric systems (where parity labels lose their meaning).

What's more, the extinction coefficients of trivalent lanthanide ions are small, and usually, in the range 0.5-3 $dm^3mol^{-1}cm^{-1}$ which makes direct excitation extremely inefficient, and only feasible with laser pulses. As a consequence, it is not practical to produce highly luminescent lanthanide ions by direct excitation.[1]

1.3 Sensitised luminescence

Since the direct excitation becomes unrealistic due to the very low molar absorptivities, therefore the method for circumventing this issue is to incorporate with a sensitising chromophore (also known as an antenna group), which can populate the emissive excited states of the lanthanide ion via energy transfer. The antenna can be covalently incorporated into the ligand manifold or bringing in via other means (e.g., co-ligand). These *f*-centred

excited states can undergo radiative processes to produce lanthanide emission with well-defined characteristics, microsecond (or longer) lifetime and large Stokes shift. These phenomena all result from the forbidden nature of f-f transitions and the antenna effect, respectively. Besides, the lanthanide luminescence can be easily quenched by the high energy oscillators (X-H, C-H, N-H)



Scheme1-1. Schematic representation of sensitised lanthanide luminescence with energy transfer.

In a classic sensitisation process, excitation of the organic chromophore starts with single or multiphoton absorption event and, following internal conversion (IC), generates the singlet excited states (S_1) of the organic chromophore. This S_1 state can be relaxed down to the ground state via non-radiative decay or undergo radiative decay to produce fluorescence. Alternatively, S_1 can undergo intersystem crossing (ISC) to populate the triplet excited states T_1 from S_1; potentially giving rise to phosphorescence, non-radiative decay, or transfer energy from T_1 to the excited states of a lanthanide acceptor. This energy transfer pathway can be mediated by either Dexter Exchange or Förster energy transfer, substantially depending on the molecular structure. It has been demonstrated that the effectiveness of energy transfer depends on the difference between the Ln^{III} acceptor state and the donor triplet state. Back energy transfer can occur to diminish the Ln^{III} emissive states when the gap is less than 2000 cm^{-1}, and therefore triplet mediated energy transfer

usually dominates the sensitisation process. It has been reported that the short-lived S_1 states of the antenna can also sensitise the lanthanide luminescence and this singlet energy transfer (^{1}ET) plays a crucial role in sensitisation of lanthanide emissive state in the presence of intra-ligand charge transfer (ILCT).[3] (Figure 1-2)

A simplified diagram is given in Figure 1-2, though the real sensitisation process of Ln^{III} ions could be more complicated. Although there has been extensive research on organic chromophore-sensitised lanthanide complexes, transition metal-containing systems also have been exploited for preparing highly luminescent lanthanide complexes, especially terbium and europium with high energy emitting levels.

Furthermore, charge transfer (CT) containing systems have also been attracting more attention due to their high photostability and broad absorbing range. Particularly, in the case of ytterbium complexes, charge transfer is of great importance in such systems since the emissive excited states $^2F_{5/2}$ of Yb^{3+} is much lower than triplet excited states of the common organic chromophore. Horrocks *et al.* postulated the fact that $^2F_{5/2}$ emissive states can be populated via a reversible ligand-to-metal electron transfer.[13] In this process, the excited organic chromophores reduce Yb^{3+} to Yb^{2+} to form ligand-to-metal charge transfer (LMCT) states, and subsequently, the radical chromophore oxidise the Yb^{2+} to generate the (Yb^{3+})* excited states, resulting in the ytterbium emission. Except for ytterbium complexes, LMCT can also occur in the energy transfer cascade of other lanthanide-containing systems. However, in these systems, LMCT states are could be lower in energy than the emissive states of lanthanide (e.g., Tb), thus leading to the quenching in lanthanide luminescence.

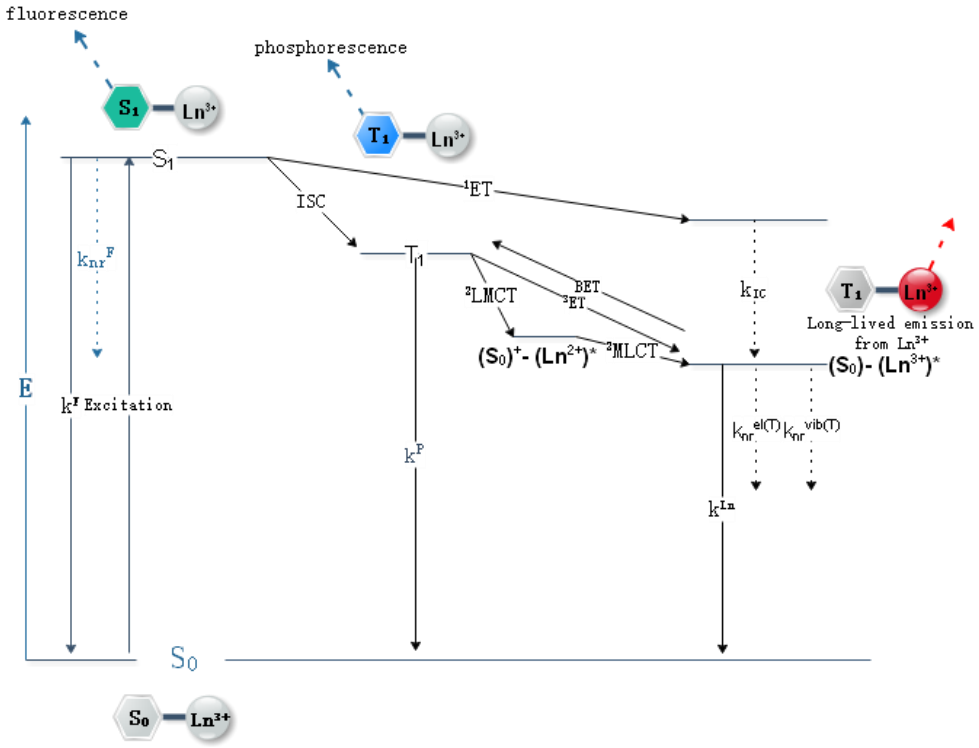


Figure 1-2. Simplified Jablonski diagram for sensitised lanthanide luminescence.

1.4 Luminescence quenching

The emissive states of Ln^{III} ions can be readily quenched by oscillators such as NH, OH and CH since their vibrational energy is quite close to the energy of f-f transition.[2] This is a non-radiative quenching process thus the intensity of Ln^{III}-centred emission is reduced. However, the energy of vibrational harmonics of deuterated oscillators (*e.g.* ND, OD and CH) are lower in energy and hence, they cannot quench the luminescence of lanthanide complexes efficiently due to the mismatch in energy between the corresponding vibrational overtone and emissive states of Ln^{III}. Indeed, the rate of depopulation of emissive states in H_2O is almost 200 times faster than that in D_2O. The energy gap between the emissive states and the lower states of a Ln^{III} ion can be bridged by the vibrational harmonics of the O-H oscillators on water molecules bound to (or close to) the metal centre. In fact, Ln^{III}

ions with larger energy gaps between excited and ground states, such as Eu^{III} and Tb^{III} are less likely to be quenched by the bound water molecule as a consequence of the reduced Franck-Condon overlap with higher vibrational harmonics. The luminescent lifetime is also significantly lengthened by the oscillators due to the increase in the rate of non-radiative relaxation.

In aqueous solution, water molecules bind to the Ln^{III} ion to complete the coordination sphere of lanthanide complexes (8-9). While the determination of hydration states can be achieved via the X-ray crystallography, this technique is limited due to the difficulty in crystal growth and frequent inconsistency in structure between solution state and solid state. More commonly, the number of bound water molecules can be calculated by employing the modified Horrocks' equation (Equation 1).[3] The decay constant of the emissive states in both water (k_H) and deuterium oxide (k_D) can be obtained from time-resolved luminescence measurements and used to calculate q, the number of inner sphere solvent molecules.[3]

$$\boldsymbol{q} = A(k_H - k_D - B) \qquad (1)$$

Where constant A indicates how likely lanthanide radiation quenched by OH oscillators and is parameterised for each lanthanide ion. Solvent molecules in the outer sphere and the donor atoms bound to the metal ion can also quench the lanthanide emission, and constant B is introduced in the equation as an empirical correction factor to account for quenching by all outer sphere solvent oscillators. In the case of ligands coordinating via amide carbonyl groups, the exchangeable N-H oscillation can quench emissive states of Eu^{III} ion, thus an additional correction needs to be applied when calculating hydrations states of europium(III) complexes.

$$\boldsymbol{q_{Eu}} = A(k_H - k_D - B - 0.075x^{\mathrm{I}}) \quad (2)$$

Values of A and B for Eu^{III} and Tb^{III} are tabulated in Table 1-1. [8]

Table1-1. Factors of A and B used in the Horrocks' equation in aqueous solution

	A	B
Eu	1.2 ms	0.25 ms^{-1}
Tb	5 ms	0.06 ms^{-1}

It worth noting that the triplet excited states of the chromophore can be quenched by molecular oxygen. In the case, the effectiveness of the radiative process is reduced by $^3O_2$ quencher via triplet-triplet annihilation, though such an effect can be partially relieved by the thermal repopulation of lanthanide excited states. Particularly, terbium-containing systems are widely adopted as oxygen probes due to its high sensitivity to the presence of molecular oxygen. [4–6]

1.5 Lanthanides as luminescent probes

Emissive lanthanide complexes have been attractive in analytical application due to their unique photophysical characteristics.[7]

In conventional fluorescence microscopy, noise arising from autofluorescence and light scattering poses a challenge in discriminating the desired luminescent signal from the background. This issue can be circumvented by taking advantage of the long-lived lanthanide luminescence arising from the nature of f-f transitions. The lifetime of

lanthanide luminescence falls down to millisecond (e.g. Tb, Eu) whilst the background luminescence has a lifetime with an order of nanoseconds.[8] In the biological environment, long-lived luminescence from lanthanide ion can be distinguished from short-lived fluorescence of background endogenous species (biological fluorescence lifetime is nanosecond scale) and thus the sensitivity of measurement is enhanced and assignment of luminescent signals can be more feasible. [9] These characteristics of emission of lanthanide complexes have attracted considerable attention in analytical applications, especially as optical analyte reporters. Considering the most recognized pathway for the population of emissive excited states of lanthanides, i.e. $^1\pi\pi^* \rightarrow {}^3\pi\pi^* \rightarrow Ln^*$, perturbation of three excited states can result in modulation of the emission of lanthanide complexes. Although many deactivation processes need to be considered when preparing highly luminescent Ln^{III} complexes, these non-radiative processes can be used as a method in designing analyte-responsive lanthanide complexes.

1.6 Paramagnetic properties

As we discussed in an earlier section, the unique chemical and physical properties of lanthanide ion are a consequence of the occupation of 4f orbitals. Among the lanthanide series, the gadolinium(III) ion has drawn much attention due to its special properties; its 4f orbitals are half-filled with seven unpaired electrons, leading to powerful paramagnetism.[10,11]

The fundamental paramagnetic properties have been extensively exploited in term of energy levels of lanthanide(III) ions, which are commonly noted applying the Russell-Saunders coupling scheme. The total spin quantum number, S, and the total orbital angular

momentum quantum number, L, are used to define the Russell Saunders term, which is represented as follows.

$$^{(2S+1)}L_j \quad (3)$$

Upon complexation, the electron distribution around the Ln(III) is disturbed by the ligand, and the molecular symmetry is broken, giving rise to the splitting in energy levels. Firstly, electron-electron repulsion contributes to the splitting in energy levels, which are further split into **J** levels following by spin-orbit coupling. The **J** states are divided into **2J+1** states by the crystal field effect, where the parameter is termed as B_q^k. Zeeman effects also contribute to the splitting but with a small magnitude. In the case of lanthanide ions, the splitting of energy levels is dominated by the spin-orbit coupling and the crystal field coupling has a trivial effect. [12]

In the context of these parameters, k, is the rank label and has a possible value from 0 to 7. The interactions between electrons in different orbitals contribute to the even numbers of the rank label (2, 4 and 6) whereas the electrical dipole transition is responsible for the odd rank labels. The component label, q, is related to the symmetry elements. The magnitude of this parameter is increased when the symmetry is reduced. Thus, for a complex with low symmetry, this parameter has a significant effect on paramagnetism.[13]

Magnetic susceptibility also plays an important role in the paramagnetism of Ln(III) ion-containing systems. An external magnetic field makes the spin of unpaired electrons precess along the direction of the magnetic field, leading to energy level being further split by the Zeeman effect and induced magnetic moments. The magnetic susceptibility becomes anisotropic when the residual orbital magnetic moment is taken into account.

In a paramagnetic system, the anisotropy of magnetic susceptibility causes direct changes to the chemical shifts of a given nucleus compared to the corresponding diamagnetic analogue; this shift is quoted as the lanthanide induced shift (LIS, Δ_ω), which is also called

the hyperfine shift. The experimental chemical shift results from three mechanisms and the hyperfine shift only contains contributions from two factors, contact shift (Δ_c) and pseudocontact shift (Δ_p). These two terms are associated with magnetic susceptibility anisotropy and hence result in a much greater impact on the experimental hyperfine shift.

$$\Delta = \Delta_d + \Delta_c + \Delta_p \qquad (4)$$

The diamagnetic term Δ_d is the change in chemical shift of the ligand proton when undergoing complexation between free ligand and Ln(III) ion. This term is only responsible for a small change in the shift difference due to the changes in the structure of complexes relative to the diamagnetic analogues like Lu(III) complexes.

The contact shift is also called ***Fermi contact shift*** and derives from the presence of charge density of unpaired electrons at a nucleus of interest via spin polarisation. The contact shift contributions are the result of through-bond spin coupling between the orbital of the unpaired electrons and resonating nucleus. The distance between paramagnetic metal centre and given nucleus can be several chemical bonds away, or even longer if the chemical bonds contains π character, therefore the contact shift implies the structural information of bonding.[14] The contact shift contributed by the paramagnetic Ln(III) ion in the complex can be calculated as follows:

$$\Delta = \frac{-A \cdot \langle S_2 \rangle_J}{h \cdot \gamma_\iota \cdot \mathrm{B}_o} \qquad (5)$$

Pseudocontact shift is named to discriminate it from another contribution which originating from the same unpaired electron but in a different mechanism, and normally used to refer to the paramagnetic shift in the NMR spectra of lanthanide complexes. Pseudocontact shifts result from the coupling between nuclear dipole and electron dipole moment. The equation

for estimating the pseudocontact shift in a paramagnetic lanthanide-containing system was first proposed by Bleaney.[15] The expression is derived under the assumption that the magnitude of the J states split by ligand field is smaller than that of kT and written as follows:

$$\Delta_p = \frac{2\beta^2 D}{60k^2T^2}\left(\frac{\langle r^2\rangle A_2^0(3\cos^2\theta - 1) + \langle r^2\rangle A_2^2(\sin^2\theta cos2\varphi)}{r^3}\right) \quad (6)$$

In this expression, β is the Bohr magneton, *k* is the Boltzmann constant, ϕ,θ are the angles of the nucleus of interest in regard to lanthanide ion as the centre of the reference frame $\langle r^2\rangle A_2^0$ and $\langle r^2\rangle A_2^2$ parameters are crystal field term, established by the polarsability of ligand donor and the symmetry character of the system. The sign of hyperfine shift can be determined by coefficient C_j, which is related to magnetic susceptibility. The equation can be simplified to equation (6) if the system contains axial symmetry characters.

$$\Delta_p = \frac{2\beta^2 C_j}{60k^2T^2}\left(\frac{\langle r^2\rangle A_2^0(3\cos^2\theta - 1)}{r^3}\right) \quad (7)$$

It is notable that the relative position of the nucleus to Ln(III) ion is only used in the determination of pseudocontact shift and the magnitude of pseudocontact shift is primarily dependent on the distance between nucleus under consideration and Ln(III) ion.

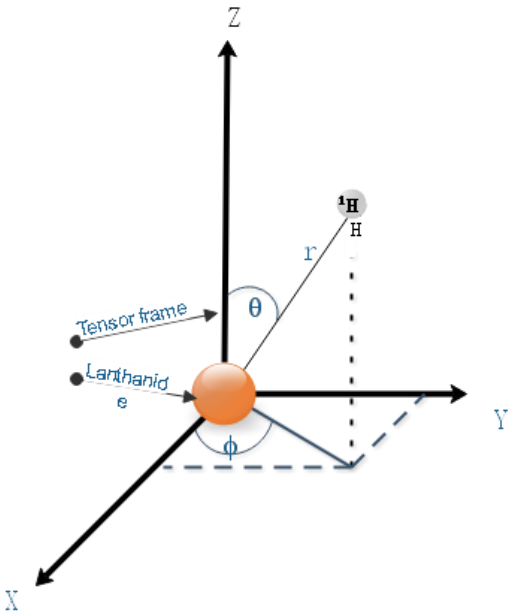


Figure1-3. Spherical coordinate system refers to the paramagnetic shift. The paramagnetic centre is located at the origin of axes (orange sphere); the nucleus of interest (grey sphere) is located with coordinates ϕ,θ and r. The direction of the external magnetic field is parallel to the z-axis.

Although both factors take effect simultaneously, there is only one dominating contributor of paramagnetic effects; the paramagnetic shifts of lanthanide complexes can be mainly ascribed to the pseudocontact contribution, which has been demonstrated by Aime and coworkers.[16] The Bleaney analysis remains a useful approach in analysing the solution behaviour of the ytterbium(III) complex with DTMA (DOTA tetrakis-methylamide) ligand as demonstrated by Blackburn et al. [17,18]

Nonetheless, Parker and co-workers have indicated that Bleaney's theory is limited in describing the magnetic anisotropy for some lanthanide complexes with low symmetry.[3] They demonstrated some assumptions in the theory needed to be revised before applying to DO3A containing lanthanide complexes. Firstly, higher-ordered crystal field terms are crucial in a system with low symmetry, and thus the contribution of such terms cannot be ignored when performing a Bleaney analysis.[19] Secondly, the electron distribution of Ln^{III} ion cannot be treated as a point charge as it is more proper to consider the electron

distribution as prolate or oblate in shape which is dependent on the lanthanide coordination environment specific for each lanthanide atom.[20] Lastly, the total angular momentum quantum number J, which is derived from spin-orbit coupling, is used to determine the Bleaney coefficient C_j. In some cases, it is more appropriate to use J-mixing rather than J when the energy of spin-orbit coupling is in the same magnitude as the ligand field.

1.7 Isomers of lanthanide complexes

Aminopolycarboxylate ligands based on the azamacrocycle12N_4 are most often adopted for complexation with Ln(III) ions (Figure) due to flexibility and adjustable size of the macrocyclic ring. The most well-known case, $[Ln.DOTA]^-$ complex, is discussed in this chapter.

The structures of these complexes depend on the interplay between ligand conformation and the metal centre. Unlike transition metals, where d- orbitals participate in bonding and define complex geometry, the core like nature of f-orbitals means that lanthanide ions can display a much broader range of coordination geometries. In the case of ligands such as DOTA and its derivatives, the structural chemistry in solution is dominated by the interplay between square antiprismatic (SAP) and twisted square antiprismatic (TSAP) coordination geometries. Both SAP and TSAP forms are found as pairs of enantiomers, meaning that a minimum of four isomers results at the lanthanide centre.

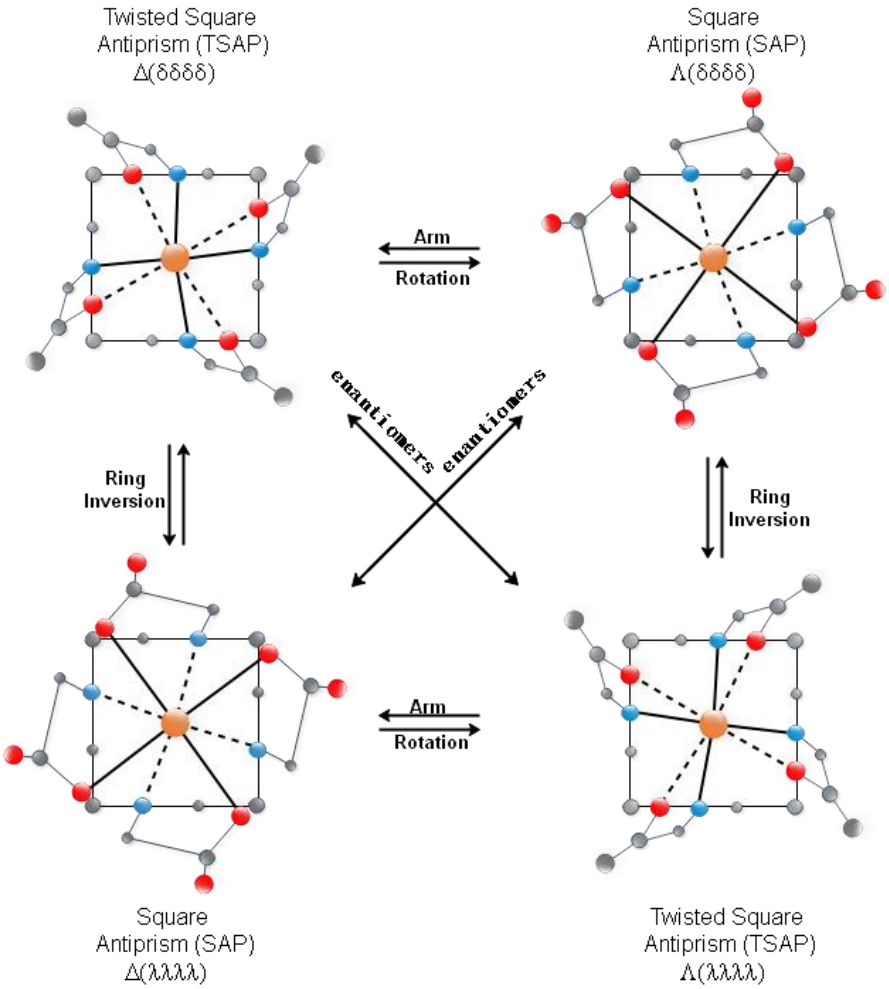


Figure 1-4. representation of possible diastereoisomers of [Ln.DOTA]$^-$ complexes.[54]

Figure 1-4 represents the four possible isomeric forms of [Ln.DOTA]$^-$ in the solution, resulting from the twist of N4 and O4 plane and the rotation of arms. These two sets of enantiomers can be mutually interconverted, and the chirality of the complexes is derived from the helicity of ethylenic moieties and the acetate arms. The macrocyclic ring has two possible conformers in C_4 symmetry in terms of helicity, where these stereoisomers are classified as δδδδ and λλλλ. Similarly, Λ and Δ are two conformers in the acetate arms referred to the difference in helicity, giving four possible isomers as two sets of enantiomers. The isomers of [Ln.DOTA]$^-$ complexes can be divided into two different species (two enantiomeric pairs), i.e. square antiprismatic isomer (SAP) and twisted square

antiprismatic isomer (TSAP), with a twist angle of approx. 40° and 30°, respectively.[21,22] Although the SAP geometry taking predominance was commonly found in the crystal structures of later lanthanide complexes with DOTA, e.g. Eu,[23] Gd,[24] and Lu. [25,26]. SAP and TSAP diastereomer can mutually interconvert in a slow exchange rate (NMR timescale) in solution. Indeed, the isomerisation between SAP and TSAP occurs in the solution via either the motion of acetate arms (by maintaining cyclen ring unchanged) or the inversion of the ring (by keeping the helicity of acetate arms untouched). The slow exchange in solution between isomers can be attributed to the high barrier of both entropy and entropy. Another fact is that in the solution, it has been observed that the geometry of earlier lanthanides from La(III) to Pm(III) is dominated by TSAP isomers whereas the later lanthanides have a preference for SAP geometry.[54] It is also worth noting that the exchange rate of coordinated water substantially relies on the conformation of the molecule that the exchange rate of SAP isomer is over 50 times slower than corresponding TSAP isomer.[27] NMR spectroscopy can be a useful tool in discriminating the basic geometry of lanthanide complexes in solution though the accurate assignment of protons could require more efforts. For instance, the resonance peaks with the most paramagnetic shift can be attributed to the axial protons on the cyclen ring, and complexes adopted SAP geometry have a larger angle towards the C_4 symmetry axis (θ) if we consider the contribution of pseudocontact shift. Similarly, this rationale can be applied to [Ln.DO3A] complexes where one nitrogen atom in the macrocycle is alkylated by a different side chain. The full assignment of ^{1}H-NMR spectra for $[Ln.DO3A]^-$ analogues could be challenging since higher-ordered crystal field parameters should be taken into consideration when performing Bleaney analysis on such heptadentate systems. Nevertheless, the discrimination between TSAP and SAP is still straightforward by comparing with the analogues of axial-symmetric species. In the $[Ln.DO3A]^-$ system, the broken axial makes the rotation of acetate arms more freely, and

thus the interconversion between TSAP and SAP isomers could be much faster than that of [Ln.DOTA]$^{-}$ analogue. Indeed, for [Eu.DO3A], the axial ring protons with SAP geometry can be found in the range from 25 to 40 ppm in the ^{1}H-NMR spectra, whereas the resonance for the corresponding TSAP isomer is broader and less shifted.

1.8 Lanthanide coordination chemistry

Lanthanide ions are hard Lewis acids with limited interaction with the ligand field as a consequence of the effectively core-like nature of the f-orbitals. As a consequence of their high charge, they form complexes most favourably with charged ligands, though neutral polydentate ligands can form stable complexes. The simple coordination chemistry of the lanthanides has been widely reviewed by Aime[16] and we will concentrate on key aspects of ligand design and complex stability for the purposes of this introduction.

1.8.1 Macrocyclic effect

Cyclic molecules have attracted chemists since the discovery of the structure of the benzene ring in the 19th century.[28] Chemists have devoted considerable efforts on investigating natural macrocycle and synthesising novel cyclic compounds. Nevertheless, the use of macrocycles as ligands for complexation of d metal ions has been substantially developed since the coordination chemistry have been outlined by pioneer Alfred Werner in the early 1890s. The lanthanide coordination chemistry has not been acknowledged as a subject until Pedersen first reported the formation of a complex between crown ether and salts of lanthanides (e.g. La^{III} and Ce^{III}) in 1967.[29] The studies of other macrocyclic compounds were systematically carried out in the early 1970s, and a significant number of lanthanide complexes were investigated with the aid of nuclear magnetic resonance spectroscopy

(NMR); the Schiff base derivatives were used to prepare the first neutral complex with lanthanum. [30] In sum, the studies of macrocyclic receptors until now has contributed to the development of coordination chemistry of lanthanide with a wide range of potential applications in regulating energy transfer pathways and in spectroscopic tools for analytical and biomedical probes.

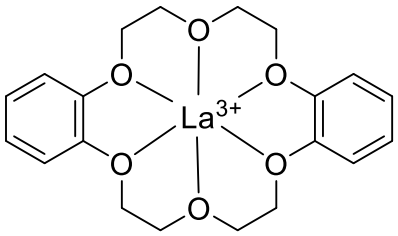


Figure1-5. The structure of dibenzo-18-crown-6 ether($B_2$16C6) lanthanum complex.

1.9 Stability

Stability is the most crucial parameter to be considered when designing ligands for preparing heterometallic lanthanide complexes with certain properties. Each lanthanide ion should be well encapsulated in its own binding pocket to avoid demetallation. As already stated, the properties of lanthanide ion arise from their high oxidation state and non-bonding 4f orbitals. Bonding is almost pure ionic, rendering hard donor atoms (e.g. oxygen, nitrogen) more favourable. Given the ionic nature of 4f-elements, the exchange between ligand and metal is extremely fast[31],[32]. Therefore, thermodynamic stability can be enhanced by implementing hard donor atoms in the macrocycle, where the strong ionic interaction between metal and ligand can minimise the possibility of demetallation. The coordination numbers of lanthanide can vary from two to twelve, where the most common ones are eight and nine. Besides, in a macrocycle, multiple chelating arms are incorporated to reduce the lability of lanthanide ion and increase the kinetic stability. As stated previously, the macrocyclic ligand can contribute to the kinetic stability due to the

macrocyclic effect. The acyclic ligand can dissociate successively from the metal ion by removing one donor atom individually, whereas, in case of macrocyclic ligands, all donor atoms must be removed at the same time to release the metal ion. This process requires much higher activation energy, and thus provides extra kinetic stability.

1.9.1 Thermodynamic Stability

Thermodynamic stability is highly related to the Gibbs free energy associated in the formation of a chelate and is represented by the stability constant. The thermodynamic stability constant can be defined as the equilibrium constant of the complexation reaction and calculated by the concentration of all species in solution.

Nevertheless, the thermodynamic stability constant can only be useful when assuming the ligand is fully protonated in a solution, which is not the case in the physiological environment. Therefore, conditional thermodynamic stability constant is introduced to predict the thermodynamic stability of lanthanide complexes under physiological conditions.

The relatively slow complexation of lanthanide (III) ions, particularly with macrocyclic ligands, hinders the exploitation of such binding by direct titrations. Thus, extensive studies are made to investigate the determination of thermodynamic stability constant, and competition methods are generally adopted depending on the pH of reaction conditions.

The thermodynamic properties of some common Gd(III) complexes are summarized in Table 1-1. Given the nature of hard donor, aminopolycarboxylate ligands exhibit superior thermodynamic stability. Although the flexibility of ligand might lead to an increase in entropy, the less steric hindrance, when encapsulating the metal ion, can significantly contribute to the thermodynamic stability.

Table 1-1. Thermodynamic stabilities for examples of linear and macrocyclic ligands with lanthanide ions.

	EDTA[34]	DPTA[31]	DOTA[37]
Eu^{3+}	17.2	22.4	23.4
Gd^{3+}	17.3	22.4	24.5
Tb^{3+}	17.8	22.9	24.3
Lu^{3+}	19.9	22.3	25.5

As shown in Table 1-1, for EDTA, the stability is dependent on the charge density of lanthanide ion. It can be rationalised by the increment in electrostatic interaction between ligand and metal resulted by each increased charge density across the lanthanide series. $[Ln.DTPA]^{2-}$ complexes also reflect a clear trend of increasing stability, however, the stability reaches a maximum with Tb(III) and Ho(III). Among the three ligands, the lanthanide complexes formed with DOTA ligand exhibit better stability. The pre-organised macrocycle requires less energy to rearrange the structure when forming the chelate, which makes it more entropic favourable, leading to the overall enhancement of thermodynamic stability of $[Ln.DOTA]^{-}$ complexes.

The stability of cyclam derived $[Ln.TETA]^{-}$ complexes is 10 orders of magnitude lower relative to the corresponding DOTA complexes. Unlike $[Ln.DOTA]^{-}$ species, $[Ln.TETA]^{-}$ complexes do not have a water molecule coordinated to the metal centre. The molecular geometry is an approximate dodecahedron which gives rise to greater repulsion. The larger macrocyclic ring also weakens the electrostatic interaction between metal ions and donor atoms. Similarly, [Ln.NOTA] complexes are also less stable than $[Ln.DOTA]^{-}$ complexes due to their inability to complete the coordination sphere of a typical lanthanide.

1.9.2 Kinetically Stability

It is well known that trivalent lanthanide ions are kinetically labile and that their rates of exchanges with water are in the order of 10^9 s^{-1}.[33] There are extensive studies on lanthanide complexes with aminopolycarboxylate ligands, particularly for gadolinium complexes given their ability to enhance the signal of magnetic resonance imaging. It can be noted that the kinetical stability is dependent on several factors including temperature, pH in H_2O and the rigidity of ligand. The complexation of Gd^{3+} ion by a flexible chain ligand (e.g. EDTA) is much faster than macrocyclic ligands like DOTA. The formation of [Gd.EDTA] involves a rapidly-formed intermediate following a slow structural rearrangement. [31] In contrast, the complexation of lanthanide Gd^{3+} with DOTA are characterised by potentiometry, luminescence spectrometry and EXAFS, proposing a mechanism that the formation of [Gd.DOTA] complex consists of three steps. Step **I** involves the formation of intermediate $[LnH_2DOTA]^+$, where the Gd^{3+} ion is first bound to the four oxygen atoms of the carboxylate arms and placed outside the cavity. Two protons are bound to the nitrogen atoms of the macrocycle follows slow proton transfer (1^{st} rate-determining step) to the carboxyl group. During Step **II**, the intermediate species is deprotonated to form [Gd.HDOTA] without changing conformation. In Step III, following a concerted rearrangement the Gd^{3+} ion enters the cavity coordinated to the four nitrogen atoms and simultaneously the last protons are lost(2^{nd} rate-determining step) to yield the final product $[Gd.DOTA]^-$, where the four nitrogen atoms and four oxygen atoms are bound to the Gd^{3+} ion. [34,35] The pH of the solution clearly influences the rate of formation of the complex. The pH of the DOTA solution was dropped dramatically once the gadolinium salt was added and remained slow decreasing for 48 hours. After stirring the mixture for 3-4 days, the pH was decreased gradually until it finally remains a constant after 7 weeks. The rate of complexation, therefore, can be optimum in the pH lower than 7, which facilitates the

deprotonating of intermediate whilst avoiding forming the insoluble lanthanide hydroxide. [36]

Table1-2. The dissociative rate constant of some gadolinium complexes discussed in this chapter. (pH dominated pathways are measured at pH < 2)

Compound	k_{obs} (s^{-1})	Reference
$[Gd.DOTA]^-$	$<5x10^{-8}$	[37]
[Gd.DTPA]	$1.2x10^{-3}$	[31]
[Gd.DO3A]	$2.3x10^{-3}$	[38]
[Gd.DTPA-BMA]	$>2x10^{-2}$	[31]
[Gd.HP-DO3A]	$2.6x10^{-5}$	[37]

It is of great importance that the dissociation of metal ion must be taken into account when exploiting the kinetics of lanthanide complexes. Many competing factors facilitate the dissociation of lanthanide complexes; protonation of chelate by decreasing pH, the presence of competitive cations like Zn^{2+}, Cu^{2+} and Fe^{3+} (transmetallation), and precipitate of lanthanide hydroxide salt. In the aspects of contrast agents, the most crucial factor is the toxicity of the compound which, in this case, is the rate of dissociation of complexes. However, The limitation of gadolinium complexes used as contrast agents is caused by the intrinsic toxicity of free Gd^{3+} ion, that the Gd^{3+} ion in the ligand cavity might be replaced by the Zn^{2+} given by its high concentration in human blood (18 μM).[39]

Indeed, for complexes with EDTA ligand, the dissociation process is primarily dominated by the proton-assisted mechanism rather than a direct attack by another competitive cation, where no space in the cavity can be accessible since all acetate arms are blocked. However, it is not the case for complexes with DTPA where the negative charges on $[Gd.DTPA]^{2-}$ make direct attack more feasible[40]. The rate of transmetallation of acyclic complexes such as $[Gd.DTPA]^{2-}$ has been shown to be directly related to the concentration of Zn^{2+} ion, suggesting that metal ions are directly attacked by another cation. As shown in Table 1-2, it is clear that the kinetic stability is considerably enhanced when the metal ion is bound to

a macrocyclic ligand. Studies by Brücher *et al.* revealed that the transmetallation of Gd^{III} complexes dominates under physiological conditions and the exchange rate of $[Gd.DTPA]^{2-}$ with Cu^{2+} is accelerated in the presence of endogenous anions like phosphate, carbonate and citrate.[41,42] The rate of dissociation of $[Gd.DOTA]^{-}$ is much lower than that of $[Gd.DTPA]^{2-}$ even under extreme acidic condition, despite the fact that the dissociation of $[Ln.DOTA]^{-}$ complexes follows proton-assisted mechanism (Table1-2). At physiological pH, the acid-catalysed dissociation has no effect on the actual rate of transmetallation of $[Gd.DOTA]^{-}$.[35] Compared to the acyclic chelate like $[Gd.DTPA]^{2-}$, the extra contribution of kinetic stability can be derived from the macrocyclic effect of DOTA ligand, leading to negligible effect in the presence of Zn^{2+} ion.

Lanthanide DO3A derivatives functionalized on the fourth nitrogen atom display much higher kinetic stability than complexes formed with DO3A itself and can be used as building blocks to prepare heterometallic lanthanide arrays, and it is necessary to understand the kinetic details of such complexes in the presence of other endogenous catalytic ions like Cu^{2+}. A thorough review of the kinetic stability of DO3A gadolinium complexes has recently been published by Long *et al.*, who found that the kinetic stability of Gd^{III} chelates was substantially dependent upon the nature of appended arms. The effect of the ligand coordination number is not obviously correlated.[43] The strong coordination of pendant arm to Gd^{3+} centre prevents the reduction in kinetic inertness of Gd^{III} complexes caused by the decrease in coordination number. It was also noted that the alkylation of 4^{th} position on cyclen nitrogen with a bulky group could make the ligand backbone less flexible and holds the Gd^{3+} ion in a tighter cavity, leading to an enhancement of kinetic inertness of the chelates. The increase of steric hindrance in the ligand cavity was supported by the reduction in hydration states upon N-alkylation.

1.10 Responsive lanthanide complexes as Sensors

1.10.1 Design Principles

Although different strategies are employed in responsive luminescent lanthanide complexes, the principle behind the design holds true for most notable examples, that is a modulation of sensitisation pathways of Ln^{III} centred emission via external analytes. As depicted in Figure 1-6, three different mechanisms are used to modulate the emission of lanthanide complexes.

The first mechanism involves an analyte that can directly interact with lanthanide ion. In this case, a coordinatively unsaturated chelate is commonly adopted to develop such sensors, and the binding sphere still has coordination sites to bind with water molecules, leading to quenching of luminescence. When these anions replace the binding solvent molecules, the luminescence is modulated, and the lifetime is lengthened simultaneously. In the second mechanism, the analyte may act on the excited states of the chromophore (e.g., singlet or triplet excited states). One way is to quench the singlet state through Photon-induced charge transfer (PeT). Another one is to change the efficiency of the intersystem cross (ISC) by affecting its energy in singlet or triplets. Another method is to direct diminish the triplet excited states, for instance, by O_2. The third mechanism is the analyte can be used as an individual antenna to sensitise the luminescence of Ln^{III} ions. This strategy can be further exploited by preparing a ternary system containing a lanthanide complex (non-luminescent) and analyte (antenna), so that the emissive states of Ln^{III} ion can only be populated once the antenna is bound.

These methods have been utilized in important research on lanthanide complexes in the development of a range of probes for neutral small molecules (O_2, H_2S), anions (F^-, CO_2^{2-}, PO_4^{3-}), cations (Zn^{2+}, K^+, Na^+) and macromolecular biological substrates (DNA, enzyme).

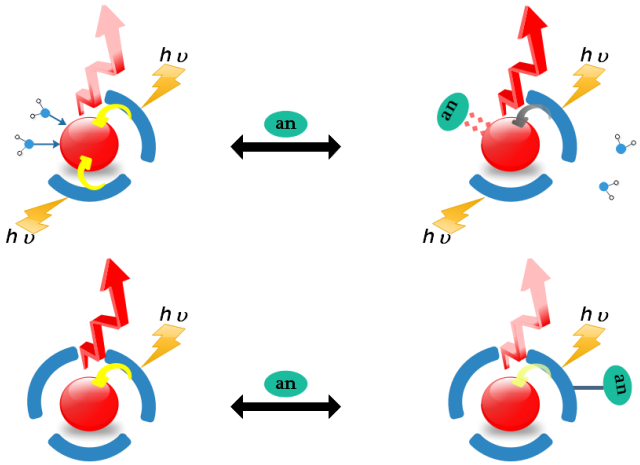


Figure 1-6: Cartoon illustration of modulation of LnIII emission by analyte-binding: (a) analyte directly binding to lanthanide ion, (b)interaction of analyte to the ligand-centred chromophore. [8,44–47]

1.10.2 pH sensors

pH sensors are one of the most important types of Ln^{III}-based luminescent probes. Modulation of lanthanide luminescence can be achieved by disrupting energy transfer pathways to control formation or quenching of the lanthanide excited state, for instance by using protonation events to switch the PeT from a group with a high HOMO like amines on or off.[48] The PeT process is governed by the energy gap between HOMO of PeT switch and singlet excited state (S_1) of an antenna. Upon the photoexcitation of the antenna S_1, the PeT switch transferred an electron to the pair with another unpaired electron in the S_0 state. This process is competitive to other radiative process and ISC process, and consequently, decrease the efficiency of sensitisation, and hence luminescence of Ln^{III} ion ('turn-off' luminescence). In a 'Turn-on' system, chemical reaction between analyte and PeT switch changed the photophysical properties of PeT switch, leading to the decrease in the energy of HOMO, and in turn, recover the sensitisation efficiency of the antenna.

As shown in Figure 1-7 (a), the Eu^{III} phenanthridyl chelate reported by Parker, is an example of a pH sensor. The sensor has a moderate intensity of characteristic Eu^{III} emission at pH around 7, whereas the emission is significantly enhanced by 5-fold when pH is less than 7, as the protonation of phenanthridyl group renders itself a poor PeT donor so that turning off the 'PeT switch'.[8]

Another method to modulate the Ln^{III} centred emission is to change its local symmetry. This method was adopted by Faulkner *et al.* to control self-assembly DO3A derivatives through changes to the pH (Figure 1-7 (b)). The hydration number changes from 2 to 1 and emission enhancement was observed when increasing the pH since, at higher pH, the deprotonation of carboxylbenzyl pendant facilitates the formation of bimetallic self-assembly. [49]

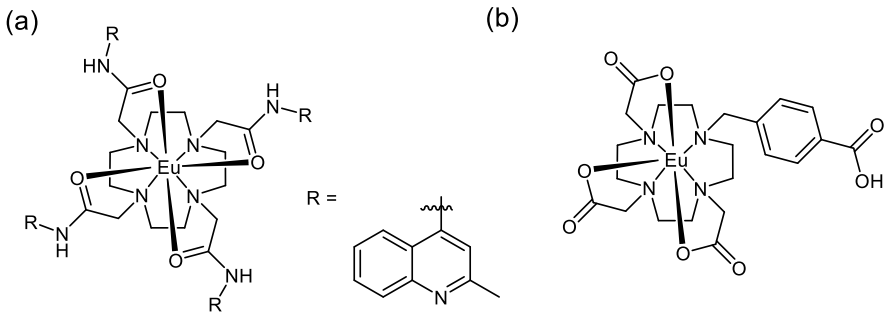


Figure 1-7. Examples of lanthanide complexes that respond to the change in pH.

1.10.3 Anion sensors

As discussed earlier, the lanthanide ion can be treated as a strong Lewis acidic centre. As expected, lanthanide ions have high affinity to anionic species; with the exception of OH^-, which gives rise to the formation of insoluble $Ln(OH)_3$. Nevertheless, we can apply such high affinity of anions into the design of lanthanide-based probe for anion recognition. The

lanthanide ions can be wrapped around by an unsaturated coordination ligand which cannot satisfy the requirement of Ln^{III} coordination (generally 8-9), and the remaining coordination sites are still accessible for binding with an external ligand, in particular, water molecules. Such binding will not lead to the precipitation of lanthanide ions, and such binding will lead to significant changes in spectroscopy, such as enhancement of Ln^{III} luminescence and lifetimes. This type of binding has been broadly applied in designing anion-responsive lanthanide complexes, and several reviews are explicitly addressed the development of such probes by Gunnlaugsson.[50–53]

Generally, the Eu^{III} ion has been most extensively used in such sensing systems since the direct interaction to the metal centre through binding will lead to huge changes in Eu^{III} emission, originating from the interruption of transition from $^5D_0$ to $^7F_2$ states. This transition called 'hypersensitive transition' and its intensity is substantially affected by the symmetry of the Eu^{III} ion and the nature of the ligand. [54] Thus, it reflects the changes in the local coordination environment of Eu^{III}. These kinds of sensors can be fairly useful in probing the presence of halides and carboxylates. As depicted in Figure 1-6, the cartoon illustration demonstrates that this type of sensing is usually reversible and contains competitive binding events. For example, a 'Turn-off' system is a competitive anion displaces the coordinating antenna, where the anion does not contain an antenna, or its excited states cannot effectively sensitise the luminescence of Ln^{III}. Alternatively, this system can be 'Turn-on', for instance, a quenching unit, such as a solvent molecule, is replaced by an anion and such process facilitates the population of Ln^{III} excited states and hence, leads to the enhancement of lanthanide emission.

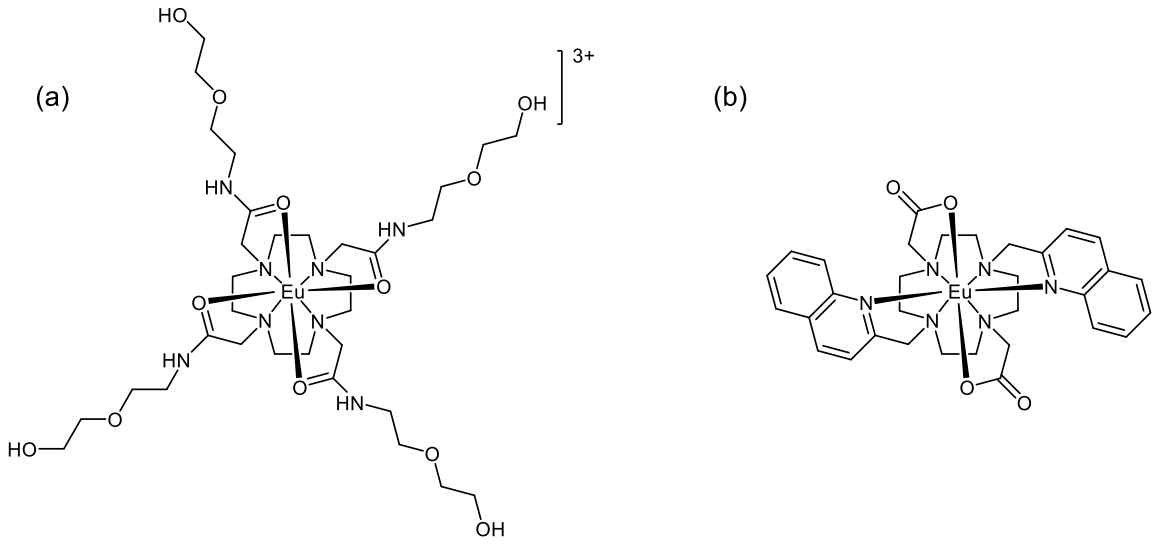


Figure 1-8. examples of lanthanide complexes used as anion sensor; complex (a): left, complex(b): right.

In aqueous solution, most of the lanthanide complexes have a low affinity for halide in exception of fluoride. The complex pictured in Figure 1-8(a), is an eight-coordinate Eu^{III} complex with hydration number q = 1 and can be used as a luminescent reporter for F^-. Upon addition of fluoride a new complex with q = 0 is generated and the intensity of Eu^{III} centred emission is enhanced, indicating the axial coordinating water molecule is replaced by fluoride ions. Another example of a 'turn-on' system is published by Butler, and example are shown in Figure 1-8(b). The complex has C2-symmetry with one positive charge, containing two quinoline antenna, and the intensity of Eu^{III} centred emission undergoes a 9-fold increase upon addition of fluoride. This can be rationalised by the increase in efficiency in sensitisation of Eu^{III} emissive states given by the closer distance between quinoline chromophore and Eu^{III} ion caused by a fluoride-induced hydrogen bond. [55]

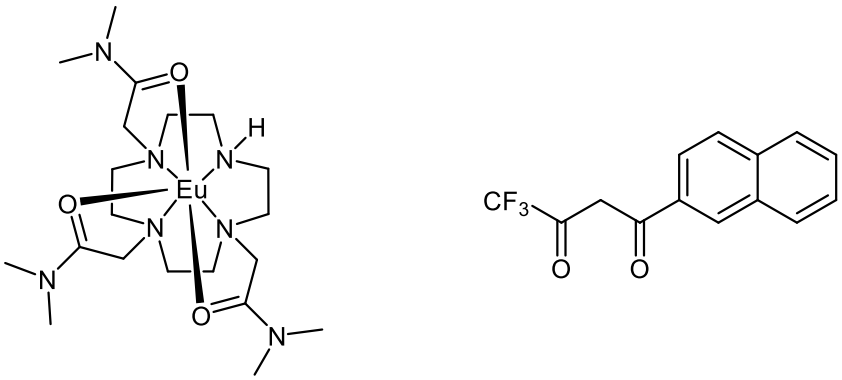


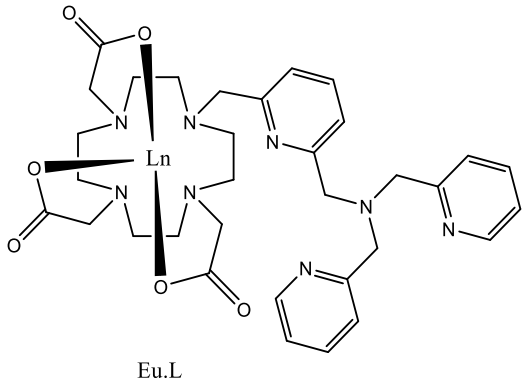
Figure 1-9. example of lanthanide complex used as anion sensor with 'turn-off' emission.

With a carefully designed method, a 'Turn-off' mode has also been developed for sensing anions. In Figure 1-9, the probe has taken advantage of self-assembly between Eu^{III} complex and a β-diketone, where the β-diketone as a chromophore is able to sensitise the Ln^{III} emission efficiently.[78] The introduction of anions will switch off the luminescence of Eu^{III} by displacing the β-diketone antenna with the anion.

1.10.4 Cation sensors

Unlike anion sensing, the requirement for cation sensors is different since they need an appended binding site which is pre-organised for encapsulation of the specific cation. In this case, for group I cations (Na^+, Li^+), crown ether moieties(12-crown-4 for Li^+, 15-crown-5 for Na^+) can be implemented into one of the appended arms of cyclen, to selectively bind these cations. The Tb^{III} complexes pictured in Figure 1-9, show pH-dependent luminescence, and these complexes are responding to the Li^+ and Na^+ ion, their emission is increased in the presence of those cations. In contrast, the emission of copper(II) sensor needs to be turned on under physiological conditions.[79] It is not a surprise that the paramagnetic Cu^{II} ion would reduce the efficiency of energy transfer, leading to the 'turn-

off' of the emission of Eu^{III} ion. Zinc(II) is an important biological role and it participates in many crucial biological activities. Hence, research on developing sensors targeted at this ion has drawn much attention.



Eu.L

Figure 1-9. Representation of DO3A-based lanthanide complex with bis-picolyl capable of sensing Zn^{2+}.

Pope *et al.* reported a novel Zn^{2+} sensor based on the DO3A skeleton[56], where one of the arms is incorporated with zinc sensing moieties (bis-picolyl moiety). Specifically, the Zn^{2+} ions are coordinated to the bis-picolyl moiety, leading to an increase in the characteristic emission of Eu(III) complexes.

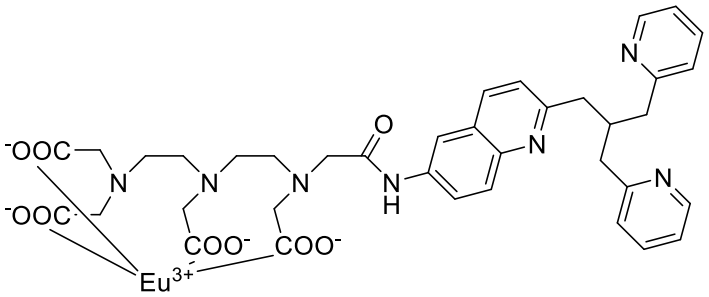


Figure 1-10. Representation of DTPA-based lanthanide complex incorporating with bis-picolyl as Zn^{2+} sensor.

A novel ligand[57] was published by Nanaoka *et al.* where bis-picolyl amines were combined into each side of the DTPA skeleton since the bis-picolyl unit is reported to respond to the presence of Zn^{2+}. Increased intensity in Eu^{III} emission was observed upon the addition of zinc, where the two picolyl units were brought closer to the Eu (III) centre

resulted by the Zn^{2+} ion binding to the ligand, leading to the enhancement in the efficiency of sensitisation of lanthanide luminescence. Also, the similar sensing moiety of Zn^{II} has been adopted into more rigid DO3A framework and the Eu^{III} complexes have been proved to be Zn(II) responsive, both intensities of emission and luminescent lifetime were modulated in the presence of Zn^{II}.

As shown in Figure 1-11, another sensing approach was published by Gunnlaugsson, where a Eu^{III} complex based chemical sensor was able to effectively detect the Fe(III) ion in water. 4,7-diphenyl-1,10-phenanthroline-disulfonate (BPS) showed perfect sensitisation to **Eu**.**1**, giving a strong red emission. The red emission from Eu centre can be "turned off" by displacement of BPS chromophore due to analyte Iron ions present stronger affinity to BPS which leads to the formation of $Fe.BPS_3$. The lack of sensitisation chromophore makes europium less emissive with increasing concentration of Fe^{II}. This "turn-off" system, thus, has provided an effective way to sense the presence of Fe^{II} selectively.

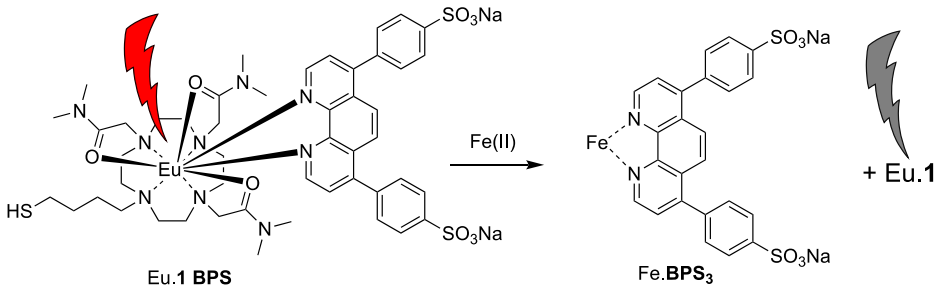


Figure 1-11. graphic representation of the lanthanide complex is capable of sensing Iron(II)[80]

1.10.5 Ratiometric sensing

A fluorescent probe is able to monitor the binding event of an analyte, but not all probes can quantify such change. The vast majority of reported molecular probes, only decrease (fluorolytic) or increase (fluorogenic) the intensity of a luminescent signal. These

fluorolytic or fluorogenic changes have been well established to monitor the qualitative tendency in spectroscopic change, however quantitative information cannot be acquired only if the accurate concentration of the probe itself is known so that the output signal can be calibrated and the concentration quantified. In a biological context, where biodistribution changes with time, such quantification needs to be done at the same time as the measurement.

For this reason, ratiometric sensing is normally difficult to be realised only by a monometallic lanthanide complex; europium complexes offer an exception to this rule since the quadrupolar $^5D_0 \rightarrow {}^7F_2$ transition is hypersensitive to local symmetry. Thus, the intensity ratio of this transition to one of the other $^5D_0 \rightarrow {}^7F_n$ transitions can be used to quantify both probe concentration and response, provided that the analyte is coordinated directly to the lanthanide ion, changing its symmetry and, consequently, changing its shape of the emission profile. In this case, a relationship between the relative intensity of emission spectrum against the concentration of the analyte can be plotted, and this relationship is independent of the concentration of probe solution, thereby allowing ratiometric measurement of the analyte of interest. Parker and Gunlaugsson are the pioneers who first systematically explored such ratiometric probes. [58–62] Alternatively, a method that used a 'cocktail' of europium and terbium complexes has been adapted into ratiometric measurement and has been extensively investigated by Poole *et al.* to develop a luminescent reporter for uric acid. [63] In this mixture, only the emission of Tb^{III} complex is selectively quenched by the uric acid, making such system is efficient to achieve the ratiometric measurement of the analyte of interest (though real-world applications can potentially be compromised if the biodistributions of the two complexes differ. Although the 'cocktail' strategy has good potential as a ratiometric reporter, the influence on the

efficiency of sensitisation of both Eu^{III} and Tb^{III} complexes, resulted by the changes of intrinsic electronic properties of antenna, is also unpredictable.

In summary, two different lanthanide complexes being covalently linked may be more preferable to be used in ratiometric reporting since two lanthanides are sensitised by two different antennas, which will not be affected by the analyte at the same time.

1.10.6 Cyanide sensing [64]

Cyanide is a well-known toxic agent. The presence of cyanide in biologically related environments is a significant cause of concern even at an extremely low level. There are various sources that can produce cyanide in the environment such as biological sources, effluents from industrial processes as well as the combustion of nitrogen-containing polymers. This has raised a non-negligible issue and results in a vast amount of research on developing strategies for the detection of cyanide. The significance of this research has been emphasised by the potential use of cyanide in cyanide-containing nerve agent such as Tabun (GA). [65]

At the outset of this project, lanthanide complexes had not been deployed to sense changes in cyanide concentration. Cyanide does not interact readily with lanthanide ions in water, owing to thermodynamics favouring the hydrated lanthanide ion.

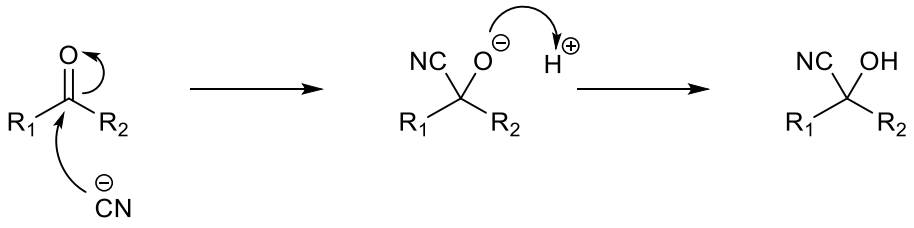
Although a variety of methods have been adopted to sense cyanide including electrochemical, potentiometric and titrimetric methods. Most of these methods require numerous procedures and involve bulky instruments. Among existing methods, optical sensors have been extensively investigated; many of these established optical sensors are based on $BMes_2$ moiety where nucleophilic cyanide attacks the electron-deficient boron centre, resulting in colourimetric changes. These changes originate from the photophysical

changes when undergoing nucleophilic addition, and the sensitivity of detection decreases drastically when performed in polar protic solvent or water due to the reactivity of the boron atom. There is only one exception reported by Gabbaï, a sulfonium borane-based reporter is able to respond to cyanide in pure water with the limit of detecting reaching to 0.2 ppm, however this cyanide responding system does not allow a fast discrimination since the responding time is up to 40 minutes.[66] The signal of cyanide was also interfered by the other competitors (e.g. F^- and OH^-) in the solution due to the high affinity of these anions for $BMes_2$ group. Consequently, such a system is not only compatible under certain pH environment, but also limited in practical analytical applications.

In summary, a prompt and quantitative method to the determination of cyanide in pure water remains an important challenge. [67,68]

1.10.7 Cyanohydrin formation

Cyanohydrin formation occurs when a ketone or aldehyde group, by treating with cyanide ion (normally as KCN), is then converted into cyanohydrin product where a cyano group and a hydroxyl group are bonded to an sp3-hybridised carbon.

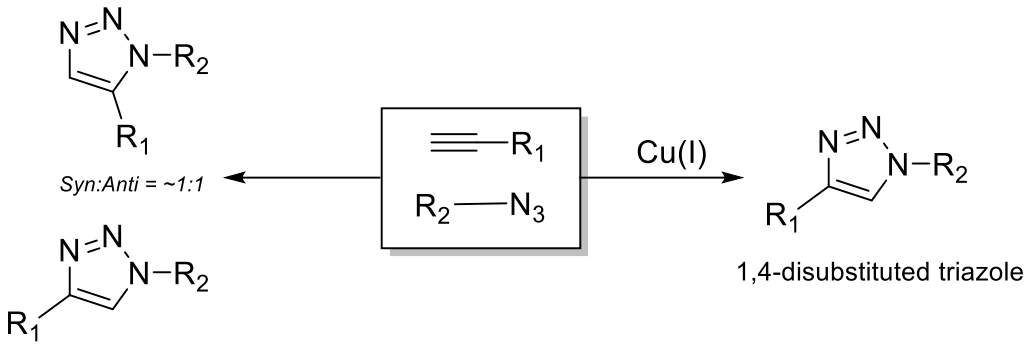


Scheme 1-2. illustration of acid-catalysed cyanohydrin formation

The carbon-based nucleophile CN^- can attack the carbonyl group of aldehydes and ketones where the formation of cyanohydrin is reversible. This process of reaction can be facilitated in the presence of catalytic acid, which can protonate the alkoxide to give the hydroxyl group. Notably, a new C-C σ–bond can be formed in this manner.

1.11 Click reaction

In 2002, the concept of 'click chemistry' first emerged as a synthetic approach in a review by Kolb, Finn and Sharpless. The synthesis of the compound is expected to be simplified via click reaction and thus development in drug discovery could be much faster. The click chemistry, therefore, must contain these characteristics including high yields, modularity, regiospecificity and stereospecificity, wide scope, inoffensive by-product and benign solvent that can be easily removed. There are several chemical reactions identified as 'click' reactions: nucleophilic substitution, Diels-Alder reaction, the addition of carbon double bond, *etc*.[69] Among these click reaction, alkyne and azide cycloaddition is obviously the most prominent example of click chemistry. The synthesis of the alkyne and azide appended with certain function group is relatively easy, given by their stability towards different chemical conditions. Therefore, the synthetic building blocks containing azide and alkyne groups have been widely used in synthetic chemistry. In particular, azide-alkyne coupling reaction can be facilitated by copper(I) catalysis and performed in the presence of water, which was discovered by Sharpless[70], Folkin and Meldal[71]. This novel reaction is extremely advantageous due to no protecting group required and no purification needed, given by the full conversion and high selectivity. This copper(I) catalysed alkyne-azide cycloaddition(CuAAC) has demonstrated great versatility in synthetic chemistry and is regarded as the synonymy of click reaction. [72]



Scheme1- 3. The copper(I) catalysed Huisgen 1,3-dipolar cycloaddition of alkynes and azides. (Right); Non-catalysed alkyne-azide cycloaddition with non-stereoselectivity. (Left)

CuAAC reaction has been broadly employed as a method to prepare supramolecular architecture with a triazole group serving as an anion receptor.[70] Additionally, Paul Beer's group has conducted extensive studies by using a modified CuAAC 'click' reaction to prepare anion responsive interlocked structures containing halogen bonds.[73,74]

CuAAC also provides endless possibilities in the scope of lanthanide chemistry, for preparing multimetallic arrays and interlocked supramolecular lanthanide complexes. The first example that CuAAC was adopted into a lanthanide-containing system was published by Hulme in 2006. The author depicted a copper(I) responsive europium(III) complex with alkyne pendant, where the luminescence of europium(III) ion was significantly enhanced by the azide containing sensitiser in the presence of the catalytic amount of Cu(I).[75]

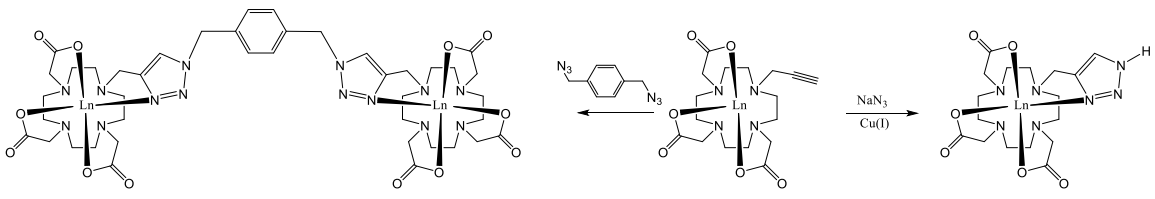


Figure 1-12. Example of the application of CuAAC click reaction on the lanthanide-containing system.

pDO3A, a heptadentate ligand appended with a propargyl arm was first introduced by Lowe and Faulkner in 2009.[76,77] The author described that lanthanide complexes were

used as synthetic precursors to couple with azide containing small molecules via the ‘click’ reaction, leading to dramatic changes in the coordination environment since the triazole group is able to coordinate to the metal centre. These changes can be directly monitored by ^{1}H-NMR and spectroscopic studies upon the formation of click product.

1.12 Project aims

This thesis deals with the development of kinetically stable lanthanide complexes-based luminescent probes for analytical applications, and more specifically for cyanide recognition. The rest of the thesis illustrates how we develop these ideas and prepare the corresponding structures.

Designing analyte responsive complexes has been achieved by different synthetic approaches, given the high lability of Ln(III) ions and versatile ligands for satisfying the requirement of large coordination numbers (CN). We first explored the development of cyanide-responsive monometallic lanthanide complexes with bright emission by employing chromophores containing donor group to the lanthanide centre. Furthermore, the monometallic lanthanide complex was used as a synthetic block to prepare heterobimetallic arrays. Such systems possess a higher binding affinity to cyanide in the pure water and are capable of determining the concentration of cyanide by ratiometric measurement. Thirdly, in a collaboration with Dr Li in the group of Prof. Beer, a novel supramolecular ligand based on rotaxane was developed which complexes lanthanide ions, especially terbium, with relatively strong binding. Lastly, the ligand structure was changed, and the coordination environment was exploited to probe different analytes.

1.13 Reference

[1] J. C. G. Bünzli, C. Piguet, *Chem. Soc. Rev.* **2005**, *34*, 1048–1077.

[2] T. Sagami, Y. O. Tahara, M. Miyata, H. Miyake, S. Shinoda, *Chem. Commun.* **2017**, *53*, 3967–3970.

[3] A. Beeby, I. M. Clarkson, R. S. Dickins, S. Faulkner, D. Parker, L. Royle, A. S. de Sousa, J. A. G. Williams, M. Woods, *J. Chem. Soc. Perkin Trans. 2* **1999**, *39*, 493–504.

[4] G. L. Law, R. Pal, L. O. Palsson, D. Parker, K. L. Wong, *Chem. Commun.* **2009**, *47*, 7321–7323.

[5] B. Song, G. Wang, M. Tan, J. Yuan, *J. Am. Chem. Soc.* **2006**, *128*, 13442–13450.

[6] T. Yoshihara, Y. Yamaguchi, M. Hosaka, T. Takeuchi, S. Tobita, *Angew. Chemie - Int. Ed.* **2012**, *51*, 4148–4151.

[7] S. Faulkner, S. J. A. Pope, B. P. Burton-Pye, *Appl. Spectrosc. Rev.* **2005**, *40*, 1–31.

[8] D. Parker, *Coord. Chem. Rev.* **2000**, *205*, 109–130.

[9] A. De Bettencourt-Dias, P. S. Barber, S. Viswanathan, *Coord. Chem. Rev.* **2014**, *273–274*, 165–200.

[10] F. Gendron, K. Sharkas, J. Autschbach, *J. Phys. Chem. Lett.* **2015**, *6*, 2183–2188.

[11] Á. Canales, Á. Mallagaray, M. Á. Berbís, A. Navarro-Vázquez, G. Domínguez, F. J. Cañada, S. André, H. J. Gabius, J. Pérez-Castells, J. Jiménez-Barbero, *J. Am. Chem. Soc.* **2014**, *136*, 8011–8017.

[12] K. H. Chalmers, E. De Luca, N. H. M. Hogg, A. M. Kenwright, I. Kuprov, D. Parker, M. Botta, J. Ian Wilson, A. M. Blamire, *Chem. - A Eur. J.* **2010**, *16*, 134–148.

[13] C. K. Duan, P. A. Tanner, *J. Phys. Chem. A* **2010**, *114*, 6055–6062.

[14] K. V. R. Chary, A. K. Srivastava, G. C. K. Roberts, L. Guan, H. R. Kaback, *Choice Rev. Online* **2013**, *50*, 50-5926-50–5926.

[15] B. Bleaney, *J. Magn. Reson.* **1972**, *8*, 91–100.

[16] S. Aime, M. Botta, G. Ermondi, *Inorg. Chem.* **1992**, *31*, 4291–4299.

[17] O. A. Blackburn, A. M. Kenwright, P. D. Beer, S. Faulkner, *Dalt. Trans.* **2015**, *44*, 19509–19517.

[18] O. A. Blackburn, N. F. Chilton, K. Keller, C. E. Tait, W. K. Myers, E. J. L. McInnes, A. M. Kenwright, P. D. Beer, C. R. Timmel, S. Faulkner, *Angew. Chemie - Int. Ed.* **2015**, *54*, 10783–10786.

[19] M. E. Boulon, G. Cucinotta, J. Luzon, C. Degl'Innocenti, M. Perfetti, K. Bernot, G. Calvez, A. Caneschi, R. Sessoli, *Angew. Chemie - Int. Ed.* **2013**, *52*, 350–354.

[20] J. D. Rinehart, J. R. Long, *Chem. Sci.* **2011**, *2*, 2078–2085.

[21] D. Parker, H. Puschmann, A. S. Batsanov, K. Senanayake, *Inorg. Chem.* **2003**, *42*, 8646–8651.

[22] J. W. Walton, L. Di Bari, D. Parker, G. Pescitelli, H. Puschmann, D. S. Yufit, *Chem. Commun.* **2011**, *47*, 12289–12291.

[23] M. R. Spirlet, J. Jean Rebizant, J. F. Desreux, M. F. Loncin, *Inorg. Chem.* **1984**, *23*, 359–363.

[24] P. Lebduková, P. Hermann, L. Helm, É. Tóth, J. Kotek, K. Binnemans, J. Rudovský, I. Luke, A. E. Merbach, *Dalt. Trans.* **2007**, 493–501.

[25] S. Aime, M. Botta, M. Fasano, M. P. M. Marques, C. F. G. C. Geraldes, D. Pubanz, A. E. Merbach, *Inorg. Chem.* **1997**, *36*, 2059–2068.

[26] S. Aime, A. Barge, M. Botta, M. Fasano, J. Danilo Ayala, G. Bombieri, *Inorganica Chim. Acta* **1996**, *246*, 423–429.

[27] S. Aime, A. Barge, M. Botta, A. S. De Sousa, D. Parker, *Angew. Chemie - Int. Ed.* **1998**, *37*, 2673–2675.

[28] O. T. Benfey, *J. Chem. Educ.* **2009**, *35*, 21.

[29] C. J. Pedersen, *J. Am. Chem. Soc.* **1967**, *89*, 7017–7036.

[30] J. D. J. Backer-Dirks, C. J. Gray, F. A. Hart, M. B. Hursthouse, B. C. Schoop, *J. Chem. Soc. Chem. Commun.* **1979**, 774–775.

[31] A. D. Sherry, P. Caravan, R. E. Lenkinski, in *J. Magn. Reson. Imaging*, **2009**, pp. 1240–1248.

[32] K. Micskei, D. H. Powell, L. Helm, E. Brücher, A. E. Merbach, *Magn. Reson. Chem.* **1993**, *31*, 1011–1020.

[33] P. Hermann, J. Kotek, V. Kubíček, I. Lukeš, *Dalt. Trans.* **2008**, 3027–3047.

[34] V. Comblin, D. Gilsoul, M. Hermann, V. Humblet, V. Jacques, M. Mesbahi, C. Sauvage, J. F. Desreux, *Coord. Chem. Rev.* **1999**, *185–186*, 451–470.

[35] E. Brücher, I. Lázár, I. Tóth, *Inorg. Chem.* **1994**, *33*, 4070–4076.

[36] J. Moreau, E. Guillon, J. C. Pierrard, J. Rimbault, M. Port, M. Aplincourt, *Chem. - A Eur. J.* **2004**, *10*, 5218–5232.

[37] É. Tóth, R. Király, J. Platzek, B. Radüchel, E. Brücher, *Inorganica Chim. Acta* **1996**, *249*, 191–199.

[38] J. M. Idée, M. Port, I. Raynal, M. Schaefer, S. Le Greneur, C. Corot, *Fundam. Clin. Pharmacol.* **2006**, *20*, 563–576.

[39] H. H. Sandsted, W. Au, *Handb. Toxicol. Met.*, Elsevier, **2007**, pp. 925–947.

[40] E. Brücher, P. Szarvas, *Inorganica Chim. Acta* **1970**, *4*, 632–636.

[41] L. Sarka, L. Burai, E. Brücher, *Chem. - A Eur. J.* **2000**, *6*, 719–724.

[42] L. Sarka, L. Burai, R. Király, L. Zékány, E. Brücher, *J. Inorg. Biochem.* **2002**, *91*, 320–326.

[43] T. J. Clough, L. Jiang, K. L. Wong, N. J. Long, *Nat. Commun.* **2019**, *10*, DOI 10.1038/s41467-019-09342-3.

[44] A. J. Moro, P. J. Cywinski, S. Körsten, G. J. Mohr, *Chem. Commun.* **2010**, *46*, 1085–1087.

[45] A. Bourdolle, M. Allali, J. C. Mulatier, B. Le Guennic, J. M. Zwier, P. L. Baldeck, J. C. G. Bünzli, C. Andraud, L. Lamarque, O. Maury, *Inorg. Chem.* **2011**, *50*, 4987–4999.

[46] S. Griesbeck, Z. Zhang, M. Gutmann, T. Lühmann, R. M. Edkins, G. Clermont, A. N. Lazar, M. Haehnel, K. Edkins, A. Eichhorn, et al., *Chem. - A Eur. J.* **2016**, *22*, 14701–14706.

[47] O. A. Blackburn, M. Tropiano, L. S. Natrajan, A. M. Kenwright, S. Faulkner, *Chem. Commun.* **2016**, *52*, 6111–6114.

[48] T. Gunnlaugsson, D. A. Mac Dónaill, D. Parker, *J. Am. Chem. Soc.* **2001**, *123*, 12866–12876.

[49] S. Faulkner, B. P. Burton-Pye, *Chem. Commun.* **2005**, 259–261.

[50] O. Kotova, S. Comby, T. Gunnlaugsson, *Chem. Commun.* **2011**, *47*, 6810–6812.

[51] J. P. Byrne, M. Martínez-Calvo, R. D. Peacock, T. Gunnlaugsson, *Chem. - A Eur. J.* **2016**, *22*, 486–490.

[52] S. E. Plush, T. Gunnlaugsson, *Org. Lett.* **2007**, *9*, 1919–1922.

[53] L. K. Truman, S. Comby, T. Gunnlaugsson, *Angew. Chemie - Int. Ed.* **2012**, *51*, 9624–9627.

[54] K. Binnemans, *Coord. Chem. Rev.* **2015**, *295*, 1–45.

[55] S. J. Butler, *Chem. Commun.* **2015**, *51*, 10879–10882.

[56] S. J. A. Pope, R. H. Laye, *Dalt. Trans.* **2006**, 3108–3113.

[57] K. Hanaoka, K. Kikuchi, H. Kojima, Y. Urano, T. Nagano, *J. Am. Chem. Soc.* **2004**, *126*, 12470–12476.

[58] E. M. Surender, S. J. Bradberry, S. A. Bright, C. P. McCoy, D. Clive Williams, T. Gunnlaugsson, *J. Am. Chem. Soc.* **2017**, *139*, 381–388.

[59] L. K. Truman, S. Comby, T. Gunnlaugsson, *Angew. Chemie - Int. Ed.* **2012**, *51*, 9624–9627.

[60] C. M. G. Dos Santos, T. Gunnlaugsson, *J. Chem. Soc. Dalt. Trans.* **2009**, *21*, 4712–4721.

[61] C. P. Montgomery, B. S. Murray, E. J. New, R. Pal, D. Parker, *Acc. Chem. Res.* **2009**, *42*, 925–937.

[62] E. R. H. Walter, J. A. G. Williams, D. Parker, *Chem. Commun.* **2017**, *53*, DOI 10.1039/c7cc08361k.

[63] R. A. Poole, F. Kielar, S. L. Richardson, P. A. Stenson, D. Parker, *Chem. Commun.* **2006**, 4084–4086.

[64] S. Y. Huang, V. C. Pierre, *Chem. Commun.* **2018**, *54*, 9210–9213.

[65] R. Misra, T. Jadhav, B. Dhokale, S. M. Mobin, *Dalt. Trans.* **2015**, *44*, 16052–16060.

[66] Y. Kim, H. Zhao, F. P. Gabbai, *Angew. Chemie - Int. Ed.* **2009**, *48*, 4957–4960.

[67] T. B. Wei, X. Bin Cheng, H. Li, Q. Lin, H. Yao, Y. M. Zhang, *Supramol. Chem.* **2016**, *28*, 913–920.

[68] T. B. Wei, X. Bin Cheng, H. Li, Q. Lin, H. Yao, Y. M. Zhang, *Supramol. Chem.* **2016**, *28*, 913–920.

[69] J. E. Moses, A. D. Moorhouse, *Chem. Soc. Rev.* **2007**, *36*, 1249–1262.

[70] V. V. Rostovtsev, L. G. Green, V. V. Fokin, K. B. Sharpless, *Angew. Chemie - Int. Ed.* **2002**, *41*, 2596–2599.

[71] C. W. Tornøe, C. Christensen, M. Meldal, *J. Org. Chem.* **2002**, *67*, 3057–3064.

[72] V. D. Bock, H. Hiemstra, J. H. van Maarseveen, *European J. Org. Chem.* **2006**, *2006*, 51–68.

[73] S. W. Robinson, C. L. Mustoe, N. G. White, A. Brown, A. L. Thompson, P. Kennepohl, P. D. Beer, *J. Am. Chem. Soc.* **2015**, *137*, 499–507.

[74] M. J. Langton, Y. Xiong, P. D. Beer, *Chem. - A Eur. J.* **2015**, *21*, 18910–18914.

[75] R. F. H. Viguier, A. N. Hulme, *J. Am. Chem. Soc.* **2006**, *128*, 11370–11371.

[76] M. Jauregui, W. S. Perry, C. Allain, L. R. Vidler, M. C. Willis, A. M. Kenwright, J. S. Snaith, G. J. Stasiuk, M. P. Lowe, S. Faulkner, *Dalt. Trans.* **2009**, 6283.

[77] G. J. Stasiuk, M. P. Lowe, *Dalt. Trans.* **2009**, 9725–9727.

[78] A. W. Woodward, A. Frazer, A. R. Morales, J. Yu, A. F. Moore, A. D. Campiglia, E. V. Jucov, T. V. Timofeeva, K. D. Belfield, *Dalt. Trans.* **2014**, *43*, 16626–16639.

[79] S. J. A. Pope, R. H. Laye, *Dalt. Trans.* **2006**, 3108–3113.

[80] H. M. Burke, T. Gunnlaugsson, E. M. Scanlan, *Chem. Commun.* **2015**, *51*, 10576–10588.

2 Study of 4'-substituted PhenacylDO3A complex as Cyanide Sensor[I]

2.1 Introduction

As we have already seen, a variety of methods have been developed to sense cyanide, and most of these are dependent on the interaction between the cyanide ion and a Lewis acidic centre, where boron-containing moieties are commonly adopted as a receptor, thus making detection of cyanide difficult in competitive solvents. The development of cyanide responsive systems in aqueous phase remains to be addressed since the effective method to detect the presence of cyanide in pure water is rare.

Luminescent lanthanide complexes have been extensively exploited as analytical tools for a variety of anions (e.g., halides[1], nitrate[2], phosphate[2], hydrogen sulfide[3]) and as luminescent tags to provide optical contrast. Thus, the general characteristics of luminescent lanthanide complexes provide numerous possibilities for the design of cyanide sensors in aqueous media. As discussed earlier, luminescent Ln^{III} complexes are remarkably sensitive to the changes in sensitisation pathway and coordination environment, leading to a great variation in the luminescent lifetime and quantum yield. Their long lifetime is one of their most essential properties for optical probes; luminescent lanthanide complexes are particularly valuable since their long-lived emission selectively collected by using time-gating instruments to eliminate the signal from background (typically, the

[I] Aspects of my work summarised in this chapter have been already published: see: J.D. Routledge, X. Zhang, M. Connolly, M. Tropiano, O. A. Blackburn, A. M. Kenwright, P. D. Beer, S. Aldridge and S. Faulkner, *Angew. Chemie - Int. Ed.*, 2017, **56**, 7783–7786.

luminescent lifetime of biological tissue is in order of nanoseconds)[4] and hence, the sensitivity of detection can be further enhanced. Lifetime is also a useful parameter for developing lanthanide complexes as analytical probes, since, from lifetime, we can obtain more information on changes in the local environment and thus the analyte of interest.

For most Ln^{III} complexes, sensitisation of emission is achieved by transferring energy from triplet excited states of the antenna to emissive excited states of Ln^{III} ion. The quantum yield is predominantly decided by the effectiveness of sensitisation, which is greatly dependent on the distance between the antenna and Ln^{III} ion. Additionally, two possible mechanisms are normally used to describe the energy transfer: Forster (through-space) or Dexter (through-bond). Faulkner has previously demonstrated that the energy transfer is generally dominated by the Dexter exchange mechanism when there is a through-bond pathway available, and that the Dexter mechanism is generally more effective than Forster mechanism, where the latter is normally unfavourable given by the limited spectral overlap between emission spectra of chromophore and absorption spectra of lanthanide(III) ion. [5,6]

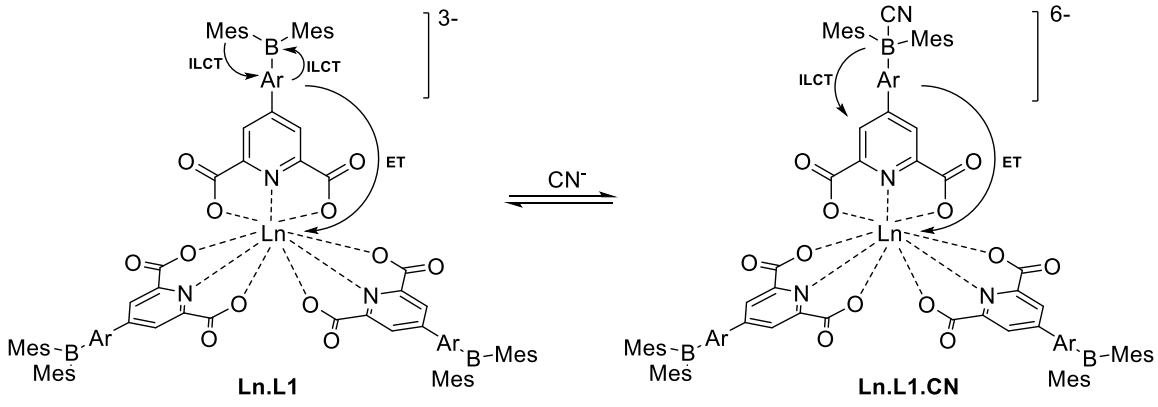


Figure 2-1. Example of a lanthanide complex that can respond to the presence of cyanide.[14]

Wang et al. prepared a triarylboron-based lanthanide complex that responds to the cyanide and fluoride ions.[7] A reduction in the intensity of emission was observed upon addition of

cyanide or fluoride. However, this system can only be effective in detecting cyanide or fluoride in non-competitive media such as THF, and the complex is not very kinetically inert in the presence of nucleophilic anions, leading to the demetallation of the complex. Besides, this lanthanide complex-based probe showed no selectivity in cyanide given by the high reactivity of Lewis acidity of boron centre. These two reasons make this probe unusable in practical applications, for instance, cyanide in the industrial effluent.

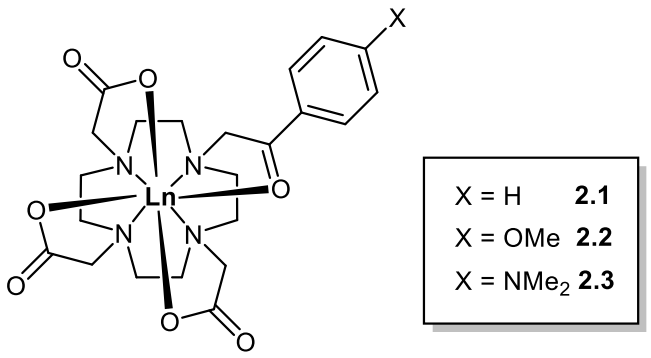


Figure2-2. Pictorial representation of phenacyl-containing DO3A lanthanide complexes. (Ln = **Eu**, **Tb**, **Yb**)

In this chapter, phenacylDO3A lanthanide complexes with different halogen atoms were selected to investigate the effect of cyanide on their photophysical properties. As shown in Figure 2-1, the phenacyl group is a good chromophore that can effectively sensitise Ln^{III} emission. The influence of *para*-substituents on phenacylDO3A lanthanide complexes has been addressed by Gareth Williams et al.[8] The unsubstituted phenacyl **2.1** ligand and methoxyl-substituted phenacyl **2.2** ligands can both effectively sensitise the emission of Eu^{III} in water, whereas the lanthanide complex with dimethylamino-phenacyl ligand **2.3** found to be strongly dependent on the solvent with no detectable emission in aqueous solution.[8]

In the phenacylDO3A complex, the metal ion is coordinated by a carbonyl oxygen atom on the phenacyl group. Such coordination can provide a through-bond energy transfer

pathway, thus facilitating the energy transfer from the antenna to Ln^{III} ion. Meanwhile, the carbonyl group is polarised by the coordination, resulted from the strong electropositive lanthanide(III) ion, and thus it becomes more feasible to attack by nucleophilic cyanide. Such nucleophilic attack has the potential to disturb the behaviour of the chromophore by removing the prospect of transferring energy via the Dexter mechanism (through-bond), thereby modifying the effectiveness of sensitisation of Ln^{III} emissive states. Although the cyanohydrin formation has been previously adapted into the development of cyanide-responsive devices, its usage with lanthanide-containing system provides a novel method to detect cyanide by eliciting the luminescent response.

Overall, it is of crucial significance to selectively detect cyanide in the application of chemical warfare agent detection and environment-related samples such as groundwater or biological sources.[15] This strategy proved effective, and lanthanide complexes can be exploited as an excellent analytical tool in selectively detecting cyanide in water. In the remainder of this chapter, my work on this topic is explored in detail.

2.2 Synthesis

Figure 2-3 shows how the key complexes were prepared, incorporating an aryl ketone coordinating to the metal centre, thus giving rise to an octadentate phenacylDO3A ligand. Such direct coordination offers a possible through-bond pathway which enhances the effectiveness of energy transfer from the antenna to metal ion. 2-Bromo-4'-fluoroacetophenone and 2,4'-dibromoacetophenone used were commercially available.

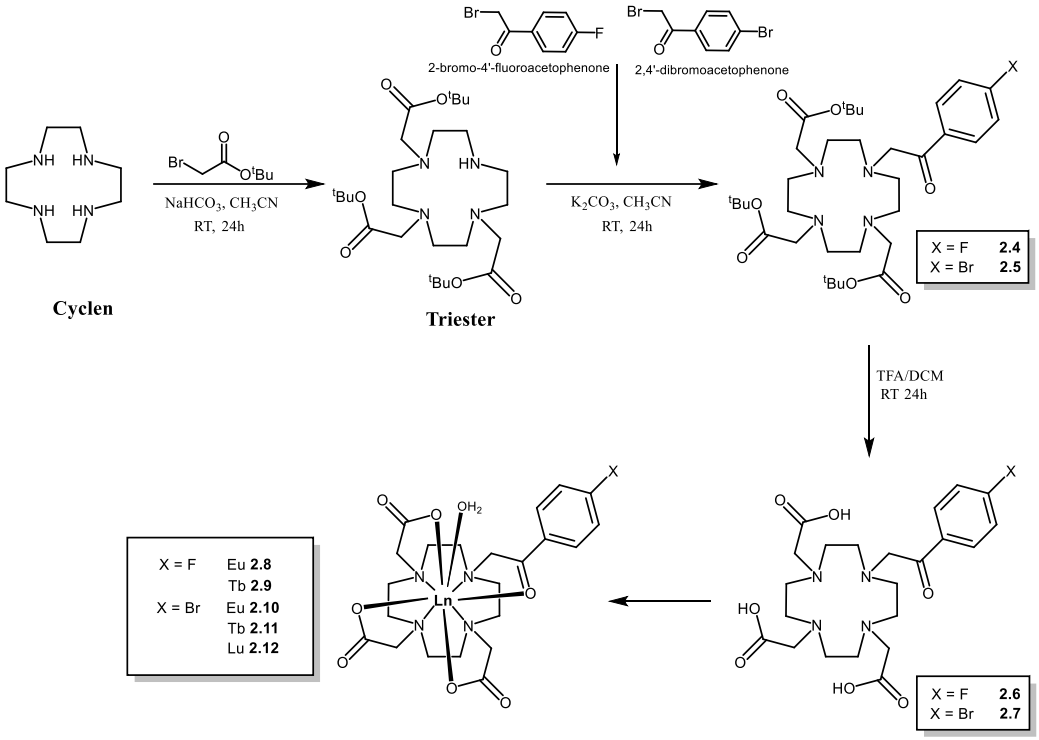


Figure 2-3. Synthetic routes of preparation of halogenated-phenacylDO3A lanthanide complexes.

The fourth nitrogen of the triester was alkylated under the same condition by using the standard procedure. The crude product was purified by flash silica gel column chromatography to give pure protected ligands. The deprotection of *tert*-butyl groups was achieved by treating with trifluoroacetic acid in dichloromethane, and the corresponding ligands were obtained in quantitative yield. The lanthanide complexes were prepared by mixing the ligand with the corresponding lanthanide triflates in MeOH and stirring for 72 hours.

2.3 NMR spectroscopy characterisation

The ^{1}H-NMR spectrum of europium complex **2.8** exhibited similar NMR profile compared to DO3A europium analogues with highly-shifted resonance peaks, as shown in Figure 2-4. The relatively sharp peaks imply the complex is an eight-coordinate complex where the

ketone is actively engaged in the coordination. The four main resonances between 25 and 35 ppm show four different proton environments on the macrocycle backbone, indicating the square antiprismatic (SAP) geometry predominates, whereas the resonances from the twisted squared antiprismatic (TSAP) have much lower chemical shifts. The predominance can be attributed to the strong ligand field formed by four oxygen donors. The favoured SAP geometry could be accounted by the free arm rotation is hindered by coordination of the bulky phenacyl group. Similar phenomena can be seen in the ^{1}H-NMR spectrum of **2.10** suggesting both europium(III) complexes (**2.8** and **2.10**) adopted very similar structures in solution. Furthermore, the ^{1}H-NMR spectra of **2.8** and **2.10** have similar profiles, indicating that the effect of different halogen substituents on the coordination environment is insignificant.

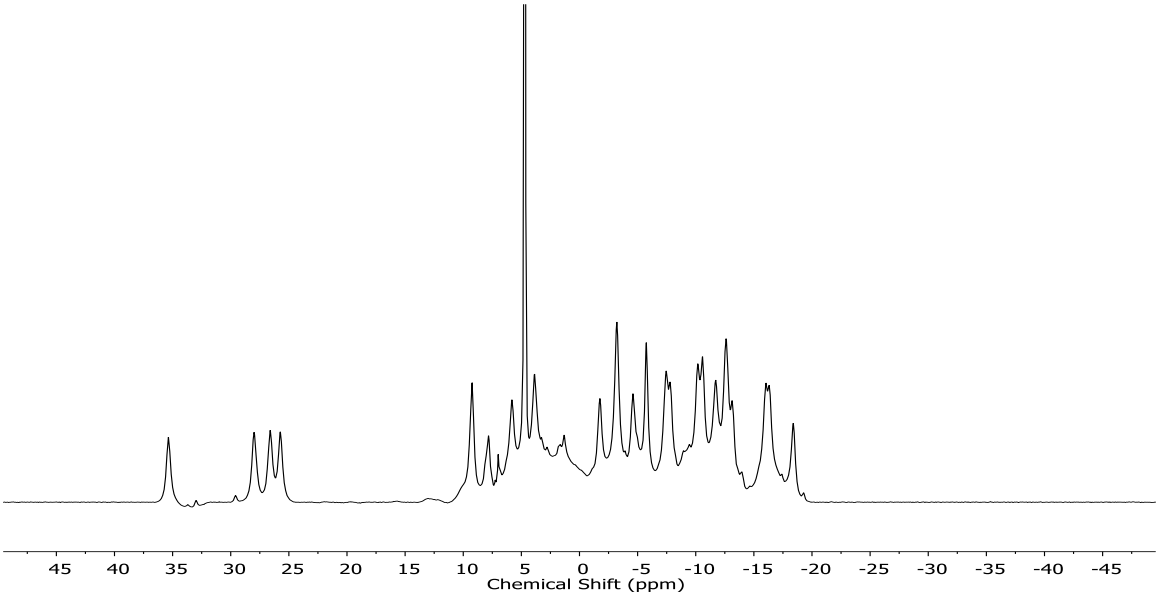


Figure 2-4. The ^{1}H-NMR spectrum of lanthanide complex **2.8** registered in D_2O.

The ^{1}H-NMR spectrum of the terbium(III) complex **2.9** also exhibits sharp resonance peaks. It is notable that there is a different contribution to the paramagnetic shift (cf. δ -250 to +410 ppm for the terbium complex of DOTA)[9]. This may indicate that there is a different

contribution of the contact (through bond) shift in this system, since geometric factors would usually mean that the pseudocontact term leads to a greater magnitude of low field shifts.

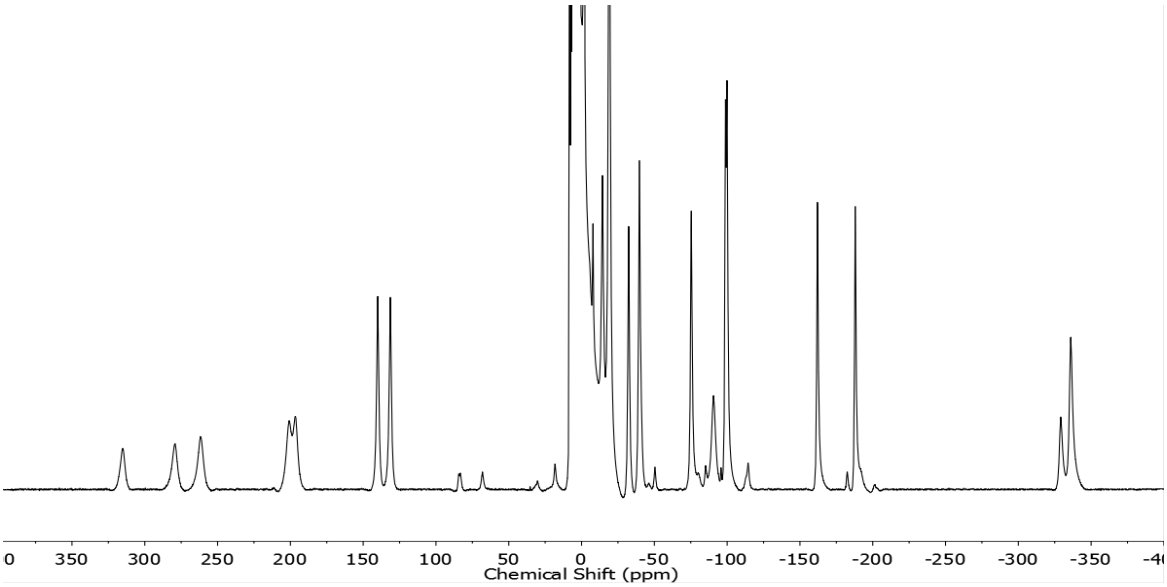


Figure 2-5. The ^{1}H-NMR spectrum of terbium(III) complex **2.9** registered in D_2O.

2.4 Photophysical studies

Photophysical studies of europium(III) and terbium(III) complexes were carried out by UV-Vis absorption and luminescence spectroscopy with time-gating techniques. When comparing the UV-Visible spectra of ligand **2.7** and Eu^{III} complex **2.10**, The absorption spectrum of ligand demonstrated a broad band with maxima centred at 250 nm in water solution which is corresponding to the ILCT transition originating from aromatic phenacyl moiety. A bathochromic shift was observed with the maximum absorption at 272 nm upon binding with europium ion, thus suggesting that there is an interaction between ligand and metal. The large redshift can be attributed to the strong coordination of carbonyl oxygen to Lewis acidic metal ion. The similar phenomenon was also observed in the bromo-

substituted analogues in the photophysical studies implying ILCT transition dominates the sensitisation mechanism.

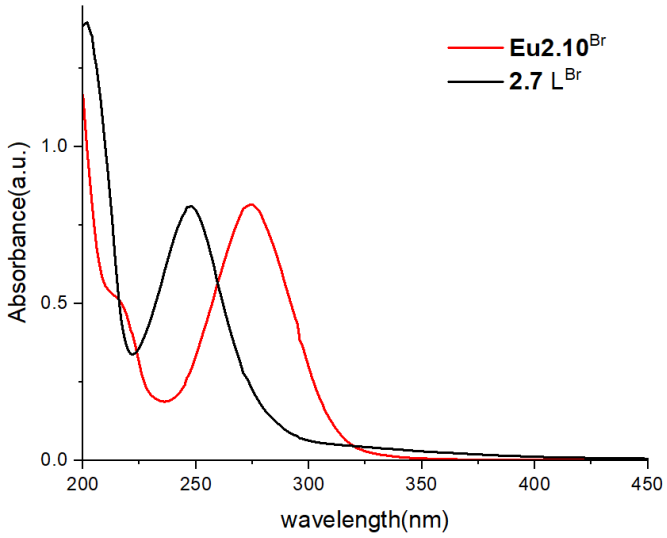


Figure 2-6. Comparison of the UV-Vis absorption spectra of ligand **2.7** (black) and europium complex **2.10** in H_2O.

The UV-Vis absorption spectra of ligand **2.7** and corresponding complex **2.10** are shown in Figure 2-6. The presence of a broad band centred at 249 nm in the ligand absorption spectrum is ascribable to the ILCT transition of aromatic phenacyl moiety. Upon complexation there is a significant bathochromic shift of ILCT band in the absorption spectrum, suggesting the ligand becomes more stabilised when binding to lanthanide(III) ion. This confirms the assumption that the carbonyl oxygen is coordinated to the metal centre, given by the strong Lewis acidity of trivalent lanthanide ion and electron-donating ability of the carbonyl group. Coordination to the Ln^{3+} ion polarises the carbonyl group, stabilising the charge induced by $n \rightarrow \pi^*$ transition and hence lowering its energy lowered. All phenacyl-containing lanthanide complexes have a redshift of approximately 16 nm compared to corresponding ligands, it is indicative that the interaction between the metal ion and carbonyl oxygen are similar in intensity.

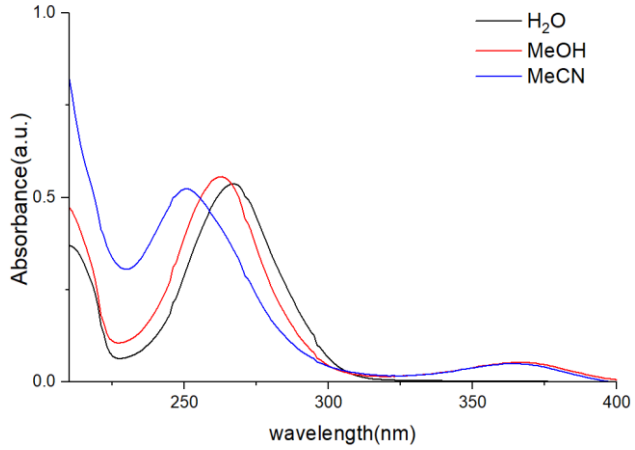


Figure 2-7. UV-Vis absorption spectra of complex **2.10** in the solvent with increasing polarity.

Intraligand charge transfer normally occurs between electron-rich and electron-deficient moieties of the ligand. For the phenacyl ligand, the position of ILCT band should be predominantly dependent on the solvent polarity due to the LUMO of donor moiety being more polar than HOMO of the acceptor. The UV-Vis spectrum of complexes **Eu2.10^{Br}** in solvents with different polarity was recorded in Figure 2-7, thus suggesting the nature of charge transfer can be confirmed. As can be seen in the spectrum, the ILCT band experienced a redshift when increasing the polarity of the solvent resulted from the increase in the stabilisation of excited states of ILCT band.

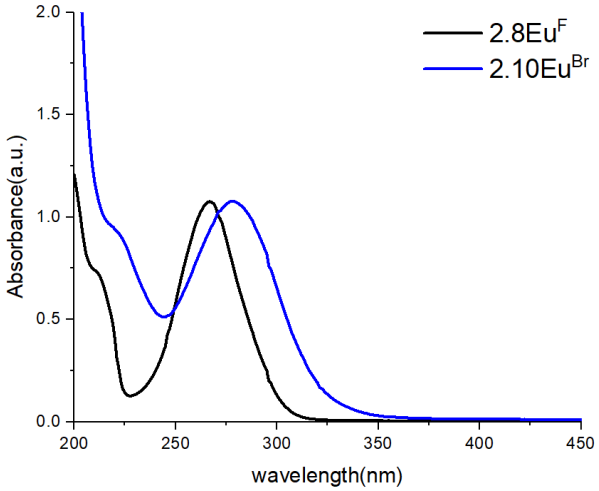


Figure 2-8. Comparison of the UV-Vis absorption spectra of europium complex **2.8** (black) and europium complex **2.10** (blue) in H_2O.

The UV-Vis absorption spectrum of europium(III) complexes of halogenated phenacylDO3A ligands is shown in Figure 2-8. An obvious redshift can be observed upon increasing the electron-donating ability of substituent. Thus this behaviour can be assumed, hypothetically, this 'mesomeric effect' of halogen substituents (see Figure 2-8), as shown in the UV-Vis absorption spectrum, can be explained by the different of electron-donating ability in the excited states in the order of Br > F.[10] The pictorial representation of ILCT state illustrate that the electronegativity of halogen atom has a profound effect on the interaction between the ketone and the lanthanide ion; making the ketone group more likely to be attacked by the nucleophile and the cyanohydrin production more stable. As shown in Figure 2-8, the C-Br bond makes a greater contribution to the corresponding excited states of phenacyl group, where the stabilisation of excited states is facilitated by the polar solvent of water, thus leading to a smaller gap between excited states and ground states and absorption in longer wavelength.

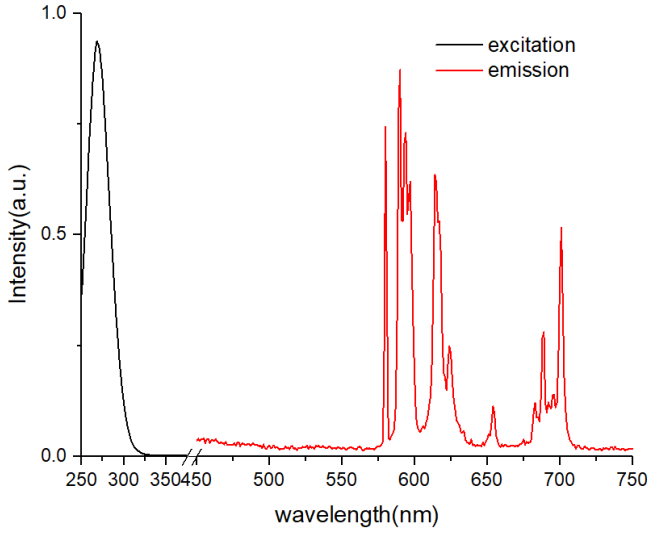


Figure 2-9. Excitation (black line) and emission (red line) of Eu(III) complex **2.8**.

The luminescence spectrum of Eu^{III} complex **2.8** is represented in Figure 2-9. The excitation spectra showed a broad band centred at around 275 nm and the overlap between absorption (Figure 2-9) and emission, indicating the sensitisation of europium^{III} emissive states is taking place at the phenacyl group. It worth noting that an intense $^5D_0 \rightarrow {}^7F_0$ transition is observed, which is indicative that the complex in solution is predominated by one isomer. Furthermore, no fluorescence band originating from of chromophore can be observed, suggesting the energy transfer triplet excited states of the chromophore to Eu^{III} emissive states is effective. To confirm this, the energy of the triplet excited state of organic chromophore was determined from the gadolinium(III) species (Figure2-10). The energy of gadolinium(III) excited states are much higher than that of ligand, and the emission originating from chromophore triplet can be recorded. From Figure 2-10 the triplet energy of ligand **2.6** is around 22200 cm^{-1}. The energy of acceptor states of Eu^{III} ($^5D_0$) and Tb^{III} ($^5D_4$) is 17200 cm^{-1} and 20500 cm^{-1}, respectively. Thus, the possibility of back energy transfer from europium(III) to the antenna can be ruled out, hence this mismatch in energy level makes repopulation of Eu^{III} emissive states by back-energy transfer impossible.

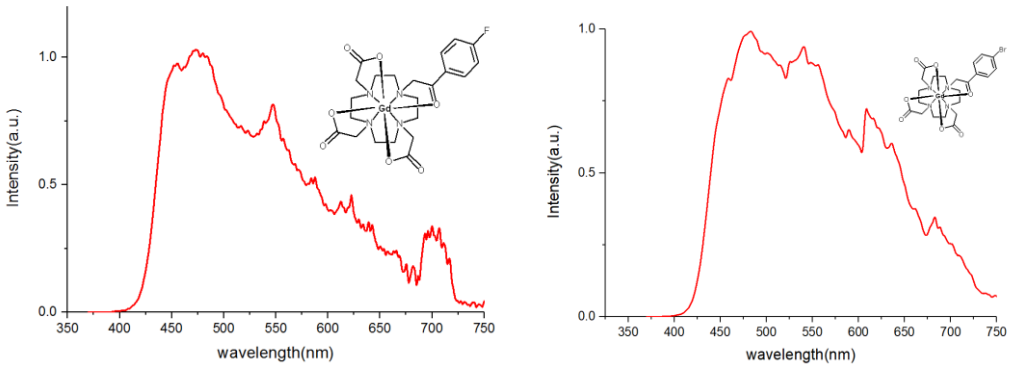


Figure 2-10. Phosphorescence spectrum of Gadolinium complex with fluoro-acetophenone pendant arm (left) and bromo-acetophenone pendant (right).

The hydration number for both europium(III) complexes prepared further proved that the lanthanide metal is wrapped by an octadentate ligand with only one water molecule saturating the coordination sphere. The terbium(III) complex **Tb2.9^{F}** also exhibited strong characteristic emission with lifetime close to one, further indicating the carbonyl oxygen is strongly coordinated to the metal. However, **Tb2.11^{Br}** exhibited a much shorter lifetime in both water and deuterium oxide compared to **Tb2.9^{F}**. This can result from the back-energy transfer from Tb^{III} emissive states to chromophore given by the lower triplet energy of ligand, or the quenching of Tb^{III} emissive states by low-energy ILCT states. However, verification of these hypotheses requires more photophysical investigation, the validation of these hypotheses is outside the scope of this work and hence has not been conducted.

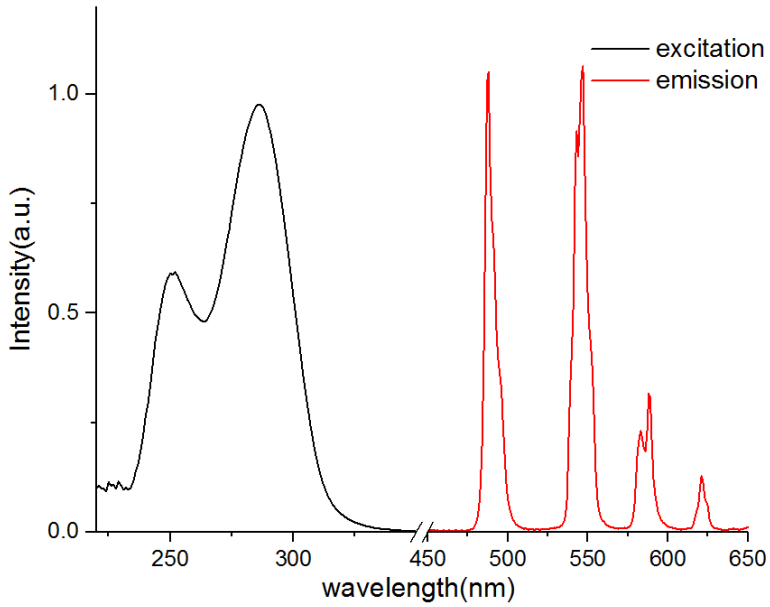


Figure 2-11. Excitation (black line) and emission (red line) of Tb(III) complex **2.9**.

The number of inner-sphere water molecule coordinated to the metal ion was calculated by using the Horrocks' equation, as summarised in Table 2-1. These results suggest that the coordination number of all complexes are nine with one water molecule in the axial position.

Table 2-1. Photophysical properties of 4'-substituted phenacylDO3A lanthanide complexes in aqueous solution.

	τ_{H2O}/ms	τ_{D2O}/ms	*q*
2.8 Eu	0.62	2.16	1.1[±0.1]
2.9 Tb	1.70	2.59	1.0[±0.2]
2.10 Eu	0.61	2.52	1.2[±0.1]
2.11 Tb	1.76	2.90	1.1[±0.1]

2.5 Fluoride and Cyanide binding of tetra-amide terbium complex

Although excess fluoride(32-64mg/kg) can cause significant health issues such as organ failure, a small amount of fluoride can beneficial to the growth of bones and prevent teeth decay. Nevertheless, the intrinsic function of fluoride in bone reproduction has not been well-established. The maximum recommended daily allowance of fluoride is 0.05mg/kg as published by WHO. Bearing this in mind, the development of analytical tools for fluoride has drawn much attention over the last decades, and the development of a quantitative luminescence probe has become important research. The presence of other competitors such as hydroxide and chloride make detection of fluoride in water is challenging. Luminescent lanthanide complexes are advantageous in the development of fluoride probe due to the nature of Lewis acidic lanthanide(III) centre and long luminescence lifetimes. Besides, only the fluoride ion can displace the axial coordinated water molecule of closed-shell lanthanide complexes, giving rise to greater selectivity over other competitive halogen atoms in water.

Many reported probes cannot effectively detect the fluoride in pure water and the majority of them can only be used in the nonpolar organic solvent.[1] The emergence of luminescent lanthanide complexes provide great water solubility and has been extensively investigated for the development of fluoride detection. For instance, bis-quinoline containing europium complexes reported by Butler for the strong binding with fluoride in water. The author reasoned that fluoride can be bind with electron-deficient quinoline moieties via hydrogen bonding, which greatly contributes to the overall fluoride binding performance.

This section describes an investigation of the interaction between a tetra-amide lanthanide complex and fluoride and cyanide ions in water. We have already explored the binding of fluoride to lanthanide tetra-amide complexes, and shown that axial fluoride binding can have profound effects on the local crystal field and, more importantly, on the spectroscopic behaviour of the lanthanide. [13]

Luminescence studies and NMR spectroscopy were used to examine both fluoride and cyanide binding in comparison with phenacylDO3A analogues. We carried out this study on the basis that fluoride is able to coordinate to lanthanides in water, while cyanide is not, reasoning that tetraamide complexes should respond only to fluoride.

Four tryptophan moieties were covalently linked to cyclen macrocycle and the corresponding lanthanide complexes were used to explore the interaction with the fluoride. Alternatively, this lanthanide complex contains an amide-propargyl pendant and can be further used as a synthetic block to prepare f-f' heterometallic lanthanide arrays via 'click reaction' (see Chapter 3). The ligand was incorporated with tryptophan to sensitise the lanthanide emission and the terbium complexes, where the indole moieties of tryptophan can be used as fluoride recognition site.

2.5.1 Synthesis and characterisation

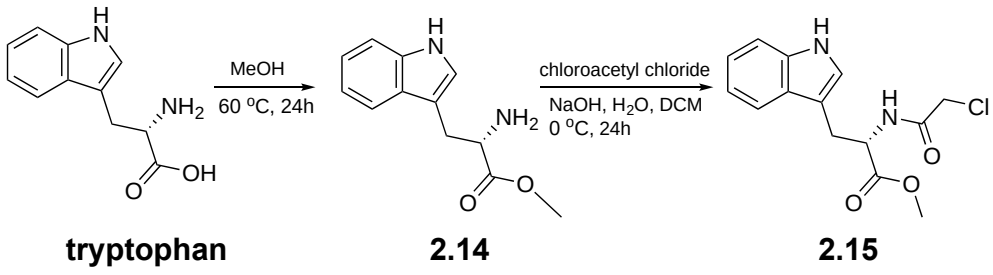


Figure 2-11. Synthetic route for the preparation of chloro-acetyl tryptophan pendant arm.

Chloro-acetyl tryptophan was obtained from the starting material of tryptophan as represented in Figure 2-11. Upon stirring in methanol, carboxylic acid group of **2.14** was protected by methyl ester. **2.14** was then converted to **2.15** by treating with an excess of chloroacetyl chloride to form an amide linker.

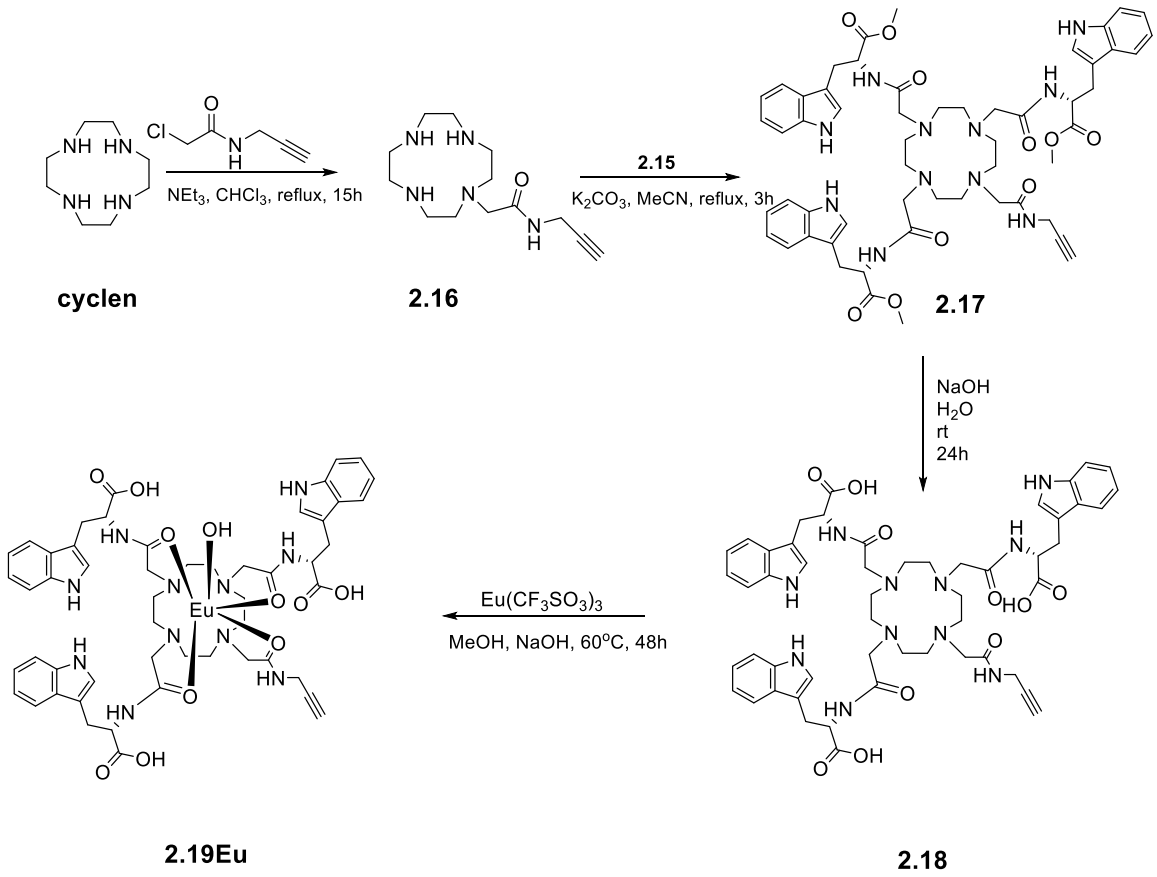


Figure 2-12. Synthetic route for the preparation of europium complexes **2.19Eu** containing a tryptophan chromophore.

The synthetic route for the target tetra-amide lanthanide complexes (**2.19Eu**) is depicted in Figure 2-12. The preparation of the mono-alkylated product **2.16** followed the literature published by Gunnlaugsson.[11] The mono-alkylation of cyclen was achieved by using an excess of cyclen (4 equiv.) and triethylamine base was used to deprotonate the amine. The resulting mixture was washed with 1M sodium hydroxide solution and water to remove the

excess cyclen. The excess cyclen was recycled from the alkaline solution via concentration and neutralisation. The crude mono-alkylated product was then acidified with HCl (1M) solution to give free amine for characterisation. The three amines in **2.16** were then alkylated with **2.15** under standard conditions (K_2CO_3, acetonitrile, reflux, 3h) to afford the crude product as an oil. Silica gel column chromatography was used to purify the oil to give pure **2.17** as a pale-yellow solid. The cleavage of methyl ester was achieved by treating **2.17** with an alkaline solution. After completion of deprotection, the solvent was removed *in vacuo* and methanol was used to extract the tetra-amide compound from the resulting solid under sonication. Pure tetra-amide with free carboxylic acid ligand **2.18** was obtained by concentrating the methanol solution after neutralisation of the solution. The targeted lanthanide complex **2.19Eu** was prepared by stirring the slightly excess europium triflate and ligand **2.18** in hot methanol for 48h. Sodium hydroxide solution was used to basify the solution to pH 10 and excess free lanthanide salt was precipitated out as insoluble lanthanide hydroxide, which was further removed by centrifugation and filtration. Upon complexation, the water solubility was improved and **2.19Eu** was characterised by ^{1}H-NMR, high-resolution ESI-MS and luminescence spectroscopy.

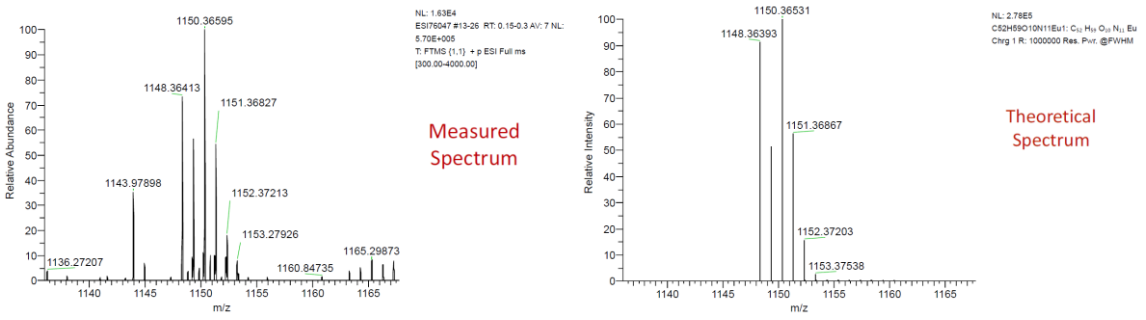


Figure 2-13. High-resolution mass spectra of experimental (left) and predicted (right) of **2.19**Eu ($[M+H]^+$)

2.5.2 Fluoride binding studies

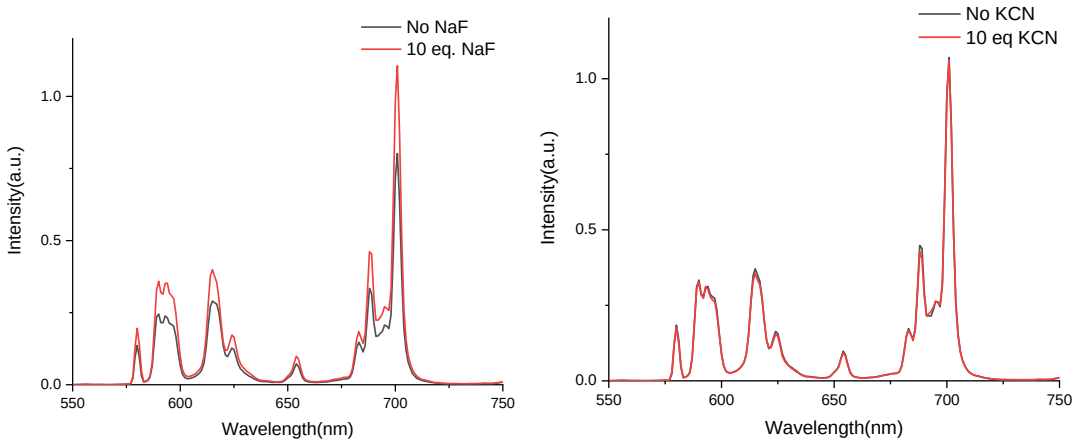


Figure 2-14: Emission spectrum of **2.19Eu**, λ_{ex} = 286 nm. Left: titration of fluoride(black line =start of titration, red line = end of titration; Right: titration of cyanide(black line =start of titration, red line = end of titration. (λ_{ex} = 302 nm, exit slit = 5 nm)

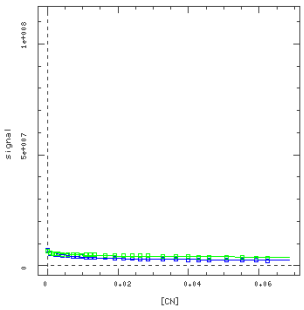
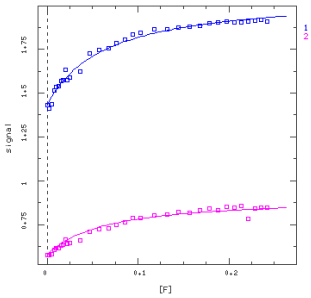
Luminescence titration was used to determine the fluoride affinity of **2.19Eu**. As shown in Figure 2-14, the addition of fluoride-induced a significant increase in the intensity of emission spectra of **2.19Eu**. Upon the addition of fluoride, the europium(III) complexes showed a significant decrease in hydration number which can be rationalised by the displacement of an axial coordinating water molecule by fluoride.

Notably, the hypersensitive transition ($\Delta J = 2$) shows a significant increase in intensity upon the addition of fluoride, implying that the introduction of fluoride results in dramatic changes in coordination environment between ligand and Eu(III). In contrast, no spectral changes can be observed upon the addition of cyanide in **2.19Eu**, reflecting there is cyanide cannot displace the coordinating water molecule due to the lack of nucleophilicity. Addition of other halides (e.g., Cl^-, Br^-) led to no observable changes in the emission spectra,

indicating that the interaction between Eu^{3+} ion and the F^- ion is stronger than the enthalpy of hydration of fluoride in water.

Dynafit® was used to fit the changes in intensity obtained from luminescence titration with 1:1 isothermal binding mode. Alternatively, the attempt of the fluoride binding process being fitted by the two-step mechanism was made but no better convergence was observed, suggesting that the displacement of axial water by fluoride is limited by the bulky nature of molecule and balanced charge.

Table 2-2. Photophysical properties of **2.19Eu**

2.19Eu	K_{CN}/M^{-1}	K_F/M^{-1}
	1.6 [1.2-1.8]	35.2 [30.3-39.2]
	No NaF	**NaF**
τ_{H2O}/ms	0.49	1.21
τ_{D2O}/ms	1.08	2.12
q	1.2	0.3
		

In summary, the interaction of lanthanide tetra-amide complexes with fluoride can result in fundamental changes in photophysical properties, whereas cyanide displayed minimal effect on tetra-amide species. Multiple factors can contribute to the enhancement in radiation processes such as changes in crystal field parameter, sterics and electrostatic interaction.

2.6 Cyanide binding studies

The interaction between cyanide and prepared complexes (2.8-2.12) was examined by using NMR spectroscopy and steady-state luminescence spectroscopy. Furthermore, the affinity of the competitor fluoride ion was also determined for comparison.

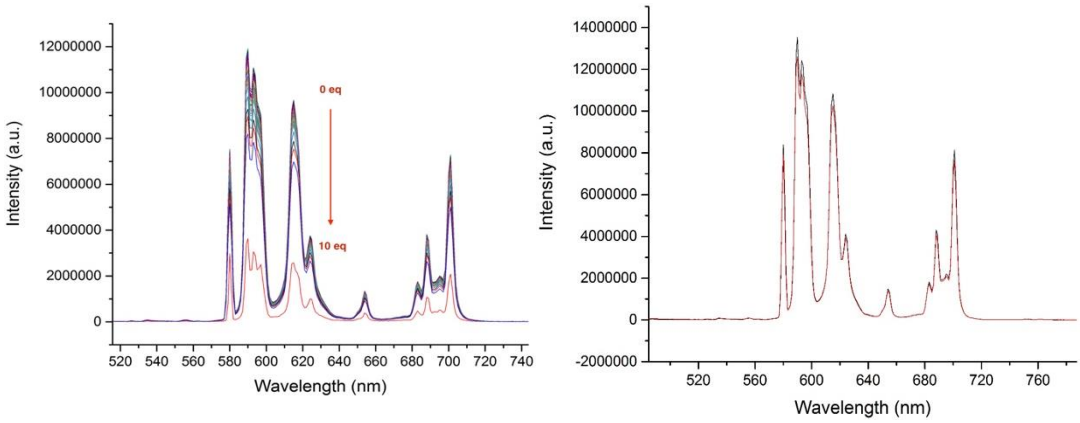


Figure 2-15**: Left**: Emission spectrum of **2.8Eu**, λ_{ex} = 286 nm, blue line = start of titration and red line = end of titration (10eq. KCN); **Right**: Emission spectra of **2.8Eu** with and without fluoride, λ_{ex} = 286 nm, Black line = start of titration and red line = end of titration(10 eqv. NaF).

As Figure 2-12 shown, all transitions (ΔJ = 1-4) experienced a dramatic reduction in intensity though the profile of the spectrum did not change significantly. This minimal changes in the relative ratio of the peaks are more likely to be attributed to the changes in the ligand donor (i.e., from ketone to alcohol) rather than the displacement of bound water by cyanide. Particularly, given that the hypersensitive transition ΔJ = 1 ($^5D_0 \rightarrow {}^7F_2$) of europium(III) complexes are essentially dependent on the local coordination environment,[12] no significant change in the relative intensity of the peaks suggests the axial coordination site is still occupied by a water molecule. The emission spectrum of **2.8Eu** exhibited negligible changes upon the addition of fluoride compared to the cyanide titration spectrum. This substantially smaller fluoride binding affinity for **2.8Eu** can be

rationalised by the charge-balanced Eu^{III} centre in the phenacylDO3A complexes, hence minimising the electrostatic interaction. Fluoride titration was also studied by UV-Vis absorption spectra where no change was observed in the absorption band when cyanide is added, suggesting that the changes in recorded luminescence intensity cannot be attributed to the interaction of fluoride on the sensitising chromophore. Cyanide possesses lower nucleophilicity compared to fluoride and hence is much less likely to displace bound water. These studies further confirmed the fact that spectroscopic changes are the result of cyanohydrin formation on the carbonyl group of phenacyl moiety.

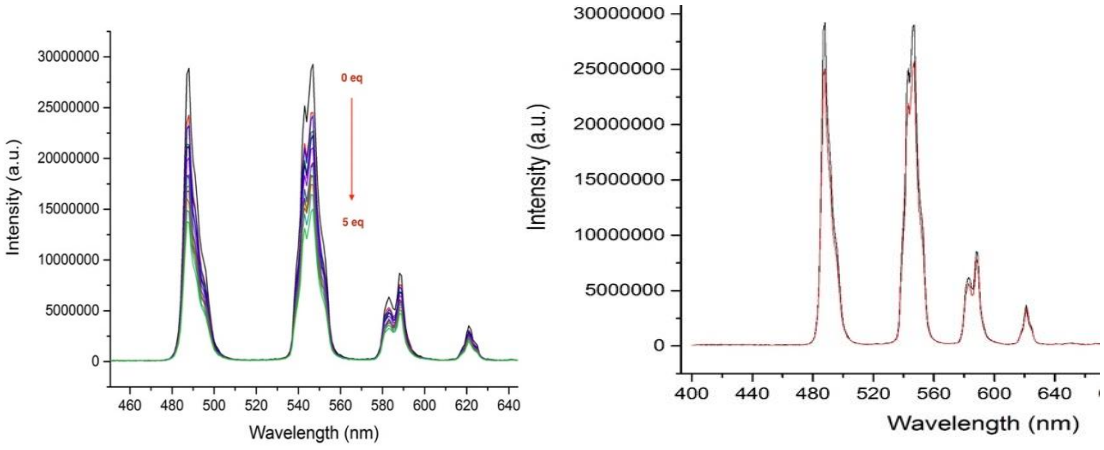


Figure 2-16: **Left**: Emission spectrum of **2.9Tb**, λ_{ex} = 286 nm, black line = start of titration and green line = end of titration (5eq. KCN); **Right**: Emission spectra of **2.9Tb** with and without fluoride, λ_{ex} = 286 nm, black line = start of titration and red line = end of titration(10 eqv. NaF).

Compared to europium(III) analogue, the emission spectrum of terbium(III) complex **2.9Tb** showed the similar phenomenon where the most sensitive transition $^5D_4 \rightarrow {}^7F_5$ has almost a half reduction upon the addition of cyanide. There is a small increase in the luminescence intensity in the presence of fluoride, implying the collisional quencher-water is replaced by the fluoride and hence enhancing the emission of terbium(III) ion.

In Table 2-3, it worth noting that the terbium(III) is less sensitive to cyanide, reasonably because of the higher emissive excited states being less affected by the changes of sensitiser in the presence of cyanide.

Lifetime and hydration states *q* in the presence of fluoride and cyanide are determined and also tabulated in Table 2-3. In the presence of KCN, there is no change in luminescence lifetime in both H_2O and D_2O, even treated with an excess of cyanide, thus suggesting cyanide cannot displace the water molecule from the europium(III) centre. However, there is a slight increase in luminescence lifetimes in H_2O and D_2O and the *q* value is reduced to 0.9, thus indicating that there is partial displacement of a water molecule from the inner coordination sphere. Another aspect of this is most of the europium(III) centres are still coordinated with water molecule with a small amount of them being bound with fluoride since the hydration number *q* remains around 1, which is consistent with the nature of weak fluoride binding of DO3A analogues.

Table 2-3. Photophysical properties of 4'-substituted phenacylDO3A lanthanide complexes in aqueous solution.

		τ_{H2O}/ms	τ_{D2O}/ms	q
2.8Eu	**No addition**	0.62	2.16	1.1[±0.1]
	KCN	0.66	2.21	1.2[±0.1]
	NaF	0.79	2.50	0.9[±0.2]

The changes in the relative intensities of transition bands in the emission spectrum were used to calculate the binding affinity for cyanide by using Dynafit® to simulate the binding behaviour and assess the fitting performance. The isothermal plot of the ratio of emission intensity against cyanide concentration was represented in Figure 2-14. The best-fitted result is given by the 1:1 ratio and higher order of isothermal fitting resulted in no significant improvement. The constants of binding affinity and confidence intervals are summarised in Table 2-4.

Although from stoichiometric analysis with 1:1 binding mode, the obtained binding affinities were low in magnitude, direct binding data for cyanide in pure water is limited and the binding of cyanide is over 100 times stronger than that of fluoride, especially in the case of **2.10Eu**. The DO3A lanthanide complexes are relatively stable in the basic environment, and hence their interaction with hydroxide can be negligible since the pK_a of such system is over 10.5. [13]

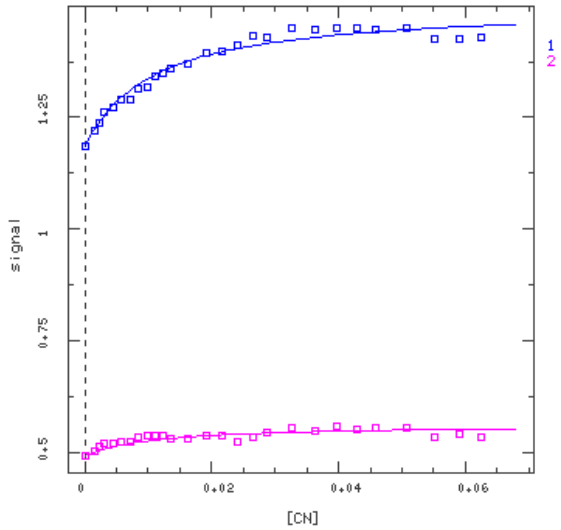


Figure 2-17. Changes in the **2.8Eu** emission spectra in H_2O upon addition of cyanide, showing the change in the peak intensity ratio or ΔJ =2: ΔJ =1 (top) and ΔJ =2: ΔJ =4 (bottom) fitted using a binding isotherm derived using DYNAFIT® (K = 94.2 [80.3 – 110.7])

From the luminescence studies, it is clear that the quenching of emissive states of lanthanide complexes cannot be explained by the collisional quenching since the binding of cyanide is much stronger than collisional quencher fluoride and there is no linear Stern-Volmer relationship (e.g., collisional process).

Table 2-4 Affinity constants for cyanide and fluoride.

	K_{CN}/M^{-1}	K_F/M^{-1}
2.8Eu	94.2 [80.3 – 110.7]	2.1 [1.9-2.3]
2.10Eu	142.7 [135.9 – 173.1]	1.5 [1.46-1.57]

In order to further explore the interaction with cyanide, NMR titration of lutetium(III) complex **2.12Lu** was performed given by the diamagnetic nature of lutetium(III) ion. The ^{1}H-NMR spectrum shows two sets of double doublets corresponding to the aromatic protons on the phenacyl group, indicating each aromatic proton have two different resonance environment and hence there are at least two isomers in solution. The addition of cyanide led to the shift of resonance peaks of aromatic protons where the resonance corresponding to *ortho*-aromatic protons being upshifted, confirming that the cyanohydrin formation indeed occurs at carbonyl carbon and magnetic shielding of *ortho* position is reduced due to the absence of electron-withdrawing carbonyl group.

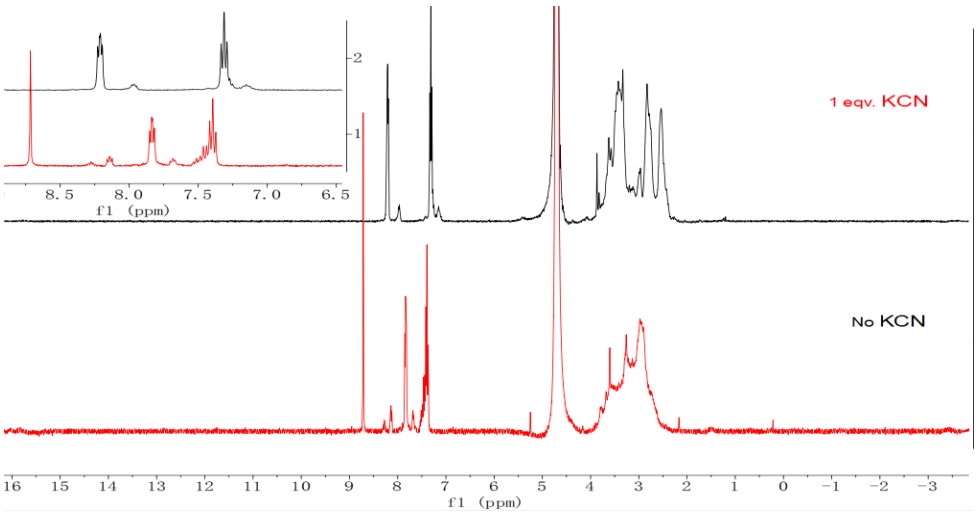


Figure 2-18. ^{1}H-NMR spectra of **2.12Lu** in the presence and absence of cyanide.

Furthermore, the ^{1}H-NMR spectrum of europium(III) complexes **2.8Eu** and **2.10Eu** also exhibited obvious changes upon addition of cyanide. These can be illustrated briefly by the example of **2.8Eu** as depicted in Figure 2-19. As discussed earlier, the ^{1}H-NMR is predominated by the major SAP isomers, while with the cyanide uptake there is a clear

increase in the intensity of resonance originating from TSAP isomers (e.g. the resonance around 20 ppm). It worth noting that the newly-formed species are in slow exchange with **2.8Eu** on the NMR timescale. Combined with luminescence studies earlier and corresponding binding affinity, it can be deduced that the introduction of bulky cyanide group led by cyanohydrin will inevitably change the coordination between the carbonyl group to the metal centre, thus disrupting the exchange equilibrium between NMR distinguishable isomers

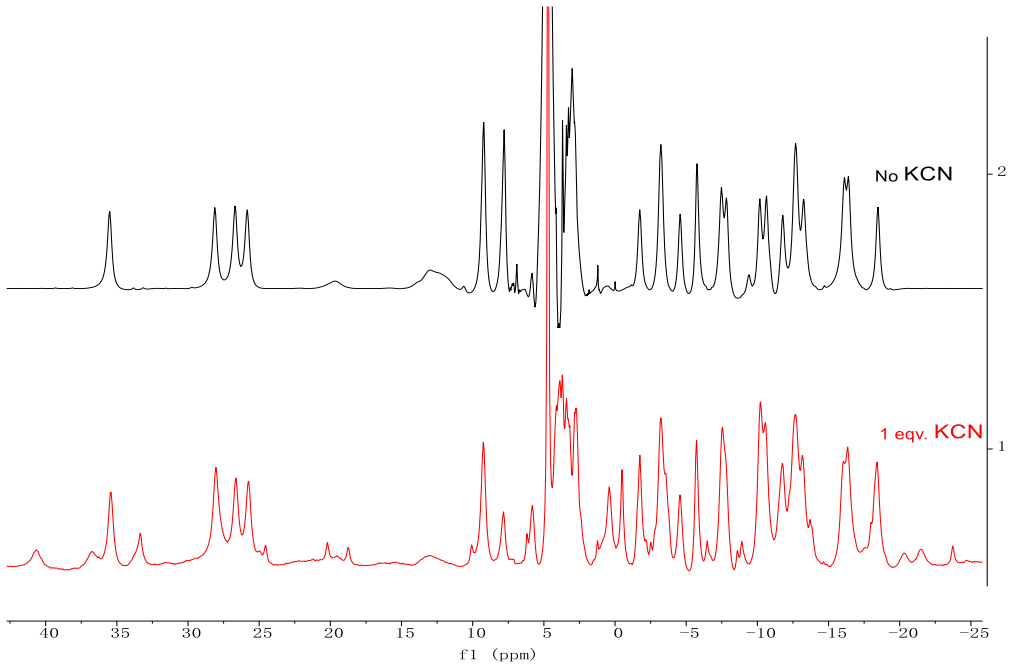


Figure 2-19. The ^{1}H-NMR of **2.8Eu** without cyanide (black) and with cyanide (red).

It is common knowledge that cyanide ions can attack carbonyl groups to form cyanohydrin products in organic systems. In this case, cyanohydrin formation can be facilitated by the coordination of the carbonyl group to the lanthanide(III) centre, which polarises the carbonyl group further. Hypothetically, we can describe the interaction between cyanide and complexed ligand as the result of cyanohydrin formation due to the possibility of direct

coordination of cyanide to the lanthanide ion being excluded by the reason of the constant luminescence lifetime. Comparatively, axial coordination of fluoride will result in significant changes in ligand coordination environment and reduce the non-radiative decay by eliminating the oscillator O-H, and hence the changes in emission profile and longer luminescence lifetimes are expected to be observed in the case of direct binding to metal. In consideration of this hypothesis, these spectroscopic changes can be properly rationalized by the proposed binding events. The sensitization is no longer dominated by Dexter exchange mechanism since the through-bond energy transfer from phenacyl moiety to lanthanide(III) centre is disrupted by the formation of cyanohydrin product, and hence is exerted by the through-space mechanism - Förster energy transfer mechanism. Compared to Dexter mechanism, the effectiveness of Förster mechanism is much lower, as the spectral overlap between triplet states of chromophore and lanthanide absorption spectra is limited, thus resulting in the reduction in luminescence intensity of emission.

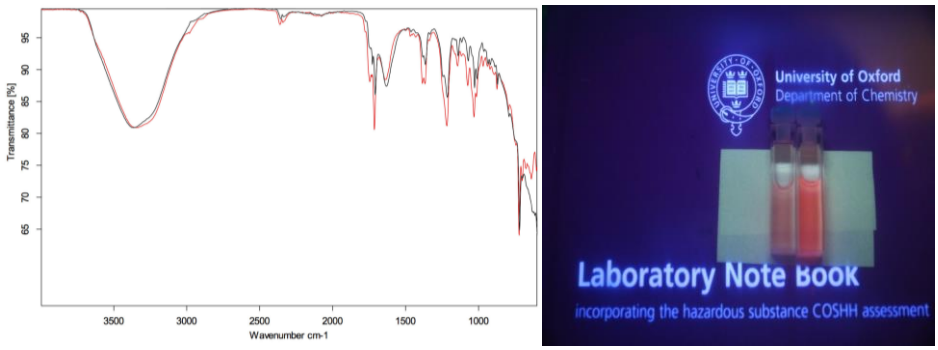


Figure 2-20. Left: Infra-red spectra of **2.8Eu** with (black) and without (red) cyanide. Right: Photography of visual change of **2.8Eu** upon addition of CN^- (10 eqv.) under UV-lamp with 266nm excitation. Right: before the addition of cyanide. Left: after addition of cyanide.

Other techniques were employed to obtain further evidence to verify the proposed hypothesis. Upon the addition of the cyanide, the IR spectra of **2.8Eu** showed similar profile but a reduction in the intensity of stretch at 1713 cm^{-1} can be observed, which is attributable to the carbonyl group, suggesting cyanohydrin indeed occurs at carbonyl group.

The similar changes can be observed in ^{13}C-NMR of lutetium complex **2.12Lu** on the addition of KCN. Furthermore, illumination of the solution of europium species under UV light exhibits difference colours of luminescence in the presence and absence of cyanide.

2.7 Conclusion

The studies in this chapter utilise the 4'-substituted phenacyl chromophore as an optical probe to report the presence of cyanide with relatively low detection limit. It has been demonstrated that phenacyl chromophore is able to sensitise the emissive states of lanthanide(III) ions and the 4'-substituents can alter the photophysical properties of these lanthanide systems. It was observed that their interaction with fluoride is extremely weak due to the low residue negative charge on the metal centre. Compared to phenacylDO3A species, **2.19Eu** exhibited a stronger affinity for fluoride as a consequence of the presence of indole moiety for fluoride capture and no cyanide response was observed for the tetra-amide lanthanide complexes. PhenacylDO3A lanthanide complexes provide a novel method to discriminate cyanide in water by appreciating the chemical interaction between cyanide and phenacyl carbonyl. The present cyanide probe cannot effectively conduct cyanide recognition in aqueous media, but this method is able to detect the presence of cyanide in pure water.

Besides, it is apparent that lanthanide complexes described in this chapter mainly focused on their interactions with fluoride and cyanide ions, which are the most likely found residues after usage of chemical warfare agents. PhenacylDO3A lanthanide complexes can selectively respond to cyanide while tetra-amide lanthanide complex can only respond

to fluoride. It could a starting point to combine the two systems into one system to crease a dual-responsive cyanide-fluoride detector in future.

2.8 Reference

[1] D. Parker, *Coord. Chem. Rev.* **2000**, *205*, 109–130.

[2] D. F. Caffrey, T. Gunnlaugsson, *Dalt. Trans.* **2014**, *43*, 17964–17970.

[3] M. Tropiano, S. Faulkner, *Chem. Commun.* **2014**, *50*, 4696–4698.

[4] W. Zheng, D. Tu, P. Huang, S. Zhou, Z. Chen, X. Chen, *Chem. Commun.* **2015**, *51*, 4129–4143.

[5] J. C. G. Bünzli, *Coord. Chem. Rev.* **2015**, *293–294*, 19–47.

[6] S. Faulkner, M. Tropiano, in *Lumin. Lanthan. Ions Coord. Compd. Nanomater.*, John Wiley & Sons Ltd, Chichester, United Kingdom, **2014**, pp. 331–358.

[7] H.-J. Park, S.-B. Ko, I. W. Wyman, S. Wang, *Inorg. Chem.* **2014**, *53*, 9751–9760.

[8] A. Beeby, L. M. Bushby, D. Maffeo, J. A. Gareth Williams, *J. Chem. Soc. Dalt. Trans.* **2002**, 48–54.

[9] S. Aime, M. Botta, G. Ermondi, *Inorg. Chem.* **1992**, *31*, 4291–4299.

[10] W. F. Forbes, *Can. J. Chem.* **1961**, *39*, 2295–2305.

[11] J. Massue, S. E. Plush, C. S. Bonnet, D. A. Moore, T. Gunnlaugsson, *Tetrahedron Lett.* **2007**, *48*, 8052–8055.

[12] K. Binnemans, *Coord. Chem. Rev.* **2015**, *295*, 1–45.

[13] O. A. Blackburn, M. Tropiano, L. S. Natrajan, A. M. Kenwright, S. Faulkner, *Chem. Commun.* **2016**, *52*, 6111–6114.

[14] S. Y. Huang, V. C. Pierre, *Chem. Commun.* **2018**, *54*, 9210–9213.

[15] Z. Xu, X. Chen, H. N. Kim, J. Yoon, *Chem. Soc. Rev.* **2010**, *39*, 127–137.

3 Heterobimetallic f-f’ Arrays as Ratiometric Cyanide Sensors

3.1 Introduction

To achieve ratiometric sensing, it is necessary to design highly defined architectures with different lanthanide moieties which can exhibit different responses to cyanide. Kinetically inert lanthanide complexes are often employed as molecular building blocks. It is also desirable to develop facile synthetic approaches to pure heterometallic systems, ideally employing starting building blocks that can be readily obtained. Routes to heterometallic assemblies must also exclude the possibility of demetallation of lanthanide complexes (which would lead to the scrambling of metal centres), though it has been shown that some cyclen derived complexes can be kinetically stable under conditions as forcing as those associated with diazotisation.[1]

3.2 Alkyne appended DO3A lanthanide complexes

3.2.1 Introduction

‘Click chemistry’ has been extensively used to prepare supramolecular chemosensors, particularly via Cu(I)-catalysed azide-alkyne cycloaddition (CuAAC). Cu(I) ions can be generated by reduction of copper sulphate with sodium ascorbate, leading to [3+2] cycloaddition reactions between the alkyne and azide components. Although the direct

coupling of protected DO3A ligands bearing alkyne and azide would be synthetically effortless, since simple column chromatography can be applied to isolate the desired coupled product, the side product, the copper DO3A complex, will be difficult to remove. The use of hepta-coordinated DO3A lanthanide complexes as synthons to perform click reactions was first reported by Lowe and Faulkner *et al.* in 2009. The authors demonstrated the propargylDO3A lanthanide complex can undergo cycloaddition with small organic azides to form a new eight coordinated species. Furthermore, the propargylDO3A complex can even react with inorganic azide, giving a simple triazole ring appended product. The formation of triazole is proved by the significant changes in ^{1}H-NMR profiles compared to the propargylDO3Aprecusor.[2] Furthermore, other alkynyl lanthanide complexes were reported to probe the presence of copper(I) in biological tissue. The mixture of equimolar dansyl azide and alkynyl europium complex were used to detect copper(I). With the catalytic effect of copper(I), a dansyl moiety was covalently linked to the alkynyl europium complex to act as an antenna to sensitise europium emission.[3]

However, propargylDO3A forms a seven-coordinated complex, where one or more water molecule might coordinate to the metal centre, leading to the possibility of water being replaced by other nucleophilic competitive anions. A coordinatively-saturated complex would be desirable to deploy as a 'reference channel' in a ratiometric reporting system. Therefore, a new reference complex is designed and derived from a DOTA monoamine where the propargyl arm is extended to link with an amide moiety. Such complexes were prepared via similar procedures as propargylDO3A and photophysical studies were carried out in comparison with propargylDO3A analogues.

3.2.2 Propargyl-appended DO3A

The preparation of alkynyl lanthanide complexes followed the synthetic procedure in the literature.[4] The triester was obtained by alkylating cyclen with *tert*-butyl bromoacetate with potassium carbonate in the acetonitrile. The open site of the fourth tertiary amine was alkylated with propargyl bromide and 2-chloro-N-prop-2-ynylacetamide, respectively. Compound **3.1** was prepared in a decent yield without further purifications and was characterised by ^{1}H-NMR spectra. The compound **3.8** was purified by the silica gel column using chloroform-methanol eluent (95:5) after removing the solvent under reduced pressure to yield white foam powder in 72% yield. Both protected compounds were deprotected using TFA in dichloromethane to remove the *tert*-butyl carboxylic acid protecting group in quantitative yield. The syntheses of all lanthanide complexes are conducted by reacting **3.2** and **3.9** with lanthanide triflates in methanol.

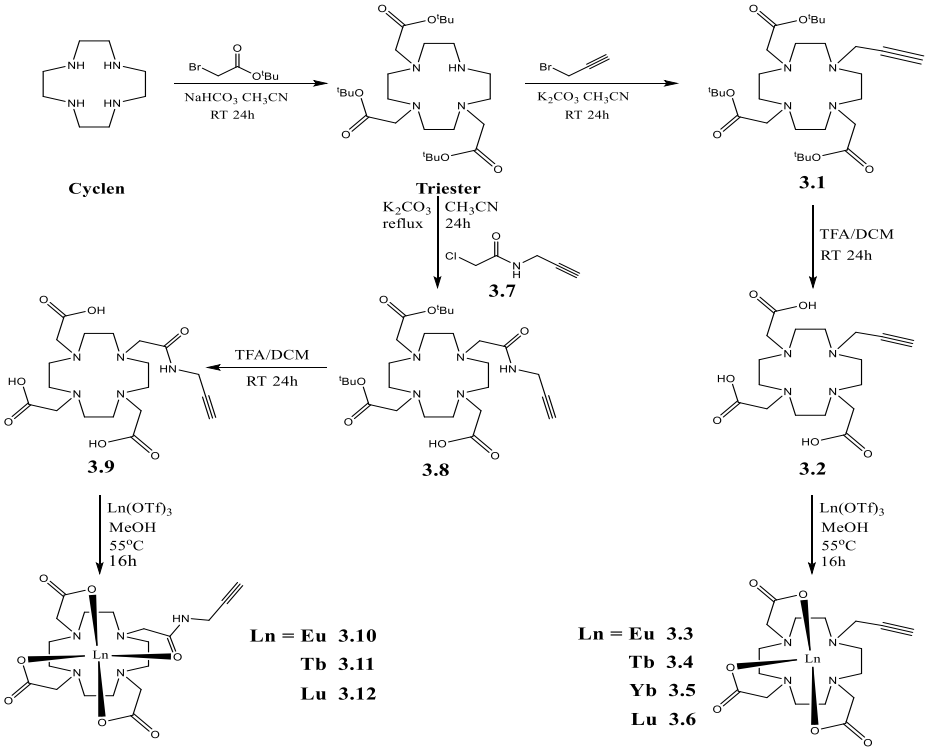


Figure 3-1. Synthetic scheme for the preparation the lanthanide complexes containing propargyl or propargyl-amide arms

3.2.3 Crystal structure of propargylDO3 [II] complex and computational studies

Single crystals of a Lu(III) complex were grown by slow evaporation of concentrated by methanol in an NMR tube. The crystal structure was obtained by X-ray analysis. (Shown in Figure 3-2) The crystal growth of the lanthanide complex is challenging, and many attempts failed. The broken symmetry of a hepta-coordinate complex makes the packing of molecules difficult. The structure of **3.12Lu** was solved and analysed by Dr Kirsten Christensen. The lutetium ion is encapsulated in the cyclen macrocyclic cavity, where the lutetium ion sits between the basal plane containing N_4 and the parallel oxygen donor plane containing O_3. The structure of Lu complex presents a squared-antiprismatic (SAP) configuration with an O_4/N_4 twist angle of approximately 39°, indicating the conformation of the complex is relatively rigid with steric crowding in the binding pocket.

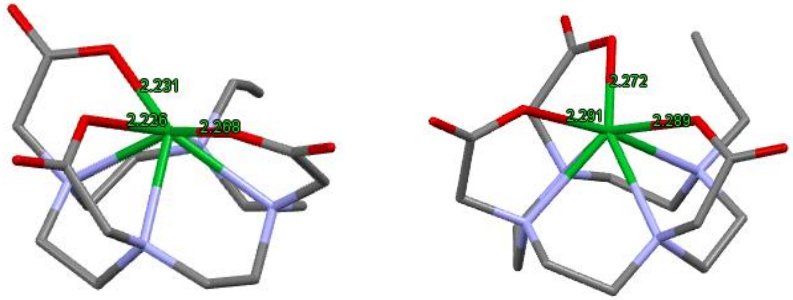


Figure 3-2. Structure of **3.6Lu** complex calculated using Sparkle/RM1 model. (Left) Structure of propargylDO3A Lu complex with capped stick representation. (Right) Hydrogen atoms are omitted for clarity. Grey, purple, red, green are carbon, nitrogen, oxygen and lutetium atoms respectively) The bond length is indicated in green with the unit(Å).

[II] Thermal ellipsoids of **3.6**Lu can be referred to **6.6** in experimental chapter.

To further study the structural behaviour of propargylDO3A complexes, Sparkle Model parameters were used within the RM1 module, which is one of the wide applied semi-empirical molecular orbital modelling methods, for optimising the lanthanide complex and predicting the lanthanide cation-coordinating atom distances. RM1 is exclusively based on monoatomic parameterisation, and limited to certain common elements H, C, N, O, P, S, F, Cl, Br and I. These elements constitute most of the elements in bio-organic compounds and are originally parameterised for highest accuracy. Compared to other new methods PM6 and PM7, which utilise diatomic parameters, RM1 still exhibits the best accuracy in predicting the molecular structure of lanthanide complexes containing common elements.[5] The Sparkle model was first parameterised by a series of crystal structures of europium complexes in 1994, and the predicted distance was in an acceptable accuracy with the deviation of the order of 0.13 Å.[6] The Sparkle Model adopted the theoretical approximation that the 4f-electrons do not possess covalent character in bond formation due to low probability of the 4f electrons in the outer shell, making the coordination electrostatic: while this is not wholly true, it represents a very good first approximation when discussing structures. Besides, a new method for simulating UV-Vis absorption spectra of lanthanide complex using the ZINDO[7] program with an INDO/S-CI model was reported by Lowdin.[8]

PropargylDO3A lutetium complex was optimised by Sparkle/RM1 parameters and calculated lanthanide ion-coordinating atom distances were compared to those obtained from the crystal structure. Alternatively, other model functions like AM1, PM6 and PM3 were also performed to compare with RM1 in terms of accuracy. In Figure 3 5, it is clear that Sparkle/RM1 shows better performance in predicting the structure of lanthanide complex.

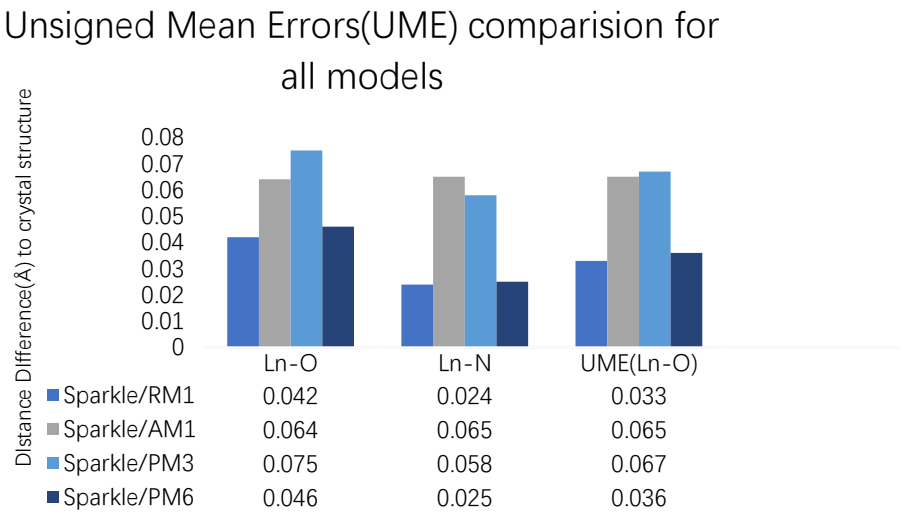


Figure3-3. Unsigned Mean Errors for parameters in Sparkle models in comparison to the crystal structure.

3.2.4 NMR spectroscopy characterisation

^{1}H-NMR spectra of **3.3Eu** and **3.4Tb** are in accordance with heptadentate and non-centrosymmetric nature of propargylDO3A complexes, where all axial protons are in different environments and resonance peaks are broad, suggesting the feasibility of arm rotations which would allow exchange between isomeric pairs. This behaviour in solution is expected due to the pendant propargyl group being unable to coordinate to the lanthanide ion. The exchange between isomers of propargylDO3A lanthanide complexes has been well-established by Faulkner,[9,10] thus detailed characterisation upon such complexes will not be covered in this chapter.

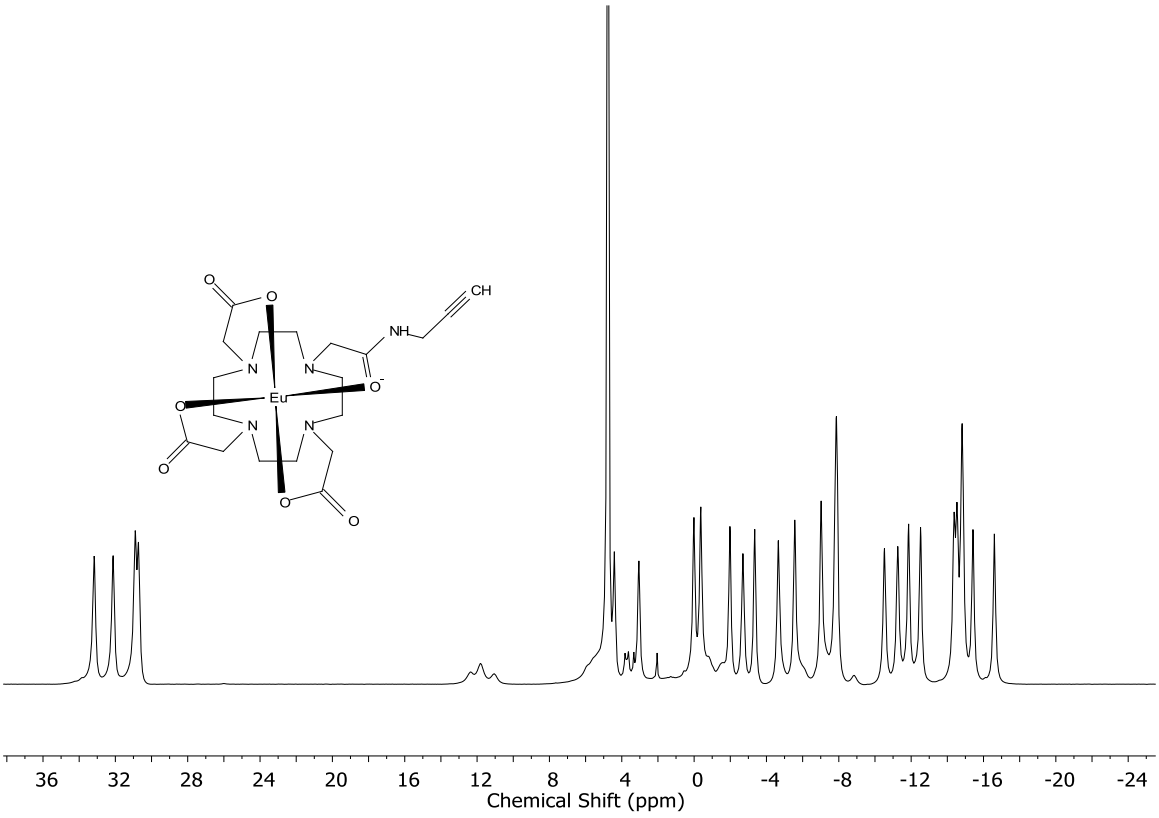


Figure 3-4. The ^{1}H-NMR spectrum of **3.10Eu** recorded in D_2O at RT.

The ^{1}H-NMR spectrum of **3.10Eu** shows sharp peaks and a clearly defined cluster of four peaks between 30 and 34 corresponding to axial ring protons on the azamacrocycle where the complex adopts square antiprismatic geometry, while a minor isomer is also observed corresponding to the twisted square antiprismatic (TSAP) form (as can be seen from the slightly broader peaks between 11 and 12.3 ppm. The ^{1}H-NMR spectrum of **3.11Tb** exhibits a similar profile, albeit over a much larger chemical shift range, as expected for a terbium complex. It is clear that rigidity of molecule is enhanced relative to heptadentate analogues of these complexes; this confirms the coordination of propargyl-amide carbonyl group to the metal centre.

3.2.5 Photophysical Studies

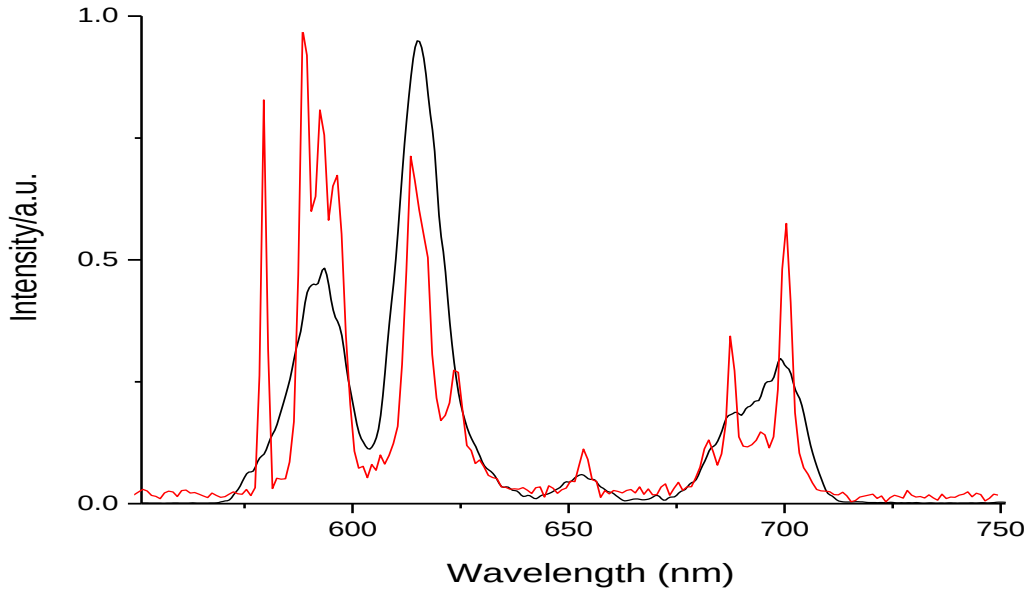


Figure 3-5. Emission spectra for **3.3Eu** (black) (slit width 10 nm, I_{ex} = 278 nm) and **3.10Eu** (slit width 1 nm, I_{ex} = 390 nm) , registered in H_2O.

Figure 3-5 shows the emission profile for the $^5D_0$ to ^7F_j transitions of **3.10Eu** (red) in comparison with **3.3Eu** complex. The ratio of hypersensitive transitions of **3.10Eu** is smaller than that of **3.3Eu**, resulting from the changes in the local environment of coordination. The profile of **3.10Eu** is similar to the [DOTA.Eu]$^-$ complex,[11,12] where both the magnitude of and the transitions are similar, suggesting the coordination number of **3.10Eu** is eight. Upon changing pH, no obvious change in the emission spectrum of **3.10Eu** was observed, and hydration states remain stable. The separation between alkyne moiety and metal centre of **3.10Eu** is relatively long, compared to **3.3Eu**, thus it is more likely that the energy transfer in such system occurs through space pathway, i.e., Förster mechanism.

The excitation spectrum (detecting the emission at λ = 614 nm) shows an intense band centre at 320 nm and a weak peak at 395 nm. The latter peak can be attributed to the direct

sensitisation of Eu^{III} ion. The band observed at 320 nm could correspond to either the sensitisation of propargyl amide moiety or an LMCT absorption. The hypersensitive transition at 615 nm was used to acquire the lifetime to determine the hydration state *q* via Horrock's equation.[13] The lifetimes of complexes are summarised in Table 3-1.

Table 3-1. lifetimes for depopulation of emissive states; hydration states, *q*, was calculated by Horrock's equation.

Compound	λ_{ex}/nm	λ_{ex}/nm	τ_{H2O}/μs	τ_{D2O}/μs	q
3.3Eu	278	615	434	1695	1.7[±0.3]
3.10Eu	277	615	466	1124	1.2[±0.1]
3.4Tb	350	544	467	1123	1.2[±0.2]
3.11Tb	350	545	1123	1430	1[±0.1]

Through the lifetime studies, a hydration number q = 1.7 was found as expected, since two water molecule can bind to the metal ion of **3.3Eu** to fulfil the coordination requirement, with a coordination number of 9. However, hydration number of the complexes with octadentate ligand (**3.10Eu** and **3.11Tb**) is reduced compared to the corresponding lanthanide complexes due to structural changes in coordination. Although cyanide ion is less nucleophilic to replace the coordinated water molecule, complexes with more compact inner sphere (smaller hydration number) might be hypothetically better to avoid the susceptibility to be attacked by other anions, like F^- and CH_3COO^-.

In summary, all these results demonstrate both alkyne appended lanthanide complexes were both kinetically stable and their photophysical characteristics can be utilised to the development of heterometallic arrays as a ratiometric sensor, particularly as a 'reference channel'. It is perhaps important to note that fluoride is an effective kinetic trap for lanthanides owing to the very low solubility of lanthanide fluoride salts. The absence of any visible precipitate over the course of the fluoride tritration lends further credence to the high stability of the complexes.

3.3 Propargyl-DO3P complex

3.3.1 Synthesis

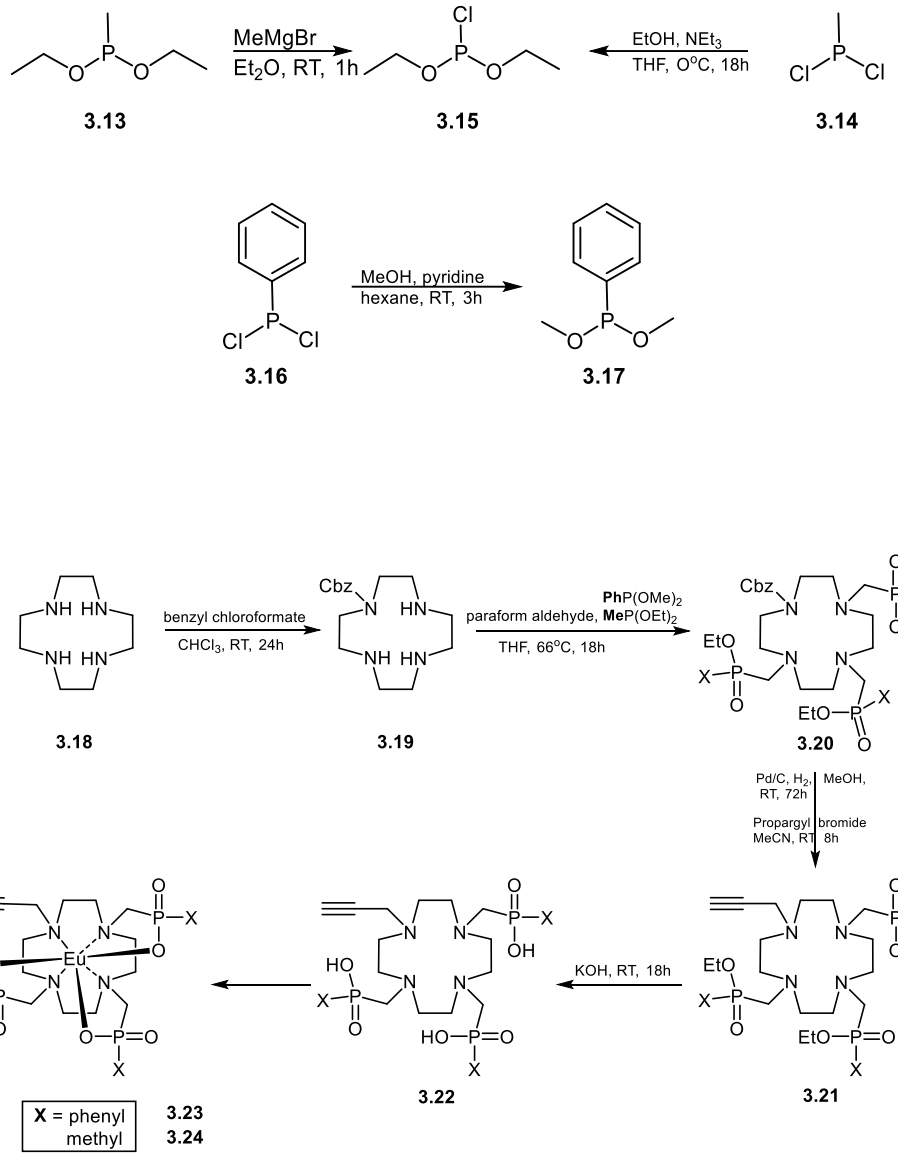


Figure 3-6. Synthetical scheme of DO3P europium complexes.

Figure 3.6 shows the route used to access the phosphinate analogues of propargyl DO3A. The mono-protected cyclen (**3.19**) was obtained by using benzylchloroformate to selectively protect one position[14], and was then treated with NaOH(1M) to remove the hydrochloride adduct and recovered by extraction with dichloromethane. The free base

compound **3.19** and paraformaldehyde were dissolved in anhydrous THF. Water was removed from the reaction mixture by refluxing the reaction mixture through a Soxhlet extractor equipped with molecular sieves and set to reflux. The mixture was stirred for 30 minutes to allow the forming of an iminium ion. The generated water was successively removed by the Soxhlet extractor to drive the reaction to completion. The tris-phosphinate ester was achieved via an Arbuzov reaction by adding diethyl-methylphosphonite or diethyl-phenylphosphonite to the mixture. The tris-substituted compound was isolated by column chromatography on neutral aluminium oxide. The Cbz protecting group was removed by hydrogenation in the presence of catalytic Pd on activated carbon. The completion of deprotection can be confirmed by the absence of phenyl protons at the aromatic region. The deprotected compound was then alkylated with propargyl bromide to yield **3.21**. The hydrolysis of ethyl ester groups was achieved using hydrochloric acid and stirring for 2 days. The pro ligand was used for complexation reactions without further purification. The complexation was carried out in methanol using slightly excess of lanthanide triflate. The excess lanthanide salt was removed by forming the insoluble lanthanide hydroxide by increasing the pH of the solution with sodium hydroxide solution.

3.3.2 NMR characterisation

^{1}H-NMR spectroscopy shows spectrum broadening and significant shift due to the paramagnetic nature of europium ion. All ^{1}H-NMR spectra show sharp resonance peaks implying that all diastereoisomers in solution are in slow exchange (NMR timescale).

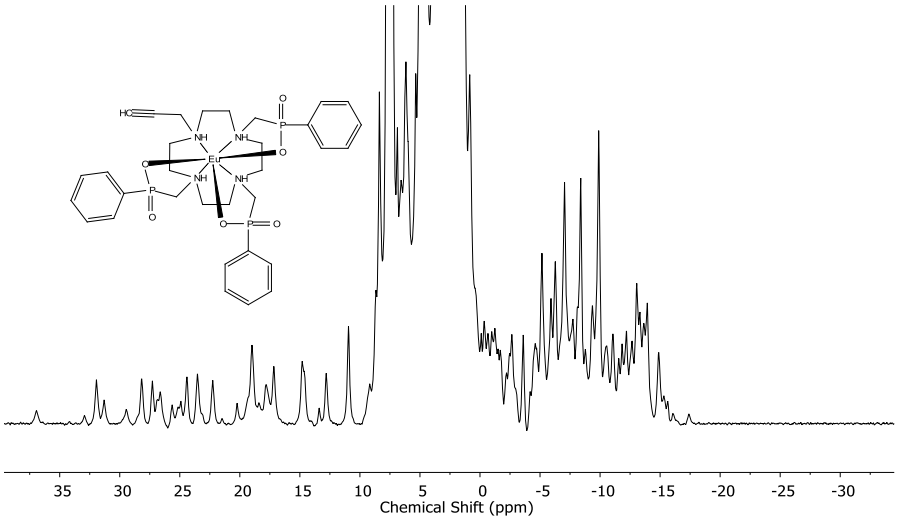


Figure 3-7. The ^{1}H-NMR spectrum of **3.23Eu** registered in D_2O at RT.

The ^{1}H-NMR spectrum of europium(III) complex **3.23** exhibits a typical paramagnetic spectrum of europium(III) complex and is shown in Figure 3-7. Many sets of different resonances at the low field can be attributed to the signals from axial protons on the cyclen macrocycle. It is indicative that the introduction of four phenyl groups on the phosphinate arms increases steric hindrance in the complex, thus leading to many NMR distinguishable isomers in solution.

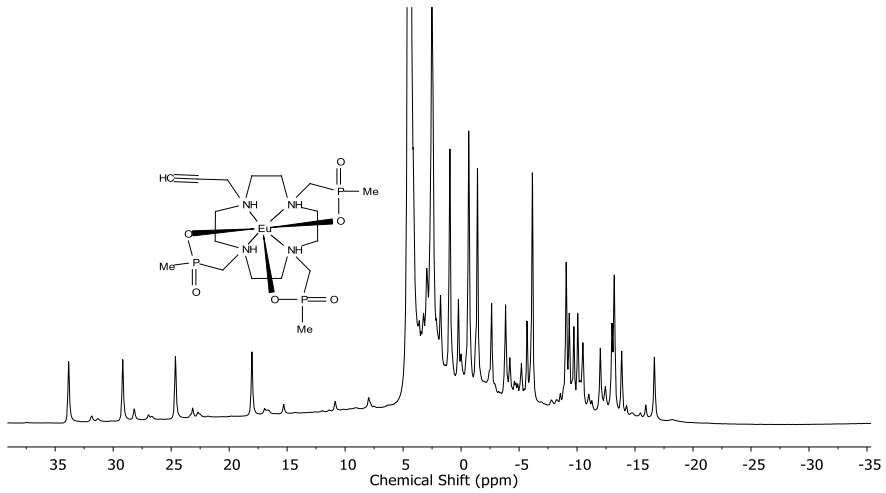


Figure 3-8. The ^{1}H-NMR spectrum of **3.24Eu** registered in D_2O at RT.

The ^{1}H-NMR spectrum of **3.24Eu** shows a similar scenario as **3.23Eu** but with one dominant diastereoisomer, suggesting that compared to **3.24Eu**, **3.23Eu** which only possesses a bulky benzyl substituent might lead to an increase in rigidity of the coordination site. This conformational rigidity is of crucial importance regarding the dynamic process involving ring inversion and arm rotation.

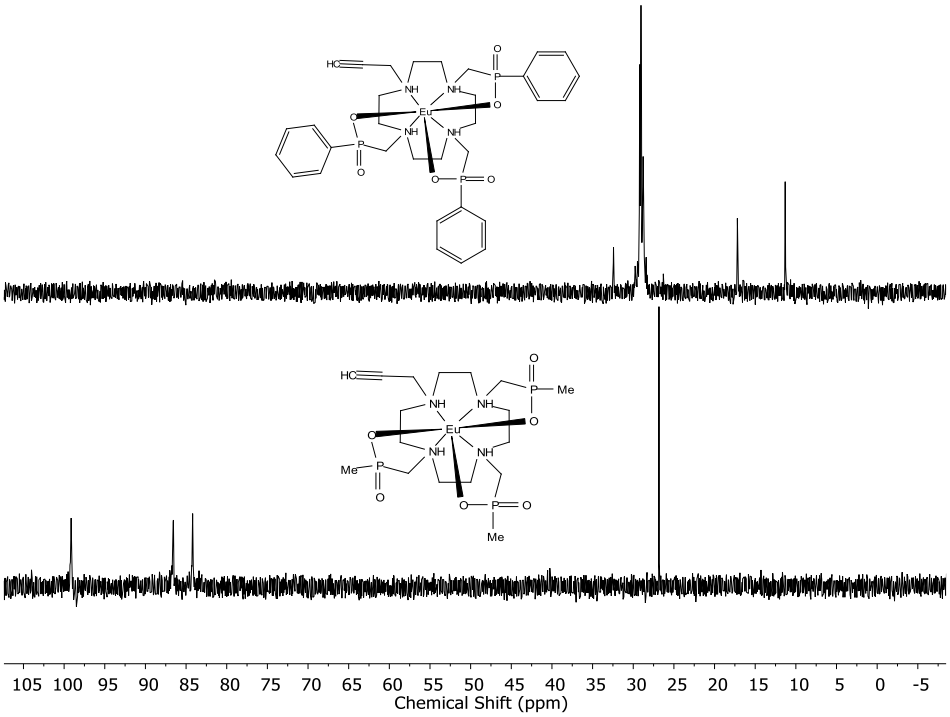


Figure 3-9. Proton decoupled ^{31}P NMR spectrum of **3.23Eu** (above) and **3.24Eu** (below) registered in D_2O at RT (pD = 7).

Many isomers of **3.23Eu** and **3.24Eu** were observed by proton and phosphorus NMR spectroscopy as ^{31}P NMR analysis of complexes revealed at least three diastereoisomers in solution, arising as a consequence of asymmetry at the phosphinate groups. These diastereoisomers can be attributed to the chiral centre at phosphorus atom arising from the coordination of phosphorus oxygen to the metal centre. Additionally, the combination of the protonation state of phosphonates makes the assignment of the spectrum more complicated.

3.3.3 Photophysical Studies

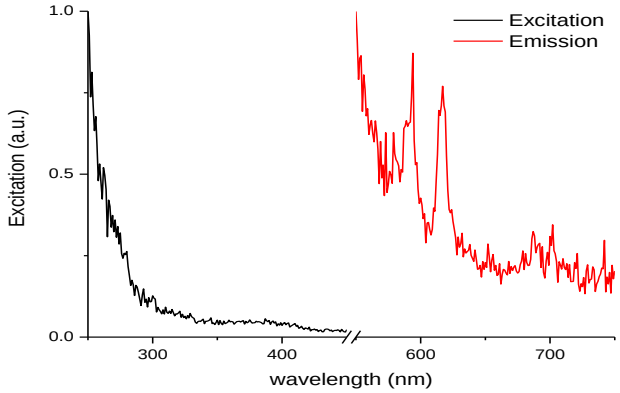


Figure 3-10 Excitation and Emission spectrum of the Eu(III) complex **3.24Eu** (slit width = 10 nm, I_{ex} = 298nm) registered at 273K in H_2O

The excitation spectrum of **3.23Eu** and **3.24Eu** were recorded by measuring the emission at 616 nm. **3.23Eu** shows very weak emission, no obvious observable excitation band on the spectrum (Figure 3-10), indicative poor sensitisation of the methyl-phosphinate chromophore, whereas excitation spectrum of **3.24Eu** demonstrates moderate sensitisation originating from phenyl-phosphinate moiety, though the sharp lines in the excitation spectrum reveal that sensitisation is not significantly more effective than direct excitation. (As shown in Figure 3-11)

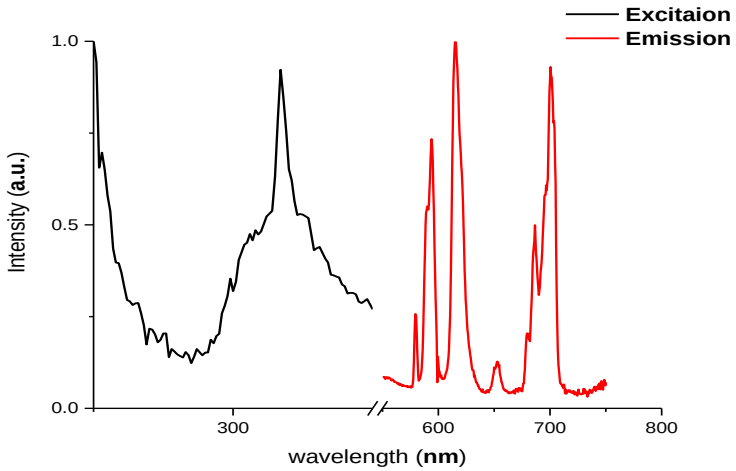


Figure 3-11. Excitation (I_{em} 615nm) and emission spectrum (I_{ex} 355nm, exit slit 8nm) of the Eu^{III} complex **3.23Eu** register at 273K in H_2O

The emission spectrum of **3.24Eu** is represented in Figure3-11. The spectrum shows the assignment of expected $^5D_0 \rightarrow {}^7F_n$ transitions. The transition $^5D_0 \rightarrow {}^7F_0$ was observed at 578 nm with relatively strong intensity, suggesting there is no centre of symmetry in the molecule as this transition rarely can be seen in complexes with D_{4h}, D_{4d} and D_4 symmetry like the $[Eu.DOTA]^-$ complex.

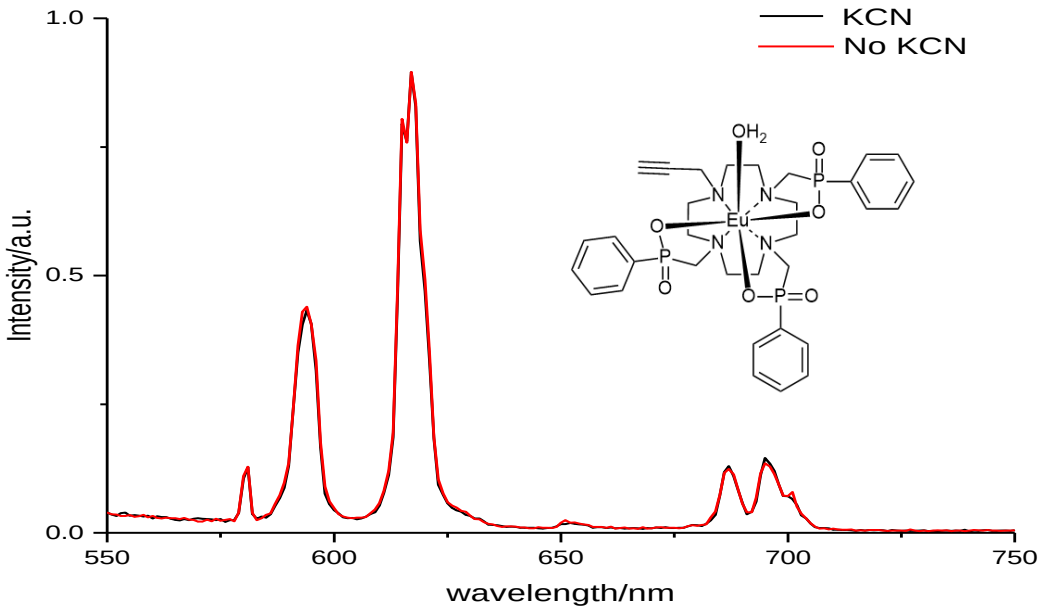


Figure 3-12. Comparison of the emission spectrum of the Eu^{III} complex **3.23Eu** (I_{ex} 310 nm, exit slit 14 nm)) upon addition of KCN registered at 273K in H_2O.

The interaction between **3.23Eu** and cyanide was studied by luminescence titration. Upon addition of 10 equivalent of KCN, no change was observed in the emission spectrum, confirming the lack of coordination of cyanide to the complex, which was further confirmed by the luminescence lifetime. However, the complex was found to be unstable upon laser excitation; the excitation spectrum of **3.23Eu** showed that the absorption band is reduced after one month, presumably losing the phenyl chromophore manifold. Given this, and the demanding nature of the syntheses of phosphinate containing complexes, DO3P lanthanide complexes were not pursued further in the development of heterobimetallic complexes.

Table 3-2.Luminescence lifetime of the propargyl tris-phosphinate complexes **3.23Eu** and corresponding hydration number **q**

Compound	λ_{ex}/nm	λ_{ex}/nm	τ_{H2O}/μs	τ_{D2O}/μs	q
3.23Eu	310	615	854	1192	0.1
3.23Eu+KCN	310	615	855	1201	0.1

The measured lifetimes of lanthanide complex **3.23** in the presence or absence of cyanide are recorded in Table 3-2. The relatively low hydration number for both cases could possibly suggest the formation of **3.23** aggregates in the solution.

3.4 EthynylbenzylDO3A

3.4.1 Synthesis

Although the propargylDO3A complex was a good precursor for preparing complicated lanthanide architectures, it is less likely to be used as a luminescent reporter as no chromophore was attached to the molecule to sensitise the emission of lanthanide ion. Thus, a ligand structure incorporating both antenna and alkyne moiety would be much superior

for the preparation of a luminescent multimetallic complex offering a ratiometric response to guests. Bearing this in mind, a DO3A manifold appended with a *p*-ethynylbenzyl moiety was proposed and synthesised to couple with azide containing lanthanide complexes. The *p*-ethynylbenzyl group has several properties: it links the alkyne to the chelate ring without ketone which is unaffected against nucleophile cyanide ion; it acts as an antenna to sensitise the emissive states of lanthanide ions.

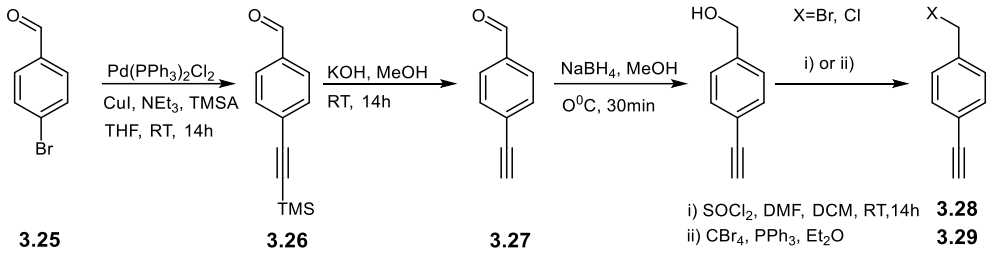


Figure 3-13. Synthetic scheme for the halogenated ethynylbenzene.

Although 4-ethynylbenzyl alcohol is commercially available, the price is extremely high even for milligrams, which is not favourable for preparing a large scale of ligands. A standard Sonogoshira reaction was adopted to couple trimethylsilyl protected ethynyl to 4-bromobenzylaldehyde, followed by a deprotection procedure under a basic condition. Reduction of **3.27** aldehyde was carried out by sodium borohydride in methanol. Halogenation of 4-ethynylbenzyl alcohol was undertaken by using thionyl chloride to generate the 4-ethynylbenzyl chloride or corresponding bromide. The chlorinated product was used for the further reaction as the chlorination gave better yield and the synthesis is more facile compared to the bromination.

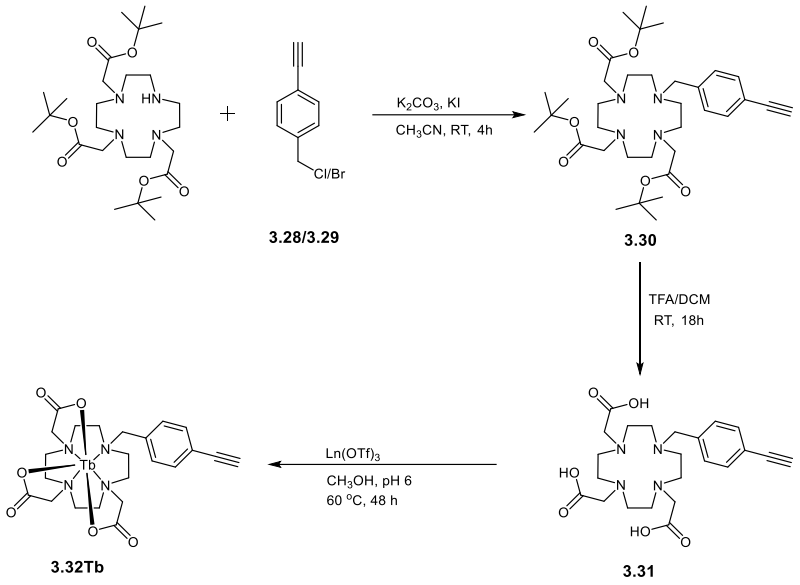


Figure 3-14. Synthetic scheme of lanthanide complex containing ethynylbenzyl pendant.

The triester was alkylated under standard basic conditions using 4-ethynylbenzyl chloride. The crude product was purified by flash column chromatography to afford the *t*-butyl protected product. Alternatively, the product could also be recrystallised from hot hexane and chloroform. Cleavage of the *tert*-butyl esters was achieved by using trifluoroacetic acid in dichloromethane to give the ligand quantitively. The complexation was achieved by using a standard procedure by mixing ligand and slightly excess corresponding lanthanide triflate in methanol and stirring at 60 °C. The reaction solution was adjusted toward neutral, making it pH 5 for best complexation condition. The excess lanthanide triflate was removed as insoluble lanthanide hydroxide precipitated by raising the pH to 12.

3.4.2 Photophysical Studies

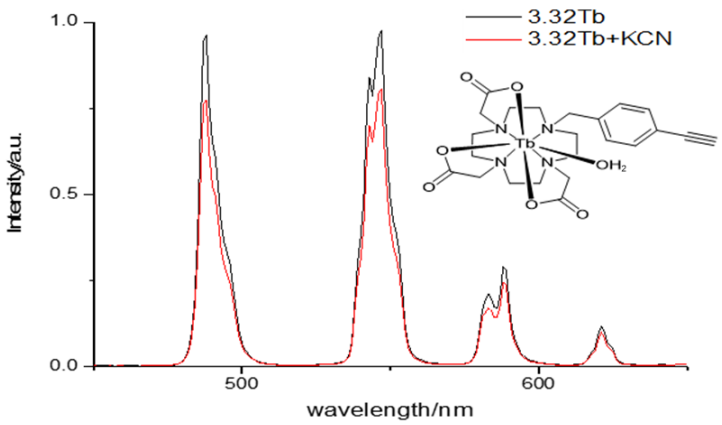


Figure 3-15. Comparison of the emission spectrum of the terbium(III) complex **3.32Tb** upon addition of KCN registered at 273K in H_2O

Cyanide titration was performed on the **3.32Tb** complex, and the emission intensity was found to change slightly while the form of the spectra remained the same. It is possible that the addition of cyanide (and the consequent change in ionic strength, leads to aggregation of the neutral complex, reducing the potential for non-radiative deactivation.

Table 3-3. Luminescence lifetime of the propargyl tris-phosphinate complexes **3.32Tb** and **3.32Tb+KCN** and corresponding hydration number **q.**

Compound	**λ_{ex}/nm**	**λ_{ex}/nm**	**τ_{H2O}/μs**	**τ_{D2O}/μs**	**q**
3.32(Tb)	355	544	1200	2051	1.4[±0.2]
3.32(Tb)+KCN	355	544	1450	2610	1.2[±0.1]

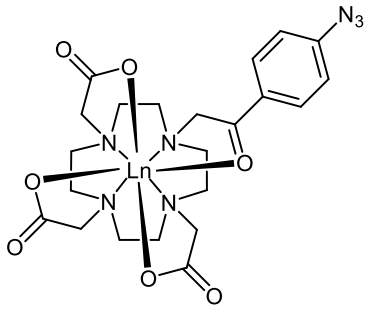
The lifetimes of **3.32** in the presence or absence of cyanide in solution were recorded in Table 3-3. The hydration number of 1.4 for terbium complex **3.32** indicates the unsaturated coordination sites allowing at least one water molecule bound to the lanthanide centre. No significant changes were observed followed by the addition of cyanide which is in accordance with the weak nucleophilic nature of cyanide ion.

3.5 Azidophenacyl DO3A lanthanide complexes

3.5.1 Introduction

The design of novel lanthanide complexes as building blocks certainly contributes to the development of analyte responsive lanthanide complexes with versatile structures. Besides, a straightforward methodology should be adopted to prepare heterometallic lanthanide complexes with decent purity. Thus, ‘click chemistry’ was chosen to apply to coupling different complexes to give hetero-multimetallic lanthanide complexes. Given the experience of alkyne appended complexes, it is reasonable to develop a new class of lanthanide complexes with a pendant azide functional group. In terms of sensing, the presence of analytes is normally monitored by spectral changes, which can be easily observed by undertaking conventional luminescent studies.

To design azide appended complexes, it was necessary to employ a chromophore to sensitise lanthanide emission, as the presence of chromophore sensitisation allows us to better understand the photophysical properties of the heterobimetallic complex. Also, such ligands should be effortless to make and are kinetically stable in competitive media. Bearing these requirements in mind, the azidophenacylDO3A complexes were selected for further investigation. (As depicted in Figure 3-16)



3.37

Figure 3-16. AzidophenacylDO3A lanthanide complexes with azidophenacyl pendant.

Complex **3.1** is based on the well-known DO3A structure containing a phenacyl side arm and has already been reported as a building block for heterometallic architectures.[10] The carbonyl oxygen allows the phenacyl moiety to directly coordinate to the metal centre, while additionally offering a chromophore to sensitise the formation of lanthanide emissive states. Carbonyl oxygen coordination facilitates the efficiency of energy transfer from chromophore to the metal centre, leading to the changes in the polarisability of carbonyl moiety, thus reducing the possibility if that electrophilic lanthanide metal ion being attacked by competitive nucleophilic ions. The azido group is linked to the aryl ring and chemically reactive to undergo 'click reactions' with other alkyne components to build up through-bond interactions between two different lanthanide complexes moieties in the heterometallic complex.

3.5.2 Synthesis

Azidophenacylbromide was synthesised from 4'-aminoacetophenone as shown in Figure 3-17. Instead of using conventional NaN_3 and $NaNO_2$ in harsh acidic conditions, a mild synthetic methodology was used to prepare the aromatic azide from a primary amine.[15] Upon treatment of *tert*-butyl nitrile, **3.34** was converted into intermediate diazonium salts followed by addition of azidotrimethylsilane at 0 °C. The reaction was accomplished

rapidly in high yield with help of the electron-withdrawing acetyl substituent, and the product, azido-acetophenone, was obtained after washing with cold hexane.

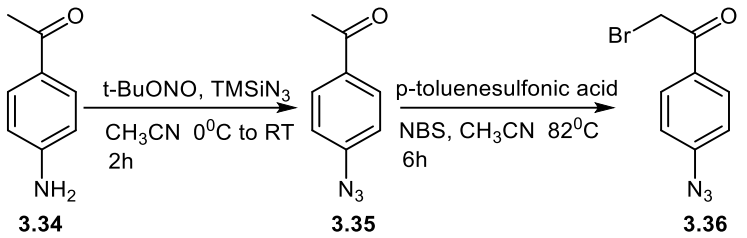


Figure 3-17. Synthesis of bromo-azidophencylDO3A pendant arm.

The bromination of azido-acetophenone with the stoichiometric amount of bromine was attempted but this reaction did not produce target product in decent conversions. A few attempts were made to increase the yield, such as lowering the temperature or dropwise addition of Br_2, but neither was successful. After catalytic amounts of aluminium trichloride were added, the reaction mainly produced undesired dibrominated side products. The target compound was eventually obtained by using 2 equivalents of *p*-toluenesulfonic acid and *N*-bromosuccinimide in acetonitrile with heating to reflux, adopting a bromination procedure by Chang reported in 2002.[16] The final product was kept in the dark at low temperature in case of decomposition by light irradiation. This methodology was applied for all the bromination of aromatic carbonyl compounds to prepare corresponding halogenated products.

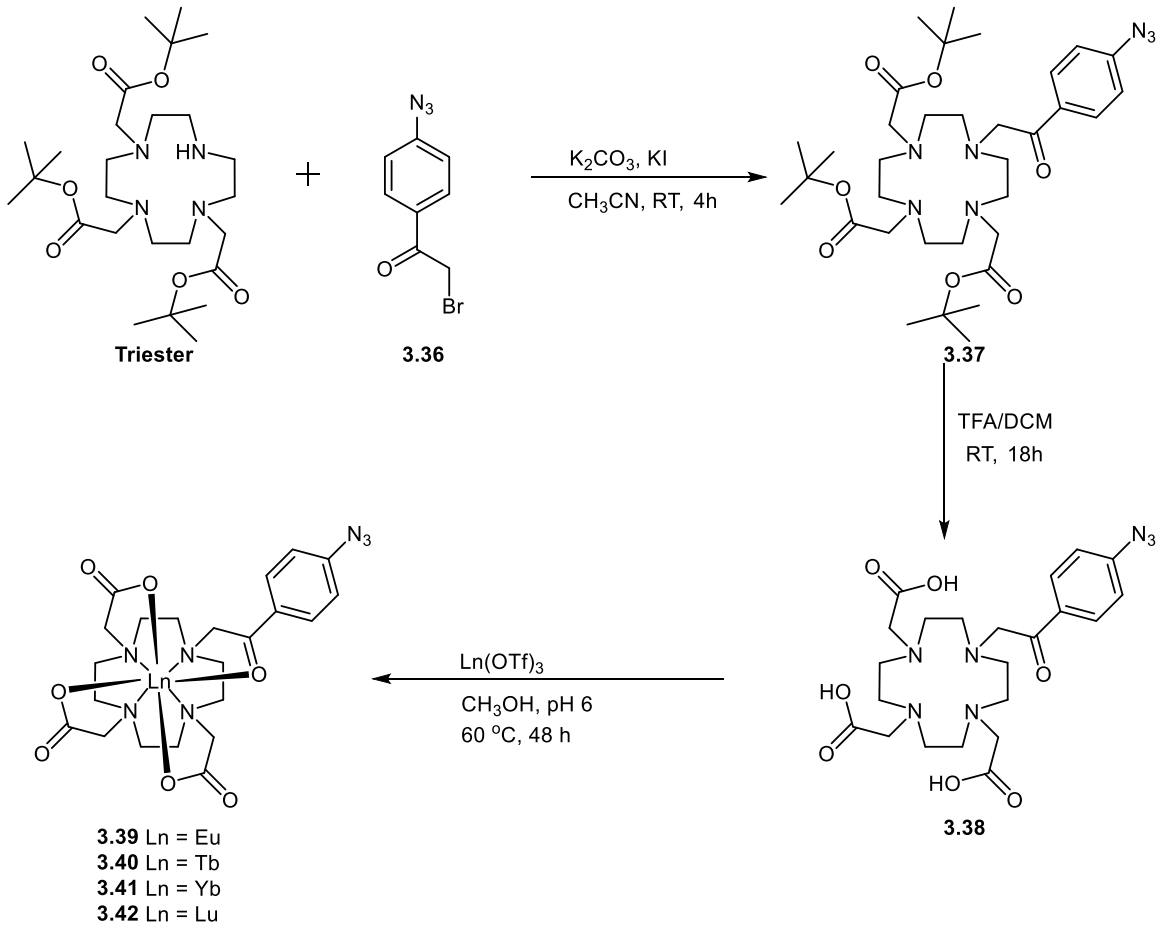


Figure 3-18. Synthetic procedure for preparation of azidophenayclDO3A complexes.

The reaction between azidophenacylbromide and *tert*-butyl protected triester in the presence of potassium carbonate and a nucleophilic catalyst (KI) yielded the crude protected ligand **3.37**. The purification was achieved by the flash column chromatography on silica gel. The deprotection of the *tert*-butyl protection group was carried out in dichloromethane with the treatment of trifluoroacetic acid in room temperature. The deprotected ligand was dissolved in methanol with corresponding lanthanide triflate salts with heating to 60 °C. Excess of lanthanide ions was removed by filtering off the precipitation of lanthanide hydroxide resulted by addition of sodium hydroxide solution.

The resulting complexes were characterised by ^{1}H-NMR spectroscopy, IR and mass spectrometry.

3.5.3 NMR spectroscopy characterisation

The ^{1}H-NMR spectrum of the europium complex **3.39** exhibited typical broad shifted resonances due to the paramagnetic nature of lanthanide ion. The four signals between 25 and 40 ppm can be assigned to the axial protons on the macrocycle backbone, indicating the square antiprismatic geometry (SAP) is predominant in the solution, while the twisted square antiprismatic (TSAP) diastereoisomer exists in trace amounts. Besides, the relative sharp peaks suggest that the oxygen atom of the carbonyl group attached to the acetophenone is coordinating to the metal ion tightly, facilitating the formation of an eight-coordinate complex. Notably, there is no significant change in the spectrum with a variation of pD from 3 to 10, confirming that the complex remains in the form of SAP without interchanging to other structural isomers (or faster than the NMR timescale).

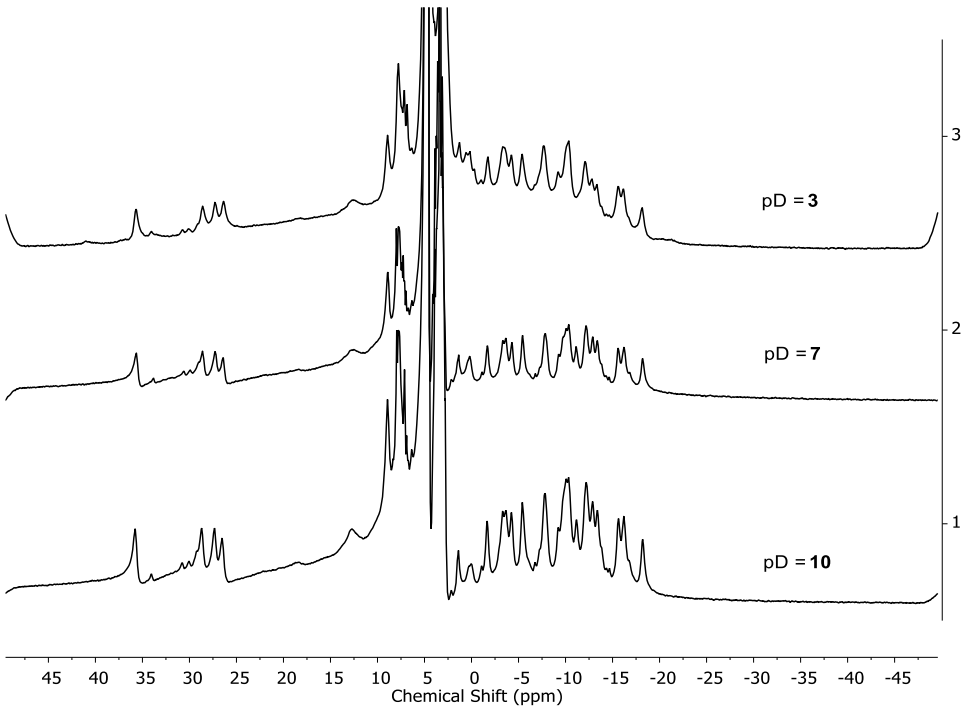


Figure 3-19. The ^{1}H-NMR spectrum of **3.39** registered in D_2O at RT with different pD.

The spectrum of ytterbium complex **3.41Yb** exhibits quite a unique scenario with two different sets of signals originating from two isomers in solution (axial protons between 90 and 140 ppm). The pD of the solution of the ytterbium complex was raised to 10 by adding sodium deuteroxide, resulting in the domination of one set of signals. This phenomenon may imply that the keto-enol tautomerism of ligand is more significant when binding to ytterbium, where the enolic form is dominating at higher pH. Hypothetically, this could be rationalised by the enhancement of interaction between ytterbium ion and carbonyl oxygen led by the strong interaction between the Lewis acidic ytterbium ion and the ketone of phenacyl chromophore (since ytterbium, being smaller than other open shell lanthanides, exhibits higher charge density and increased Lewis acidity). This validation of this assumption can be referred to as the 'mesomeric effect' discussed in chapter 2 in the case of halogenated-phenacylDO3A lanthanide complexes.

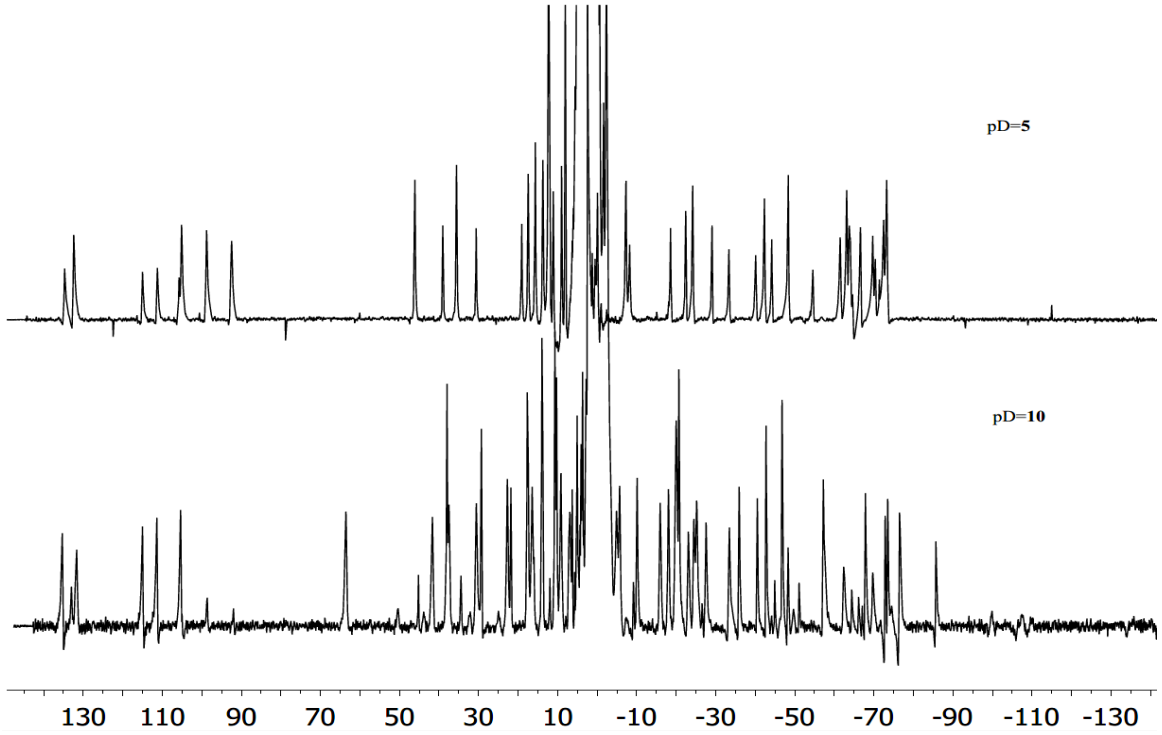


Figure 3-20. The ^{1}H-NMR spectrum of **3.41** registered in D_2O at RT with different pD.

3.5.4 Photophysical Studies

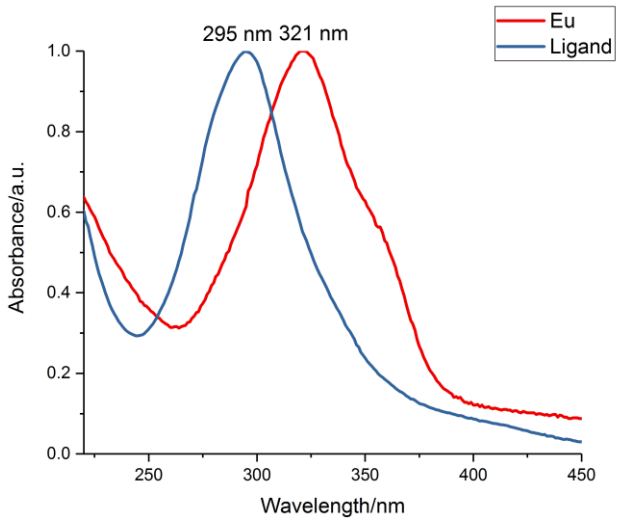


Figure 3-21. Comparison of the UV-Vis absorption spectra of ligand **3.38** (blue) and europium complex **3.39** in H_2O.

Figure 3-21 illustrates the comparison of UV-Vis absorption spectra of ligand and complex in water. The ligand exhibits a broad absorption band centred at 300 nm in aqueous solution which corresponds to the charge-transfer (CT) originating from aromatic moiety in phenacyl chromophore. Upon complexation a bathochromic shift can be observed in the absorption spectrum, indicating there is substantial interaction between the carbonyl group on the chromophore and lanthanide centre. The presence of electropositive lanthanide ion in the macrocyclic cavity facilitates the polarisation of carbonyl group while simultaneously stabilising the polar charge-transfer excited states, thus decreasing their energy.

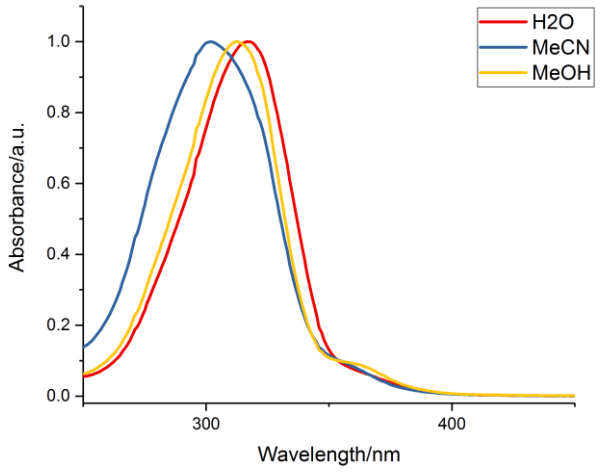


Figure 3-22. UV-Vis absorption spectra of europium(III) complex **3.39** in solvent with increasing polarity.

The solvatochromic effect was observed in the absorption spectra where the stock solution of complex was prepared in different solvent with increasing polarity. As shown in Figure 3-22, the major absorption band experienced a red shift when increasing the solvent polarity. This suggests the charge-transfer induced excited state is stabilised by the polar solvent. Therefore, the coordination of carbonyl oxygen to the metal centre plays a crucial

role in sensitising the lanthanide luminescence and forming the azidophenacylDO3A species.

In such coordination, the carbonyl group is polarised by the electropositive lanthanide ion, giving rise to the susceptibility to attack by a nucleophile (*e.g.* CN^-). Furthermore, it facilitates the energy transfer from chromophore to the metal centre, given the susceptibility to disrupt the chromophore, making it possible to reduce the effectiveness of energy transfer by removing the Dexter-type (through-bond) sensitisation mechanism. Thus, the carbonyl provides a possible route to detect the presence of cyanide species via monitoring the spectral changes.

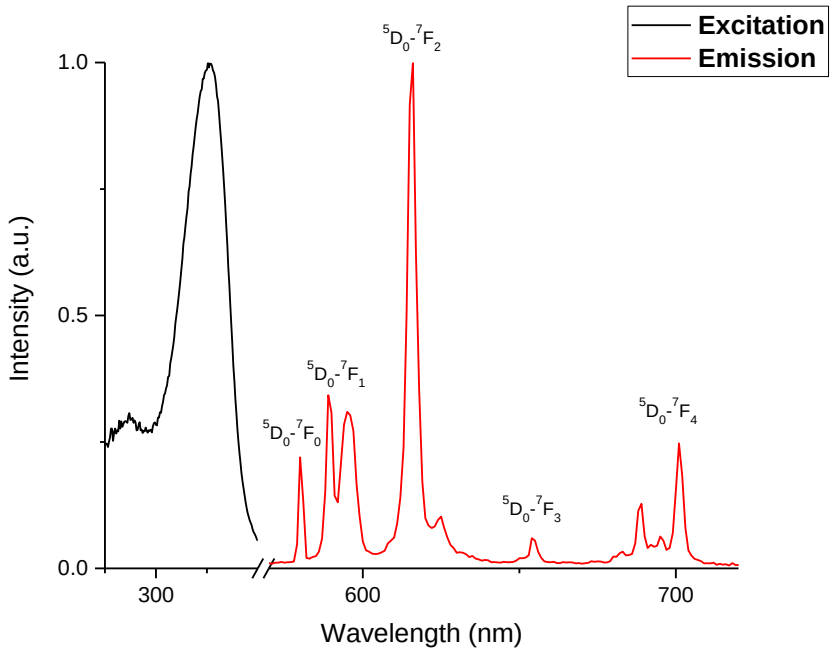


Figure 3-23. Excitation and emission spectrum of the Eu(III) complex **3.39** registered at 273K in H_2O

The europium complex exhibits a strong luminescence upon the excitation of the phenacyl chromophore. Notably, a single sharp $^5D_0 \rightarrow {}^7F_0$ transition was observed, which indicates that the Eu^{3+} ion exists as a single isomer with low symmetry (*e.g.* C_{nv}, C_n and C_s

symmetry).[17] Furthermore, the $^5D_0 \rightarrow {}^7F_2$ transition dominates the spectrum and the relative intensity to the $^5D_0 \rightarrow {}^7F_2$ transition $^5D_0 \rightarrow {}^7F_1$ is 1.7. This high intensity cannot just be attributed to the low symmetry of coordination site, but, more importantly, the high polarizability of azidophenacylDO3A ligand.[18] The excitation spectrum shows a relatively broad band which is extended to the visible region. By employing two-photon excitation microscopy, it is possible to use this molecule as an imaging agent under sensitisation by NIR light source. As shown in Table 3-4, the lifetimes of corresponding complexes in H_2O and D_2O were obtained by fitting the luminescent decay curve. From lifetimes, the hydration number $\boldsymbol{q}$ (the number of solvent molecules coordinated to the lanthanide centre) was determined by employing modified Horrocks' equation (Eqn 3.1).

$$\boldsymbol{q} = A(k_H - k_D - B) \qquad 3.1$$

The hydration number of **3.39Eu** implies that azidophenacylDO3A ligand is octadentate in water, where an average one water molecule saturated the lanthanide coordination sphere by directly coordinating to the metal centre. Through these studies, we can confirm that the phenacyl group indeed coordinates to the metal centre through the carbonyl group.

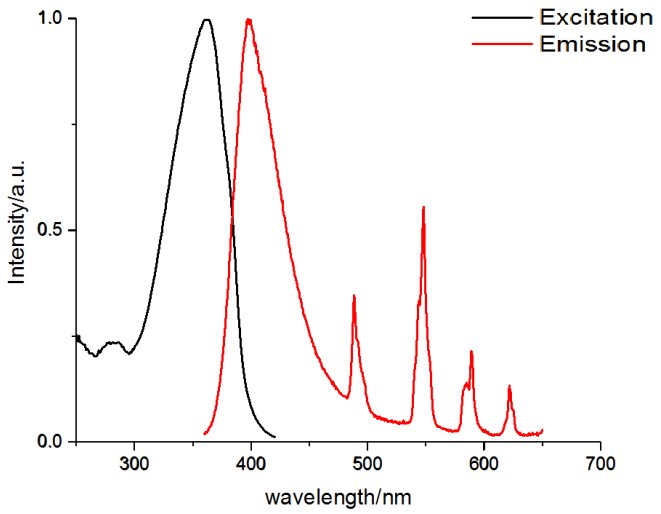


Figure 3-24. Excitation and emission spectrum of the Tb(III) complex **3.40** registered at 273K in H_2O

Complexes **3.39Eu** and **3.40Tb** have similar excitation profiles in aqueous media (both have a broad band centred at around 350 nm), while the emission spectra show an unusual band where a broad fluorescence peak originating from the phenacyl chromophore is overlapping with terbium luminescence. This indicates that the azidophenacyl cannot sensitise the emission of terbium efficiently. (Figure 3-24) Besides, DO3A-type Tb(III) complexes normally show luminescent lifetimes of the order of 2-3 ms in the deuterated solvent. The excited state lifetime of **3.40Tb** was found to be 1.02 ms in deuterium oxide, suggesting the emissive state of Tb^{3+} is deactivated by the non-radiative process, especially, back energy transfer. To investigate such a phenomenon, the spectrum of the terbium complex was taken in both aerated and deoxygenated condition.

This behaviour can be rationalised by the misalignment between the triplet state of the organic chromophore and the $^5D_4$ excited state of Tb(III), further evidenced by the observed intense fluorescence of aryl chromophore when exciting the molecule. Hypothetically, the luminescence of terbium ion could be quenched by energy back transfer from emissive states of Tb^{3+} to organic chromophore via thermal repopulation.

Table 3-4. Luminescence lifetime of the propargyl tris-phosphinate complexes **3.32Tb** and **3.32Tb+KCN** and corresponding hydration number **q.**

Compound	λ_{ex}/nm	λ_{ex}/nm	τ_{H2O}/μs	τ_{D2O}/μs	q
3.39(Eu)	300	615	421	1030	1.4[±0.2]
3.40(Tb)	305	545	650	1020	2.5[±0.5][III]

3.6 Preparation and study of Heterobimetallic arrays

3.6.1 Introduction

While a variety of alkynyl appended complexes were investigated in the previous section, further functionalisation is still required to access heterometallic complexes for ratiometric sensing of cyanide. In the presence of azidophenacylDO3A complexes, the alknyl group would easily undergo [3+2] cycloaddition with the azido group to afford pure heterometallic complexes in high selectivity. The mild reaction conditions would prevent transmetallation from occurring when forming the heterobimetallic species.

A series of heterometallic lanthanide complexes were prepared via CuAAC reactions and characterised by NMR spectroscopy and luminescent studies. In particular, these bimetallic complexes were examined to assess their ability to detect cyanide in a luminescence titration with potassium cyanide. The desired cyanide reporter should be able to exhibit the ratiometric response to the presence of cyanide, where the emission of one lanthanide centre is selectively quenched by cyanide, as a 'detection channel', while the other lanthanide centre remains constant as a 'reference channel'.

[III] The significant luminescence lifetime of the terbium(III) complex was the consequence of weak back energy transfer.

For a monometallic complex, the luminescence of a lanthanide ion is sensitised by a single antenna which responds to the presence of the analyte in solution, but it is nonetheless very difficult to determine the concentration of the analyte accurately unless the concentration of the complex itself is known. However, it would be much easier to employ a heterometallic system where the introduction of the analyte can perturb the energy transfer to only one lanthanide ion, while leaving the energy transfer pathway of the other lanthanide ion unaffected. In this chapter, the sensitisation of luminescence of the lanthanide complex containing a linear alkyne is more likely to be achieved by through-space mechanism (Förster mechanism) due to the lack of through-bond pathway available and no coordination between the alkyne group and the metal ion. The other azide-containing binding pocket has a ketone coordinating to the lanthanide ion, facilitating the energy transfer from chromophore to lanthanide ion via direct coordination, that is through-bond energy transfer pathway. Thus, it is reasonable that formation of conjugated linker between two lanthanide complexes will change the photophysical properties of two lanthanide systems, allowing possible through-bond and through-space communication to two individual lanthanide moieties, respectively.

Above all, the heterometallic complexes have the potential to be used as a ratiometric detector of cyanide. However, the sensitivity and accuracy should be both taken into consideration when examining the performance of these complexes regarding the detection of cyanide.

3.6.2 Synthesis

The preparation of heterobimetallic complexes was achieved via classical CuAAC ‘click’ reactions. The two lanthanide complexes and copper sulphate were dissolved in methanol and the Cu(I) catalyst was generated *in situ* by using sodium ascorbate to reduce Cu(II).

The conversion of click reaction was low by starting with 1:1 equivalent of azide and alkyne added and hence, excess alkyne was added to drive the reaction to completion. This issue could be rationalised by the bulky nature of phenacylDO3A precursor and low reactivity of the azide group. 'Freeze-pump-thaw' was used to eliminate the oxygen of the reaction vessel, and the reaction was conducted at 40 °C.

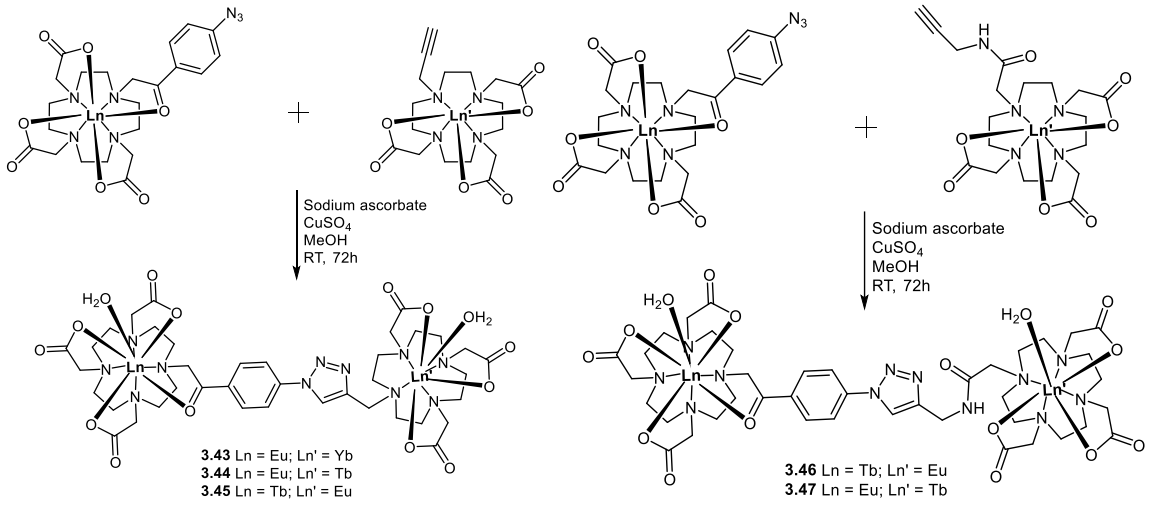


Figure 3-25. synthetic procedure for preparation of the heterometallic f-f' arrays.

Alternatively, for the click reactions, other polar solvents and different Cu(I) source were attempted but none of them improved the yield to the desired product. Dialysis was adopted to purify the targeted product by using 1000 MWCO cellulose membrane. This purification successfully removed the residue of lanthanide complex precursors and catalytic copper source, which can effectively quench the luminescence of lanthanides. Different methods of mass spectrometry failed to characterise the final product due to the demetallation of lanthanide ions induced by the ionisation process.

3.6.3 NMR Spectroscopy

The NMR study of these heterobimetallic complexes confirmed that each lanthanide resides in rigid binding moiety and that the coordination number of propargylDO3A precursors had increased to eight (both binding ligands are octadentate): each complex showed peaks with chemical shifts in regions corresponding to protons in the neighbourhood of the expected lanthanide ions. Compared to the propargyl precursors, the sharper peaks in ^{1}H-NMR spectra indicate that the barrier of interconversion between TSAP and SAP isomers has increased, and both binding centres are in the slow exchange between diastereoisomers on the NMR timescale. The ^{1}H-NMR spectrum of **3.43EuYb** (Figure 3-26) reveals that the most shifted resonances correspond to shifts related to ytterbium complexes, while the centre of the spectrum contains resonances corresponding to protons in the europium complex domain.

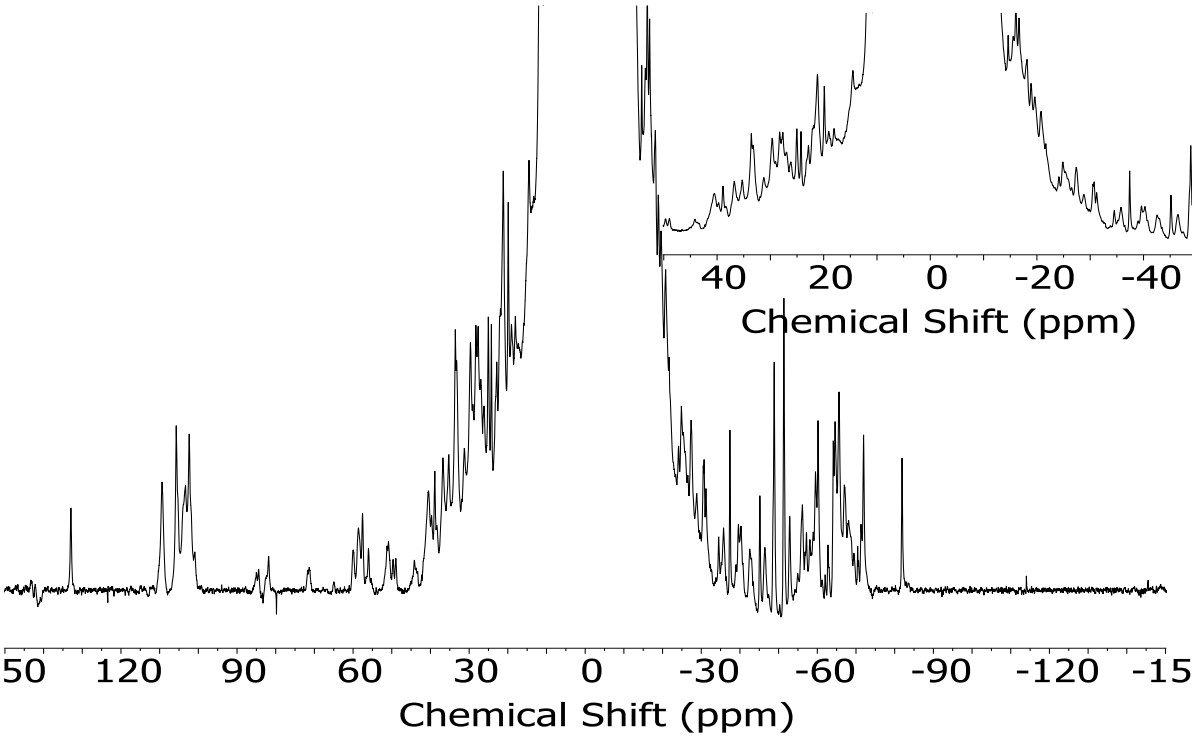


Figure 3-26. ^{1}H-NMR spectrum of **3.43EuYb** registered in D_2O at RT (pD 7)

If considering the resonance associated with axial protons on the ring, there are more diastereoisomers than would be seen in the NMR studies compared to the monometallic species since TSAP and SAP enantiomeric pairs in different binding pockets can be detected as NMR distinguishable species. In Figure 3-26, the spectrum of **3.43EuYb**, there are more than four peaks around 100 ppm corresponding to the axial protons on cyclen ring of the Yb^{III} complex, indicating the presence multiple isomers, whereas the resonances with a lower chemical shift at ca. 55 ppm can be accounted for the minor isomer (TSAP). Effectively it is clear that the second metal centre acts as a chiral auxiliary for the first: in the case of **3.43EuYb**, the introduction of Eu^{III} complex moiety results in another chiral centre on the Yb^{III} complex, leading to two different species regarding the Yb^{III} binding pocket. The paramagnetic signals ascribable to the Eu^{III} binding pocket are still distributed in the range between 50 ppm to -50 ppm while the resonance of protons near the Yb^{III} ion dominated the spectra of **3.43EuYb**.

In the case of propargylDO3A derivatives as precursors, it is obvious that the NMR spectra of the heterometallic product are significantly different from the azide and alkyne containing precursors, indicating the heterometallic complex undergoes dramatical structural changes upon the 'click' reaction. These changes result from the increase in coordination number of the propargyl-containing binding pocket, led by the formation of a triazole group, and the existence of two chiral centres, formed by the two lanthanide complexes containing the DO3A ligand. Theoretically, upon the formation of click product, a total of sixteen diastereoisomers in the solution can be detected by NMR, though it is obvious from the spectra some isomers are more favoured than the others.

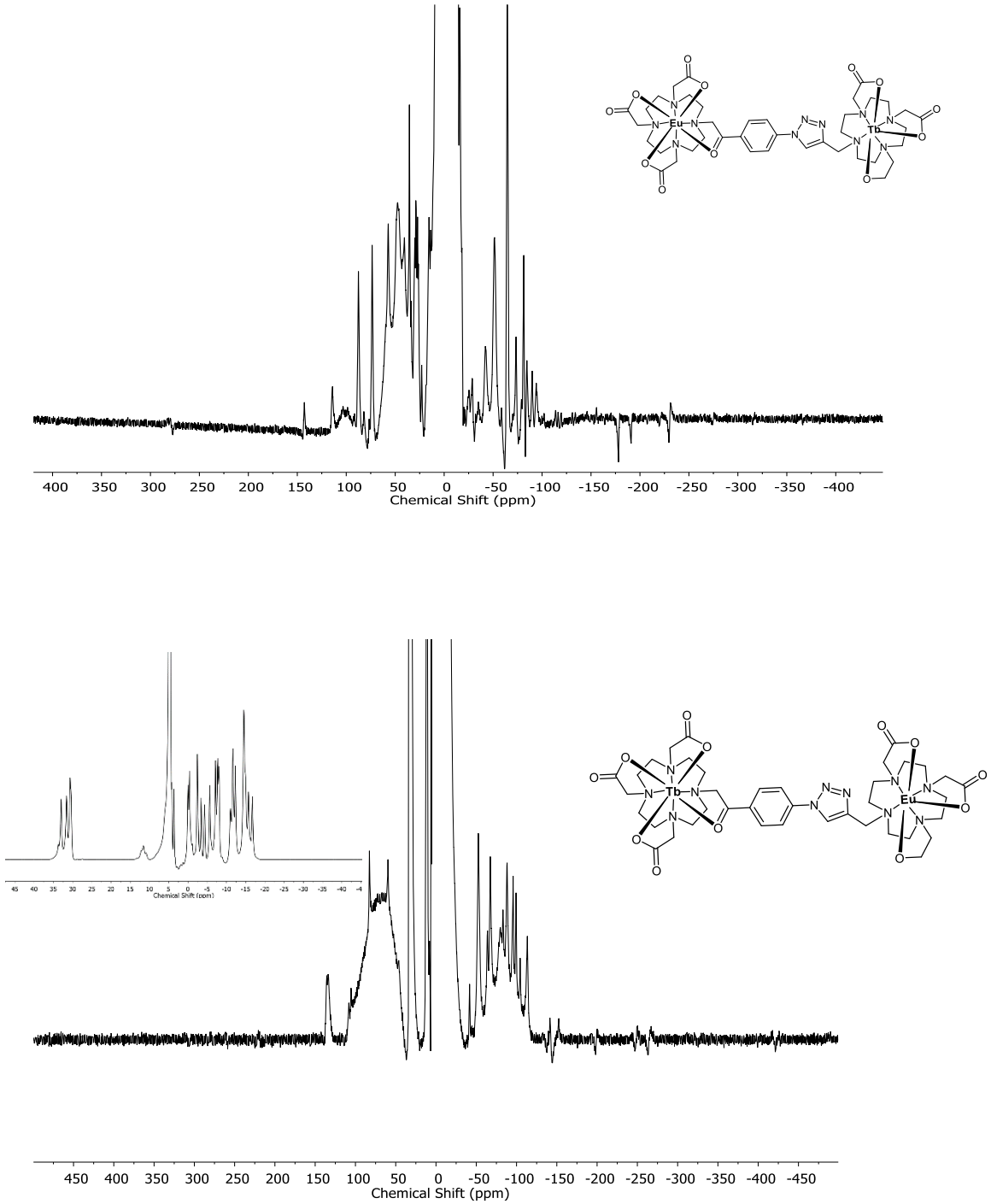


Figure 3-17. The ^{1}H-NMR spectrum of **3.44EuTb** (above) and **3.45TbEu** (below) registered in D_2O at RT (pD 7).

The comparison of the ^{1}H-NMR spectrum of **3.44EuTb** and **3.45TbEu** are presented in Figure 3-27. The ^{1}H-NMR spectrum of **3.45TbEu** shows the Eu^{III} binding site is dominated by the SAP geometry where only less than 5% of TSAP isomer was observed. In contrast, no geometric information can be acquired from the NMR spectrum of **3.44EuTb** since

signals of axial protons on europium(III) cyclen are subsumed by the broad resonances associated with terbium(III). It is clearly shown that two spectra are totally different, and the difference of their NMR properties are predominantly dependent on which lanthanide ion is in which binding pocket.

Heterometallic complexes **3.46TbEu** and **3.47EuTb** were prepared by using the amide-propargylDO3A (**3.10** and **3.11**) complex as precursor and following the 'click' reaction, the ^{1}H-NMR spectra reveal evidence for ring protons on the cyclen backbone: the resonances with reduced chemical shift are associated with europium moiety, and the wider-spread peaks are the protons closed to the terbium ion.

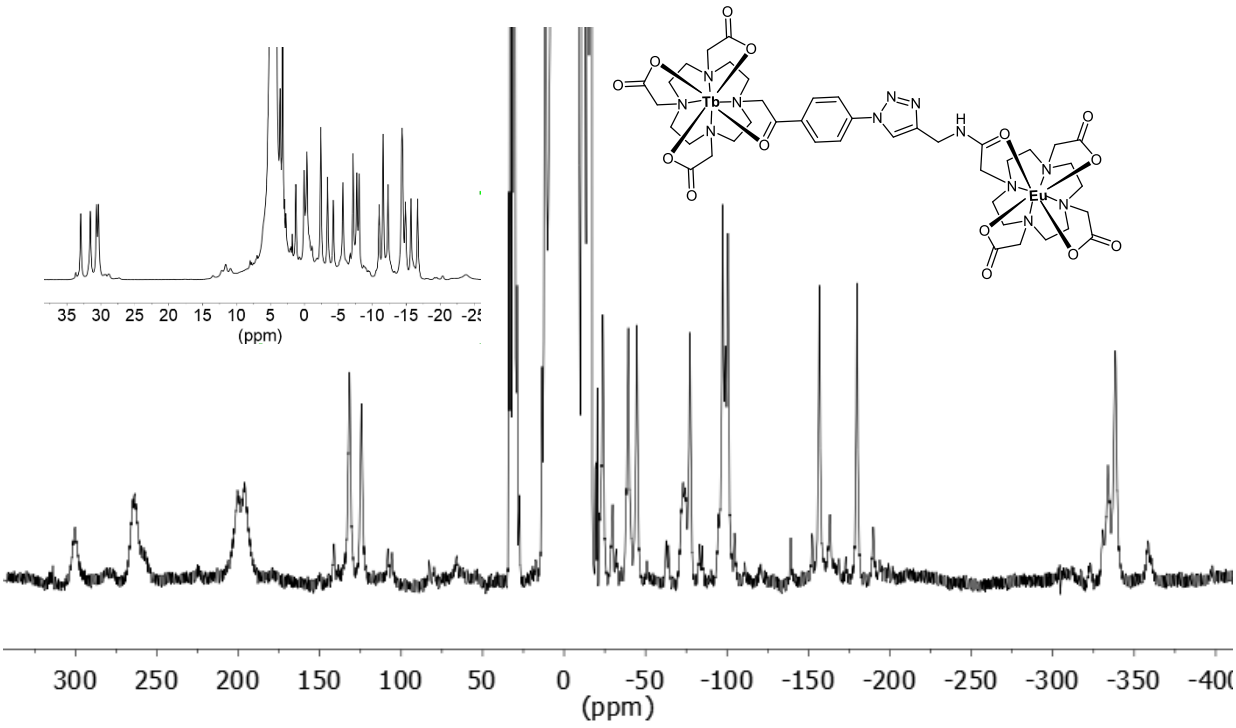


Figure 3-28. The ^{1}H-NMR spectrum of **3.46TbEu** registered in D_2O at RT (pD 7)

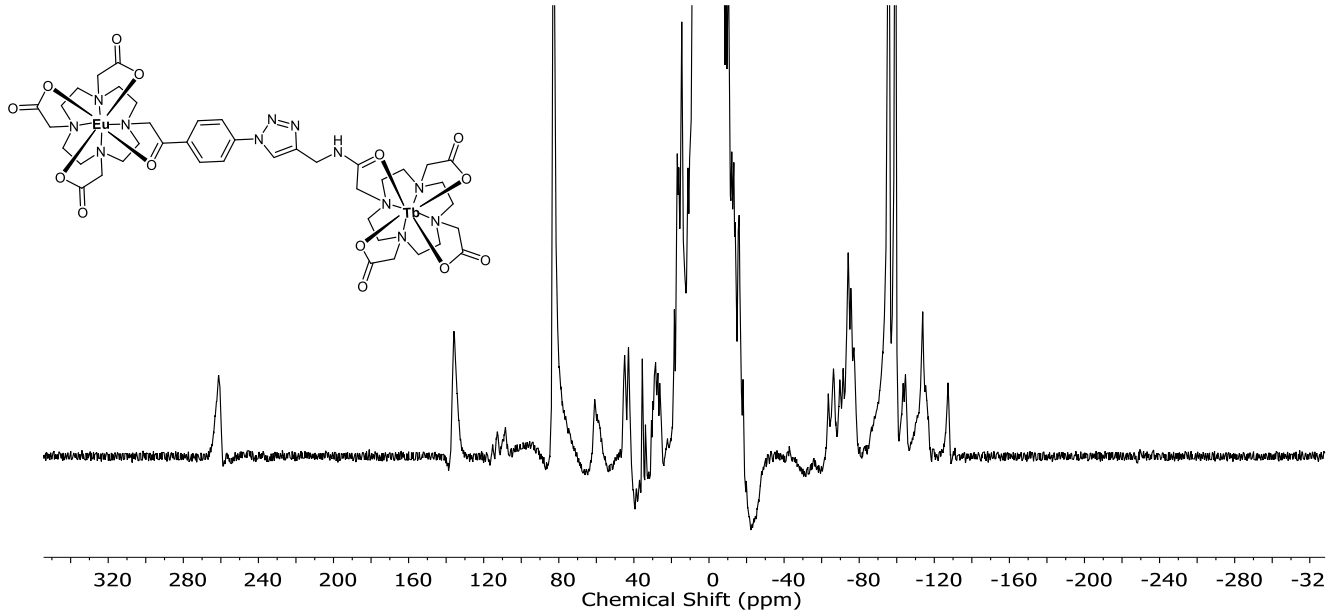


Figure 3-29. The ^{1}H-NMR spectrum of **3.47EuTb** registered in D_2O at RT (pD 7)

Nevertheless, the ^{1}H-NMR spectra of **3.46TbEu** and **3.47TbEu** reflect a totally different scenario compared to the bimetallic complexes being prepared from propargylDO3A complexes. For example, in complex **3.46EuTb**, the ^{1}H-NMR spectrum shows peaks corresponding to both europium and terbium binding pockets, and the SAP diastereoisomers dominate both europium binding sites (as shown in the inset of Figure 3-28). Compared to the mononuclear precursor complexes, no significant changes in the chemical shift was observed for both NMR spectra, which is different from the previous bimetallic complexes. In a paramagnetic system, it is expected that changes in the local environment would result in changes in the contribution of pseudocontact shift, hence leading to changes in the paramagnetic shift. Therefore, we can conclude that in this case, the formation of bimetallic complexes does not lead to obvious structural changes at either binding pocket.

In contrast, in the case of **3.47TbEu**, the ^{1}H-NMR spectrum reflects a reduction in contribution from pseudocontact shift by comparison with **3.46EuTb** analogue, where

europium(III) binding site exists in the form of both SAP and TSAP isomers. It is indicative that azide-containing binding pocket can make a greater contribution to the overall appearance of the NMR spectra probably due to chirality in the phenacyl appended arm given by the strong coordination of ketone oxygen to the metal centre.

3.6.4 Photophysical Cyanide binding studies

All bimetallic complexes and the precursor complexes are luminescent, and their photophysical properties were summarised in Table 3-5. Each bimetallic complex was characterised by using time-resolved fluorescence and UV-Vis absorption spectroscopy.

As shown in the Figure 3-30, excitation of the chromophore at 300 nm in **3.43EuYb** results in the population of emissive states for both lanthanide ions, leading to the sensitised emission in visible (Eu^{3+}) and near-IR (Yb^{3+}). The broad band centred at approximately 500 nm is attributable to the residual fluorescence from phenacyl-triazole manifold (which is difficult to remove by time gating owing to the similarity between the pulse length of the flash lamp and the lifetime of the ytterbium centred luminescence). More detailed information about the spectrum can be inferred from the europium(III) emission bands.

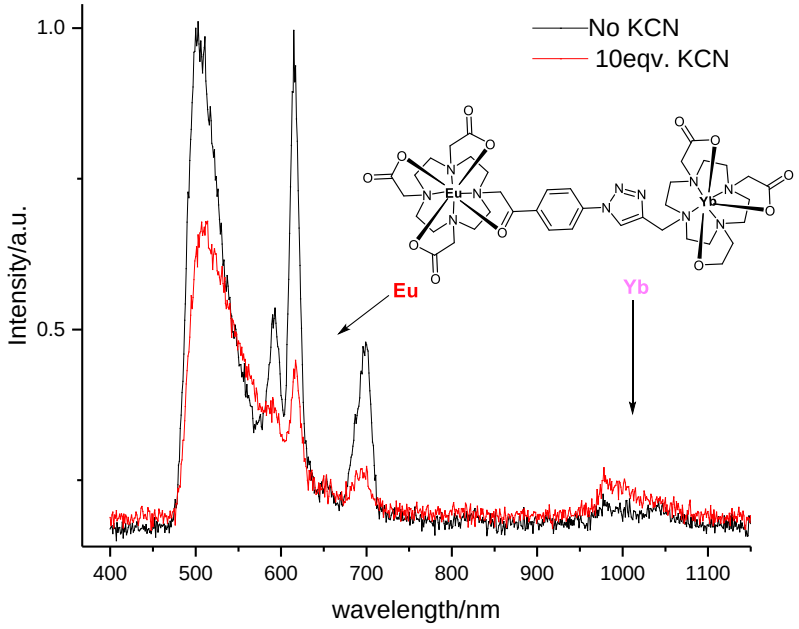


Figure 3-30. Changes in the **3.43EuYb** emission spectra in H_2O upon addition of KCN; I_{ex}=300 nm, exit slits 1 nm. Start of titration (black), end of titration (red; 1.5 eq.), and intermediate concentrations (gray) are shown.

As we previously discussed, in the azide-containing complex **3.39Eu**, the $[\Delta J = 2]$ transition dominates the emission spectrum. However, notable changes in the ratio in relative intensities $\frac{[\Delta J = 2]}{[\Delta J = 1]}$ is observed upon the coupling with propargylDO3A Yb^{III} complex via the 'click' reaction, since the transition $[\Delta J = 2]$ is hypersensitive to the changes in the local environment. The Yb-centred emission is observed in the near-IR region, and its intensity is relatively small compared to the europium(III) emission. The poor sensitisation of ytterbium ion could be explained by the large gap in energy between triplet excited of triazole and emissive state of Yb^{3+} ion, given by the high-energy emission of triazole moiety. Furthermore, hydration numbers were obtained by time-dependent luminescent studies and summarised in Table 3-5. From **3.39Eu** to **3.43EuYb**, decreased hydration number at the europium-containing binding site was observed, indicating there is an increase in steric hindrance around the Eu^{III} binding site.

The interaction between **3.43EuYb** and cyanide in water was explored by titration of cyanide into the complex solution. As shown in Figure 3-30, as expected, there is a dramatic reduction in the intensity of europium $^5D_0 \rightarrow {}^7F_0$, $^5D_0 \rightarrow {}^7F_1$, $^5D_0 \rightarrow {}^7F_2$ and $^5D_0 \rightarrow {}^7F_3$ transitions. Concurrently, a small increase in the intensity at Yb-centred emission was observed, which makes the ytterbium luminescence less than ideal as a reference signal-while ratiometric imaging would still be theoretically possible on the basis of the ratio between the intensities of europium and ytterbium centred emission bands. The cyanide ion cannot displace solvent from the metal centre (vide Chapter 2), and thus the enhanced luminescence from ytterbium arises from the change in the chromophore manifold if considering triazole as a sensitizer to Yb^{3+} ion. Indeed, the cyanohydrin formation removes an electron-withdrawing carbonyl group from conjugation with the chromophore, making a charge transfer mediated energy transfer pathway to Yb^{3+} ion more likely. Unfortunately, this hypothesis cannot be proved by detailed luminescent studies on Yb^{3+} ion, since the available time resolution is insufficient to monitor energy transfer through fast charge transfer processes. Although the binding of **3.43EuYb** to cyanide ion is promising, **3.43EuYb** offers limited scope as a ratiometric probe as a consequence of the dramatic difference in luminescence quantum yield between the two components.

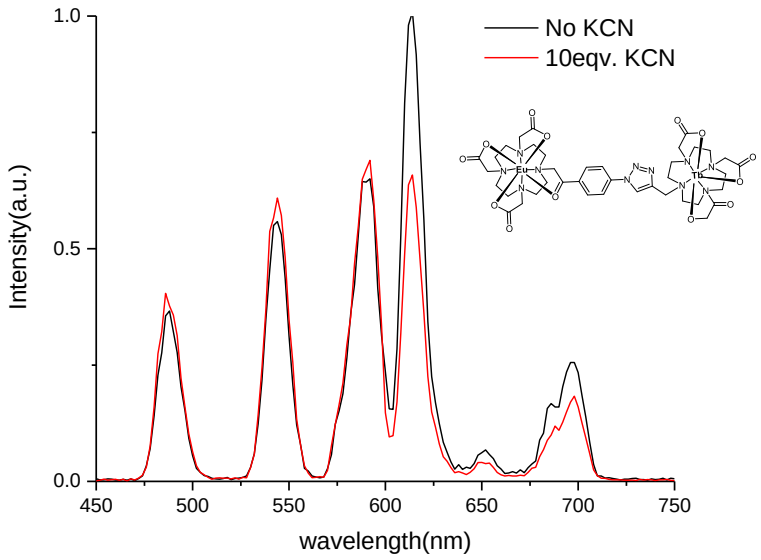


Figure 3-31. Changes in the **3.44EuTb** emission spectra in H_2O upon addition of KCN; I_{ex}=325 nm, exit slits 2 nm. Start of titration (black), end of titration (red; 2 eq.).

This issue can be overcome by using two lanthanide ions with similar quantum yields and lifetimes. As shown in Figure 3-31, a drastic reduction in the luminescent intensity of europium(III)-centred emission, especially for Eu: $^5D_0 \rightarrow {}^7F_2$ transition, the intensity decreased by a third. However, the signal of terbium^{III} emission is slightly enhanced with the addition of cyanide, indicating the effectiveness of energy transfer from bridging chromophore is increased due to the structural changes led by the cyanohydrin reaction. The luminescent lifetimes remained unchanged for both terbium^{III} and europium^{III} even upon adding an excess of cyanide, suggesting the no water from the inner coordination sphere is replaced by cyanide. Furthermore, the luminescent lifetimes of all bimetallic complexes are comparable with other DO3A-based lanthanide complexes, which demonstrates any unnecessary non-radiative process is eliminated in such a system.

Figure 3-32 shows the emission spectrum of complex **3.45TbEu**. The spectrum exhibits the characteristic europium and terbium luminescent bands covering the red and green region of visible wavelength, implying that the chromophore manifold can effectively sensitise the emission for both lanthanides as expected from the research from phenacylDO3A derivatives. The profile of europium(III) emission is similar to the complex where the $^5D_0 \rightarrow {}^7F_2$ transition dominates the luminescence spectra. Since the $^5D_0 \rightarrow {}^7F_1$ transition of europium(III) is overlapped with $^5D_4 \rightarrow {}^7F_5$ transition of terbium^{III}, the ratio of intensities of is thus compared with complex **3.43EuYb**. The intensity of terbium^{III} emission is comparable in magnitude to the europium(III) emission, indicating that the triplet excited state of triazole is higher in energy than excited states of terbium^{III} ion and thus triazole is an excellent sensitiser to populate the emissive states of terbium^{III}.

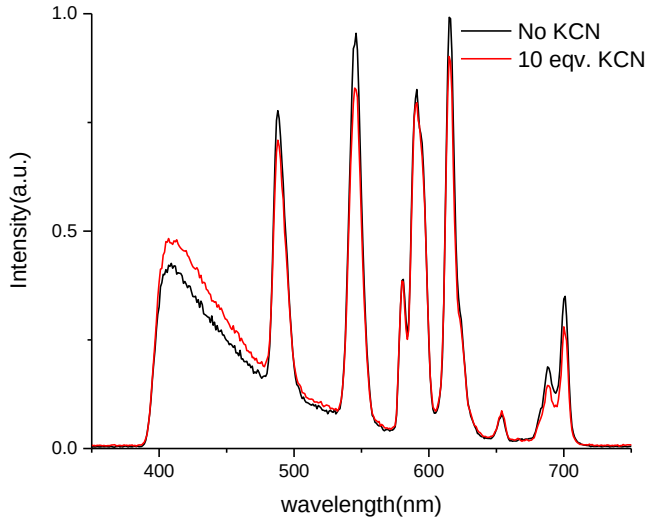


Figure 2-32. Changes in the **3.45TbEu** emission spectra in H_2O upon addition of KCN; I_{ex}=305 nm, exit slits 2 nm. Start of titration (black), end of titration (red; 2 equiv).

Table3-5. Luminescence lifetime of the bimetallic lanthanide complexes and corresponding hydration number **q.**

Compound	Ln	λ_{ex}/nm	λ_{em}/nm	τ_{H2O}/μs	τ_{D2O}/μs	q
3.43	**Eu**	300	615	471	1030	1.1[±0.1]
	Yb	300	980	<3	<3	
3.44	**Tb**	273	544	1767	2860	0.8[±0.1]
	Eu	325	701	464	1024	1.1[±0.1]
3.45	**Eu**	307	615	563	1466	1.0[±0.1]
	Tb	268	544	1050	1600	1.6[±0.1]
3.46	**Eu**	368	701	560	1910	1.2[±0.2]
	Tb	354	545	650	1020	2.5[±0.3]
3.47	**Eu**	374	701	562	1611	1.1[±0.1]
	Tb	350	545	660	990	2.2[±0.3]

We can conclude that bimetallic complexes derived from monometallic propargylDO3A complexes can effectively sensitise both lanthanide ions, and their emission profiles are different compared to the precursor complexes. Two bimetallic complexes (**3.43EuYb** and **3.44EuTb**) have been investigated and their binding performance towards cyanide examined. Although each complex demonstrated luminescence quenching from the phenacyl-containing binding site (detection channel) in the presence of cyanide, neither showed steady reference luminescence from the binding site near the triazole group (as would be desired from an ideal reference channel). The response from the "reference" channel could be the consequence of sensitisation being mediated through a mixture of through-space and through-bond mechanisms. Such bimetallic systems could be an excellent mean to develop heterobimetallic lanthanide complexes as ratiometric cyanide sensors. Additionally, it is possible to enhance the performance of the reference channel by making the sensitisation of the reference channel merely dependent on the through-space

mechanism (Forster mechanism). In particular, this could be achieved by extending the separation between the chromophore and the metal ion.

Bearing this in mind, two bimetallic complexes **3.46TbEu** and **3.47EuTb** derived from propargyl-amide complexes were prepared where the propargyl pendant arm incorporated an amide moiety and an aliphatic spacer to obviate the possibility of Dexter mediated energy transfer to one metal centre.

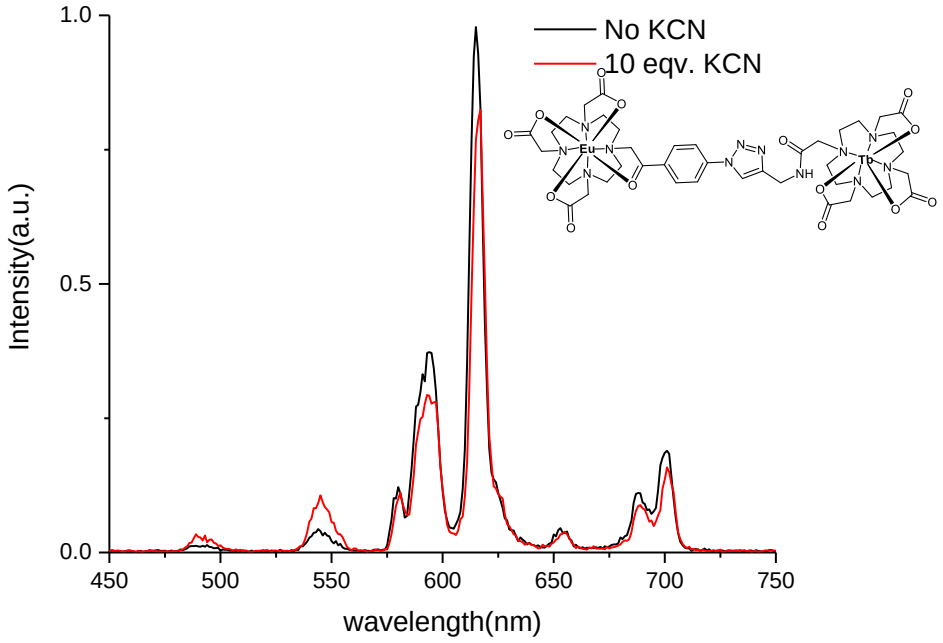


Figure 3-33. Changes in the **3.47TbEu** emission spectra in H_2O upon addition of KCN; I_{ex}=320 nm, exit slits 2 nm. Start of titration (black), end of titration (red; 2 eq).

3.47EuTb was prepared by coupling the europium(III) complex of azidophenacylDO3A and the terbium(III) complex of propargyl-amideDO3A, catalysed by Cu(I). Compared to its analogue **3.44EuTb**, the triazole group in complex **3.47EuTb** is further separated from terbium^{III} ion by an amide moiety, and the Figure 3-33 shows the luminescence intensity of terbium, as expected, is significantly weak comparable to the emission of europium, suggesting that the effectiveness of energy transfer from triazole to terbium^{III} is reduced by spatial distance. The addition of cyanide led to the reduction in luminescence intensity of

europium(III) centred emissions, whereas, an almost two-fold enhancement in the luminescent signal from terbium^{III} ion was observed, which is similar to the emission spectrum of complex **3.44EuTb**.

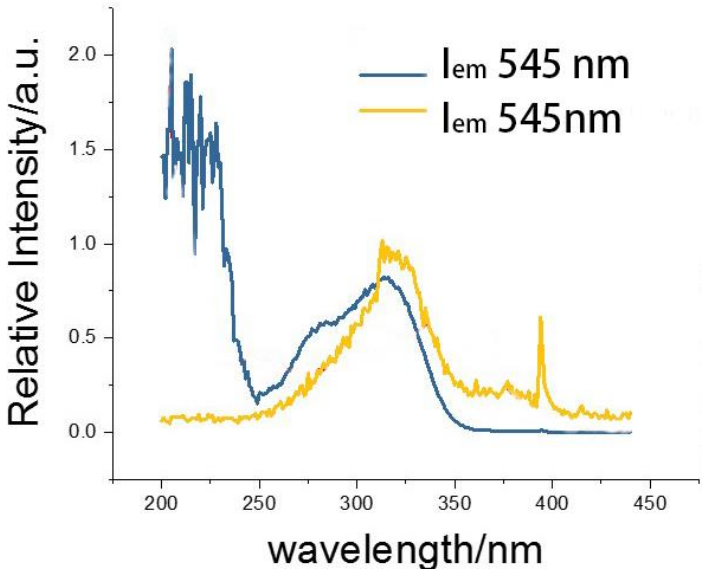


Figure 3-34. Left: excitation spectra registered in H_2O (6 x 10^{-4} M). Right: Simultaneous fluorescence excitation and emission spectra of **3.46TbEu** registered in H_2O (6 x 10^{-4} M).

There is a broad band centred at ca. 350 nm in the UV-Vis absorption spectrum of **3.46TbEu**, which can be attributed to the ILCT transition located on the phenacyl triazole moiety. The excitation spectrum was recorded by measuring the emission intensity at 545 nm (Tb^{3+}: $^5D_4 \rightarrow {}^7F_5$) and 700 nm ($Eu^{3+}$: $^5D_0 \rightarrow {}^7F_4$), respectively, implying the difference between the excitation spectra is dependent on the emission wavelength monitored. It worth noting that these excitation spectra indicate the sensitisation of europium and terbium emissive states are accomplished to different degrees, though the profile of the main

excitation band looks similar; emission of the terbium ion is more effectively sensitised by the phenacyl chromophore. Both lanthanide complexes exhibited strong luminescence when excited the organic chromophore around 350 nm. The spatial distance between the metal ion and the chromophore is relatively small, hence the sensitisation of lanthanide luminescence could be facilitated by the Dexter-mediated energy transfer pathway. Besides, the excitation spectra for europium^{III} ion displays the intensity of Eu^{III} sensitised emission ion is comparable in magnitude to the peak upon the direct sensitisation of Eu^{III} ion at 397 nm; this clearly reveals the sensitisation of Eu^{III} centred emission is achieved through an inefficient though-space energy transfer pathway originating from a remote chromophore.

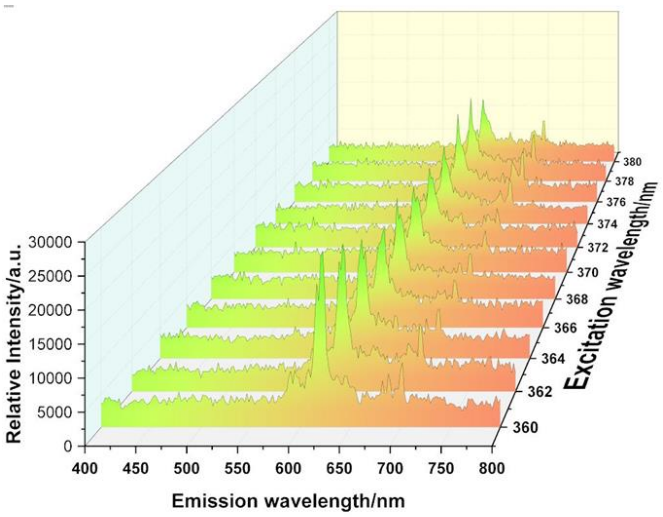


Figure 3-35. Simultaneous fluorescence excitation and emission of **3.46TbEu** recorded in H_2O. (exit slits = 2 nm)

It would be desirable to have an emission spectrum with a similar contribution from europium(III) and terbium(III) luminescence under single excitation at a certain wavelength. Therefore a 3D excitation-emission spectrum was obtained by varying the excitation wavelength from 360 to 380 nm. As shown in Figure 3-36, the wavelength of emission spread the majority of the visible spectrum extending from green to near-IR. The

emission from terbium(III) centre is significantly more intense than europium(III), indicating the sensitisation of europium(III)-centred emission is relatively weak.

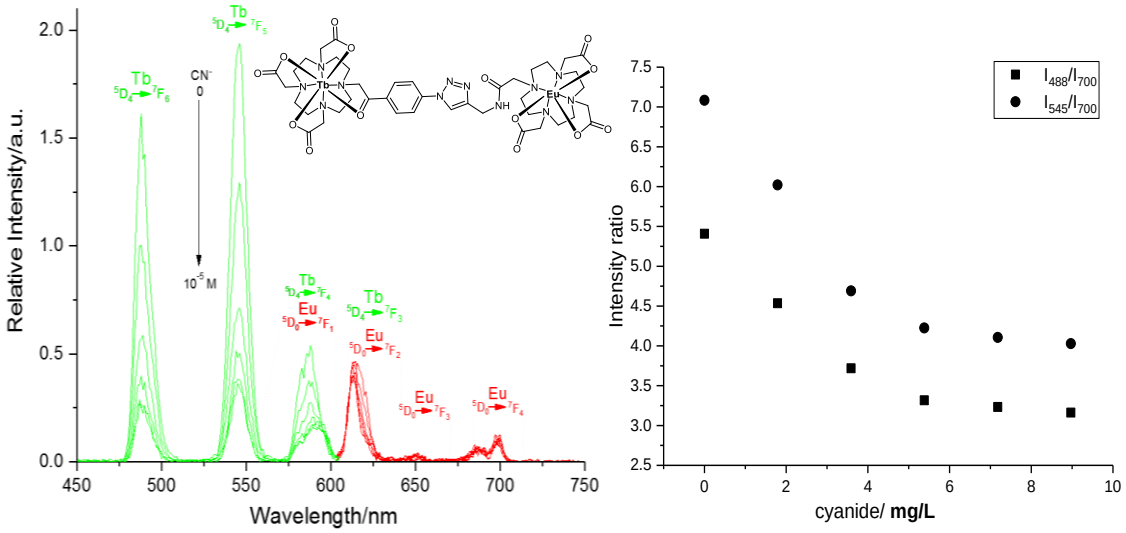


Figure 3-36. Left: Emission spectra of **3.46TbEu** (60 μM) in the presence of cyanide. (λ_{ex} = 360nm, exit slit = 5nm). Right: the ratios of intensity of Eu and Tb centred emission as a function of the concentration of cyanide in water.

The interaction between complex **3.46TbEu** and cyanide was then investigated in the aqueous solution. As shown in the Figure 3-36 dramatic reduction in the intensity of terbium(III)-centred emission (e.g., $^5D_4 \rightarrow {}^7F_6$ $^5D_4 \rightarrow {}^7F_5$ and $^5D_4 \rightarrow {}^7F_4$ transitions) was observed with addition of cyanide while the $^5D_0 \rightarrow {}^7F_4$ transition essentially keeps constant, thus suggesting that the luminescence of europium is possible to be used as an internal reference signal. To further investigate the cyanide binding event, the ratio of luminescence intensity of terbium (transition $^5D_4 \rightarrow {}^7F_j$, j = 4,5) to europium (transition $^5D_0 \rightarrow {}^7F_4$) was calculated, and the plot of the ratio of intensities and cyanide concentration is shown in Figure 3-36 (Right). The plot clearly indicates that the ratio is strongly dependent on the cyanide concentration, allowing the detection of cyanide in the water at the lowest 20 ppb.



Figure 3-37. Emission from aqueous solutions of **3.46TbEu** in the presence (left) and absence (right) of cyanide under UV illumination (366 nm)

These results have shown that the **3.46TbEu** is able to respond to cyanide ion ratiometrically, offering a potential method to quantify the cyanide in the practical context. Besides, the presence of cyanide can be directly visualised by illuminating the solutions under UV light irradiation (Figure 3-37).

3.7 Conclusion

In this chapter, a series of precursor lanthanide complexes have been prepared and their photophysical properties have been investigated. Four different alkyne-appended DO3A complexes were examined to explore the interaction with cyanide ion and two propargyl-containing complexes were employed to couple with azidophenacylDO3A complexes. Also, we can infer that, from the photophysical studies of azidophenacyl Tb^{III} complex, the formation of Tb^{III} emissive states is mediated via ILCT state. Derived from 4-halogenated phenacyl chromophore, azidophenacylDO3A complexes can be used as an analytical probe to detect cyanide and the presence of azido group can be exploited as a synthon, allowing further functionalization to prepare heterobimetallic f-f' arrays for ratiometric sensing purposes. A series of heterobimetallic lanthanide complexes were prepared by a 'click' reaction between alkyne-appended complexes and lanthanide complexes of azidophenacylDO3A. NMR spectroscopy and luminescent studies were applied to characterise and understand precursor complexes and 'click' products. It has been shown that for click reaction, the building blocks are kinetically stable, and this method can be exploited as an effective method to prepare heterobimetallic lanthanide complexes. Since there is no proof that the two metal ions can mutually communicate, the heterobimetallic arrays with two independent lanthanide centres could be explored to the development of luminescent probe with dual emission, where a reference channel can be directly incorporated into the cyanide detection channel, allowing quantification of cyanide via ratiometric response.

3.8 Reference

[1] M. P. Placidi, A. J. L. Villaraza, L. S. Natrajan, D. Sykes, A. M. Kenwright, S. Faulkner, *J. Am. Chem. Soc.* **2009**, *131*, 9916–9917.

[2] M. Jauregui, W. S. Perry, C. Allain, L. R. Vidler, M. C. Willis, A. M. Kenwright, J. S. Snaith, G. J. Stasiuk, M. P. Lowe, S. Faulkner, *J. Chem. Soc. Dalt. Trans.* **2009**, 6283–6285.

[3] R. F. H. Viguier, A. N. Hulme, *J. Am. Chem. Soc.* **2006**, *128*, 11370–11371.

[4] G. J. Stasiuk, M. P. Lowe, *Dalt. Trans.* **2009**, 9725–9727.

[5] M. A. M. Filho, J. D. L. Dutra, G. B. Rocha, R. O. Freire, A. M. Simas, *RSC Adv.* **2013**, *3*, 16747–16755.

[6] A. V. M. de Andrade, N. B. da Costa, A. M. Simas, G. F. de Sá, *Chem. Phys. Lett.* **1994**, *227*, 349–353.

[7] M.C.Zerner, *Univ. Florida, Gainesville, FL* **1990**, 32611.

[8] A. V. M. De Andrade, N. B. Da Costa, O. L. Malta, R. L. Longo, A. M. Simas, G. F. De Sá, *J. Alloys Compd.* **1997**, *250*, 412–416.

[9] C. Allain, P. D. Beer, S. Faulkner, M. W. Jones, A. M. Kenwright, N. L. Kilah, R. C. Knighton, T. J. Sørensen, M. Tropiano, *Chem. Sci.* **2013**, *4*, 489–493.

[10] M. Tropiano, A. M. Kenwright, S. Faulkner, *Chem. - A Eur. J.* **2015**, *21*, 5697–5699.

[11] É. Tóth, R. Király, J. Platzek, B. Radüchel, E. Brücher, *Inorganica Chim. Acta* **1996**, *249*, 191–199.

[12] W. S. Perry, S. J. A. Pope, C. Allain, B. J. Coe, A. M. Kenwright, S. Faulkner, *Dalt. Trans.* **2010**, *39*, 10974–10983.

[13] R. M. Supkowski, W. D. W. Horrocks, *Inorganica Chim. Acta* **2002**, *340*, 44–48.

[14] M. Woods, G. E. Kiefer, S. Bott, A. Castillo-Muzquiz, C. Eshelbrenner, L. Michaudet, K. McMillan, S. D. K. Mudigunda, D. Ogrin, G. Tircsó, et al., *J. Am. Chem. Soc.* **2004**, *126*, 9248–9256.

[15] K. Barral, A. D. Moorhouse, J. E. Moses, *Org. Lett.* **2007**, *9*, 1809–1811.

[16] J. C. Lee, Y. H. Bae, S. K. Chang, *Bull. Korean Chem. Soc.* **2003**, *24*, 407–408.

[17] K. Binnemans, *Coord. Chem. Rev.* **2015**, *295*, 1–45.

[18] A. F. Kirby, F. S. Richardson, *J. Phys. Chem.* **2005**, *87*, 2544–2556.

4 Novel Rotaxane Ligands for Lanthanide Complexation

4.1 Introduction

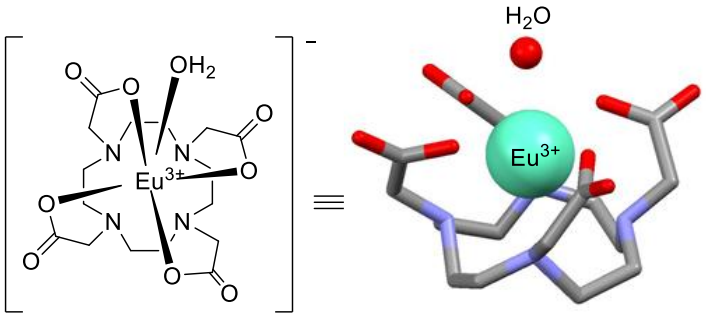
Although lanthanide complexes have been extensively investigated over the past decades due to their potential as luminescent materials and contrast media, examples related to the direct coordination between a supramolecular ligand and a lanthanide ion are rare, particularly for interlocked molecules. Herein, we outline a series of novel supramolecular ligands which can be directly coordinated to lanthanide metal ions with moderate affinity, by using donor atoms from both components in a mechanically interlocked structure. The rotaxane possesses a rigid macrocycle containing triazole group, where this chromophore can sensitise the emission of the lanthanide. All three ligands proved effective in complexing and sensitising lanthanide metals as a result of strong emission in the green region (e.g. Tb^{3+}). Significant improvement in association constant was also observed by tuning the size of rotaxane macrocycle and the number of carboxylate arms.

As we discussed in the introduction chapter, luminescent lanthanide complexes have been attracting considerable attention for many areas on account of their sharp emission bands, micro-second scale lifetimes and versatile luminescence, making lanthanides promising optical materials in many applications such as displays and lasers. Especially, lanthanide complexes responding to certain biological species (e.g. F^-, Ca^{2+}) could be extremely desirable for potential medical applications. Such highly-emissive and analyte responsive lanthanide complexes require selection of a suitable chromophore and elaborate design of the analyte binding cavity. The development of analyte-responsive lanthanide complexes

remains a significant challenge due to the difficulty in purification and the hard metal nature of lanthanide ions.

The emergence of supramolecular chemistry has offered a solution to analyte-responsive lanthanide complexes. Anion-responsive supramolecular structures are becoming gradually attractive due to their versatile anion recognition sites with different degrees of selectivity. To the best of our knowledge, there is no rotaxane ligands directly complexing lanthanide metals have been reported so far.

A number of ligands for binding with lanthanide ions have been prepared and investigated over the last four decades. Polyaminocarboxylate-based macrocyclic ligands such as 1,4,7,10-tetraazacyclododecane-1,4,7,10-tetraacetic acid (DOTA) exhibit excellent kinetic and thermodynamic stability in binding with lanthanide ions due to the macrocyclic effect and the nature of strong donor atoms. Four secondary amine groups of cyclen (a 12-membered tetraazacyclodecane macrocycle) are further modified by incorporating with N-CH_2CO_2H groups to give DOTA. For instance, the structure of an Eu.DOTA complex is represented in Scheme 4-1. Given the crystal structure, the Eu^{3+} ion is bound with four nitrogen atoms and wrapped by four carboxyl oxygen atoms where a water molecule is coordinated to the Eu^{3+} ion in the axial position. Lanthanide DOTA complexes hence demonstrate greater stability due to the macrocyclic effect compared to the acyclic analogues EDTA (ethylenediaminetetraacetic acid). [1,2]



Scheme 4-1. The chemical structure and crystal structure of $[Eu.DOTA]^-$ complex[3]

Although several lanthanide complexes containing supramolecular ligands have been reported[4,5], examples of lanthanide direct binding with interlocked ligands are still rare. Beer and co-workers are pioneers for reporting the first complex of a [2]rotaxane binding with lanthanide. As illustrated below (Figure 4-1 (a)[6]) propargylDO3A europium complex is covalently linked to a [2]rotaxane via CuAAC reaction, demonstrating response to the presence of Cl^-. Besides, lanthanide rotaxanes can be prepared by using anion/lanthanide ion template to form pseudo-rotaxanes or lanthanide-cation templates by using the 'stoppering' methodology. (Figure 4.1(b)[7] and (c)[8]).

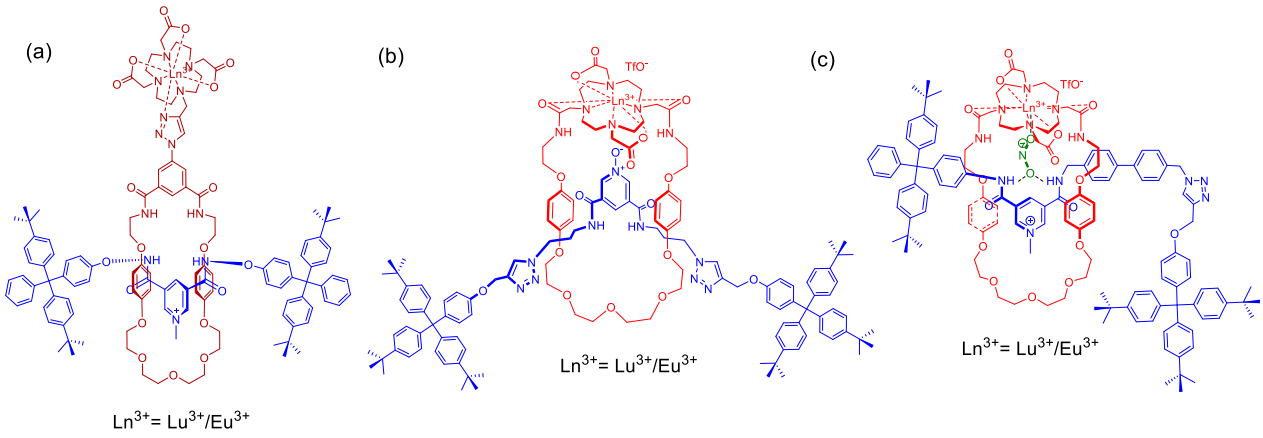


Figure 4-1. (a) Crystal structure of Leigh's Eu-containing knots; (b) structure of a europium(III)-[3]catenane.

Other than DO3A complexes, a number of rotaxane-containing lanthanide complexes were prepared using a 2, 6-pyridinedicarboxamide. Leigh and co-workers[9,10] reported the preparation of trefoil knots facilitated by the interactions between a lanthanide ion and three 2,6-pyridinedicarboxamide ligands (Figure 4-2(a)). Gunnlaugsson and co-workers also published the supramolecular lanthanide complexes containing interlocked [2] and [3] catenanes using ring-closing metathesis reactions, though the purification of these two components seems to be difficult due to the similar chemical properties between the [2] and [3] catenanes (Figure 4-2 (b)). [11]

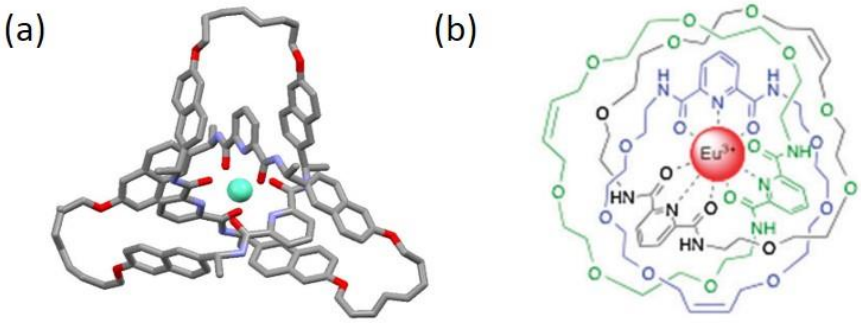


Figure 4-2. (a) Crystal structure of Leigh's Eu-containing knots[10]; (b) structure of a europium(III)-[3]catenane.[11]

Bearing this in mind, a supramolecular ligand containing a rotaxane structure was carefully designed and synthesised. The macrocycle component of the rotaxane, incorporating nitrogen and oxygen donor atoms, can interact with the Lewis acidic lanthanide ion. Furthermore, carboxylic acid pendant chains on the rotaxane axle can increase the negative charge density around the metal ion, thus potentially giving rise to a stronger electrostatic interaction between the lanthanide and the ligand.[12] Figure 4.3 shows a representation of how such cooperative interactions might work in practice.

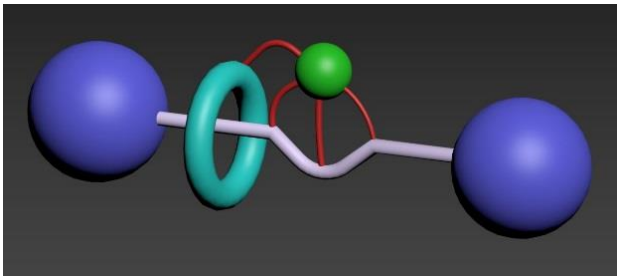


Figure 4-3. Cartoon representation of rotaxane-lanthanide complex.

Additionally, the triazole which results from the copper catalysed click reaction is used to clip the rotaxane macrocycle together, is an effective and simple sensitising chromophore for a proximate lanthanide. Similar triazoles have already been shown to sensitise luminescence from a wide variety of lanthanide ions from the visible emitter with high-energy excited states to NIR region.[13,14] The rotaxane ring closure was achieved by click reaction, employing phenyl group and triazole as a sensitiser to lanthanide ions, giving rise to the multiple energy transfer pathways.

4.2 Origin of the design and strategy of synthesis

Although several cases of lanthanide incorporating interlocked structures have been reported, they all employed the well-developed ligands (e.g. DO3A) as binding sites for accommodating lanthanide ions. To the best of our knowledge, interlocked ligands designed explicitly for lanthanide complexation are unprecedented. This chapter will mainly focus on the synthesis and lanthanide ion binding studies of such novel rotaxane ligands.

The design of the rotaxane host was informed by the structure of DOTA complexes. In DOTA, the four secondary amine groups of cyclen are further modified by the addition of

N-CH_2CO_2H groups, giving an octadentate ligand which forms an array of five-membered chelate rings around the host lanthanide. The relative rigidity of the macrocycle backbone and the need for a concerted motion of the molecule to release the lanthanide gives rise to kinetic as well as thermodynamic stability. Since DOTA was first used for lanthanide complexation, there have been numerous reported modifications of the ligands, including replacement of carboxylate arms for other flexible chains (e.g., amides) or altering the size of the macrocycle. However, all these structural modifications are limited in using covalent bonds to link multiple ligands. On the other hand, the structural possibilities of multiple ligands linked by mechanical bonds have been overlooked for a long time. These structures were found to be rigid as a consequence of their compact structures, hence offering new ways to control the local coordination environment.

In this project, the main idea is to replace some of the covalent bonds of the cyclen cycle in DOTA by mechanical bonds which can be formed in a [2]rotaxane (Figure 4.4). Also, it is possible to modulate the binding affinity for lanthanide ions by changing the number of binding sites and the size of macrocycles.

Despite the existence of lanthanide-containing interlocked structures, all these examples use the well-developed/studied ligands (e.g. DO3A and 2,6-pyridinedicarboxamide) for lanthanide complexation and rotaxanes bearing three-dimensional cavities for lanthanide complexation are unprecedented. This project will mainly focus on the synthesis and Ln^{3+} binding studies of novel rotaxane ligands.

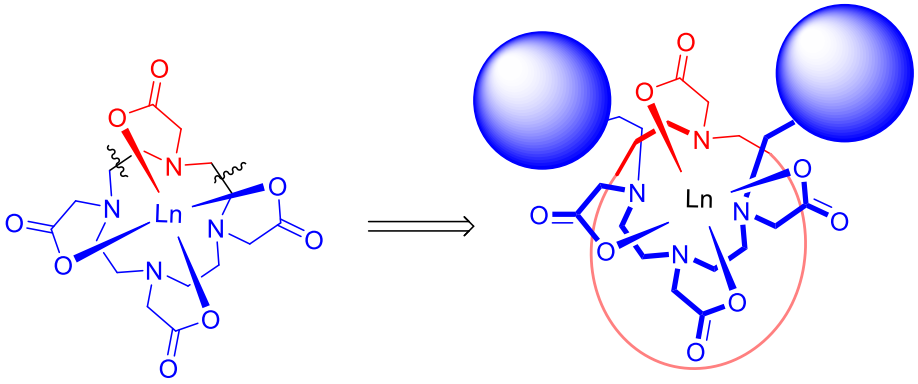
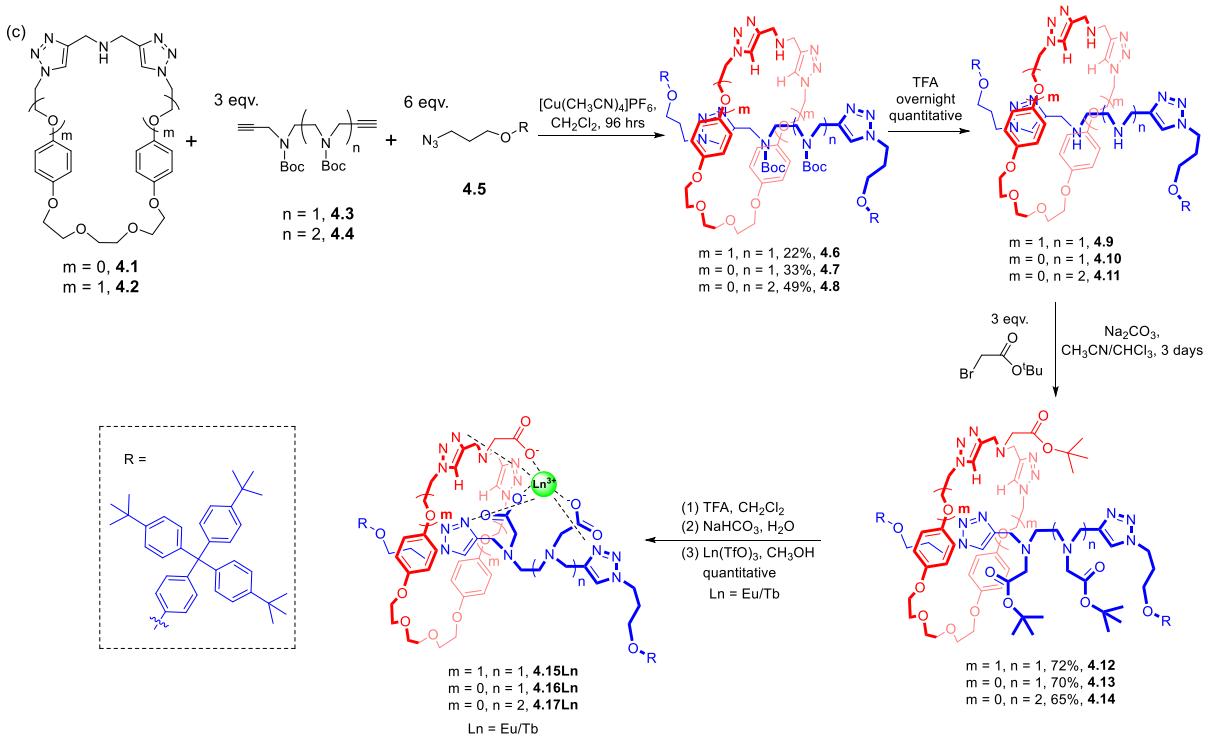


Figure 4-4. The graphic illustration of idea of novel rotaxane ligands for lanthanide complexation

4.3 Synthesis of the ligating rotaxane



Scheme 4-2. Synthesis of rotaxanes-lanthanide complexes.

The synthesis of the rotaxane-appended ligand was carried out by Dr Xiaoxiong Li, a member of the Beer group in Oxford. As shown in Scheme 4-1, target rotaxanes were prepared through an azide-alkyne cycloaddition active-metal template (CuAAC-AMT)

method consisting of rotaxane synthesis – deprotection – post-rotaxane functionalisation. The macrocycle components **4.1** and **4.2** were prepared by 'clicking' dipropargyl alkyne and bis azide. This macrocycle was incorporated with a triazole moiety, which can facilitate the formation of the mechanical bond. By comparing the ^{1}H NMR spectra of macrocycle **4.1**, rotaxane **4.7** and the corresponding free axle component (which was isolated as a by-product from the AMT rotaxane forming reaction), the interlocked nature of **4.6** was confirmed from the evidence of upfield shifts of macrocycle component hydroquinone proton signals, arising from the aromatic π- π donor-acceptor interactions with the electron-deficient triazole motifs on the axle. After removal of *N*-Boc-protecting groups, the proton signals become quite sharp and display assignable coupling patterns due to the elimination of the slow exchange N-CO bond rotation process of the N-Boc moieties. However, the appendage of three methylene tert-butyl acetate groups resulted in the rotaxane adopting an unsymmetric co-conformation as evidenced by the signal splitting in the ^{1}H NMR spectrum of **4.12**. Also, the alkyl proton signals in the region between 3.0 – 4.5 ppm become more complicated and difficult to interpret compared to rotaxane **4.9**. This indicates that the macrocycle is stationed on one side of the axle and cannot shuttle along the axle freely.

Removal of the tert-butyl protecting groups using trifluoroacetic acid, followed by washing with saturated $NaHCO_3$ solution, afforded the trianionic-rotaxane sodium salt **4.15**, **4.16** and **4.17**. The ^{1}H-NMR spectrum of the ligand **4.17** clearly shows the disappearance of the tert-butyl signals and mass spectrometry also confirms the generation of target rotaxanes.

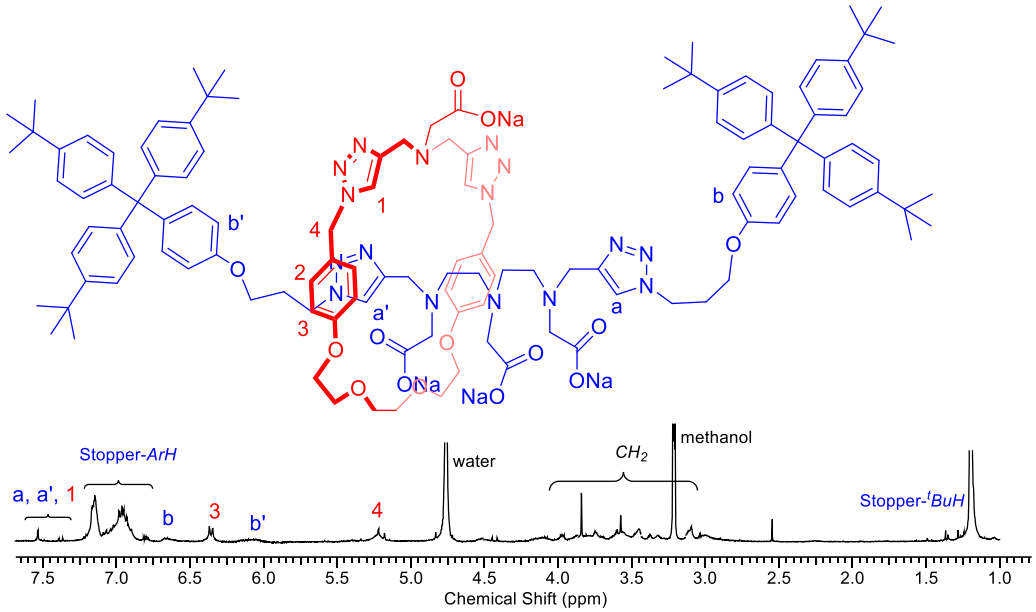


Figure 4-5.The ^{1}H-NMR spectrum of ligand **4.17** in CD_3OD (T = 298 K).

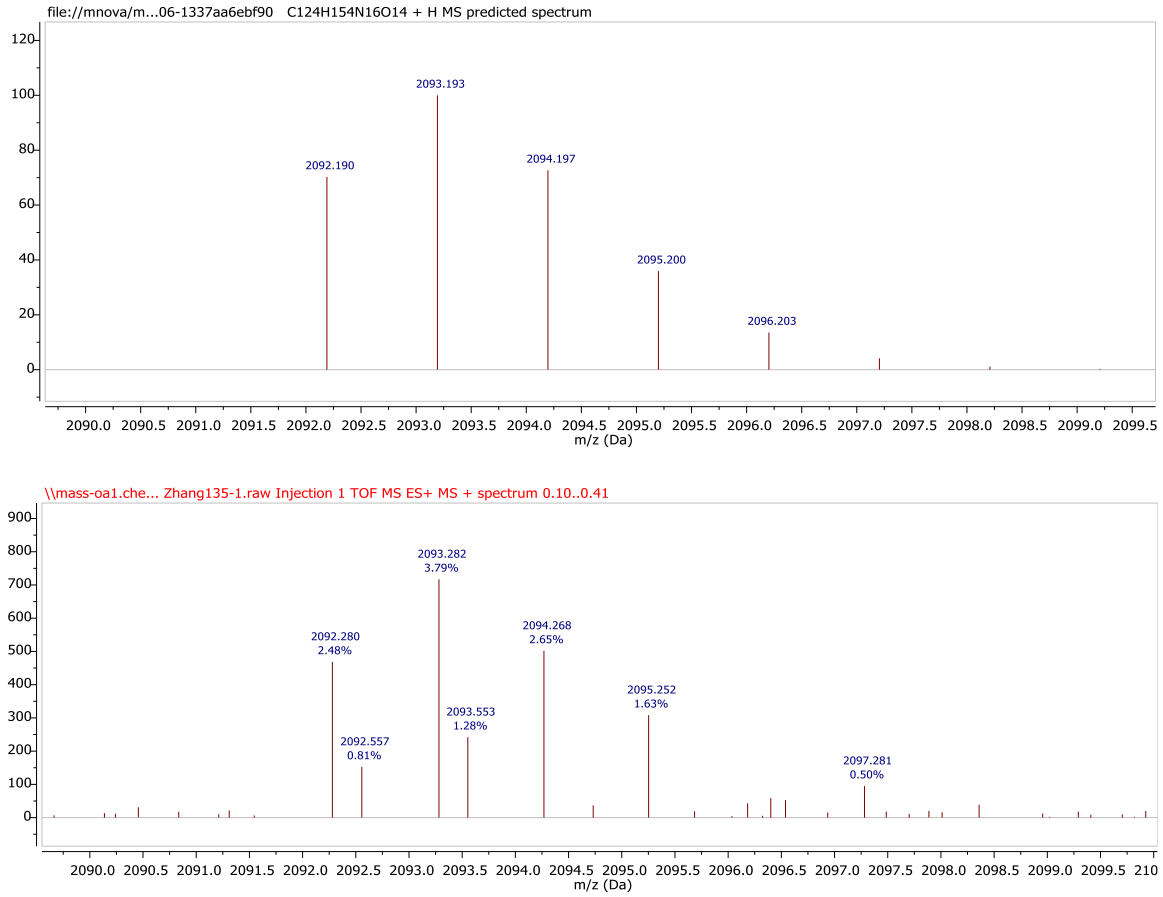


Figure 4-6. Mass spectrometry of rotaxane **4.17** (top) theoretical (bottom) experimental

Finally, complexation was carried out in methanol: dichloromethane (10:1) solvent mixture. This was achieved by mixing the ligand and corresponding lanthanide triflate at 60°C with a slight excess of lanthanide triflate. After the reaction was completed, the resulting mixture was concentrated and dried under vacuum, followed by altering the pH to basic by adding sodium hydroxide solution. The excess lanthanide triflate salt was removed by filtration. The filtrate was dried by freeze dryer to yield the targeted product as pale yellow solid. The product was characterised by ^{1}H-NMR spectroscopy and TOF-MS. The mass spectrum clearly exhibited the disappearance of the peak ascribed to the starting rotaxane ligand and the emergence of a new peak corresponding to the formation of the complex.

4.4 Structure optimisation

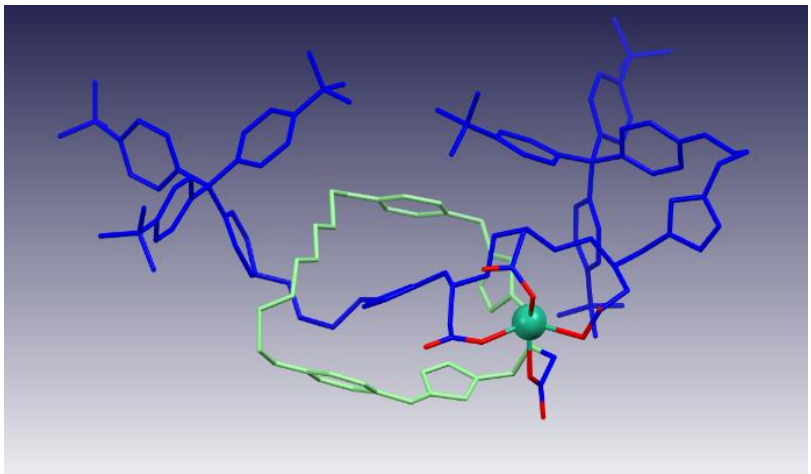
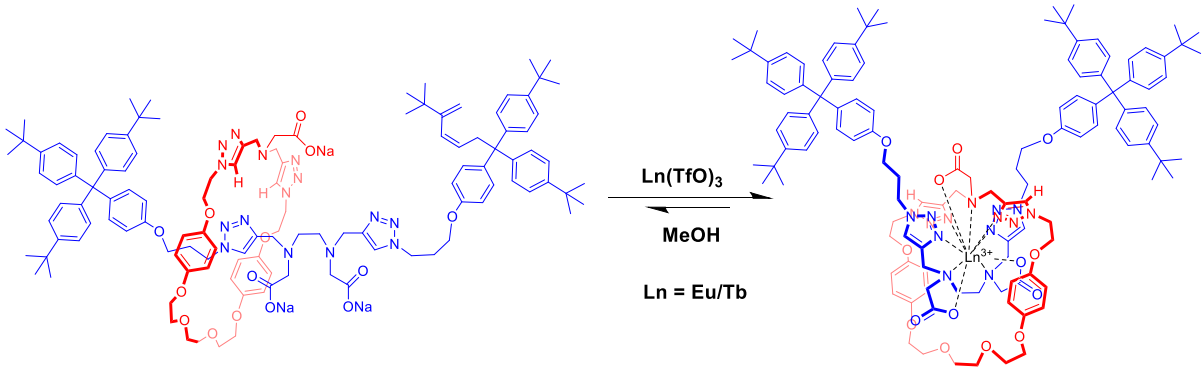


Figure 4-7. Computational structure of **4.17**Tb (MOPAC2016)

To further understand the complex, MOPAC 2016 was used to optimize the structure of **4.19Tb**. MOPAC is a computational chemistry package that can be used to study lanthanide complexes on the basis of Dewar and Thiel's NDDO approximation. In this case, MOPAC was implemented with Sparkle Model parameters with RM1, which is one of the most

accurate semi-empirical molecular orbital models.[15] This approach was used to predict the geometry of **4.19Tb**. Compared to conventional DFT method, MOPAC has certain advantages like low computational cost and relatively high accuracy. Taking into account of computational cost, we sought to predict the structure of **4.19Tb** with MOPAC Sparkle/RM1 model.[16] The optimized structure demonstrates the binding site is not happening inside the macrocycle ring, leading to weaker binding ability compared to the conventional ligand, which can be rationalized by the steric effect and bulky nature of the ligand. The average bond length between Tb^{3+} and the carboxylic oxygen atoms is 2.23 Å on average, which is relatively close to the order of Tb-DOTA system with oxygen-terbium(III) distance of 2.35 Å.[17] This observation can be rationalized by the formal negative charge on carboxylic acid oxygen which facilitates the electrostatic effects to enhance the binding to the Lewis acidic Tb^{3+} cation, implying the predicted structure can coordinates to Tb^{3+} with strong kinetic stability.

4.5 Lanthanide Binding Studies



Scheme 4-3. A synthetic method for preparation of rotaxane-lanthanide complex

Preliminary qualitative lanthanide complexation experiments were initially achieved via mixing one equivalent of lanthanide triflate with a methanolic solution of the deprotected rotaxane ligand and monitoring the luminescence properties of the resulting mixture (Scheme 4-3).

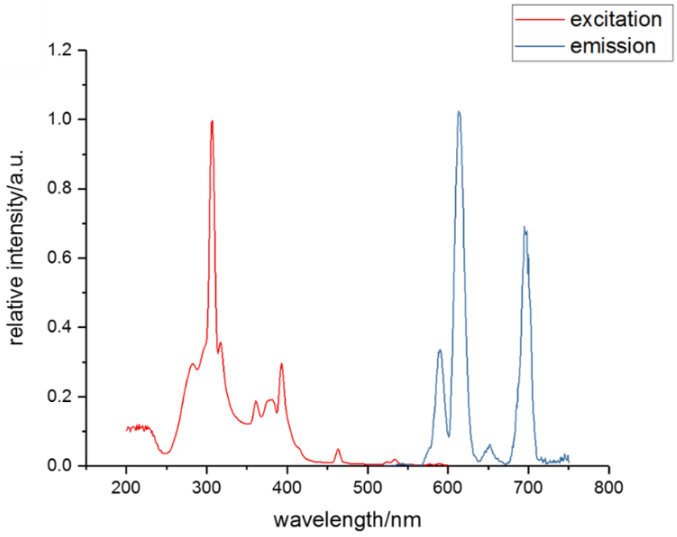


Figure 4-8. (Red) Excitation spectra of **4.15Eu** and (blue) emission spectra of **4.15Eu** (λ_{ex} = 315 nm).

Upon the addition of europium triflate, the excitation spectrum of complex **4.15Eu** exhibited a ligand-metal charge transfer (LMCT) band with a sharp peak at 315 nm with relatively low intensity (Figure 4-8). The corresponding emission spectrum showed weak luminescence when exciting the molecule with 315 nm light, implying the LMCT process is responsible for the quenching of europium luminescence. This can be further confirmed by the fact that the appearance of direct excitation of europium(III) ion at 395 nm strongly implies that indirect sensitisation through the sensitising chromophore is very inefficient. In this case, the acyl-triazole chromophore cannot effectively sensitise the emission of Eu^{3+}. This can be rationalised by the mismatch in energy between the lowest triplet state of the triazole moiety and emissive states of Eu^{3+}, which limits the rate of through space energy transfer to the lanthanide centre. In most literature reports that use triazoles as sensitising

chromophores, the triazole is coordinated directly to the lanthanide centre.[21] It seems reasonable to infer that the triazole does not coordinate the lanthanide in this case, precluding effective Dexter exchange while the low spectral overlap between the emission spectrum of the triazolyl group and the absorption spectrum of the lanthanide is likely to make Förster transfer too slow to be effective. Furthermore, quenching of the triazole excited states by photoelectron transfer from nearby lone pairs is also likely to limit the usefulness of the sensitisation pathway. Although further investigation is required to reveal the photophysical details behind this phenomenon, it was clear that the europium(III) complex was not appropriate for studying the complexation of rotaxane ligand with lanthanide ions.

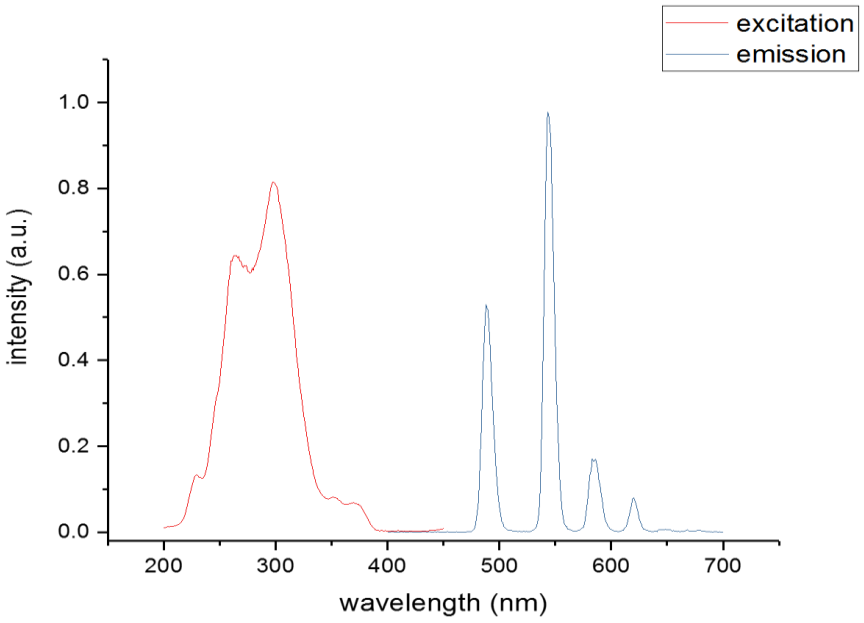


Figure 4-9. (Red) Excitation spectra of **4.15Tb**and (blue) emission spectra of **4.15Tb** (λ_{ex} = 315 nm).

Comparatively, the emission spectra of complex **4.15Tb** showed a strong green luminescence in the methanolic solution which corresponds to the unique luminescence profile of the terbium(III) ion. The complexes showed four emission bands corresponding to the $^5D_4 \rightarrow {}^7F_6$, $^5D_4 \rightarrow {}^7F_5$, $^5D_4 \rightarrow {}^7F_4$ and $^5D_4 \rightarrow {}^7F_3$ transitions. The strong luminescence

intensity indicates that there is an effective energy transfer from the triazole chromophore to the terbium centre via a Dexter mechanism.

With an equimolar of sodium fluoride to a solution of **4.17Tb**, no significant change was observed in either excitation or emission spectra. This indicates the Tb^{3+} was strongly bound to the rotaxane: lanthanide fluorides have very low solubilities, and precipitation of any free (or indeed labile) ions would be expected. Similar observations were also noted for both **4.15Tb** and **4.16Tb**.

All the Tb complexes were further characterised by high-resolution mass spectrometry and ^{1}H NMR spectroscopy. High resolution ESI mass spectrometry confirmed the successful complexation (e.g. observed mass spectra of **4.15Tb** m/z = 2208.07099, assigned as [**16.Tb**+H]$^+$, $C_{122}H_{149}O_{14}N_{15}Tb$, theoretical calculated 2208.06900, Figure 4-10).

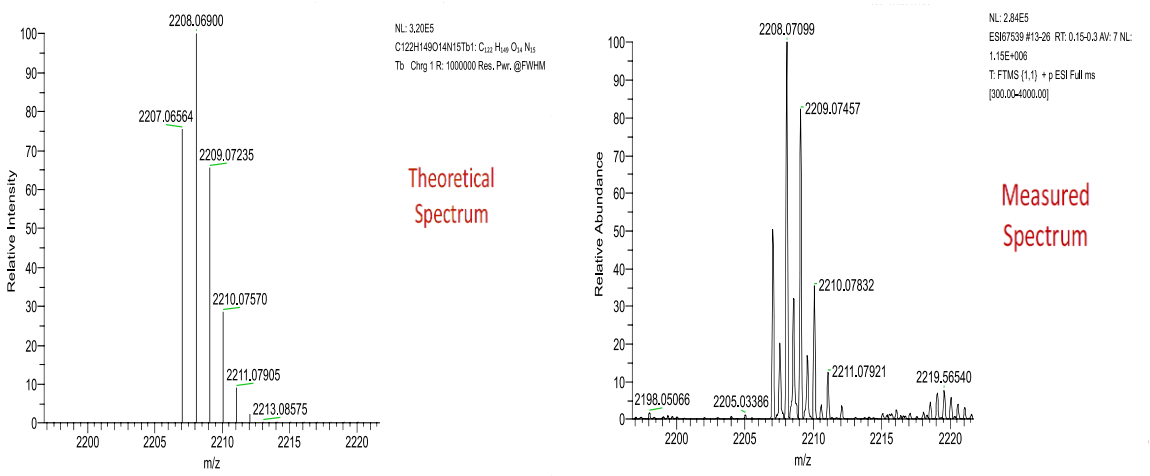


Figure 4-10. High-resolution Mass Spectrometry Spectrum of Complex **4.15Tb**

Unfortunately, only **4.17Tb** displayed a clearly defined set of paramagnetically shifted peaks in the proton NMR spectrum, while no well-defined signals were observed in either **4.15Tb** or **4.16Tb.** Compared to the free ligand **4.17**, **4.17Tb** (Figure 4-11) showed a broad range of spectrum with line broadening, which corresponds to the paramagnetic

nature of terbium, strongly suggesting a novel lanthanide-rotaxane system was successfully established with significant kinetic stability.

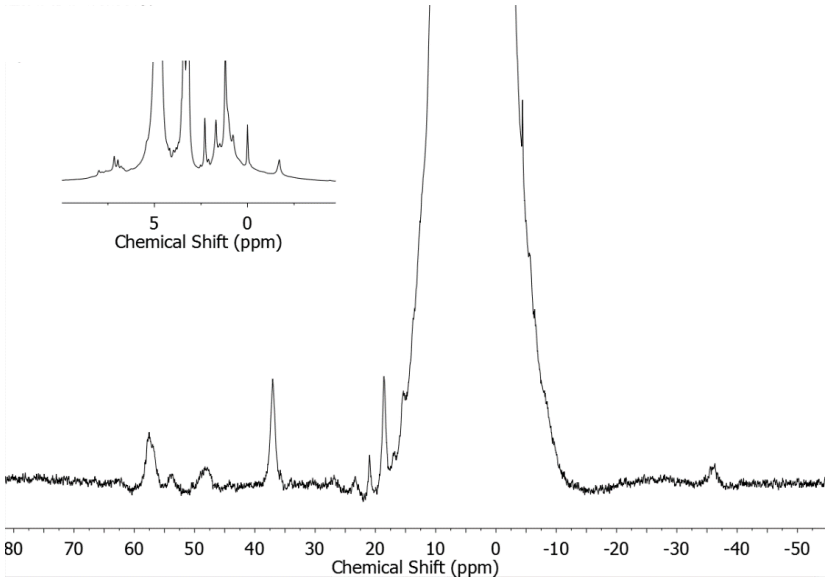


Figure 4-11. The ^{1}H-NMR spectrum of **4.17Tb** in the d_4-methanol

The structures of the Tb^{3+} complex were further investigated for the hydration number (**q**). The hydration number can reflect the number of an axial coordinating water molecule, hence indicating the size of free site in the cavity and revealing the local coordination environment of these complexes.

Thus, the hydration state (**q**) was determined by measuring the lifetimes in deuterated and non-deuterated methanol and the curve was fitted with 1st order exponential decay, with the number of theoretical bound water less than one. Also, no free Tb^{3+} was detected in the solution since fitting to a second exponential component yielded no significant improvement. The non-radiative process can quench the Tb^{3+} luminescence via vibration of surrounding solvent molecules containing O-H oscillators.

Compared to X-H oscillators, lanthanide luminescence tends to be less sensitive to deuterated oscillators (O-D, N-D) as deuterated oscillation has a higher frequency, hence,

requires more energy to quench the luminescence from lanthanide. Kinetically, the rate of quenching of the excited state of terbium in methanol consists of several contributors:

$$k_{MeOH} = k_R + k_{NR} + \sum k_{XH} + \sum k_{CO}$$

where k_R is the rate of the radiative pathway, k_{NR} is the rate of non-radiative relaxation, and k_{XH} and k_{CO} are the sums of rates of surrounding X-H and C=O stretches, respectively. In deuterated methanol MeOD-d_4, all X-H stretches are treated as irrelevant factors to the overall quenching process. Thus, the rate of quenching of excited states of terbium in deuterated methanol can be written as:

$$k_{MeOD} = k_R + k_{NR} + \sum k_{CO}$$

As explained earlier, the quenching in deuterated media is no longer dominated by X-H stretches. These two equations can be rearranged to give Horrocks equation to determine the number of methanol coordinated to the lanthanide ion centre.

$$q_{MeOH} = A(k_{MeOH} - k_{MeOD} - B)$$

It is meaningful to theoretically calculate the coordinated water molecules as it helps to understand the local coordination environment. When calculating the number of coordinated methanol molecules, it is reasonable to assume that, since methanol only has a single O-H oscillator, the value of the proportionality constant A must be doubled if we are to estimate inner sphere solvation. If further, we assume that there are the same number of water or methanol molecules in the outer sphere, it is reasonable to assume that the correction constant, B, must be halved in value. Thus,

$$q_{H_2O} = 2 * A\left(k_{MeOH} - k_{MeOD} - \frac{B}{2}\right) = 2 * A\left(\frac{1}{\tau_{MeOH}} - \frac{1}{\tau_{MeOD}} - \frac{B}{2}\right)$$

where A is a parameter which is proportional to each lanthanide and B is the correction factor.[11] The curve was fitted with single exponential luminescence decays in MeOH and d_4-MeOD with the parameter of Beeby et al. (A = 5.0, B = 0.06),[18,19] suggesting a hydration number of 2.2 for **4.17Tb**, which is slightly surprising for an octadentate ligand species in solution, implying that there is more "space" around the lanthanide than might be expected in a conventional structure (Figure 4-12).

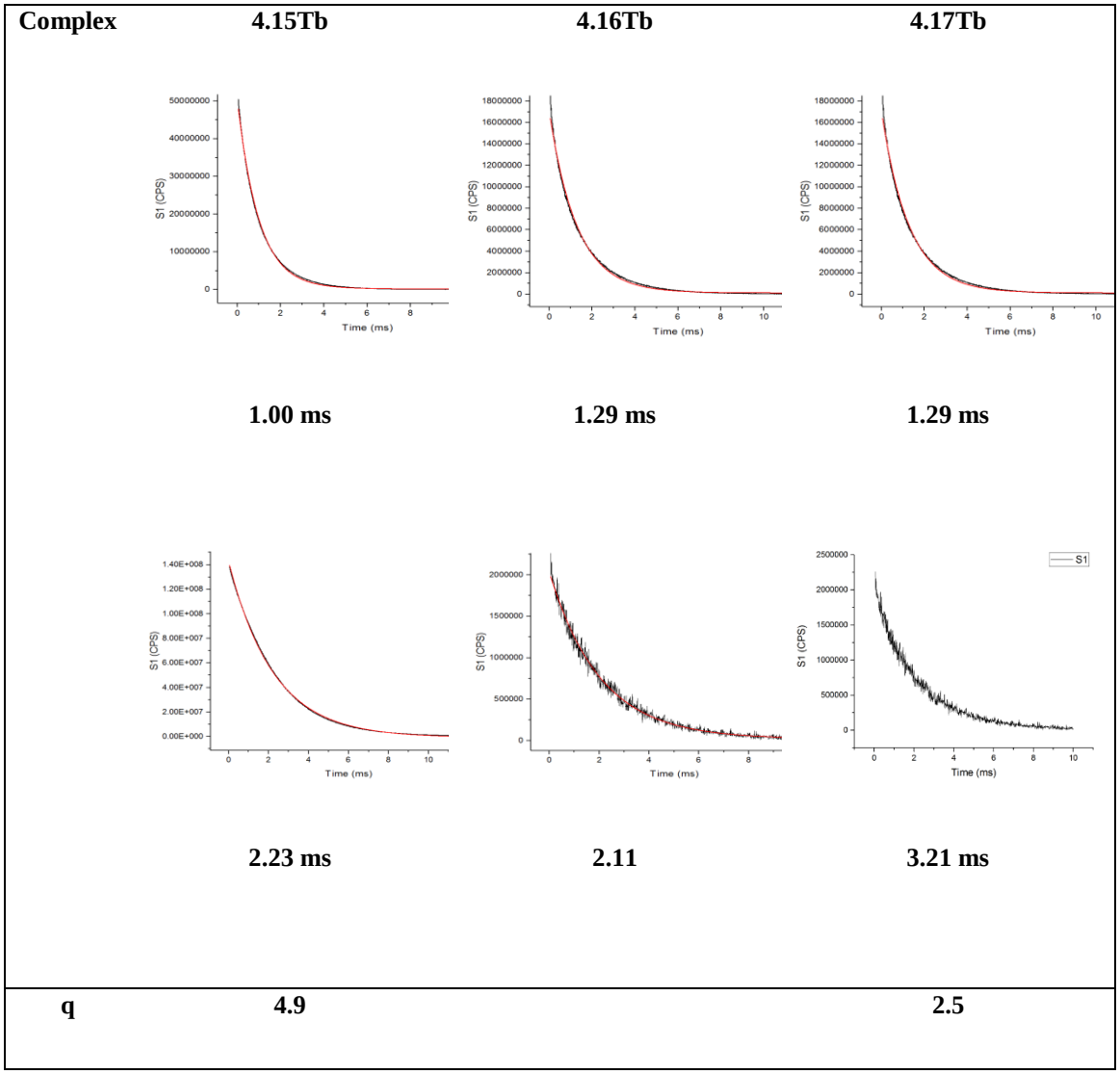


Figure 4-12. Lifetimes and hydration states for **4.15Tb** and **4.17Tb**. (Fitted curved: red, observed curve: black)

Compared to **4.17Tb**, the hydration number of complex **4.15Tb** is much larger indicating the binding of the lanthanide ion is facile. However, these values must be treated with extreme caution given the approximations described above. The large multiplier effect of the A factor means that two such different q values can be calculated from lifetime measurements that are essentially within experimental error of one another. It is, however, clear that both systems exhibit significant solvation at the metal centre, implying that not all of the potential donor atoms of the interlocked host are coordinated to the metal centre.

While small, the changes in a lifetime are likely to reflect at least some degree of structural change. The hydration of ligand **4.17** is the smallest, reflecting there are limited coordination sites in the lanthanide ions given by the smaller size of the macrocycle and another carboxylate arms. A multi-ordered fitting attempt was unsuccessful indicating no residue Tb^{3+} ion in the solution.

4.6 Association Constant Determination

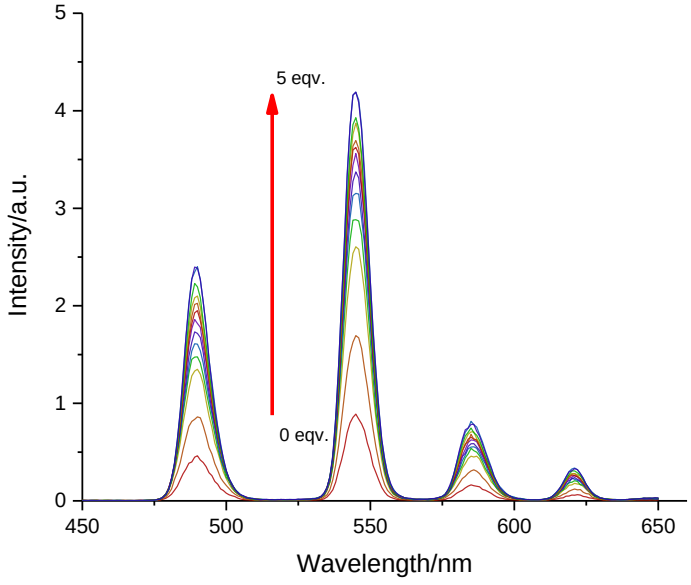
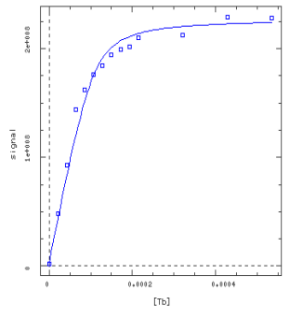
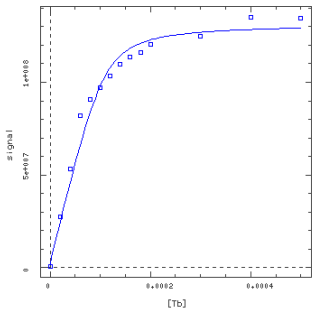


Figure 4-13. Phosphorescence spectra: Titration of free terbium ion in ligand solution **4.15Tb** (excitation at 298 nm, exit slit = 5 nm, gated time = 1 ms)

After the preliminary studies of rotaxane ligands binding with lanthanide ions, the binding affinities were determined by luminescence titration between terbium ion and ligands (**4.15**, **4.16** and **4.17**) in methanolic solution, where $Tb(OTf)_3$ was used as titrant to be added to methanol solutions of the ligands when exciting the molecule. The addition of Tb^{3+} gave rise to a significant spectral increase in emission spectra (Figure 4-13) and no changes can be observed when adding Tb^{3+} into pure methanol in the controlled experiment. Moreover, a binding stoichiometry with 1: 1 relationship was observed (Figure 4-14) when fitting spectral data (J = - 2 or J = -1) with the concentration of titrant using Dynafit[20], indicating that the binding site of the rotaxane ligand can only accommodate only one lanthanide ion given by the bulky nature of ligand. The binding affinity between the terbium ion and interlocked ligands **4.15**, **4.16** and **4.17** were afforded by fitting the luminescence titration with a 1:1 binding and results are depicted in Table 4-1.

Hypersensitive	Δ_J = -2	Δ_J = -1
4.15Tb		

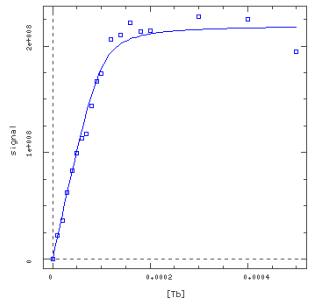
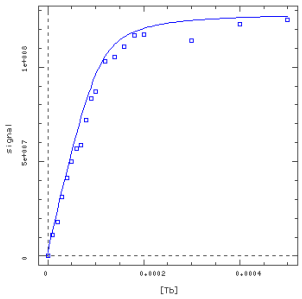
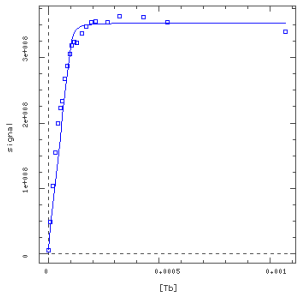
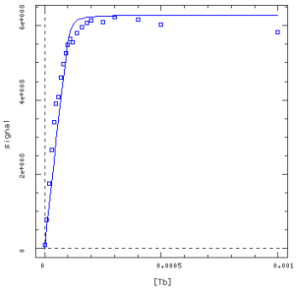
4.16Tb		
4.17Tb		

Figure 4.14. Fitted curve of the concentration of terbium solution to the intensity of integrated luminescence by Dynafit(ΔJ = -2(left); ΔJ = -1(right); vertical axis: integrated luminescence intensity; horizontal axis: concentration of terbium ion (mM))[1st row: **4.15Tb**; 2nd row: **4.16Tb** ; 3rd row: **4.17Tb**]

Table 4-1. Association Constants of different rotaxane ligands with Tb^{3+}

Ligand	Log (K_a/M^{-1})[a]	
	ΔJ = -2 (488 nm)	ΔJ = -1 (545 nm)
4.15	5.04 ± 0.09	5.12 ± 0.07
4.16	5.30 ± 0.08	5.37 ± 0.09
4.17	6.17 ± 0.04	6.08 ± 0.05

[a] Solvent = CH_3OH, T = 293 K.

Both ligands (**4.15** and **4.16)** have three carboxylate arms whereas the size of macrocycle of ligand **4.16** is smaller. The greater binding affinity between terbium and ligand **4.16** implies that smaller macrocycle size contributes to enhance the stability of the complex, probably due to the increased electrostatic interactions arisen from a shorter spatial separation between donor atoms and terbium ion. The comparison between **4.16** and **4.17**, whose macrocycles are identical, indicates that the stability of the complex molecule can be significantly influenced by the number of carboxylate arms, hence giving a greater interaction between terbium ion and supramolecular ligand.

4.7 Conclusions

By adopting an AMT synthetic methodology and post-functionalisation, three novel supramolecular ligands containing interlocked structure were synthesised and exploited for binding with lanthanide ions. The asymmetric properties were confirmed by NMR studies.

The successful binding of the ligands with lanthanide ions was monitored by luminescence spectroscopy, NMR studies and HR-MS. Detailed local coordination information was acquired by computational studies and hydration number calculations. These results reflect the binding of lanthanide can occur in competitive media such as methanol. The Horrocks equation was modified to calculate the hydration number of the complex in the non-water solvent.

The binding affinity of rotaxane ligand with terbium was determined by luminescence titrations. The magnitude of binding affinity confirms the complexation between lanthanide ion and ligand. Additionally, changes in binding affinity illustrate the stability of such

complexes are dependent on the size of macrocycle and number of carboxylate arms, which can give more donor atoms to enhance the kinetical stability.

4.8 Reference

[1] D. E. Barry, D. F. Caffrey, T. Gunnlaugsson, *Chem. Soc. Rev.* **2016**, *45*, 3244–3274.

[2] M. C. Heffern, L. M. Matosziuk, T. J. Meade, *Chem. Rev.* **2014**, *114*, 4496–4539.

[3] M. R. Spirlet, J. Jean Rebizant, J. F. Desreux, M. F. Loncin, *Inorg. Chem.* **1984**, *23*, 359–363.

[4] H. B. Cheng, H. Y. Zhang, Y. Liu, *J. Am. Chem. Soc.* **2013**, *135*, 10190–10193.

[5] Y. Zhou, H. Y. Zhang, Z. Y. Zhang, Y. Liu, *J. Am. Chem. Soc.* **2017**, *139*, 7168–7171.

[6] C. Allain, P. D. Beer, S. Faulkner, M. W. Jones, A. M. Kenwright, N. L. Kilah, R. C. Knighton, T. J. Sørensen, M. Tropiano, *Chem. Sci.* **2013**, *4*, 489–493.

[7] M. J. Langton, O. A. Blackburn, T. Lang, S. Faulkner, P. D. Beer, *Angew. Chemie - Int. Ed.* **2014**, *53*, 11463–11466.

[8] F. Zapata, O. A. Blackburn, M. J. Langton, S. Faulkner, P. D. Beer, *Chem. Commun.* **2013**, *49*, 8157–8159.

[9] G. Gil-Ramírez, S. Hoekman, M. O. Kitching, D. A. Leigh, I. J. Vitorica-Yrezabal, G. Zhang, *J. Am. Chem. Soc.* **2016**, *138*, 13159–13162.

[10] G. Zhang, G. Gil-Ramírez, A. Markevicius, C. Browne, I. J. Vitorica-Yrezabal, D. A. Leigh, *J. Am. Chem. Soc.* **2015**, *137*, 10437–10442.

[11] C. Lincheneau, B. Jean-Denis, T. Gunnlaugsson, *Chem. Commun.* **2014**, *50*, 2857–2860.

[12] J. Lehr, P. D. Beer, S. Faulkner, J. J. Davis, *Chem. Commun.* **2014**, *50*, 5678–5687.

[13] C. Allain, P. D. Beer, S. Faulkner, M. W. Jones, A. M. Kenwright, N. L. Kilah, R. C. Knighton, T. J. Sørensen, M. Tropiano, *Chem. Sci.* **2013**, *4*, 489–493.

[14] M. Tropiano, A. M. Kenwright, S. Faulkner, *Chem. - A Eur. J.* **2015**, *21*, 5697–5699.

[15] M. E. De Mesquita, *Inorg. Chem. Commun.* **2002**, *5*, 292–295.

[16] M. A. M. Filho, J. D. L. Dutra, G. B. Rocha, R. O. Freire, A. M. Simas, *RSC Adv.* **2013**, *3*, 16747–16755.

[17] D. Parker, H. Puschmann, A. S. Batsanov, K. Senanayake, *Inorg. Chem.* **2003**, *42*, 8646–8651.

[18] A. Beeby, I. M. Clarkson, R. S. Dickins, S. Faulkner, D. Parker, L. Royle, A. S. de Sousa, J. A. G. Williams, M. Woods, *J. Chem. Soc. Perkin Trans. 2* **1999**, *39*, 493–504.

[19] D. Sykes, A. J. Cankut, N. M. Ali, A. Stephenson, S. J. P. Spall, S. C. Parker, J. A. Weinstein, M. D. Ward, *Dalt. Trans.* **2014**, *43*, 6414–6428.

[20] P. Kuzmič, *Anal. Biochem.* **1996**, *237*, 260–273.

[21] M. Sengar, A. K. Narula, *Sensors Actuators, B Chem.* **2017**, *241*, 567–576.

5 Conclusion and Future Perspective

This thesis has described the scope and the most important aspects of the work conducted during my DPhil. The versatility of CuAAC chemistry has been widely adapted into preparing lanthanide-containing complexes. Lanthanide complexes obtained during the course of DPhil has been used to demonstrate several aspects as follows:

The PhenacylDO3A complexes as cyanide sensor

In the studies in chapter 2, we have demonstrated that the phenacylDO3A derivatives have a minimal binding affinity for fluoride. However, they respond to the presence of cyanide in water as a consequence of the cyanohydrin reaction between cyanide and the carbonyl group at phenacyl chromophore. The PhenacylDO3A species have great potential in selectively detecting cyanide in water and pushed the detection limit to a higher level. Since the tetra-amide complex can respond to fluoride ions, resulting from the displacement of axial coordinated water by fluoride, the tetra-amide complex can be further exploited as a fluoride sensor and incorporated into the preparation of dual sensor which can respond to the presence of fluoride and cyanide simultaneously. In future studies, the binding affinity of tetra-amide complexes can be greatly enhanced by incorporating a more effective sensitiser and chemically active alkyne pendant, in which can be used as synthon to prepare multi-metallic arrays.

The Heterbimetallic complexes *f-f'* arrays as a potential ratiometric probe

Azide-containing lanthanide complexes demonstrated great potential to be used as synthons to prepare heterometallic lanthanide complexes. In the scope of my studies, this

synthon has demonstrated great versatility in preparing a bimetallic system as a ratiometric probe for sensing cyanide. A variety of alkyne-containing derivatives have been also examined and propargyl-amide complexes were selected to preparing the ratiometric sensor due to the limited response to other competitive anions such as fluoride. In further studies, the exploitation of such systems can be made: the preparations of dual-sensing f-f' arrays for fluoride and cyanide - this requires the preparation of fluoride-responsive lanthanide complexes containing multiple alkyne groups whereas the rigidity of such alkyne-appended synthon must be maintained through the 'click' reaction. In contrast to the bimetallic system, the multimetallic system containing multiple phenacylDO3A binding sites - cyanide responding channel, could further enhance its ability in detecting cyanide in competitive media. This aspect of work has clear implications for the development of novel optical probe for chemical weapons.

The synthesis and study of supramolecular lanthanide complexes

We have demonstrated that it is possible to use a rotaxane ligand, which was prepared via AMT rotaxane synthesis followed by a post-functionalisation, to directly bind a lanthanide ion. This investigation is still ongoing, but the moderate binding strength makes such ligands promising for further development, in particular, through modifying the structural properties to achieve better sensitisation efficiency and stability. These supramolecular structures can be further exploited for the development of anion recognition by incorporating the lanthanide ion into the anion binding site, and the strong Lewis acidic lanthanide centre can facilitate the selectivity of binding between monodentate anions with different sizes and the supramolecular architecture.

6 Experimental

6.1 General procedures

Commercially available solvents and chemicals were used without purification unless stated. The anhydrous solvents used during the course of DPhil, were dried by passing through an *MBraun MPSP-800* column, degassed by freeze-pump-thaw and then used immediately. Diethyl phosphorochloridite was used stored under vacuum in a Schlenk flask. Propargyl bromide was used as 80 wt% solution in toluene. All other chemicals were used as received. Deionised water was obtained by microfilteration using a Milli-Q Millipore machine. TLC Silica gel 60 plates were purchased from Merck and used by cutting manually. TLC Aluminium oxide 60 F_{254} with *60* Å pore size (neutral Al_2O_3) were purchased from Merck. Geduran® Si 60 Silica gel for column chromatography was purchased from Merck (*particle size 25 – 45 μm*). Neutral alumina was purchased from Sigma-Aldrich (activated Al_2O_3, Type I, *70 – 290 mesh*) and the neutral alumina was dry-loaded before used. Dialysis tubes (500, 1000 MWCO) equipped with regenerated cellulose were purchased from Sigma-Aldrich and used to purify the lanthanide complexes. The dialysis tube was activated by 10% ethanol solution in water and pure water before being used. The corresponding lanthanide complexes were dissolved in pure water and transferred into dialysis tube with the appropriated membrane according to molecular weight. The dialysis tube was placed in a 5L-beaker filled with deionised water. The dialysis normally lasts for two days under stirring and the deionised water was changed three times during the course of dialysis.

All NMR spectra were registered at temperature of 298 K unless otherwise mentioned. 400 MHz ^{1}H, 400 MHz ^{13}C and 400MHz ^{31}P NMR spectra were recorded on a Bruker Avance

III HD nanobay NMR equipped with a 9.4T magnet. 500 MHz ^{1}H NMR, 470 MHz ^{19}F NMR, EXSY spectra, COSY spectra, variable temperature (VT) measurements and NMR titrations were recorded on a Bruker Avance III NMR equipped with a 11.75T magnet. Hz are the unit for all coupling constants mentioned in this thesis and all chemical shifts (δ) are quoted in parts per million (ppm). Abbreviations for referring the NMR resonance peaks are listed as follows: singlet (s), doublet (d), triplet (t), quartet (q), multiplet (m) and broad (br).

An Aligent Technology 1260 Infinity instrument were used to obtain low-resolution mass spectra. Bruker μTOF and Micromass GCT spectrometers were used to record the accurate mass spectra. Bruker Tensor 27 FT-IR equipped with an ATR unit was used to record the IR spectra.

PG instruments T60u UV-Vis spectrophotometer was used to acquire the UV-Visible absorption spectra. HORIBA Jobin Yvon FluoroLog3 fluorimeter (Hamamatsu R928 detector and a double-grating emission monochromator) was used to acquire the luminescence spectra. The standard conditions for acquiring emission and excitation spectra are room temperature and steady-stated mode unless otherwise stated. HORIBA Jobin Yvon FluoroLog3 fluorimeter system equipped with a Xenon flash lamp was used to acquire emission lifetimes. Luminescence lifetimes were obtained by tail fit for Eu(III) and Tb(III) complexes using Origin software. Near-infrared luminescence spectra from Yb(III) complexes were measured on the HORIBA Jobin Yvon FluoroLog3 fluorimeter system equipped with a Hamamatsu R5509-42 NIR PMT InGaAs detector cooled to -80 °C.

A pulsed nitrogen laser (PTI-3301-337nm) was used to excite Yb(III) lanthanide luminescence and record the luminescence lifetimes. Light is combined into the excitation

beam and then was focused onto a monochromator. Exit lighting was selected with right emission wavelength (980 nm).

Triplet state emission spectra were prepared by cooling the samples in liquid nitrogen (77K) and recorded on a Perkin Elmer LS55 spectrophotometer.

pH of solution of all complexes in water and deuterium oxide are recorded in a Hannah pH meter. The values for D_2O is the pH measured by the instrument with modification (pD = pH + 0.45) by following literature.[1]

6.2 X-ray crystallography

Crystallographic studies were performed by Dr Kirsten Christensen. For single crystal X-ray analysis of compound **2.6**, the oil drop technique was used to mount the crystal, in perfluoropolyether oil at 150(2) K using a Cryostream N_2 open-flow cooling device.[2] Graphite monochromatic Mo-K_α radiation (λ = 0.71073 Å) on a Nonius Kappa CCD diffractometer was used to acquire the diffraction data. Series of ω-scans were performed in such a way as to collect a complete data set to a maximum resolution of 0.77 Å for all data collections. DENZO-SMN/SCALEPACK[2] was used to perform data reduction and inter-frame scaling. The multi-scan method was employed for processing the intensity data and correcting the absorption effects, based on repeat measurements of identical and Laue equivalent reflections. SIR92[3] within the CRYSTALS software suite.[4] was directly used to solve the crystal structure. Free refinements were applied for coordinates of all non-hydrogen atoms related to anisotropic displacement parameters. In the difference map, soft restraints was used to refine the hydrogen atoms before using a riding model to final refine the molecule. [5] A summary of the X-ray crystallographic data is provided in **6.6** and the

ORTEP depiction of the single crystal X-ray structure is included in chapter six (Figure 6-1).

6.3 Titration methodology

The interaction between lanthanide complexes and anions is studied by luminescence and NMR titration via a non-dilution method. The concentration of titrant solution is normally 100 times more concentrated than that of stock solution, ensuring the intensity of emission was not interfered by dilution of stock solution. The information of titration is summarised in Table 7-1.

Table 6-1. Concentrations of solutions used for titrations.

	λ_{ex} / nm	**[Ln] / mM**	**[Anion] / M**	**Solvent**	**Method**
Eu.2.19 + F^-	320	0.05	0.05	H_2O	Luminescence
3.46EuTb+ CN^-	395	0.05	0.08	H_2O	Luminescence

6.4 Dynafit

Dynafit153® was used in fitting the changes in observed luminescence spectrum of the lanthanide complexes upon addition of analyte to the solution. The intensity ratio of luminescence is independent with concentration as the dilution method was adopted in titrations (see titration methodology). Only data obtained with a dilution of less than 5% can be used in fitting if we take intensity into consideration. [6]

Examples of Dynafit scripts

One-event binding – sum of peaks

[task]

data = equilibria

task = fit

[mechanism]

Tb + rot <==> complex1 : K1 association

[constants]

K1 = 133000??

[concentrations]

rot = 1.07e-4

[equil]

variable Tb

file C:\Users\SFgroup\Desktop\James\dynafit\XZ230\rotaxane.txt | response rot = 2.039e10 , complex1 = 2.129719626e12

[output]

directory C:\Users\SFgroup\Desktop\James\dynafit\result_rotaxane

[end]

Two-event binding – sum of peaks

[task]

data = equilibria

task = fit

[mechanism]

Tb + rot <==> complex1 : K1 association

complex1 + rot <==> complex2 : K2 association

[constants]

K1 = 234000?

K1 = 2340?

[concentrations]

rot = 1e-4

[equil]

variable Tb

file C:\Users\SFgroup\Desktop\James\dynafit\rotaxane2\j-2try.txt | response rot = 100 , complex1 = 2.2e12, complex2 = 2.2e12

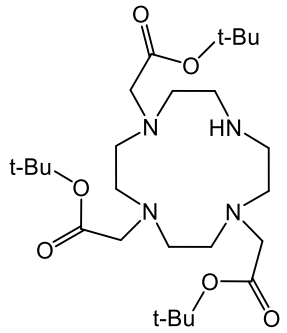
[output]

directory C:\Users\SFgroup\Desktop\James\dynafit\result_rotaxane2

[end]

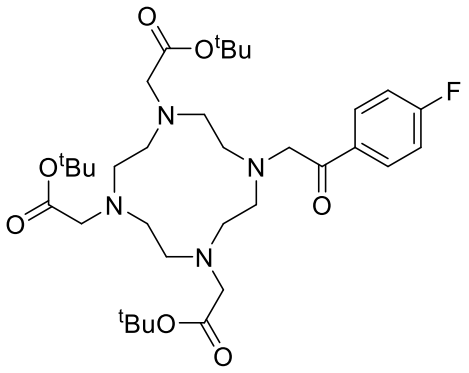
6.5 Synthesis

Triester tri-tert-butyl-2,2',2''-(1,4,7,10-tetraazacyclododecane-1,4,7-triyl) triacetate (triester)[7]



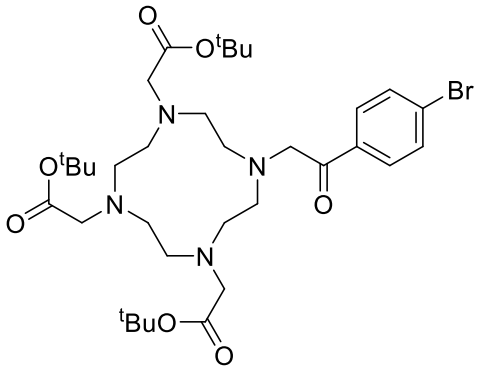
To anhydrous acetonitrile (100 ml), cyclen (5.00 g, 29 mmol) was added and stirred until fully dissolved. $NaHCO_3$ (8.16 g, 97.2 mmol) was then added and stirred in an ice bath for 30 minutes. Tert-butyl bromoacetate (17.2 mL, 116.7 mmol) in anhydrous acetonitrile (80 ml) was added dropwise over 30 minutes. The reaction stirred at room temperature for 48 hours under nitrogen. Inorganic salts were filtered and the filtrate was concentrated under reduced pressure to give a white solid. The title compound was obtained by recrystallisation from toluene as a white powder. (9.32 g, 54 %). δ_H 10.4 (br. s, 1H), 3.40 (s, 4H), 3.33 (s, 2H), 3.14 (s, br, 4H), 2.98 (s, br, 8H), 2.92 (s, br, 4H), 1.49(s, 27H) ppm. TOF-MS found *m/z* 515.3821 for $[M+H]^+$.

2.4 1-(4'-fluoro-2-acetophenone)-4,7,10-tris(*tert*-butoxycarboxymethyl)-1,4,7,10-tetraazacyclododecane (2.4)[8]



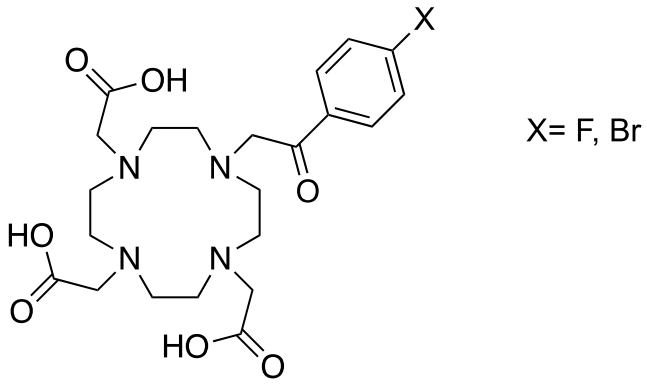
1,4,7-Tris(tert-butoxycarbonylmethyl)-1,4,7,10-tetraazacyclododecane (2.100 g, 3.5 mmol) were dissolved in anhydrous MeCN (50 mL). K_2CO_3 (1.100 g, 8 mmol) and a catalytic amount of KI were added. The solution was heated at 78°C for 30 minutes following an addition of 2-chloro-4'-fluoroacetophenone (0.665 g, 3.86 mmol). The mixture was allowed stirred for further 6 hours. The completion of reaction was confirmed by checking with TLC (10% methanol in $CHCl_3$) the mixture was allowed to cool down to room temperature, and inorganic salts were removed by filtration. The filtrate was concentrated under reduced pressure to afford dark oil. The crude product was purified by the silica gel column chromatography (0-10% MeOH in $CHCl_3$, gradient) affording the title compound as a yellow solid (1.153 g, 50%). ^{1}H NMR (400 MHz, $CDCl_3$, 373K) δ_H 8.00 (dd, 2H, Ar*H*), 7.16 (t, 2H), 3.62-2.00 (m, 24H), 1.44 (s, br, 27H) ppm. ^{13}C NMR (400 MHz, $CDCl_3$) δ_c 199.1, 173.9, 173.6, 166.8, 132.9, 132.3, 115.6 (d, $^2J_{CF}$ = 22.5 Hz), 81.94, 81.90, 61.2, 56.7, 56.4, 53.5, 49.6, 28.8, 28.7 ppm. ES-MS found *m/z* 673.3 for $[M+Na]^+$.

2.5 1-(4'-bromo-2-acetophenone)-4,7,10-tris(*tert*-butoxycarboxymethyl)-1,4,7,10-tetraazacyclododecane(2.5)



1,4,7-Tris(tert-butoxycarbonylmethyl)-1,4,7,10-tetraazacyclododecane (2.100 g, 3.5 mmol) was dissolved in anhydrous MeCN (50 mL). K_2CO_3 (1.100 g, 8 mmol) and a catalytic amount of KI were added and the solution was heated at 78°C for 30 minutes following addition of 2,4'-dibromoacetophenone (1.074 g, 3.86 mmol). The mixture was allowed to stir for further 6 hours. The completion of the reaction was confirmed by checking with TLC (10% methanol in $CHCl_3$). The mixture was allowed to cool down to room temperature, and the inorganic salt was removed by filtration. The filtrate was concentrated under reduced pressure to afford dark oil. The crude product was purified by silica gel column chromatography (0-10% MeOH in $CHCl_3$, gradient) affording the title compound as a yellow solid (1.416 g, 57%). ^{1}H NMR (400 MHz, $CDCl_3$) δ_H 7.81 (d, 2H), 7.58 (d, 2H), 3.60-2.04 (m, 24H, CH_2 ring and arms), 1.41 (s, 27H) ppm. $^{13}C\{^1H\}$ NMR (400 MHz, $CDCl_3$) δ_c 198.8, 172.7, 172.5, 136.1, 131.7, 129.1, 128.3, 81.7, 60.0, 54.9 (br), 52.8, 47.9 (br), 27.5, 27.4 ppm. ES-MS found *m/z* 711.2 for $[M+H]^+$.

2.6-2.7 General procedure for the deprotection of ligands (2.6 and 2.7)



The corresponding protected ligand was dissolved in DCM (5 mL) and the solution was cooled in an ice bath when adding dropwise TFA (5 mL). The mixture was stirred at RT for overnight and the solvent was evaporated *in vacuo*. MeOH (3 x 1 mL) and DCM (3 x 5 mL) were added and the solvent was removed *in vacuo*. This step was repeated three times to fully remove the TFA residues. The resulting compound was dissolved in a minimum amount of MeOH and precipitated with Et_2O. The title compound was precipitated out and obtained in quantitative yield.

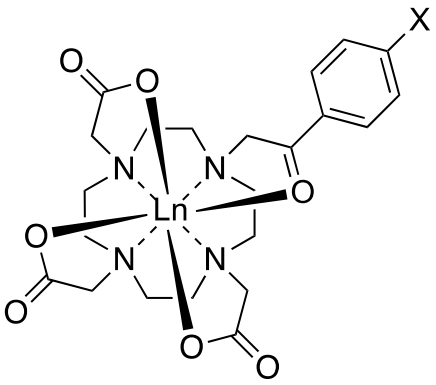
2.6 1-(4'-fluoro-2-acetophenone)-4,7,10-tris(carboxymethyl)-1,4,7,10-tetraazacyclododecane (2.6)

2.6 (0.652 g, 1.00 mmol). ^{1}H NMR (400 MHz, D_2O) δ_H 8.01 (dd, 2H), 7.26 (d, 2H), 4.10 – 2.91 (m, 24H) ppm. ES-MS found *m/z* 483.1 for $[M+H]^+$. UV-Vis (H_2O): λ_{max} 250 nm.

2.7 1-(4'-bromo-2-acetophenone)-4,7,10-tris(carboxymethyl)-1,4,7,10-tetraazacyclododecane (2.7)

2.7 (0.761 g, 1.00 mmol). ^{1}H NMR (400 MHz, D_2O) δ_H 7.84 (d, 2H), 7.78 (d, 2H), 3.90 – 2.71 (m, br, 24H) ppm. ESMS found *m/z* 543.1 for $[M+H]^+$, λ_{max} 258 nm.

2.8-2.12 General procedure for the synthesis of phenacylDO3A lanthanide complexes (2.8-2.12)[9]



X= F, Br

To a solution of the ligand in MeOH the appropriate $Ln(OTf)_3$ salts were added (1.05 eq.) and the mixture was allowed to stir at 60°C for 30 min. The pH was adjusted to 4 by the dropwise addition of an aqueous NaOH (1 M) solution. The reaction was allowed to stir at 60°C for a further 48 h. The methanol was removed under reduced pressure to leave an oil and was then dissolved in a minimum amount of water. The pH of the solution was raised to 10 by the addition of aqueous NaOH (1 M) to remove excess of lanthanide as its insoluble hydroxide salt. The precipitate was centrifuged, and the supernatant was collected by the syringe filtration. The solvent was neutralised by the addition of 1 M HCl before the solvent was removed. The residues were dissolved in a minimum amount of MeOH and precipitated with Et_2O. Trituration with Et_2O afforded the desired lanthanide complexes.

Eu 2.8. Yield: 89%. ^{1}H NMR (500 MHz, D_2O, pH = 4) δ_H 35.5 (s), 28.1 (s), 26.7 (s), 25.9 (s), 9.2 (s), 7.8 (s), 5.8 (s), -1.8 (s), -3.2 (s), -4.6 (s), -5.8 (s), -7.5 (s), -7.9 (s), -10.2 (s), -10.7 (s), -10.7 (s), -11.8 (s), -12.7 (s), -13.3 (s), -16.1 (s), -16.4 (s), -18.5 (s) ppm. Only resolved peaks outside the 0 to 5 ppm region are reported. $^{19}F\{^{1}H\}$ (400 MHz, D_2O) δ_F -98.0 (s) ppm. ESMS found *m/z* 633.0 for $[M+H]^+$. HR-ESMS found *m/z* 633.1215, calculated *m/z* 633.1227 for $[C_{22}H_{29}N_4O_7{}^{151}Eu^{19}F]^+$. UV-Vis ($H_2O$): λ_{max} 266 nm. Luminescence lifetimes: H_2O: 0.60 ms, D_2O: 2.16 ms, q = 1.2.

Tb 2.9. Yield: 74%. ^{1}H NMR (500 MHz, D_2O, pH = 4) δ_H 311.1 (s), 275.0 (s), 263.5 (s), 201.1 (s), 197.1 (s), 137.3 (s), 129.1 (s), -10.4 (s), -20.6 (s), -35.1 (s), -41.7 (s), -76.1 (s), -84.2 (s), -98.2 (s), -100.3 (s), -160.4 (s), -185.2 (s), -332.1 (s), -338.0 (s) ppm. Only resolved peaks outside the 10 to -10 ppm region are reported. $^{19}F\{^{1}H\}$ (470 MHz, D_2O) δ_F -102.7 (s) ppm. ESMS found *m/z* 639.0 for $[M+H]^+$. HR-ESMS found *m/z* 639.1257, calculated *m/z* 639.1268 for $[C_{22}H_{29}N_4O_7{}^{159}Tb^{19}F]^+$. UV-Vis ($H_2O$): λ_{max} 266 nm. Luminescence lifetimes: H_2O: 1.77 ms, D_2O: 2.91 ms, q = 1.1.

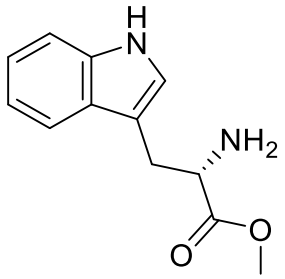
Eu 2.10. Yield: 82%. ^{1}H NMR (500 MHz, D_2O, pH = 4) δ_H 35.6 (s), 27.9 (s), 26.4 (s), 25.6 (s), 9.3 (s), 8.4 (s), 7.65 (s), 7.60 (s), 6.4 (s), -1.7 (s), -3.0 (s), -4.7 (s), -6.0 (s), -7.2 (s), -7.9 (s), -10.3 (s), -10.8 (s), -11.6 (s), -12.8 (s), -13.2 (s), -16.5 (s), -18.7 (s) ppm. Only resolved peaks outside the 0 to 5 ppm region are reported. ESMS found *m/z* 693.1 for $[M+H]^+$. HR-ESMS found *m/z* 713.0219, calculated *m/z* 713.0232 for

$[C_{22}H_{28}N_4O_7{}^{151}Eu^{79}Br^{23}Na]^+$. UV-Vis ($H_2O$): λ_{max} 278 nm. Luminescence lifetimes: H_2O: 0.61 ms, D_2O: 2.52 ms, q = 1.2.

Tb 2.11. Yield: 78%. ^1H NMR (500 MHz, D_2O, pH = 4) δ_H 314.5 (s), 278.9 (s), 260.0 (s), 200.4 (s), 196.0 (s), 140.0 (s), 131.1 (s), -15.0 (s), -19.3 (s), -31.8 (s), -39.5 (s), -75.2 (s), -92.0 (s), -98.9 (s), -99.7 (s), -162.4 (s), -188.4 (s), -327.9 (s), -335.0 (s) ESMS found *m/z* 699.1 for $[M+H]^+$. HR-ESMS found *m/z* 721.0269, calculated *m/z* 721.0287 for $[C_{22}H_{28}N_4O_7{}^{159}Tb^{79}Br^{23}Na]^+$. UV-Vis ($H_2O$): λ_{max} 278 nm. Luminescence lifetimes: H_2O: 0.86 ms, D_2O: 1.24 ms, q = 1.7.

Lu 2.12. Yield: 52.7 mg, 60%. ^1H NMR (400 MHz, D_2O) δ_H 8.22 (m, 2H, Ar*H*), 7.31 (m, 2H, Ar*H*), 4.95 (d, 1H, ArH), 4.47 (d, 1H, ArH), 3.87-2.21 (m, br, 24H, CH2 ring and arms). ES-MS found *m/z* 655 for $[M+H]^+$.

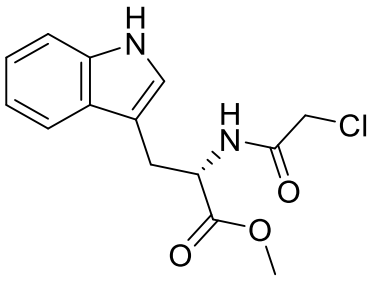
2.14 methyl L-tryptophanate (2.14)



L-tryptophan (4) (10.00 g, 49.00 mmol) was added to a solution of thionyl chloride (8.5 mL) in MeOH (250 mL) at 0°C. The solution was refluxed for 18 h and the solvent was removed to afford colourless crystals (12.27 g, 48.00 mmol, 98%) The free base was

characterized analytically: For this reason, the crystals were re-dissolved in water, alkalized with aqueous Na_2CO_3 (10%), and the precipitate was collected by filtration. ^{1}H-NMR (400 MHz, $CDCl_3$) δ 7.54 (d, J = 7.4 Hz, 1H), 7.30 (d, J = 8.1 Hz, 1H), 7.13 – 7.12 (m, 1H), 7.08 – 7.06 (m, 1H), 6.98 (d, J = 6.7 Hz, 1H), 3.91 – 3.87 (m, 1H), 3.63 (s, 3H), 3.10 (dd, J = 15.4, 5.9 Hz, 1H), 2.76 (dd, J = 15.5, 5.8 Hz, 1H), 1.72 (s, 2H). ES-MS found *m/z* 219.1 for $[M+H]^+$

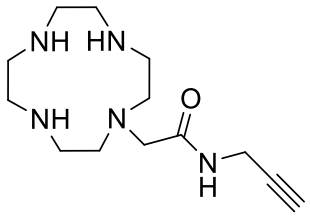
2.15 methyl (2-chloroacetyl)-L-tryptophanate (2.15)



L-Tryptophan methyl ester (5 g, 19.6 mmol) was dissolved in dichloromethane (100 mL) and was allowed to stir in a three-necked round bottom flask. Potassium carbonate (8.68 g, 63 mmol) was dissolved in water (100 mL) and a solution of 2-chloroacetyl chloride (3.1 mL, 39.2 mmol) in dichloromethane (30 mL) were added to the reaction mixture over a period of 30 min at 0°C. The reaction was first allowed to stir at 0°C for 2 h and a further stirred for 18 h after raised to room temperature. The progress of the reaction was monitored by TLC (CH_3Cl:CH_3OH/9.5:0.5) and on completion, and the organic layer of the reaction mixture was separated. The aqueous portion was extracted twice with dichloromethane (3 x 250 mL). The organic portions were combined and dried over sodium sulphate. The organic solvent was removed under reduced pressure to afford an oily liquid **2.15** in 88.3%

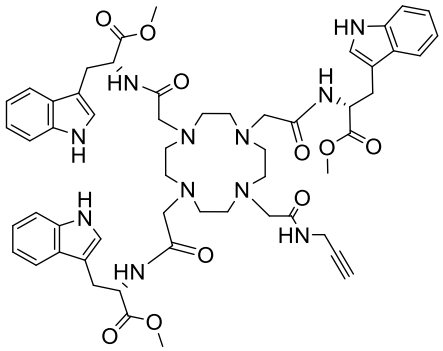
yield. No further purification was conducted. ^{1}H-NMR (400 MHz, $CDCl_3$) δ 8.09 (d, 1H), 7.67 – 7.60 (m, 1H), 7.57 (d, 1H), 7.43 – 7.36 (m, 1H), 7.26 – 7.12 (m, 2H), 7.08 (d, 0H), 4.78 (dt, 1H), 4.06 (d, 1H), 3.96 (d, 1H), 3.70 (s, 3H), 3.20 (dd, 1H), 2.86 (dd, 1H). ES-MS found *m/z* 317.1 for $[M+Na]^+$

2.16 2-(1,4,7,10-tetraazacyclododecan-1-yl)-N-(prop-2-yn-1-yl)acetamide (2.16)



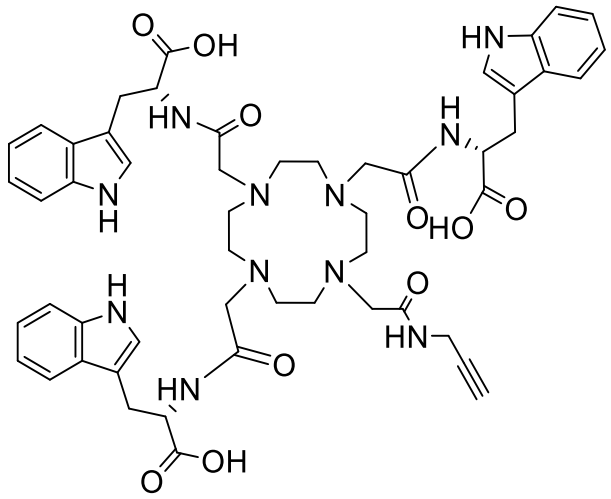
The synthesis of mono-alkylated cyclen involved the use of an alkyl halide (bromo/chloro) (1 mmol). To the solution of alkyl halide in $CHCl_3$ (15 mL), a solution of cyclen (4 mmol, 4 equiv) and triethylamine (1.2 mmol, 1.2 equiv) in freshly distilled $CHCl_3$ (15 mL) was added in one portion. The resulting solution was then refluxed gently for 15 h under nitrogen. After cooling, the organic solution was washed three times with the 1 M sodium hydroxide solution (3 x 15mL) to remove the excess of cyclen and dried over $MgSO_4$. The solvent was removed under reduced pressure to afford a colourless oil. The unreacted cyclen could be recycled by concentrating the previous alkaline solution under reduced pressure and adjusting the pH of this concentrate to neutral pH using HCl (1 M). ^{1}H-NMR (400 MHz, Chloroform-d) δ 4.01 (dd, 2H), 3.11 (d, 2H), 2.61 (d, 16H), 2.15 (q, J = 2.4 Hz, 1H). TOF-MS found *m/z* 268.2063 for $[M+H]^+$

2.17 Dimethyl-2,2'-((2,2'-(7-(2-(((S)-3-(1H-indol-3-yl)-1-methoxy-1-oxopropan-2-yl)amino)-2-oxoethyl)-10-(2-oxo-2-(prop-2-yn-1-ylamino)ethyl)-1,4,7,10-tetraazacyclododecane-1,4diyl)-bis(acetyl))bis(azanediyl))(2R,2'R)-bis(3-(1H-indol-3-yl)propanoate) (2.17)



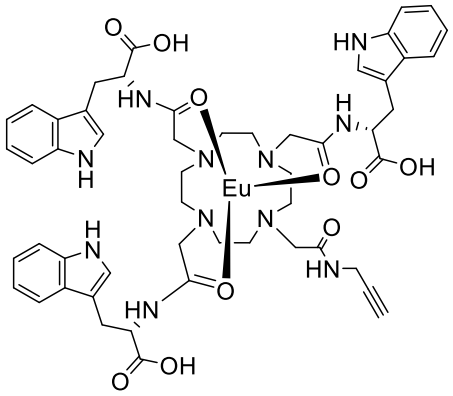
K_2CO_3 (2.38 g, 5.9 mmol) was added to a solution of compound **2.16** (0.5 g, 1.8 mmol) in acetonitrile (25 mL). Compound **2.15** (1.68 g, 5.6 mmol) was added to the suspension and the suspension was left stirring under N_2 overnight at 70 °C. After the reaction was completed, the filtration was used to remove the inorganic salt and filtrate was concentrated under reduced pressure. The crude product was further purified by gradient column chromatography (0 % MeOH in $CHCl_3$ to 10 MeOH in $CHCl_3$) to give yellow solid (1.19 g, 65 %). NMR: ^{1}H-NMR (400 MHz, MeOD-d_4) δ 7.53 – 7.29 (m, 3H), 7.30 – 7.14 (m, 3H), 7.10 – 6.76 (m, 9H), 4.73 – 4.54 (m, 3H), 3.87 – 3.41 (m, 9H), 3.21 – 1.61 (m, 30H).^{13}C-NMR (500 MHz, MeOD-d_4) δ 172. 4, 172. 4, 172.1, 170.8, 170.7, 169.6, 137.5, 137.4, 137.3, 128.6, 124.1, 123.9, 121.4, 121.2, 119.3, 117.9, 117.7, 113.2, 113.1, 113.0, 111.4, 111.3, 111.2, 77.9, 72.0, 58.1, 58.1, 57.1, 53.6, 53.6, 53.6, 53., 53.01, 52.96, 52.91, 52.9, 52.9, 28.71, 28.6, 28.5. TOF-MS found *m/z* 1042.5070 for $[M+H]^+$

2.19 (2R,2'R)-2,2'-((2,2'-(7-(2-(((S)-1-carboxy-2-(1H-indol-3-yl)ethyl)amino)-2-oxoethyl)-10-(2-oxo-2-(prop-2-yn-1-ylamino)ethyl)-1,4,7,10-tetraazacyclododecane-1,4 diyl)bis(acetyl))bis(azanediyl)) bis(3-(1H-indol-3-yl)propanoic acid) (2.19)



Compound **2.18** (1.0 g, 0.96 mmol) was dissolved in DCM (5 mL) and TFA (5 mL) was added dropwise. The solution was stirred at RT for 24 h. The solvent was removed under reduced pressure and the residue dissolved in the minimum amount of methanol and precipitated with diethyl ether. Trituration with diethyl ether yielded the TFA salt of the title compound as a white solid in quantitative yield. ^{1}H-NMR (400 MHz; MeOD-d4): δ δ7.69 – 7.62 (m, 1H), 7.41 (d, J = 7.5, 1H), 7.21 (dt, J = 21.2Hz, 2H), 6.98 (d, J = 9.3 Hz, 1H), 4.62 – 4.50 (m, 2H), 3.36 – 3.24 (m, 2H), 3.09 (d, J = 14.6, 1H), 2.93 (d, J = 0.7 Hz, 5H), 2.75 (d, J = 14.6, 1H). TOF-MS found *m/z* 1022.4603 for $[M+Na]^{+}$

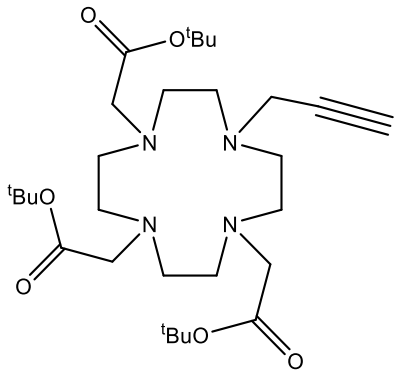
2.19 General procedure for the preparation of the europium complexes



A slight excess of europium triflate salt was added to a solution of **2.18** in methanol, and the reaction mixture was stirred at 60º C for 30 min. The pH was raised to 4 by dropwise addition of an aqueous NaOH solution. The reaction was left stirring at 60º C for 72 h. The methanol was removed under reduced pressure leaving an oil that was dissolved in water. The pH of this solution was adjusted to 10 by the addition of aqueous NaOH to remove excess of lanthanide as its insoluble hydroxide. The resulting precipitate was centrifuged and the supernatant was collected after filtration. The solvent was removed under reduced pressure to afford the product as a beige solid.

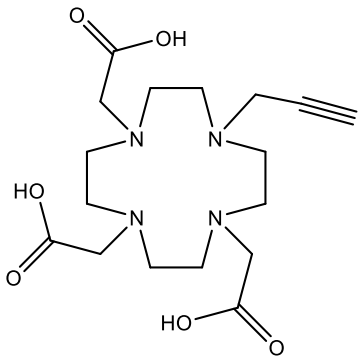
^{1}H-NMR (400 MHz, D_2O) δ 46.36, 43.88, 39.74, 36.14, 34.49, 33.95, 32.62, 30.92, 28.76, 25.28, 20.85, 9.08, 8.14, 7.89, 7.60, 7.52, 7.39, 6.90, 6.45, 3.79, 3.47, 3.29, 3.06, 2.96, 2.71, 2.50, 2.30, 1.80, 1.57, 1.13, -17.42, -24.34, -26.11, -35.23, -36.46, -37.46, -39.38, -39.73, -40.12, -40.89, -42.39, -43.63. TOF-MS found *m/z* 1042.5070 for $[M+H]^+$ 1153.3815

tri-tert-butyl-2,2',2''-(10-(prop-2-yn-1-yl)-1,4,7,10-tetraazacyclodo-decane-1,4,7-triyl)triacetate (3.1) [10–12]



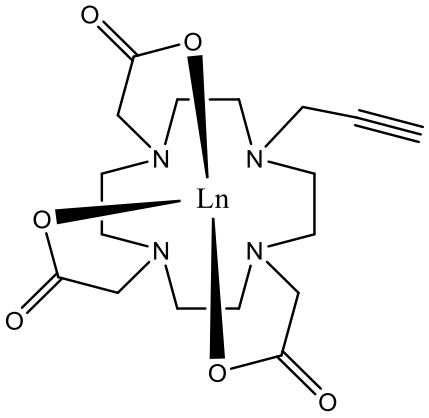
To a solution of **2.3** (2.50 g, 4.2 mmol) in 30 ml of dry acetonitrile was added potassium carbonate (1.45 g, 10.5 mmol) and this suspension was left stirring for 20 min. Propargyl bromide (0.62 g, 4.2 mmol) was added dropwise while keeping the reaction flask in an ice bath. The reaction was left stirring under nitrogen for 8 h at RT and monitored by ES-MS. The inorganic solids were removed by filtration and the solvent evaporated under reduced pressure. The product was obtained as a beige oil after successive filtrations from toluene to remove residual inorganic solid. (2.14 g, 92 %). ^{1}H-NMR (400 MHz; $CDCl_3$): δ 3.43 (d, J = 2.0, 2H), 3.28 (s, 6H), 2.82-2.79 (m, 12H), 2.69 (m, 4H), 2.14 (t, J = 2.0, 1H), 1.45 (s, 27H). 13C NMR (500 MHz; $CDCl_3$): δ 171.2, 129.1, 128.3, 125.4, 80.8, 79.4, 72.6, 56.9, 52.2, 51.90, 51.71, 43.2, 28.3. ES-MS: m/z calc. for [M+H]+ 553.40, found 553.37.

3.2 2,2',2''-(10-(prop-2-yn-1-yl)-1,4,7,10-tetraazacyclododecane-1,4,7-triyl)triacetic acid[13]



Compound **2.4** (0.7 g, 1.26 mmol) was dissolved in DCM (8 mL) and TFA (8 mL) was added dropwise. The solution was stirred overnight at RT. The solvent was removed under reduced pressure and the residue dissolved in the minimum amount of methanol and precipitated with diethyl ether. Trituration with diethyl ether yielded the TFA salt of the title compound as a white solid in quantitative yield. ^{1}H-NMR (400MHz; D_2O): δ 3.84-3.66 (br, 8H), 3.31-3.22 (m, br, 16H), 2.82 (s, br, 1H). ^{13}C-NMR (500MHz, D_2O) δ = 31.38, 36.89, 43.61, 45.49, 48.86, 49.74, 51.78, 52.86, 53.10, 53.28, 54.44, 56.84, 72.62, 77.65, 171.98, 174.36. LR-ESMS: m/z calc. for $[M+H]^+$ 384.20, found 385.22.

3.3 General procedure for preparation of lanthanide propargylDO3A complexes from[13]



A slight excess of europium triflate salt (1.1 eq.) was added to a solution of the **3.2** in methanol, and the reaction mixture was stirred at 60º C for 30 min. The pH was raised to 4 by dropwise addition of an aqueous NaOH (2M) solution. The reaction was left stirring at 60º C for 72 h. The methanol was removed under reduced pressure to afford a glassy solid. The residue was dissolved in a minimum amount of water. The pH of this solution was adjusted to 10 by an addition of aqueous NaOH (2M) to remove excess of lanthanide as its insoluble hydroxide. The resulting precipitate was centrifuged and the supernatants were collected after filtration. The solvent was removed under reduced pressure to afford the product as a white solid.

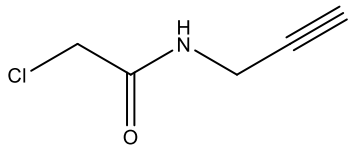
3.3 (Ln: Eu). Yield: 92%. ^{1}H-NMR (300 MHz; D_2O): δ 23.3 (s), 14.0 (s), 11.5 (s), 10.2 (s), -3.9 (s), -6.1 (s), -6.6 (s), -9.5 (s), -11.2 (s), -11.7 (s), -12.5 (s), -12.7 (s), - 13.1 (s), -14.8 (s), -17.7 (s). Only resolved peaks outside 0 to 10 ppm region are reported. MALDI-MS (α- MeOH): m/z calc. for [M+Na]+ 556.36, found 555.43. Luminescence: H2O: 0.40 ms, D_2O: 1.85 MS. q = 2.1.

3.4 (Ln: Tb). Yield: 89%. ^{1}H-NMR (500 MHz; D2O, pD7): δ 333.9, 317.1, 275.1, 141.3, 87.3, 72.3, -49.9, -63.8, -80.2, -84.6, -93.8, -101.3, -154.2, -162.9, -176.4, - 196.9, -208.4, -227.6, -313.0. Only resolved peaks related to the major isomer outside the +40 to -40 ppm region reported. MALDI-MS (α- MeOH): calc. for [M+Na]+ 563.32, found 565.01. Lifetimes: H_2O: 1.13 ms, D_2O: 2.69 ms; q=2.3.

3.5 (Ln: Yb). Yield: 87%. ^{1}H-NMR (300 MHz; D2O): δ 85.7, 62.6, 53.3, 39.7, 29.9, 23.9, 23.5, 12.4, -4.9, -8.4, -11.1, -12.1, -17.9, -18.3, -20.1, -30.1, -52.5, -56.9. Only resolved peaks outside 0 to 10 ppm region are reported. LR-ESMS: m/z calc. for $[M+Na]^+$ 578.11, found 578.13.

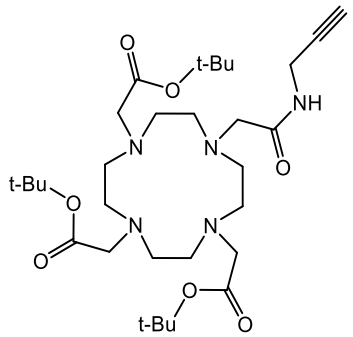
3.6 (Ln: Lu) Yield: 92%. ^{1}H-NMR (300 MHz; D2O): δ 3.93 (s, br, 1H), 3.33 (s, br, 8H), 3.03-2.63 (m, br, 17H). LR-ESMS: m/z calc. for $[M+Na]^+$ 579.11, found 579.15.

3.7 2-bromo-N-(prop-2-yn-1-yl) acetamide (3.7)[14]



Propargylamine (1.7 g, 31.2 mmol) was dissolved in dry DCM (50 ml) and cooled to 0 ^{o}C in an ice bath. Chloroacetyl chloride (1.76 g, 15.6 mmol) was added dropwise and the reaction mixture was allowed to stir for 30 min at RT under nitrogen. The reaction was washed with water (4 x 30 ml) and brine (2 x 30 ml). The organic solvent was dried over anhydrous NaSO4, filtered and evaporated under reduced. The product was isolated as a brown solid and used immediately. ^{1}H-NMR (400 MHz; $CDCl_3$): δ 6.78 (s, 1H), 4.10 (br, 2H), 4.06 (s, 2H), 2.27 (br, 1H).

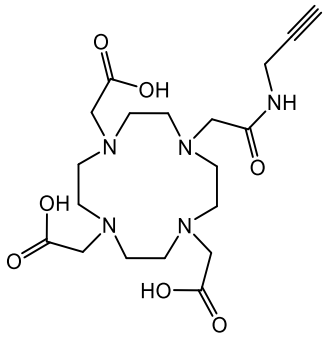
3.8 tri-tert-butyl2,2',2''-(10-(2-oxo-2-(prop-2-yn-1-ylamino)ethyl)-1,4,7,10-tetraazacyclo-dodecane-1,4,7-triyl)triacetate (3.8)



To a solution of **triester** (1g, 1.67) mmol) in dry acetonitrile, potassium carbonate was added (0.46g, 3.3 mmol) followed by **3.7** (0.22g, 1.67 mmol). The reaction was left stirring

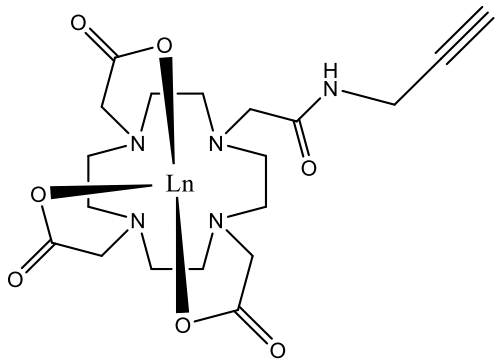
at RT under nitrogen for 24 hours. The suspension was then filtered and the solvent was removed under reduced pressure. The crude was purified by silica get column chromatography (gradient eluent DCM:MeOH = from 100:0 to 90:10, v:v) to obtain a yellow solid. (0.82g, 80%). ^{1}H-NMR (400 MHz, Methanol-d_4) δ 3.96 (s, 2H), 3.72 – 1.77 (m, 22H), 1.63 (s, 9H), 1.46 (s, 18H). TOF-MS found *m/z* 610.4103 for $[M+H]^+$

3.9 2,2',2''-(10-(2-oxo-2-(prop-2-yn-1-ylamino)ethyl)-1,4,7,10-tetraaza cyclododecane-1,4,7-triyl)triacetic acid (3.9)



DCM (8 ml) and TFA (8ml) was added dropwise to a solution of **2** (0.82 g, 1.34 mmol). The reaction was stirred at RT for 24 h before removing solvent under reduced pressure. The resulting solid was treated with a small amount of methanol following addition of diethyl ether to triturate the target product as white powder. The solvent was decanted and the solid was dried under vacuum to afford target ligand as white powder. ^{1}H-NMR (400 MHz, D_2O-d2) δ 4.13 – 3.47 (m, 12H), 3.27 (s, 16H). TOF-MS found *m/z* 442.2226 for $[M+H]^+$.

3.10 General procedure for preparation of lanthanide amide-propargyl DO3A complexes from 3.10



The ligand was dissolved in methanol and the lanthanide chloride hexahydrate was added. The suspension was stirred at 60 ^{o}C for 1 hour. And the pH was adjusted to 4 by adding dropwise sodium hydroxide (1M) solution. The reaction was left stirring at 60 ^{o}C for 48 hours. The resulting oil was re-dissolved in methanol after the solvent was removed. The pH of solution was raised to 10 by dropwise addition of sodium hydroxide solution (1 M). The insoluble inorganic salt was removed by centrifuge and the supernatant was filtered by a syringe filter. The aqueous solvent was removed under freeze dryer to obtain product.

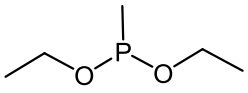
3.10 (Ln: Eu). Yield: 92%. ^{1}H-NMR (400 MHz; D_2O): δ 24.2, 14.2, 12.5, 11.2, -3.7, -6.1, -6.3, -6.5,, -11.2, -12.4 -12.9, - 13.3, -14.9, -18.7. Only resolved peaks outside 0 to 10 ppm region are reported. TOF-MS (MeOH): m/z calc. for $[M+H]^+$ 637.19, found 637.20.

3.11 (Ln: Tb). Yield: 92%. 1H NMR (400 MHz; D2O, pD7): δ 334.0, 310.2, 271.5, 143.4, 83.2, -51.2, -68.8, -89.2, -89.6, -98.2, -113.3, -145.2, -169.9, -179.8, - 199.6, -224.5, -226.7,

-343.0. Only resolved peaks related to the major isomer outside the +40 to -40 ppm region reported. LR-ESMS: m/z calc. found 565.01 for $[M+Na]^+$,

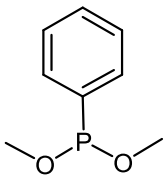
3.12 (Ln: Lu) Yield: 89%. ^{1}H-NMR (400 MHz; D_2O): δ 3.01 (s, 1H), 3.42 (s, 8H), 3.03-2.69 (m 17H). ES-MS: m/z calc. for [M+Na]+ 579.11, found 579.15.

3.14 Diethyl methylphosphonite



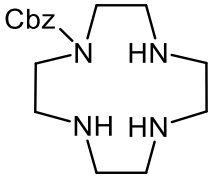
To a 3-neck 2 L round bottom flask were added pentane (6 mL), ethanol (1.1 mL, 18 mol), and N, N-dimethylaniline (235.8 mL, 1.860 mol). The mixture was cooled to 0° C in an ice bath and was allowed to stir under nitrogen. Dichloromethylphosphine (1 g, 8.5 mmol) was dropwise added through an addition funnel over a period of about 20 minutes. After the addition was complete, the mixture was stirred for an additional 1.5 h at 0° C. The reaction mixture was then filtered through a cannula filter. The filter cake was washed with 10 mL of pentane. The cloudy filtrate was then concentrated on a rotary evaporator at 0° C and then distilled. The target product was collected between 300 and 400 mTorr at a distillation head temperature of 20-22° C. The product was isolated as a clear oil (0.7 g, 62%) and used directly in the next step. ^{1}H-NMR (400 MHz, $CDCl_3$) δ 3.87 – 3.75 (m, 4H), 1.22 (td, 6H), 1.06 (d, 3H). ^{31}P-NMR (400 MHz, $CDCl_3$) δ 173.2

3.17 Dimethyl phenylphosphonite



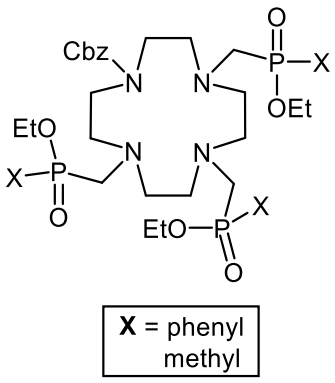
Degassed pyridine (1.8 g, 22 mmol) was dropwise added to a solution of dichlorophenylphosphine (2 g, 11 mmol) in 20 mL of hexane (degassed) under argon at 25 °C. After stirring for 30 min, the mixture was cooled to 0 °C. Whilst vigorous stirring was maintained, methanol (12 mL, 0.22 mol) was added dropwise. The reaction was allowed to stir overnight, and the pyridine hydrochloride salts were removed by canula filtration. The solvent was then removed under reduced pressure and the residue was distilled at reduced pressure (53-54 °C/1 Torr) to afford the product as a colourless liquid 1.7 g (10 mmol, 95 %). ^{1}H-NMR (400 MHz, $CDCl_3$) δ 7.50 – 7.43 (m, 2H), 7.34 – 7.20 (m, 3H), 3.53 (d, 5H).

3.19 Benzyl 1,4,7,10-tetraazacyclododecane-1-carboxylate



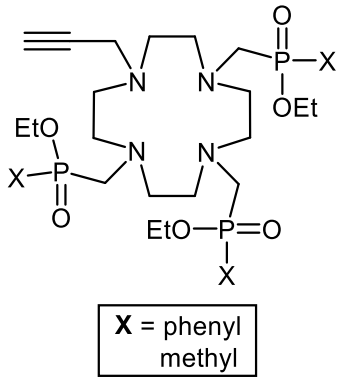
To a cooled solution (0 °C) of the protected cyclen 3 (8.0 g, 13.2 mmol) in methanol (10 mL) was added concentrated HCl (10 mL) dropwise. The resulting solution was allowed to warm to room temperature and stirred for 8 h. The reaction was concentrated at room temperature under reduced pressure to a volume of 15 mL, and the precipitates were removed by filtration. The residue was then crystallized from a mixture of water and tetrahydrofuran to afford the title compound as a colourless crystalline solid (5.1 g, 94%). ^{1}H-NMR (400 MHz, CD_3OD): δ = 7.40 (5H, m), 5.15 (2H, s), 3.14 (16H, m). ES-MS found *m/z* 329.1 for $[M+Na]^+$

3.20 Benzyl-4,7,10-tris((ethoxy(methyl)phosphoryl)methyl/benzyl)-1,4,7,10-tetraaza-cyclododecane-1-carboxylate



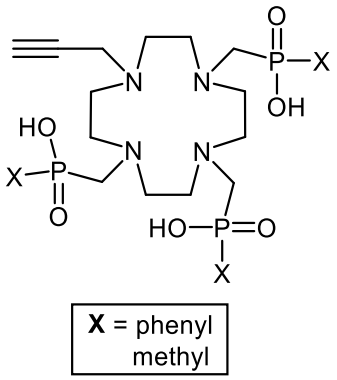
Molecular sieves were activated in the oven (200 °C) and loaded in a Soxhlet apparatus. Benzyl 1,4,7,10-tetraazacyclododecane-1-carboxylate (0.52g, 1.91 mmol) and paraform-aldehyde(1.15 g, 38.2 mmol) were dissolved in anhydrous THF (30mL) and the resulting suspension was heated at 80 °C for 3h. Diethylmethylphosphonite (1.7 mL, 11.5 mmol) was added and the solution stirred at 80 °C for a further 18 h. The solution was cooled and filtered, before the solvent was removed under reduced pressure. The residual brown oil was purified by alumina gel column chromatography, eluting with a gradient starting from 100% CH2Cl2 to 2% MeOH/ CH_2Cl_2 to yield a pale-yellow oil (0.4 g, 33%). ^{1}H-NMR (Methyl, 400 MHz, Chloroform-d) δ 7.33 (s, 2H), 7.38 – 7.29 (m, 0H), 5.16 (d, J = 0.8 Hz, 1H), 4.25 (d, J = 8.53H), 3.25 (t, J = 5.4 Hz, 2H), 3.07 (d, J = 12.3 Hz, 6H), 2.75 (d, J = 11.9 Hz, 3H), 1.34 (d, J = 13.8, 2H), 1.26 (d, J = 12.9 Hz, 4H). ^{1}H-NMR (Phenyl, 400 MHz, Chloroform-d) δδ7.82 – 7.71 (m, 2H), 7.49 – 7.37 (m, 3H), 7.23 (s, 1H), 5.06 (d, J = 0.8 Hz, 1H), 4.15 (d, J = 8.5, 2H), 3.53 (d, J = 11.9 Hz, 2H), 3.15 (t, J = 5.4 Hz, 1H), 2.97 (d, J = 12.3 Hz, 4H), 1.24 (d, J = 7.1 3H). ES-MS found m/z 756.3 for $[M^{phenyl}+H]^+$.

3.21 Diethyl ((4-((ethoxy(methyl/phenyl)phosphoryl)methyl)-10-(prop-2-yn-1-yl)-1,4,7,10-tetraazacyclo-dodecane-1,7-diyl)bis(methylene))bis(methylphosphinate)



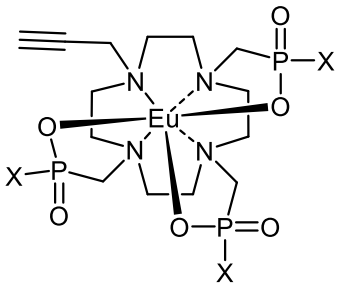
Compound **3.20** was placed in Schlenk flask and the flask was charged with Pd/C (10 wt %) and methanol (25 mL). The air was replaced by hydrogen gas via freeze-pump-thaw. The suspension was left stirring for 1 week at RT. The resulting mixture was filtered through the Celite pad and the solvent was removed *in vacuo*. The oil obtained was used for next step. The oil was dissolved in acetonitrile (5 mL / mmol) cooled in ice bath and 2 equivalent K_2CO_3 was added following dropwise addition of 1.1 equivalent propargyl bromide over 20 minutes. The reaction was left under nitrogen for overnight at RT and checked with TLC (10 % MeOH in $CHCl_3$). The inorganic salt was removed by filtration and the solvent was removed *in vacuo*. The target product was obtained as yellow oil after washed with toluene to removed excess propargyl bromide. ^{1}H-NMR (methyl, 400 MHz, $CDCl_3$) δ 4.20 (d, J = 8.5, 2H), 3.72 (d, J = 2.9 Hz, 1H), 3.04 (s, 5H), 2.70 (d, J = 11.9 Hz, 2H), 1.29 (d, J = 6.9, 3H), 1.21 (m, 3H). ^{1}H-NMR (phenyl, 400 MHz, $CDCl_3$) δ 8.22 – 8.15 (m, 6H), 7.88 – 7.81 (m, 9H), 4.58 (d, *J* = 8.5, , 6H), 4.10 (d, *J* = 2.9 Hz, 2H), 3.96 (d, *J* = 11.9 Hz, 6H), 3.42-2.60 (m, 16H), 2.64 (d, *J* = 6.0 Hz, 1H), 1.67 (t, *J* = 7.0, 9H). ES-MS found m/z 852.3 for $[M^{phenyl}+H]^+$

3.22 ((4-((hydroxy(methyl/phenyl)phosphoryl)methyl)-10-(prop-2-yn-1-yl)-1,4,7,10-tetraazacyclododecane-1,7-diyl)bis(methylene))bis(methylphosphinic acid)



Compound **3.21** (0.5 mmol) and KOH (1.1 g, 20 mmol) were dissolved in H_2O (25 mL) and a small amount of MeOH(0.1 mL) was added into mixture. The reaction mixture was allow to stir at RT for 2 days. The pH of solution was raised by the addition of conc. HCl and the solvent was removed under reduced pressure. The resulting solids were re-dissolved in a 2mL MeOH and filtered. The filtrate was collected and the solvent was removed under reduced pressure to afford a pale-yellow solid. ^{1}H-NMR (methyl, 400 MHz, $CDCl_3$) δ 3.72 (d, *J* = 2.9 Hz, 2H), 3.04-2.52 (m, 16H), 2.70 (d, *J* = 11.9 Hz, 6H), 2.26 (m, 1H), 1.21 (m, 9H). ^{1}H-NMR (phenyl, 400 MHz, $CDCl_3$) δ 7.82 – 7.71 (m, 6H), 7.49 – 7.37 (m, 9H), 3.67 (d, *J* = 2.9 Hz, 2H), 3.53 (d, *J* = 11.9 Hz, 5H), 2.99-2.21 (m, 16H). ES-MS found m/z 486.1 for $[M^{methyl}+H]^+$

3.23-3.24 General procedure for preparation of lanthanide propargyl phosphinate DO3A complexes



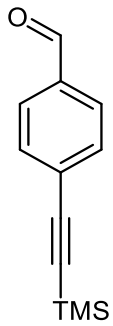
X = phenyl methyl	**3.23** **3.24**

The ligand was dissolved in methanol and lanthanide chloride hexahydrate was added. The suspension was stirred at 60 ^{o}C for 1 hour. And the pH was adjusted to 4 by adding dropwise sodium hydroxide (1M) solution. The reaction was left stirring at 60 ^{o}C for 48 hours. The resulting oil was re-dissolved in methanol after the solvent was removed. The pH of solution was raised to 10 by dropwise addition of sodium hydroxide solution (1 M). The insoluble inorganic salt was removed by centrifuge and the supernatant was filtered by a syringe filter. The aqueous solvent was removed under freeze dryer to obtain product.

3.23 (Ln: Eu X: Phenyl) ^{1}H NMR (400 MHz, D_2O) δ 36.9, 31.9, 28.8, 27.5, 25.8, 26.3, 24.0, 23.5, 22.2, 21.4, 21.1, 15.5, 14.2, 13.1, 10.9, -2.0, -3.2, -3.6, -4.0, -6.6, -7.0, -7.7, -7.8, -8.5, -8.7, -9.6, -10.8, -11.3, -12.3, -12.8, -13.3, -14.4, -14.8, -15.1, -16.2, -17.3.

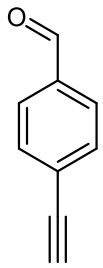
3.24 (Ln: Eu X: Methyl) ^{1}H NMR (400 MHz, D_2O) δ 34.7, 29.8, 24.7, 16.5, 1.7, 0.9, 0.1, -0.6, -1.4, -3.8, -5.9, -9.0, -9.3, -9.7, -13.1, -13.6, -14.5, -14.7, -15.8, -16.2.

3.26 4-((trimethylsilyl)ethynyl)benzaldehyde



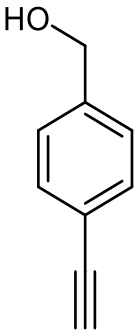
4-iodobenzaldehyde was dissolved in 5.4 mL THF and trimethylsilylacetylene (0.9 mL, 6.44 mmol), diisopropylethylamine(1.2 mL, 6.88 mmol), dichlorobis-(triphenylphosphine) palladium(II) (20 mg) and copper iodide (10 mg, 0.06 mmol) were added into Schlenk flask. The mixture was degassed three times by freeze-pump-thaw and the reaction solution was left stirring for overnight at RT. After reaction completed, the reaction solution was filtered and washed with 1M sodium chloride solution for three times. The organic layers were combined and dried over $MgSO_4$ before removing the solvent under reduced pressure. The crude product was further purified by silica gel column chromatography (EtOAc/hexane = 1/10) to give 0.8 g (96%) product as white powder. ^{1}H-NMR (400 MHz, $CDCl_3$): δ 9.89 (s, 1H), 7.69 (d, 2H), 7.45 (d, 2H), 0.14 (s, 9H)

3.27 4-ethynylbenzaldehyde



K_2CO_3 (0.056 g, 0.04 mmol) was added to the solution of **3.26** (0.8 g, 4 mmol) in methanol (50 mL). The reaction was allowed to stir at RT for 1h and the solvent was removed under reduced pressure. The resulting crude product was re-dissolved in dichloromethane (20 mL) and washed with saturated sodium bicarbonate solution for 3 times. The organic fractions were combined and dried over magnesium sulphate to afford pale yellow solid in quantitative yield after further dried in Schlenk line. ^{1}H-NMR (400 MHz, $CDCl_3$): δ = 9.8 ppm (s, 1H), 7.7 ppm (d, J = 8.2 Hz, 2H), 7.6 ppm (d, J = 8.1 Hz, 2H), 3.1 ppm (s, 1H).

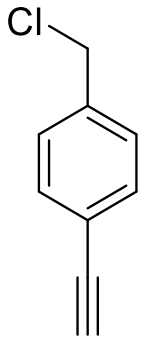
3.28 (4-ethynylphenyl)methanol



To the solution of **3.27** (0.5 g, 3.7 mmol) in methanol, sodium borohydrate (150 mg, 4 mmol) was added portionwise at 0 °C. The resulting mixture was allowed to stir for 10

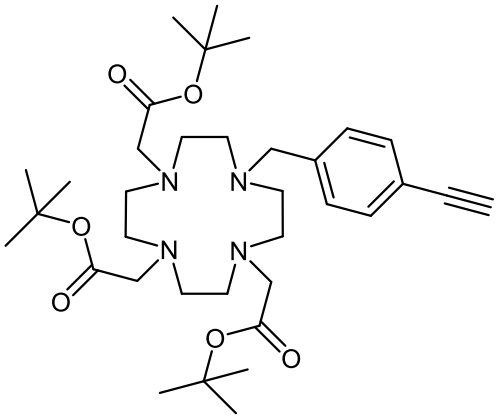
minutes. The reaction mixture was then quenched by the addition of 1M HCl solution before water (10 mL) was added to the solution. Chloroform (15 mL x 3) was used to extract the crude product from mixture and the organic solution was dried over magnisum sulphate. The crude product was purified by silica gel column chromatography (EtOAc/hexane = 3/2) to give target product as transparent oil (490 mg, 94 %). ^{1}H-NMR (400 MHz, $CDCl_3$) δ 7.44 – 7.36 (m, 2H), 7.32 (d, *J* = 8.3, 2H), 5.65 (d, *J* = 5.6Hz, 2H), 3.20 (t, *J* = 5.6 Hz, 1H), 3.00 (s, 1H).

3.29 1-(chloromethyl)-4-ethynylbenzene



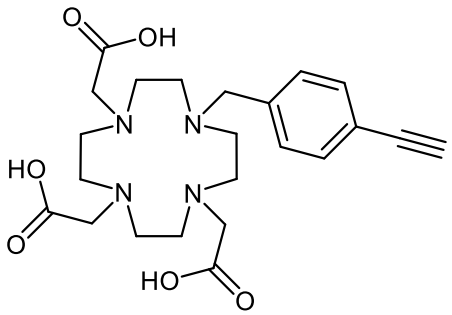
To the solution of **3.28** (0.49 g, 3.7 mmol) in dichloromethane (2 mL) methanesulfonyl chloride (0.311 mL, 4 mmol) was added dropwise to the mixture at 0 °C following an addition of triethylamine (0.55 mL, 4 mmol). The resulting mixture was heated to 60 °C for 6 hours before solvent was removed *in vacuo*. The crude product was purified by silica gel column chromatography (100 % hexane) to afford desired compound as colourless oil (0.28 g, 50 %). ^{1}H-NMR (400 MHz, $CDCl_3$) δ 7.54 – 7.46 (d, J = 7.4 Hz, 2H), 7.26 (d, *J* = 7.9 Hz, 2cH), 4.62 (s, 2 H), 3.10 (s, 1H).

3.30 tri-tert-butyl-2,2',2''-(10-(4-ethynylbenzyl)-1,4,7,10-tetraazacyclododecane-1,4,7-triyl)triacetate



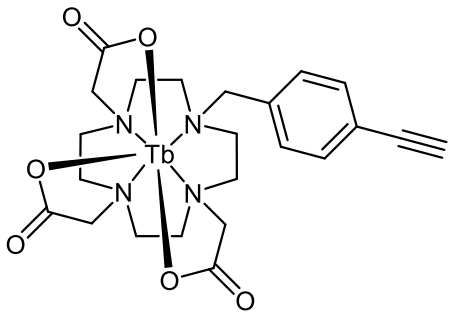
Potassium carbonate (0.42 g, 3.0 mmol) and **3.29** (0.22 g, 1.8 mmol) was added to a solution of **triester**(1.05 g, 1.75 mmol) in dry acetonitrile (50 mL). The reaction was allowed to stir at RT for overnight. The resulting mixture was then filtered and the solvent was removed under reduced pressure. The crude product was further purified by silica gel column chromatography (gradient eluent 0 % to 10 % MeOH in $CHCl_3$) to afford a yellow solid. (0.88 g, 78 %). ^{1}H-NMR (400 MHz, $CDCl_3$) δ 7.57 (d, *J* = 8.2, 2H), 7.36 (dt, *J* = 8.3, 2H), 3.86 (s, 2H), 3.26 – 2.60 (m, 22 H), 1.49 (s, 18H). ES-MS found *m/z* 629.4 for $[M+H]^+$

3.31 2,2',2''-(10-(4-ethynylbenzyl)-1,4,7,10-tetraazacyclododecane-1,4,7-triyl)triacetic acid



DCM (4 ml) and TFA (4 ml) were added dropwise to a solution of **2** (0.88 g, 2.34 mmol). The reaction was allowed to stir at RT for 24 h before removing solvent under reduced pressure. The resulting solid was treated with a small amount of methanol followed by addition of diethyl ether to triturate the target product as white powder. The solvent was decanted and the solid was dried under vacuum to afford target ligand in quantitative yield. ^{1}H-NMR (400 MHz, Chloroform-*d*) δ 7.50 (d, J = 8.7 Hz, 2H), 7.28 (d *J* = 8.3, 2H), 3.79 (s, 2H), 3.44 (s, 2H), 3.24 - 2.8 (m, 22H). 3.06 (s, 1H).

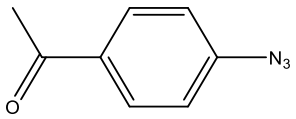
3.32 General procedure for preparation of lanthanide ethynyl propargyl DO3A complexes



The ligand was dissolved in methanol and lanthanide chloride hexahydrate was added. The suspension was allowed to stir at 60 ^{o}C for 1 hour. And the pH was adjusted to 4 by adding dropwise sodium hydroxide (1M) solution. The reaction was left stirring at 60 ^{o}C for 48 hours. The resulting oil was re-dissolved in methanol after the solvent was removed. The pH of solution was raised to 10 by dropwise addition of sodium hydroxide solution (1 M). The insoluble inorganic salts were removed by centrifuge and the supernatant was filtered by a syringe filter. The aqueous solvent was removed under freeze dryer to obtain product.

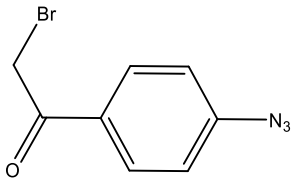
3.32 (Ln = Tb) ^{1}H-NMR (400 MHz; D_2O, pD7): δ 339.32, 143.06, 114.54, -10.49, -12.29, -14.12, -16.11, -64.72, -146.30, -155.91, -180.57, -192.41, -343.85, -499.60. Only resolved peaks outside -10 to 10 ppm are reported.

3.35 4-Azido acetophenone



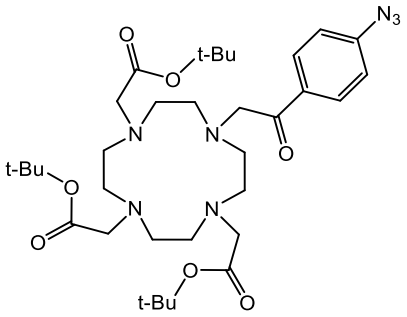
To a solution of 4-aminoacetophenone (1.2 g, 8.8 mmol) in acetonitrile (25 mL), *t*-BuONO (1.37 g, 13 mmol) was added at 0°C followed by dropwise addition of $TMSN_3$ (1.2 g, 11 mmol). The mixture was allowed stirring at RT for 4 h before the solvent was removed *in vacuo*. The resulting solid was washed with hexane, and concentrated *in vacuo* and dried in Schlenk line to give the target compoundas pure yellow crystals (1.35 g , 92%). ^{1}H-NMR (400 MHz, $CDCl_3$) δ: 2.62 (s, 3H), 7.14 (d, J = 8.0 Hz, 2H), 8.00 (d, J = 8.0 Hz, 2H).

3.36 1-(4-azidophenyl)-2-bromoethan-1-one



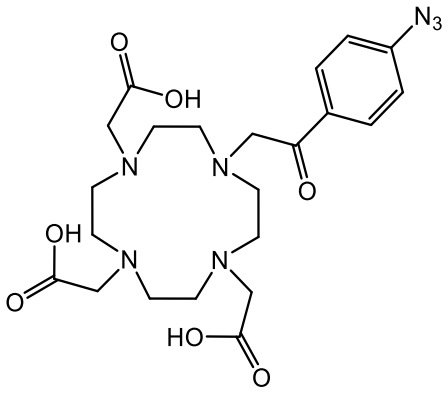
To a solution of **3.35** (2.00 g, 12.4 mmol) and p-toluenesulfonic acid monohydrate (4.70 g, 24.8 mmol) in MeCN (200 mL), N-Bromosuccinimide (2.20 g, 12.4 mmol) was added portionwise. The resulting mixture was refluxed under vigorous stirring for 2h. After reaction completed, the mixture was allowed to cool down at RT and the solvent was removed *in vacuo.* The resulting solid re-dissolved in dichloromethane (60 mL) and washed with water (2 x 60 mL). The organic layers were combined and dried over $MgSO_4$ before solvent was removed *in vacuo*. The crude product was purified by silica gel chromatography (hexane : dichloromethane = 1:1) to give the target compound as a white solid (1.48 g, 50%). ^{1}H NMR (400 MHz; $CDCl_3$): δ 8.03 (d, J = 8.5, 2H), 7.10 (d, J = 8.4, 2H), 4.5 (s, 2H).

3.37 tri-tert-butyl−2,2',2''-(10-(2-(4-azidophenyl)-2-oxoethyl)-1,4,7,10-tetraazacyclododecane-1,4,7-triyl)triacetate



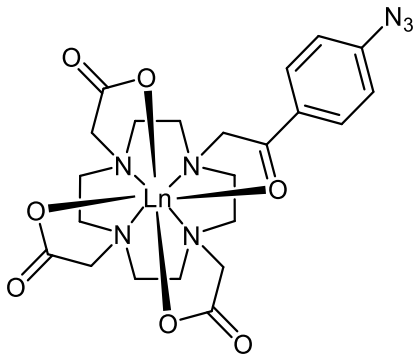
Triester (1 g, 1.67 mmol) was dissolved in dry acetonitrile (50 ml) and potassium carbonate (0.40 g, 3 mmol) was then added before addition of **3.35** (407 mg, 1.67 mmol). The reaction was left stirring at RT under nitrogen for 24 hours and the solvent was removed *in vacuo*. The crude was purified by silica get column chromatography (gradient eluent DCM:MeOH = from 100:0 to 90:10, v:v) to obtain an orange solid. (1.01g, 90%). ^{1}H-NMR (400 MHz; $CDCl_3$): δ 7.9-8.1 m, 2H), 7.0-7.2 (m, 2H), 3.45 – 2.06 (m, 24H), 1.45 (s, 27H). TOF-MS: found m/z 696.4061 for $[M+Na]^+$

3.38 2,2',2''-(10-(2-(4-azidophenyl)-2-oxoethyl)-1,4,7,10-tetraazacyclododecane-1,4,7-triyl)triacetic acid



DCM (6 ml) and TFA (6 ml) were added dropwise to a solution of **3.37** (0.97 g, 1.44 mmol). The reaction was stirred at RT for 24 h before removing solvent *in vacuo*. The resulting solid was treated with a small amount of methanol following addition of diethyl ether to triturate the target product as white powder. The solvent was decanted and the solid was dried under vacuum to afford target ligand in quantitative yield. ^{1}H-NMR (400 MHz, D_2O) δ 7.8-8.0 (m, 2H), 7.0.-7.2 (m, 2H), 4.04 – 2.76 (m, 24H). TOF-MS found *m/z* 506.234 for $[M+H]^+$

3.39-3.42 General procedure for preparation of lanthanide azido-phenacylDO3A complexes (3.39-3.42)



The ligand **3.38** was dissolved in methanol and lanthanide chloride hexahydrate was added. The suspension was stirred at 60 ^{o}C for 1 hour. The pH was adjusted to 4 by adding dropwise sodium hydroxide (1M) solution. The reaction was left stirring at 60 ^{o}C for 48 hours. The resulting oil was re-dissolved in methanol after the solvent was removed. The pH of solution was raised to 10 by dropwise addition of sodium hydroxide solution (1 M). The insoluble inorganic salt was removed by centrifuge and the supernatant was filtered by a syringe filter. The aqueous solvent was removed under freeze dryer to obtain product.

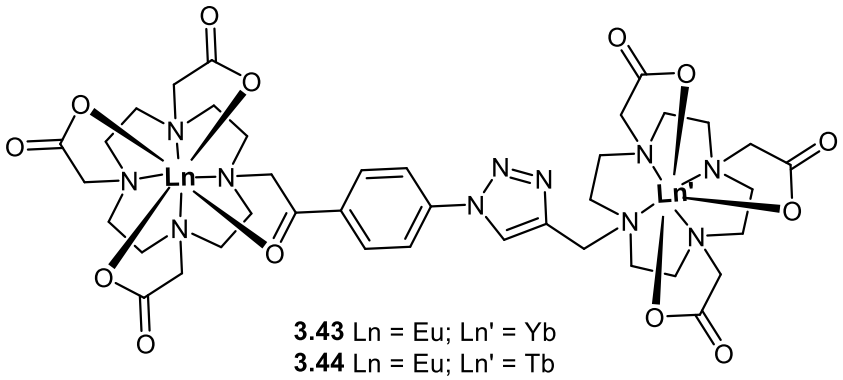
3.39 (Ln: Eu). ^{1}H-NMR (400 MHz; D_2O, pD7): δ 33.6, 31.8, 22.3, 20.1, 15.8, 9.6, -3.6, -5.0, -7.5, -8.9, -9.8, -11.2, -11.9, -15.8, -17.2. Only resolved peaks outside 0 to 5 ppm are reported. TOF-MS found *m/z* 678.1167 for $[M+Na]^{+}$.

3.40 (Ln: Tb). Yield: 87%. ^{1}H-NMR (500 MHz; D_2O, pD7): δ 309.0, 219.4, 186.7, 135.3, -53.9, -68.8, -141.3, -141.79, -197.1, -250.0, -264.1, -329.7. Only resolved peaks outside -20 to 20 ppm are reported. ES-MS found *m/z* 629.2 for $[M+H]^{+}$.

3.41 (Ln: Yb). Yield: 86%. ^{1}H-NMR (400 MHz; D_2O, pD7): δ 132.7, 125.7, 118.2, 89.5, 84.4, 79.9, 69.6, 66.1, 56.7, 42.5, 36.4, 29.0, 27.0, 23.7 22.8, 22.5, 17.8, 17.6, 15.2, 9.7, 7.0, 6.5, 6.2, 4.5, 3.8, 3.5, 2.7, 2.4, -6.6, -15.2, -18.2, -18.5, -18.9, -25.6, -28.5, -35.7, -37.5, -40.3, -43.5, -46.1, -48.1, -52.3, -69.5, -81.84. Only resolved peaks outside -20 to 20 ppm are reported. TOF-MS found *m/z* 699.1331 for $[M+Na]^+$

3.42 (Ln: Lu). ^{1}H-NMR (400 MHz; D_2O): δ 8.18 (d, J = 8.9, 2H), 7.27 (d, J = 8.9, 2H), 3.50 (br, 16H), 2.82 (br, 8H), 2.50 (br, 4H). TOF-MS found *m/z* 700.1351 for $[M+Na]^+$

General methods for the heterobimetallic complexes (3.39-3.42)



3.43 Ln = Eu; Ln' = Yb
3.44 Ln = Eu; Ln' = Tb
3.45 Ln = Tb; Ln' = Eu

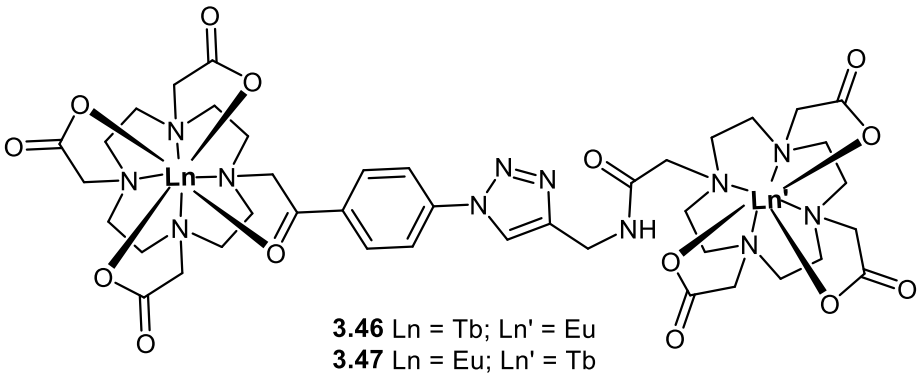
2 equivalents of propargylDO3A complexes was added into 1 equivalent of azidophenacylDO3A complexes in water. After addition of sodium ascorbate (10 mol%.) and copper (II) sulphate (2 mol%), the solution was stirred at 40 ˚C for 3 days, filtered by syringe filter and dialysed for 3 days using a 1000 MWCO membrane. The aqueous solvent was removed by freeze dryer to obtain a glazed solid, which was trituration by methanol and diethyl ether. The precipitate was collected and dried under high vacuum to yield green solid. The yield was calculated based on the starting azide

3.43. Yield 85 %. ^{1}H-NMR (400 MHz; D_2O, 293 K, pD7): δ 133.0, 109.6, 105.3, 104.2, 102.9, 101.9, 35.4, 33.9, 29.9, 24.3, 21.4, 19.9, -25.1, -27.4, -37.5, -45.2, -48.9, -51.5, -59.7, -62.9, -65.2, -65.9, -71.5, -82.1. Only resolved peaks outside -10 to 10 ppm are reported.

3.44. ^{1}H-NMR (400 MHz, D_2O, 293 K, pD7) δ 142.80, 114.02, 87.57, 73.62, 57.09, 47.50, 40.56, 35.47, 33.86, 29.94, 28.95, 27.18, 26.28, 22.97, 15.44, 13.71, -10.43, -12.21, -14.11, -15.70, -25.40, -28.60, -34.86, -42.06, -51.48, -64.51, -73.41, -81.32, -84.50, -90.01, -94.09, -231.18. Only resolved peaks outside -10 to 10 ppm are reported.

3.45 ^{1}H-NMR (400 MHz, D_2O, 293 K, pD7): δ 133.96, 105.56, 82.65, 59.67, 33.69, 32.95, 31.55, 30.60, 30.37, 27.39, 13.26, 11.54, 10.86, -11.05, -11.71, -12.32, -14.55, -14.93, -15.73, -16.76, -41.73, -52.59, -64.03, -67.47, -83.14, -88.32, -95.75, -99.39, -104.48, -113.41, -141.44, -152.49. Only resolved peaks outside -10 to 10 ppm are reported.

3.46 – 3.47 General methods for the heterobimetallic complexes (3.46 and 3.47)



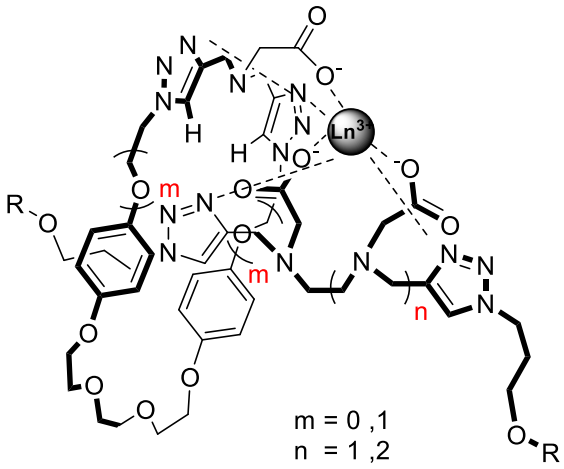
2 equivalents of propargylDO3A complexes (**3.11**) was added into 1 equivalent of azidophenacylDO3A complexes (**3.39**) in water: methanol (1:1). After addition of sodium ascorbate (10 mol%.) and copper (II) sulphate (2 mol%), the solution was degassed by three cycles of freeze-pump-thaw. The reaction was stirred at 40 ^{O}C for 3 days, filtered by syringe filter and dialysed for 3 days using a 1000 MWCO membrane. The aqueous solvent was removed by freeze dryer to obtain a glazed solid, which was trituration by methanol and diethyl ether. The precipitate was collected and dried under high vacuum to yield green solid. The yield was calculated based on the starting azide.

3.46 ^{1}H NMR (400 MHz, D_2O, 293 K, pD7): δ 307.2, 257.0, 198.9, 131.6, 105.3, 78.83 (s, 11H), 33.7, 33.0, 31.6, 30.7, -11.0, -12.3, -14.7, -15.7, -16.8, -54.7, -67.5, -80.2, -84.8, -

90.6, -95.9, -102.6, -106.8, -117.5, -147.1, -152.5, -204.6, -246.1, -263.3, -419.7. Only resolved peaks outside -10 to 10 ppm are reported.

3.47 ^{1}H NMR (400 MHz, D_2O, 293 K, pD7) δ 261.20, 135.91, 112.74, 108.40, 95.46, 82.79, 60.87, 44.93, 42.86, 35.51, 33.83, 30.63, 29.10, 28.43, 27.21, 26.24, 25.56, 18.42, 16.88, 16.09, 14.49, 11.17, -10.38, -12.10, -13.23, -13.87, -15.57, -16.09, -18.13, -63.55, -66.20, -69.67, -71.47, -74.14, -75.54, -95.66, -99.31, -103.42, -104.67, -113.84, -127.27. Only resolved peaks outside -10 to 10 ppm are reported.

4.15 General procedure of synthesis of the supramolecular rotaxane-lanthanide complexes (4.15-4.17)



DCM (1 ml) and TFA (1ml) were added dropwise to a solution of rotaxane (0.5 mmol) in. The reaction was stirred at RT for 48 h, the solvents were removed under reduced pressure and the product was obtained quantitatively from methanol by precipitation using diethyl ether. The precipitate was dried over high vacuum to afford ligand as an oil. To a solution of the ligand (**4.15-4.17**) in deuterated methanol (0.5 ml) the appropriate lanthanide triflate salt was added (1.0 eq.) and the reaction mixture was allowed to stir at 60º C for 24 hours. The reaction was left stirring at 60º C for 48 h. The methanol was removed under reduced pressure leaving an oil that was dissolved in water. The pH of this solution was adjusted to 10 by addition of aqueous sodium deuterium oxide to remove excess of lanthanide as its insoluble hydroxide. The resulting precipitate was centrifuged and the supernatant filtered. The solution was neutralised by addition of deuterium chloride. The solvent was removed under reduced pressure to yield the product as a colourless solid.

6.6 X-ray crystallographic data

Table 6-2. Summary of the X-ray crystallographic data.

Compound	**3.6Lu**	
Empirical formula	C17 H30 Lu N4 O9	
Formula weight	609.42	
Temperature	150 K	
Wavelength	0.71073 Å	
Crystal system	Monoclinic	
Space group	P 21/n	
Unit cell dimensions	a = 10.8230(2) Å	α= 90°.
b = 18.4055(3) Å	β= 106.695(2)°.	
c = 11.2150(2) Å	γ = 90°.	
Volume	2139.89(7) $Å^3$	
Z	4	
Density (calculated)	1.891 Mg/m^3	
Absorption coefficient	4.670 mm^{-1}	
F(000)	1212	
Crystal size	0.30 x 0.25 x 0.23 mm^3	
Theta range for data collection	2.195 to 30.456°.	
Index ranges	-15<=h<=15, -25<=k<=26, -15<=l<=15	
Reflections collected	48801	
Independent reflections	6132 [R(int) = 0.048]	
Completeness to theta = 26.497°	99.5 %	
Absorption correction	Semi-empirical from equivalents	

Max. and min. transmission	0.34 and 0.26	
Refinement method	Full-matrix least-squares on F^2	
Data / restraints / parameters	6127 / 0 / 280	
Goodness-of-fit on F_2	1.0000	
Final R indices [I>2sigma(I)]	R1 = 0.0321, wR2 = 0.0653	
R indices (all data)	R1 = 0.0352, wR2 = 0.0670	
Largest diff. peak and hole	1.39 and -1.82 e.$Å^{-3}$	

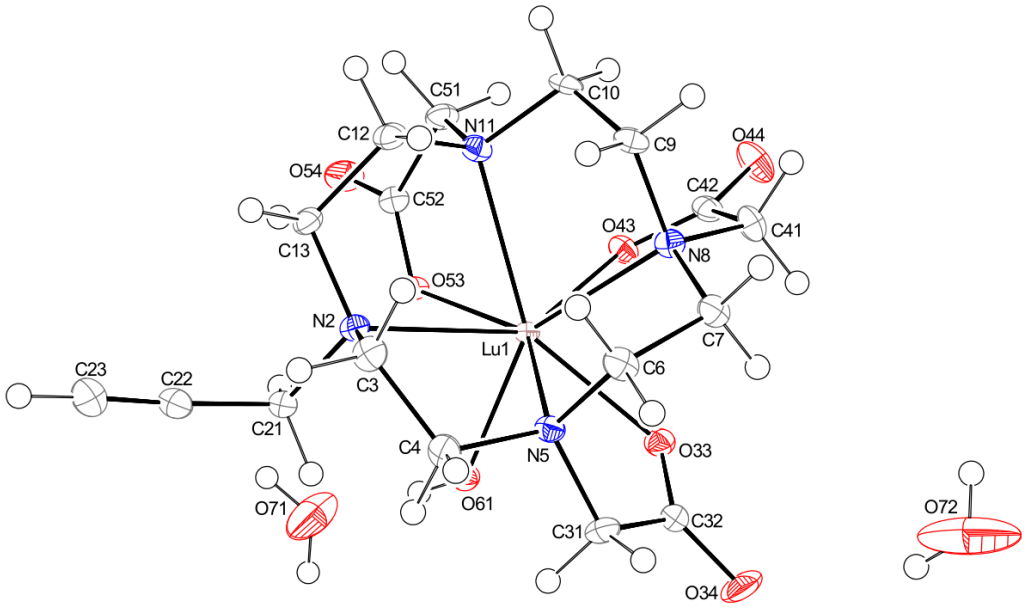


Figure 6-1. ORTEP representation of the X-ray crystal structure of 2.6 with thermal ellipsoids at 50% probability.

6.7 Reference

[1] A. Krężel, W. Bal, *J. Inorg. Biochem.* **2004**, *98*, 161–166.

[2] B. J. Cosier, A. M. Glazer, *J. Appl. Crystallogr.* **1986**, *19*, 105–107.

[3] A. Altomare, G. Cascarano, C. Giacovazzo, A. Guagliardi, *J. Appl. Crystallogr.* **1994**, *27*, 1045–1050.

[4] D. Watkin, R. Cooper, C. K. Prout, *Zeitschrift fur Krist.* **2002**, *217*, 429–430.

[5] R. I. Cooper, A. L. Thompson, D. J. Watkin, *J. Appl. Crystallogr.* **2010**, *43*, 1100–1107.

[6] P. Kuzmič, *Anal. Biochem.* **1996**, *237*, 260–273.

[7] A. Beeby, I. M. Clarkson, R. S. Dickins, S. Faulkner, D. Parker, L. Royle, A. S. de Sousa, J. A. G. Williams, M. Woods, *J. Chem. Soc. Perkin Trans. 2* **1999**, *39*, 493–504.

[8] A. Beeby, L. M. Bushby, D. Maffeo, J. A. Gareth Williams, *J. Chem. Soc. Dalt. Trans.* **2002**, 48–54.

[9] S. Faulkner, M. Tropiano, in *Lumin. Lanthan. Ions Coord. Compd. Nanomater.*, John Wiley & Sons Ltd, Chichester, United Kingdom, **2014**, pp. 331–358.

[10] G. J. Stasiuk, M. P. Lowe, *Dalt. Trans.* **2009**, 9725–9727.

[11] C. Allain, P. D. Beer, S. Faulkner, M. W. Jones, A. M. Kenwright, N. L. Kilah, R. C. Knighton, T. J. Sørensen, M. Tropiano, *Chem. Sci.* **2013**, *4*, 489–493.

[12] M. Tropiano, A. M. Kenwright, S. Faulkner, *Chem. - A Eur. J.* **2015**, *21*, 5697–5699.

[13] C. Allain, P. D. Beer, S. Faulkner, M. W. Jones, A. M. Kenwright, N. L. Kilah, R. C. Knighton, T. J. Sørensen, M. Tropiano, *Chem. Sci.* **2013**, *4*, 489–493.